



PHD

Chemical investigations into the constituents of I, *Rhodomyrtus macrocarpa* (Myrtaceae) II, some British marine red algae.

Igboechi, Chike A.

Award date:
1983

Awarding institution:
University of Bath

[Link to publication](#)

Alternative formats

If you require this document in an alternative format, please contact:
openaccess@bath.ac.uk

General rights

Copyright and moral rights for the publications made accessible in the public portal are retained by the authors and/or other copyright owners and it is a condition of accessing publications that users recognise and abide by the legal requirements associated with these rights.

- Users may download and print one copy of any publication from the public portal for the purpose of private study or research.
- You may not further distribute the material or use it for any profit-making activity or commercial gain
- You may freely distribute the URL identifying the publication in the public portal ?

Take down policy

If you believe that this document breaches copyright please contact us providing details, and we will remove access to the work immediately and investigate your claim.

UNIVERSITY OF BATH		
LIBRARY		
23	23 MAR 1984	
PMD		

CHEMICAL INVESTIGATION INTO THE CONSTITUENTS OF

I, *RHODOMYRTUS MACROCARPA* (MYRTACEAE)

II, SOME BRITISH MARINE RED ALGAE

THESIS

Submitted by

CHIKE A. IGBOECHI, B. Pharm.

for the degree of Doctor of Philosophy

of the University of Bath

1983

This research has been carried out in the School of Pharmacy and Pharmacology of the University of Bath under the supervision of Dr. M.G. Rowan

COPYRIGHT

Attention is drawn to the fact that copyright of this thesis rests with its author. This copy of the thesis has been supplied on condition that anyone who consults it is understood to recognise that its copyright rests with its author and that no quotation from the thesis and no information derived from it may be published without the prior written consent of the author.

This thesis may be made available for consultation within the University Library and may be photocopied or lent to other libraries for the purpose of consultation.

SIGNED:



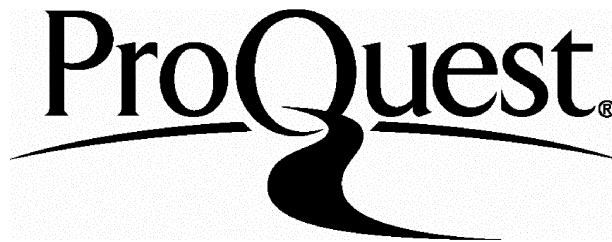
ProQuest Number: U343269

All rights reserved

INFORMATION TO ALL USERS

The quality of this reproduction is dependent upon the quality of the copy submitted.

In the unlikely event that the author did not send a complete manuscript and there are missing pages, these will be noted. Also, if material had to be removed, a note will indicate the deletion.



ProQuest U343269

Published by ProQuest LLC(2015). Copyright of the Dissertation is held by the Author.

All rights reserved.

This work is protected against unauthorized copying under Title 17, United States Code.
Microform Edition © ProQuest LLC.

ProQuest LLC
789 East Eisenhower Parkway
P.O. Box 1346
Ann Arbor, MI 48106-1346

SUMMARY

The "Australian finger cherry", *Rhodomyrtus macrocarpa*, was re-examined resulting in the isolation and characterisation of two new isomers of the natural dibenzofuran derivative, rhodomyrtoxin, and smaller quantities of a third isomer, possibly ψ -rhodomyrtoxin. A high performance liquid chromatographic method is described which offers a rapid and sensitive approach to both quantitative and qualitative analysis of the dibenzofuran derivatives from *Rhodomyrtus macrocarpa*. This could be used to investigate the possibility of geographical or seasonal variations, or variations linked with the stage of maturity, in the dibenzofuran constituents of the fruits.

A pentacyclic triterpenoid acid was also isolated from *Rhodomyrtus macrocarpa* and this raises the possibility of the presence of pharmacologically active glycosides which may be responsible for the reported toxicity of the fruits.

Five species of British marine algae were examined chemically. The known heterosides, floridoside and sodium mannopyranosylglycerate were isolated from *Palmaria palmata* and *Polysiphonia lanosa* respectively. Comprehensive spectroscopic data are given and the usefulness of spectroscopic techniques in determining the configuration at the anomeric carbon atom, and position of glycosidic linkage is highlighted .

The known potassium sulphate ester salt, lanosol sulphate, was isolated from samples of *Polysiphonia lanosa* collected from two different geographical locations but the related ether-soluble brominated phenols were found only in a sample from Kimmeridge Bay and not in one from Berwick-on-Tweed. The possibility that they may be extraction artifacts was investigated.

A fatty acid isolated from *Corallina officinalis* is shown to have an unusual arrangement of double bonds and the structure was in all probability limited to two possible isomers, 4,8,11,14, 17 - or 4,7,10,13,17 - eicosapentaenoic acid.

An aliphatic aldehyde isolated from *Laurencia pinnatifida* was assigned a tentative structure by a combination of NMR, infrared, and mass spectral evidence as well as results obtained from oxidative cleavage and gas-liquid chromatographic analysis.

Sterols, free fatty acids and amino acids were routinely isolated and analyzed.

ACKNOWLEDGEMENTS

I wish to express my profound gratitude to Dr. M.G. Rowan, whose generous efforts and stimulating ideas were invaluable in this work, and Prof. R.T. Parfitt, for suggesting, and providing material for the work on *Rhodomirtus macrocarpa*, and for his overall interest and discussions.

I would also like to thank the following: Dr. A.F. Casy for his helpful discussions; Mrs B. Dunning and D. Belk, Messrs R. Hartell, D. Wood, K. Smith, R. Sadler, and P. Reynolds, for technical assistance; Mrs J. Harbutt for the good typing and my friends and colleagues for their interest and support.

May I also acknowledge the University of Benin, Nigeria, for granting me training leave and sponsorship, and the Committee of Vice Chancellors and Principals (UK) for Overseas Research Studentship award.

Finally, I would like to express my sincere gratitude to members of my family who patiently suffered my neglect throughout the duration of this work.

Dedicated to the memory of my dad,

V.D.O. Igboechi

TABLE OF CONTENTS

	<u>Page</u>
Summary	i
Acknowledgements	iii
Part I. - CHEMICAL INVESTIGATION INTO THE CONSTITUENTS OF <i>RHODOMYRTUS MACROCARPA</i>	
Chapter 1. Introduction	
1.1 Plant material	3
1.2 Previous chemical work	4
1.3 Scope of present work	8
Chapter 2. Experimental	
2.1 Extraction	11
2.2 Thin layer chromatography	11
2.3 Preparative thin layer chromatography	12
2.4 Column chromatography	13
2.5 Spectroscopic examination	14
2.6 High performance liquid chromatography (HPLC)	15
2.6.1 Instrument	15
2.6.2 Column packing procedure	15
2.6.3 Column testing	16
2.7 HPLC of mixed crystalline Dibenzofurans (DB) from <i>R. Macrocarpa</i>	
2.7.1 Sample	20
2.7.2 Straight phase HPLC	20
2.7.3 Reversed phase HPLC	21
2.8 Chemical derivatisation	
2.8.1 Methylation of the phenolic hydroxyl	

	<u>Page</u>
groups in DB	21
2.8.2 Deuterium exchange of protons α to the carbonyl group in 2-hydroxy-4-methyl- propiophenone	22
2.8.2 Attempted deuterium exchange on DB	23
Chapter 3. Results and Discussion	
3.1 Preliminary thin layer chromatography	25
3.2 Isolation of components from the unripe fruit extract	25
3.3 Characterisation of DB	27
3.4 Analytical data on isolated dibenzofurans	
3.4.1 DB-I	30
3.4.2 DB-II	30
3.4.3 RL	33
3.5 Discussion	33
3.6 Fractionation of the ripe fruit extract	52
3.7 Deuterium exchange	53
3.8 High performance liquid chromatography	58
3.9 Analytical data on RH	63
3.10 Characterisation of RH	63
3.11 Possible relationship between biological activity and chemical structure	75
References to Part I	78

	<u>Page</u>
Part II. - CHEMICAL INVESTIGATION INTO THE CONSTITUENTS OF SOME BRITISH MARINE RED ALGAE	
Chapter 1. Introduction	
1.1 General characteristics of seaweeds	82
1.2 Uses	83
1.3 Chemistry of the seaweeds	85
1.3.1 Terpenes	87
1.3.2 Sterols	94
1.3.3 Non-terpenoid acetylenes	101
1.3.4 Non-terpenoid phenols	103
1.3.5 Fatty acids	107
1.3.6 Low molecular weight carbohydrates	108
1.3.7 Amino acids and other low molecular weight nitrogenous compounds	109
Chapter 2. General Materials and Methods	
2.1 Plant material	114
2.2 Preliminary extraction	116
2.3 Chromatography	118
2.3.1 Column and thin layer chromatography	118
2.3.2 Ion-exchange chromatography	118
2.3.3 Paper chromatography	119
2.3.4 Gas-liquid chromatography	120
2.4 Spectroscopic examination	121
2.5 Preparation of fatty acid methyl esters	122
2.6 Syntheses of potassium sulphate esters of phenol and benzyl alcohol	123
2.7 Screening for antibacterial activity	128

	<u>Page</u>
Chapter 3. <i>Polysiphonia lanosa</i>	
3.1 Extraction and isolation of water-soluble compounds	136
3.2 Characterisation of sodium 2'-(1-O- α -D-mannopyranosyl) glycerate	
3.2.1 Analytical data on KPL-2S	138
3.2.2 Ion-exchange chromatography of KPL-2S	139
3.2.3 Analytical data on KPL-2H	139
3.2.4 Acid hydrolysis of KPL-2S	140
3.2.5 Discussion	142
3.3 Characterisation of 2,3-dibromo-5-hydroxybenzyl-1'-4-disulphate, dipotassium salt	
3.3.1 Analytical data on KPL-2R	153
3.3.2 Hydrolysis of KPL-2R	155
3.3.3 Analytical data on KPL-RH	156
3.3.4 Discussion	156
3.4 ^{13}C -NMR studies on 2,3-dibromo-5-hydroxybenzyl-1',4-disulphate, dipotassium salt	160
3.5 Fractionation of the ether-soluble acidic extract	171
3.6 Characterisation of brominated phenolic compounds	
3.6.1 Analytical data on compound A	172
3.6.2 Analytical data on compound B	173
3.6.3 Discussion	174
3.7 Fractionation of the ether-soluble neutral extract	186
Chapter 4. <i>Palmaria palmata</i>	
4.1 Extraction and isolation	189
4.2 Formation of acetyl derivative of KPP-A	190

	<u>Page</u>
4.3 Acid hydrolysis of KPP-A	191
4.4 Analytical data on KPP-A	191
4.5 Analytical data on PP-1	193
4.6 Discussion	195
Chapter 5. <i>Corallina officinalis</i>	
5.1 Extraction and isolation	217
5.2 Isolation of C ₂₀ polyunsaturated fatty acid as the methyl ester	219
5.3 Formation of pyrrolidide of CA-A	220
5.4 Analytical data on CN-A	221
5.5 Analytical data on CA-A	222
5.6 Discussion	222
Chapter 6. <i>Laurencia pinnatifida</i>	
6.1 Extraction and isolation	241
6.2 Permanganate-periodate oxidation of PLP-NB	242
6.3 Results and Discussion	243
Chapter 7. Analyses of sterol, free fatty acid and free amino acid composition of some Rhodophyta species	
7.1 Sterol analyses by gas-liquid chromatography	252
7.2 Analyses of free fatty acids by gas-liquid chromatography	261
7.3 Analyses of free amino acids by two dimensional paper chromatography	266
References to Part II	269

PART I

CHEMICAL INVESTIGATION INTO THE CONSTITUENTS
OF *RHODOMYRTUS MACROCARPA*
(BENTH)

CHAPTER ONE
INTRODUCTION

1.1 PLANT MATERIAL

Rhodomyrtus macrocarpa (Benth) belongs to the family Myrtaceae and has the vernacular names "Australian Finger Cherry" and "Cooktown Loquat" . It occurs in tropical scrub and is indigenous to North Queensland and New Guinea.¹ Bailey¹ describes it as follows: A tall shrub, the young branches and inflorescence heavy with a close tomentum. The leaves are oval-elliptical or obovate, obtuse or shortly acuminate , and often 6 - 10 inches long, penniveined and reticulate, glabrous or minutely pubescent underneath. The peduncles are in the upper axils - short, bearing either 1 or 3 flowers in a short compact leafy raceme. The calyx tube is cylindrical with five unequal lobes. The petals are tardily expanding and the style is large and peltate. The ovules are usually superposed in two rows on a parietal placenta protruding between the rows (the ovary reduced to a single cell).^{The is} fruit cylindrical, $\frac{3}{4}$ - $1\frac{1}{4}$ inches long, often torulose when dry . The seeds are large, superposed usually in a single row, or very rarely two rows, and separated by firm partitions.

The fruit of *Rhodomyrtus macrocarpa* has been said to cause sporadic blindness and sometimes death when eaten by both humans and livestock. The fruit, which when ripe is bright red, at certain times of the year may be eaten with impunity and made into palatable preserves. However, during the wet summer season ingestion of the fruit often causes paralysis,

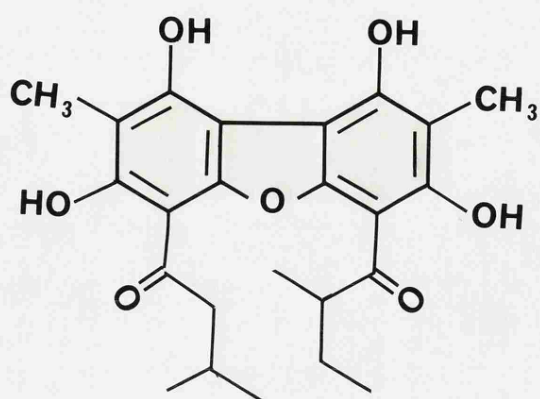
permanent blindness and sometimes death.² Although many well authenticated cases of blindness and death caused by *Rhodomyrtus macrocarpa* poisoning have been reported^{3,4}, other evidence is conflicting. There are reports of children having eaten simultaneously from the same tree, some having been blinded and others not². A number of reasons for this sporadic toxicity have been proposed. Thus it has been suggested that the immature fruit containing a glycoside may be responsible, the glycoside being destroyed during the ripening. There was also a suggestion that the loss of sight might be caused by the juice of the fruit being put in the eyes from the eater's fingers². A further suggestion was that a fungal infestation of the fruit might be responsible. The ripe fruit is said to be infested by a fungus, *Gleosporium periculosum* which occurs in the form of pustules occupying the whole or part of the surface of the ripe fruit, forming sulphur-coloured nodules half a millimetre in diameter beneath the cuticle¹. There is no evidence for or against any of these theories.

1.2 PREVIOUS CHEMICAL WORK

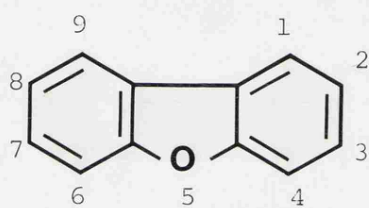
In an attempt to identify the toxic principle in the fruit of *Rhodomyrtus macrocarpa*, Trippett⁵ examined the extractives of the dried immature fruit and isolated a yellow crystalline natural product. Progress towards the definition of the constitution of this compound included the establishment of

its molecular formula, $C_{24}H_{28}O_7$, and the recognition that it was a dibenzofuran derivative associated with two methyl groups, four hydroxyl groups and two isovaleryl residues. These were achieved by chemical degradation and ultra-violet and infra-red spectroscopy. This tetrahydroxydimethyl-diisovaleryldibenzofuran was called rhodomyrtxin. On investigating the extracts of the fresh, mature fruit, Trippett⁵ found a substance isomeric with rhodomyrtxin and showing similar chemical behaviour but differing in its ultra-violet spectrum.

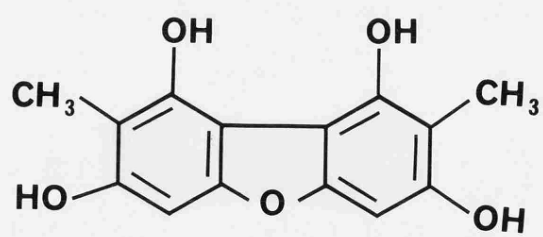
Further examination of a fresh sample of the immature fruit of *Rhodomyrtus macrocarpa* by Anderson et al.⁶ did not yield rhodomyrtxin but an isomer which they named ψ -rhodomyrtxin. ψ -Rhodomyrtxin was found to possess one isovaleryl residue and one 2-methylbutyryl residue as opposed to the two isovaleryl residues in rhodomyrtxin. On the basis of chemical degradation, ultra-violet and infra-red spectroscopy, and proton magnetic resonance (1H -NMR) spectroscopy ψ -rhodomyrtxin was assigned the structure (1) in which the acyl side chains are in positions 4 and 6 of the dibenzofuran nucleus (2). Each acyl substituent was placed *ortho* and *para* to the two hydroxyl groups on each of the two benzene rings. Anderson et al.⁶ also commented on the constitution of rhodomyrtxin and isorhodomyrtxin, the product of a boron trifluoride-catalysed reaction between dideisovaleryl rhodomyrtxin (3)⁶ and isovaleric acid. They suggested that isorhodomyrtxin has the structure (4) and that rhodomyrtxin is limited to two constitutional possibilities (5) and (6).



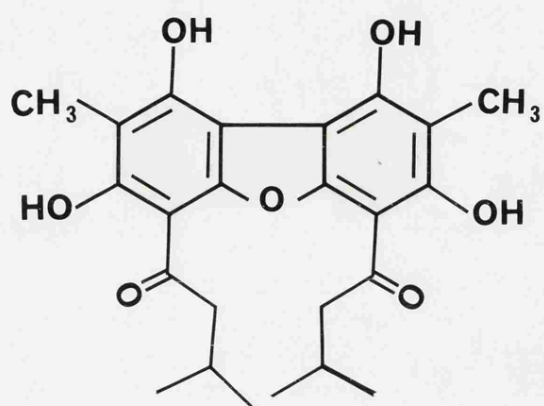
(1)



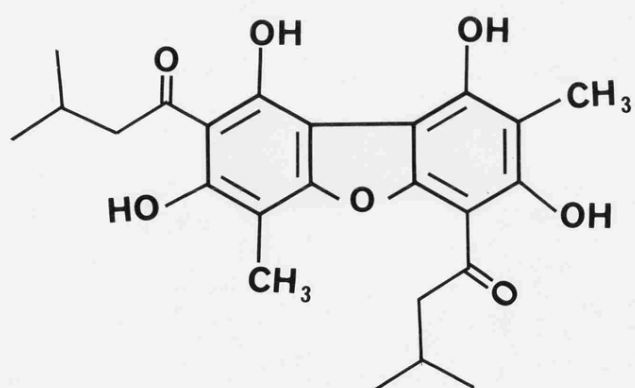
(2)



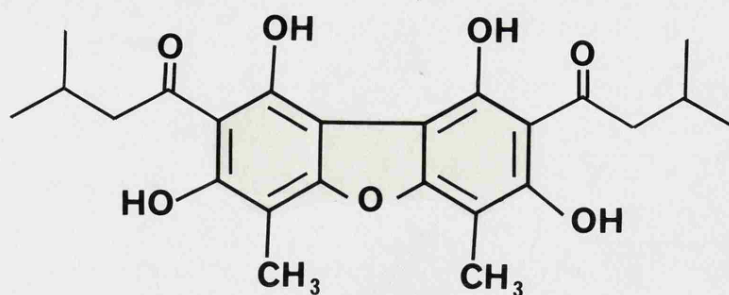
(3)



(4)



(5)



(6)

More recently Sargent *et al.*¹⁸, on the basis of synthetic studies, have confirmed the structure, (1) for ψ -rhodomyrtoxin but suggest (4) for rhodomyrtoxin and (6) for isorhodomyrtoxin.

Trippett⁵ reported an LD₅₀ of 12 mg per kg (mice) for rhodomyrtoxin. Anderson *et al.*⁶ however reported (for ψ -rhodomyrtoxin) the absence of toxic effects upon a single rat (oral administration 13 mg/kg) or upon a single cat (subcutaneous administration 6 mg/kg) but some toxic effects on mice at doses of about 30 mg/kg. No symptoms of temporary or permanent blindness were detected by various animal tests on ψ -rhodomyrtoxin, and no effect was observed upon the eye when it was administered directly to the eyes of rabbits.

1.3 SCOPE OF THE PRESENT WORK

The present work is concerned with a re-examination of

Rhodomyrtus macrocarpa, and the isolation and characterisation of further dibenzofuran derivatives. By the use of chromatographic separation on silica gel and high performance liquid chromatography (HPLC), separation of three dibenzofuran derivatives was achieved. ^{13}C - and ^1H -NMR spectroscopy, ultraviolet and infrared spectroscopy and chemical derivatisation were used to elucidate the precise structure of the isolated dibenzofurans.

The nature of the constituents of the fruit appears to vary with the season (wet or dry season crop) and the degree of maturity of the fruit. An investigation of this, using the developed HPLC system, was envisaged with the collaboration of Dr. W. Griffin (University of Queensland, Australia) who supplied the extract used in this project. Unfortunately, this aspect of the work could not be realised due to difficulties in obtaining suitable samples.

CHAPTER TWO
EXPERIMENTAL

2.1 EXTRACTION

Two separate crude extracts, R_A (1.9 g) and R_B (0.2 g) from the unripe and ripe fruits respectively were supplied as reddish-brown powdery solids by Dr. W. Griffin (University of Queensland Australia). The extraction procedure involved grinding the dried fruits to coarse powder and extraction at room temperature with acetone until further extracts were colourless. The acetone extract was evaporated to dryness under reduced pressure. The residue was dissolved in ether and treated with petroleum ether ($40^{\circ} - 60^{\circ}$) to give a suspension which was then filtered. The filtrate was concentrated and set aside at room temperature for several days. The resulting solid was collected by filtration and dried to give the crude extracts.

2.2 THIN LAYER CHROMATOGRAPHY (TLC)

Preliminary chromatographic investigations were carried out on glass plates coated with silica gel G type 60 (Merck) to a thickness of 0.25 mm. In some cases precoated TLC-Plastic sheets silica gel 60, layer thickness 0.2 mm were used. The following solvent systems were investigated:

1. Chloroform
2. Chloroform-methanol (9:1)
3. Chloroform-methanol (4:1)

4. Toluene-methanol (4:1)
5. Dichloromethane
6. Dichloromethane-methanol (9:1)
7. 1,2-dichloroethane
8. 1,2-dichloroethane-methanol (9:1)

The TLC plates were activated at 110°C for 60 minutes and allowed to cool. 2 μl samples of each dilute solution of the crude extracts in acetone were spotted on to the plates and developed for about an hour. The developed plates were dried and observed in visible light and under ultraviolet light at wavelengths of 254 and 366 nm. The plates were then sprayed with 50 per cent sulphuric acid and heated to 110°C for 5 - 10 minutes. The chromatogram was again observed in visible light and under ultraviolet light.

2.3 PREPARATIVE THIN LAYER CHROMATOGRAPHY (PREP. TLC)

Preparative thin layer chromatography was carried out on glass plates coated with silica gel 60 PF₂₅₄ to a thickness of 1.5 mm and activated at 120°C for two hours. The sample was applied as a continuous straight line, and after development in the appropriate solvent system the plates were removed from the tank and dried with a hot air drier. The bands were observed in ordinary light and under ultraviolet light. The desired band was carefully scraped off the plates into a beaker

and the components eluted with an appropriate organic solvent.

2.4 COLUMN CHROMATOGRAPHY

Column chromatography on a preparative scale was carried out on two different grades of silica gel - the relatively coarse column grade silica gel (particle size 100 - 200 μm) and silica gel H type 60, TLC grade. An open glass column was filled with an appropriate solvent of relatively low polarity compared to the solvent system that achieved a satisfactory resolution on TLC. An appropriate weight of adsorbent was made into a slurry with the packing solvent and the slurry carefully transferred into the column taking care to eliminate air from the system. The solvent was allowed to drain from the column at a very slow rate while packing was in progress but never allowing the liquid level to fall below the top of the bed. The packed column was left to settle for at least one hour before use. A layer of filter paper was placed over the bed and excess solvent drained off before the sample was introduced as a concentrated solution with the aid of a Pasteur pipette. Where sample solubility in the packing solvent was found to be poor, a concentrated solution of the sample in a suitable solvent was slurried with some adsorbent material, and solvent removed from the slurry *in vacuo* or with a stream of nitrogen to leave the organic material coated on the adsorbent. The coated adsorbent was then

deposited on top of the packed column. Fractions were eluted with solvent of gradually increasing eluting power. Components were eluted from the column in order of their increasing polarity. The progress of the elution was followed by collecting fractions from the eluate, concentrating and monitoring by analytical TLC. Appropriate combination of fractions was determined by their TLC behaviour.

2.5 SPECTROSCOPIC EXAMINATION

Ultraviolet spectra were measured for solutions in ethanol (95%) with or without the addition of sodium ethoxide using a Perkin-Elmer 550S UV-VIS double beam recording spectrophotometer.

Infrared spectra were recorded for solutions in chloroform, and for potassium bromide discs using a Unicam SP 200 G Grating Infrared spectrophotometer.

Electron impact mass spectra (E.I.M.S.) were determined on an AEI MS 12 Single focussing mass spectrometer, at ionising potentials of 12 eV and 70eV.

Proton magnetic resonance (^1H -NMR) spectra at 100 MHz were recorded on a JEOL PS100 NMR Spectrophotometer, and the ^{13}C -NMR spectra on a JEOL FX 90Q Fourier Transform NMR Spectrometer. Solutions were in either deuteriochloroform (CDCl_3) or deuteriated dimethyl sulphoxide (DMSO-d_6) or a

mixture of both solvents. Tetramethylsilane (TMS) was used as internal reference.

2.6 HIGH PERFORMANCE LIQUID CHROMATOGRAPHY (HPLC)

2.6.1 Instrument

The HPLC instrument consisted of a Talbot model LP 1 solvent delivery system equipped with a Milton Roy constant volume mini-pump plus pulse dampener, and monitored by a Pye-Unicam LC Variable wavelength ultraviolet detector. The traces were recorded on a Servoscribe 1S recorder.

2.6.2 Column packing procedure

Straight precision base stainless steel columns were used. For the straight phase HPLC a column 150 mm x 5 mm i.d. was packed with Lichrosorb Si 60 particle size 5 μ m. 2.4 g of the packing material was slurried in chloroform-methanol (4:1), shaken vigorously in a small sample tube and then placed in an ultrasonic bath for 5 - 10 minutes to effect complete dispersal of the adsorbent. Meanwhile, the column with its bottom gauze and fitting in place was filled with the support liquid (3 mls of tetrachloroethane). The packing chamber (a 75 ml bomb) was attached and the whole

mounted vertically with the column outlet downwards. The slurry was removed from the ultrasonic bath, shaken vigorously, and poured into the packing chamber. The lead from the pressure pump was connected and a pressure of 5000 p.s.i. was applied. The driver liquid (chloroform) was frequently topped up in the reservoir. The flow rate for every 50 mls of effluent from the column was determined. When a constant flow rate was attained the air pump was depressurized very slowly and the column left for a while before it was disconnected. The top of the column packing was made level by carefully removing excess packing material with a micro-spatula. The top of the packing was finally smoothed with a tamping rod. The top gauze, ring and glass beads were then put in place.

For the reversed phase HPLC a column 100 mm x 4 mm i.d. was packed with Spherisorb S5 ODS (octadecylsilane chemically bonded to silica) particle size 5 μm . The packing procedure was essentially the same as for the straight phase column. The packing material was slurried in chloroform-methanol (4:1) and packed downward with methanol at 5000 p.s.i. initially displacing 2 mls of tetrachloroethane, slammed to constant flow rate at 5500 p.s.i. and depressurized slowly.

2.6.3 Column testing

It is essential to determine the efficiency of a

column before it is put to use. In this way it is possible to monitor deterioration in performance at a later stage or to assess whether a poor separation obtained in a new application is due to a poorly packed column or to the use of the wrong stationary phase or eluant.

Column efficiency is expressed by height equivalent to a theoretical plate, HETP (H) and is given by

$$H = \frac{L}{N}$$

where L is the length of the column in mm,

$$\text{and } N = 5.54 \left(\frac{t_R}{W_{\frac{1}{2}}} \right)^2$$

t_R = retention time of a retained solute in mm,

$W_{\frac{1}{2}}$ = Width at half height of the retained peak in mm.

Typical values of N with modern HPLC columns are in the range 1000 - 20,000⁷. Efficient columns are characterized by high values of N and small values of H. Column performance may also be expressed by the value of the reduced plate height, h at different flow rates.

$$h = \frac{H}{d_p}$$

where d_p is the particle size of the packing material in millimetres.

Typical values for h range between 2 and 4⁸.

Test Conditions:

1. Column: Lichrosorb Si 60. Particle size 5 μm
Size: 150 mm x 5 mm i.d.
Test sample: 20 μl injections of $1 \times 10^{-6}\%$ (w/v) solution
of nitrobenzene in mobile phase
Mobile phase: 1% acetonitrile in n-hexane at different
flow rates

2. Column: Spherisorb ODS S5 particle size 5 μm
Size: 100 mm x 4 mm i.d.
Test sample: 5 μl injections of $3 \times 10^{-4}\%$ (v/v) solution
of anisole in mobile phase.
Mobile phase: Methanol-water (70:30) at different flow
rates.

2.6.4 Results of column testing

Table 1.1

Column 1: Lichrosorb Si 60. Particle size 5 μm ;

(L) 150 mm x 5 mm i.d.

Column 2: Spherisorb ODS S5: Particle size 5 μm ,

(L) 100 mm x 4 mm i.d.

	Column 1		Column 2	
Flow rate (ml/min)	1.96	1.46	0.90	0.70
t_R (mm)	61	92	163	184
t_o (mm)	13	17	72	79
$W^{\frac{1}{2}}$ (mm)	1.6	2.0	4.0	4.9
Plate No. (N)				
$5.54 \left(\frac{t_R}{W^{\frac{1}{2}}} \right)^2$	8052	11722	9200	7812
Capacity ratio (K')				
$\frac{t_R - t_o}{t_o}$	3.7	4.4	1.54	1.33
Column efficiency (H)				
L/N (mm)	0.0186	0.0128	0.0109	0.0128
Reduced plate height (h)				
H/d_p	3.72	2.56	2.18	2.56

The efficiency of the two columns as determined by the values of 'height equivalent to a theoretical plate' (H), the 'reduced plate height' (h), and 'plate number' (N), is satisfactory and is indicative of well-packed columns.

2.7 HPLC OF MIXED CRYSTALLINE DIBENZOFURANS (DB) FROM RHODOMYRTUS MACROCARPA

2.7.1 Sample

The sample coded DB is a yellow crystalline mixture of dibenzofuran derivatives isolated from the extracts of *Rhodomyrtus macrocarpa* by open gravity column chromatography, on coarse silica gel (column grade) eluted with chloroform.

2.7.2 Straight Phase HPLC

Straight phase HPLC was carried out on a column (150 mm x 5 mm i.d.) of Lichrosorb Si 60 particle size 5 µm. 20 µl injections of dilute solutions of DB in the mobile phase were used, and monitored at a wavelength of 280 nm.

The following mobile phases were investigated:

1. 1,2-dichloroethane
2. 1,2-dichloroethane-methanol (95:5) v/v
3. 1,2-dichloroethane-methanol (99.5:0.5) v/v
4. Dichloromethane
5. Dichloromethane-methanol (99.5:0.5) v/v
6. Dichloromethane-acetonitrile (90:10) v/v
7. Dichloromethane-acetonitrile (80:20) v/v

2.7.3 Reversed Phase HPLC

Reversed phase HPLC was carried out on a column (100 mm x 4 mm i.d.) of Spherisorb S5 ODS particle size 5 μ m. 20 μ l Injections of dilute solutions of DB in the different mobile phases were used, and monitored at a wavelength of 280 nm. The following mobile phases were investigated:

1. Methanol-water mixtures ranging from 100 percent methanol to 60 percent aqueous methanol.
2. Isopropanol-water mixtures containing 55 to 30 percent isopropanol.
3. Tetrahydrofuran-water (40:60) v/v
4. Tetrahydrofuran-water (35:65) v/v.

Solute peaks in an HPLC elution chromatogram are usually identified by their K' values,

$$K' = \frac{t_r - t_o}{t_o}$$

where K' or α value represents the capacity ratio, t_r the retention time of the retained peak and t_o the retention time of the solvent peak.

2.8 CHEMICAL DERIVATISATION

2.8.1 Methylation⁶ of the phenolic hydroxyl groups in DB

90 mg of the yellow crystalline solid (DB) was dissolved

in 200 ml of acetone. 2 g of anhydrous potassium carbonate was added and the mixture heated under reflux. Methyl iodide was added in portions at regular intervals (5 x 5 ml) during 60 hour of heating. The hot mixture was filtered and the filtrate concentrated *in vacuo* to give a residue which was extracted with diethyl ether. The ether was removed under reduced pressure to give a residue which was recrystallized from aqueous ethanol.

2.8.2 Deuterium exchange of protons α to the carbonyl group in 2-hydroxy-4-methylpropiophenone

2-Hydroxy-4-^{methyl}propiophenone was chosen as a suitable model compound for the dibenzofuran derivatives from *Rhodomyrtus macrocarpa* because of the similarity in their acyl substituents, and the relative position of the phenolic hydroxyl group with respect to the acyl side-chain.

Sodium (0.23 g; 0.01 mole) was carefully cleaned, cut into small pieces and added cautiously to deuterium oxide (4 ml; 0.5 mole) in a 50 ml conical flask. When all the sodium had dissolved, 2-hydroxy-4-methyl propiophenone, recrystallized from hot methanol, (1.6 g; 0.01 mole) in deuterio-chloroform (10 ml) was added all at once. The flask was securely stoppered and the reaction mixture was shaken continuously at room temperature for 20 hours using a magnetic stirrer. The organic layer was then separated and the aqueous fraction

extracted with more deuteriochloroform (2 x 10 ml). The combined organic fraction was dried over anhydrous magnesium sulphate and the solvent removed *in vacuo* (yield 1.31 g). The product was examined by ^1H -NMR and mass spectrometry.

2.8.3 Attempted deuterium exchange on DB

Deuterium exchange of the exchangeable protons in DB was attempted by the same method used on 2-hydroxy-4-methyl propiophenone. The product was examined by mass spectrometry.

CHAPTER THREE

RESULTS AND DISCUSSION

3.1 PRELIMINARY THIN LAYER CHROMATOGRAPHY

Three of the solvent systems used in the TLC investigation of the *Rhodomyrtus macrocarpa* extracts gave separations that were good enough for further considerations. The R_f values obtained for the major spots in the extracts are shown in Table 1.II.

3.2 ISOLATION OF COMPONENTS FROM THE UNRIPE FRUIT EXTRACT

The unripe fruit extract was fractionated on a column of silica gel eluted with chloroform and chloroform-methanol mixtures of gradually increasing polarity. The chloroform eluates furnished a major component R_f 0.58 (TLC silica gel CHCl_3 -MeOH, 4:1). Similar fractions were combined and concentrated *in vacuo* to give a yellow crystalline solid coded DB. Further development of the column with chloroform-methanol mixtures yielded a mixture of products which on TLC analysis showed up as two prominent spots with R_f values of 0.29 and 0.82 (Si gel, CHCl_3 -MeOH, 4:1) and traces of components in between. This fraction was further subjected to preparative thin layer chromatography on silica gel developed in chloroform-methanol (4:1) to separate the two main components. The component with the higher R_f value was coded RH, and that with the lower R_f value, RL.

Table I.II. TLC analysis of crude extract, R_A and R_B .

a. Solvent system: chloroform

R_f	Visualisation in daylight	UV lamp $\lambda 366$ nm	50% H_2SO_4
0.03	-	-	purple
0.09	-	blue	faint grey
0.12	yellow	dark	grey
0.41	yellow	dark	grey

b. Solvent system: chloroform-methanol (9:1)

R_f	Visualisation in daylight	UV lamp $\lambda 366$ nm	50% H_2SO_4
0.22	yellow	light brown	reddish brown
0.32	-	-	grey
0.52	yellow	dark	grey
0.67	-	-	purple
0.71	-	blue	faint grey

c. Solvent system: chloroform-methanol (4:1)

R_f	Visualisation in daylight	UV lamp $\lambda 366$ nm	50% H_2SO_4
0.29	yellow	light brown	reddish brown
0.58	yellow	dark	grey
0.82	-	-	purple
0.91	-	blue	faint grey

The chromatograms for R_A (extract from unripe fruit) and R_B (extract from ripe fruit) were virtually identical.

3.3 CHARACTERISATION OF DB

The yellow solid (DB) from the chloroform fraction was recrystallized twice from toluene to give yellow crystals, melting point 196 - 199°C. The electron impact mass spectrum showed a molecular ion at m/z 428 which was also the base peak, and consistent with the molecular formula $C_{24}H_{28}O_7$. The presence of phenolic hydroxyl groups were indicated by infrared absorption bands at 3650 and 3300 cm^{-1} . On methylation, DB formed a tetramethyl ether with a molecular ion at m/z 484. The absence of peaks corresponding to the loss of 18 atomic mass units in the mass spectrum of the tetramethyl ether which were evident in the mass spectrum of the parent compound (m/z 428 - 410, 371 - 353), would suggest that all the hydroxyl groups have been successfully methylated. The infrared spectrum of the tetramethyl ether showed a carbonyl absorption band at ν_{max} 1690 cm^{-1} as opposed to 1610 cm^{-1} in the parent compound. This would imply that the carbonyl group(s) in the parent compound are chelated whereas those in the tetramethyl ether are not. Hence, the carbonyl group(s) in DB must be in close proximity to the hydroxyl groups.

The 1H -NMR spectrum of DB indicated the presence of 2-methylbutanoyl and 3-methylbutanoyl moieties as well as two strongly deshielded methyl groups (δ 2.29). The 1H -NMR spectrum of the methylated derivative showed additional peaks at δ 3.80 (s, 2-OCH₃) and δ 3.86 (s, 2-OCH₃) which replaced the signals at δ 12.45 and δ 11.45 attributed to chelated hydroxyl

protons in the parent compound. This observation is again consistent with the formation of a tetramethyl ether derivative. The infrared, ^1H -NMR and mass spectral data on DB and the tetramethyl ether are reminiscent of the rhodomyrtoxin structure^{5,6}. However, the integral values of the ^1H -NMR spectrum did not conform with the rhodomyrtoxin structure. Further investigation revealed that DB was in fact not homogenous. TLC on silica gel developed with 1,2-dichloroethane gave two yellow spots with R_f values of 0.55 and 0.48. Developing with dichloromethane also gave two yellow spots R_f 0.71 and 0.64. Accordingly, DB was further chromatographed on a column of silica gel H (TLC grade) and eluted with 1,2-dichloroethane. 10 ml fractions were collected using an automatic fraction collector. The fractions were monitored by analytical TLC on silica gel developed with the same solvent. Combination of fractions based on TLC behaviour gave three combinations of yellow solutions. The first, containing the component with R_f 0.55 (Table 1.III) was taken to dryness to give yellow crystals coded DB-I. The third contained the component with R_f value 0.48 which on evaporation gave yellow needles, coded DB-II. The second combination of fractions contained a mixture of the two components

Table 1.III TLC analysis of dibenzofurans isolated from *Rhodomirtus macrocarpa*

Compound	R_F			Visualisation in daylight	UV lamp 366 nm	50% H_2SO_4
	a	b	c			
DB-I	0.71	0.55	0.60	light yellow	dark	grey
DB-II	0.64	0.48	0.59	light yellow	dark	grey
RL	0.03	0.03	0.48	light yellow	light brown	reddish- brown

Solvent systems:

- a) dichloromethane
- b) 1,2-dichloroethane
- c) 1,2-dichloroethane-methanol (4:1)

3.4 ANALYTICAL DATA ON ISOLATED DIBENZOFURANS

3.4.1 DB-I

DB-I was isolated in the pure form as yellow crystals.

Melting point $178 - 9^{\circ}\text{C}$. Infrared spectrum for solution in chloroform is shown in Fig. 1.1.

Mass spectrum, E.I.M.S. m/z (relative intensity):

$428 [M]^+$ (100.0), $410 [M-H_2O]^+$ (20.1), $371 [M-C_4H_9]^+$ (88.4),
 $353 [M-C_4H_9-H_2O]^+$ (55.1), $314 [M-C_4H_9-C_4H_9]^+$ (8.9). (see Fig. 1.4).

Ultraviolet spectrum, $\lambda_{\text{max}}^{\text{EtOH}}$ nm (log ϵ):

234 (4.38), 295 (4.56), 307 (4.47), 395 (3.62 (see Fig. 1.7).

$\lambda_{\text{max}}^{\text{NaOEt}}$ nm (log ϵ): 294 (4.56), 388 (4.23), 409 (4.35), 434 (4.31)

^1H and ^{13}C -NMR chemical shifts are shown in Tables 1.IV and I.V respectively.

3.4.2 DB-II

Obtained as yellow needles after recrystallisation from dichloromethane-petroleum ether (40° - 60°C). Melting point $200-201^{\circ}\text{C}$. Infrared spectrum for solution in chloroform is shown in Fig. 1.2.

Mass spectrum, E.I.M.S. m/z (relative intensity).

$428 [M]^+$ (100.0), 410 (22.3), 371 (92.1), 353 (35.6), 314 (5.4)
 (see Fig. 1.5)

Fig.1:1 Infrared spectrum of DB-I (Rhodomyrtoxin-B)

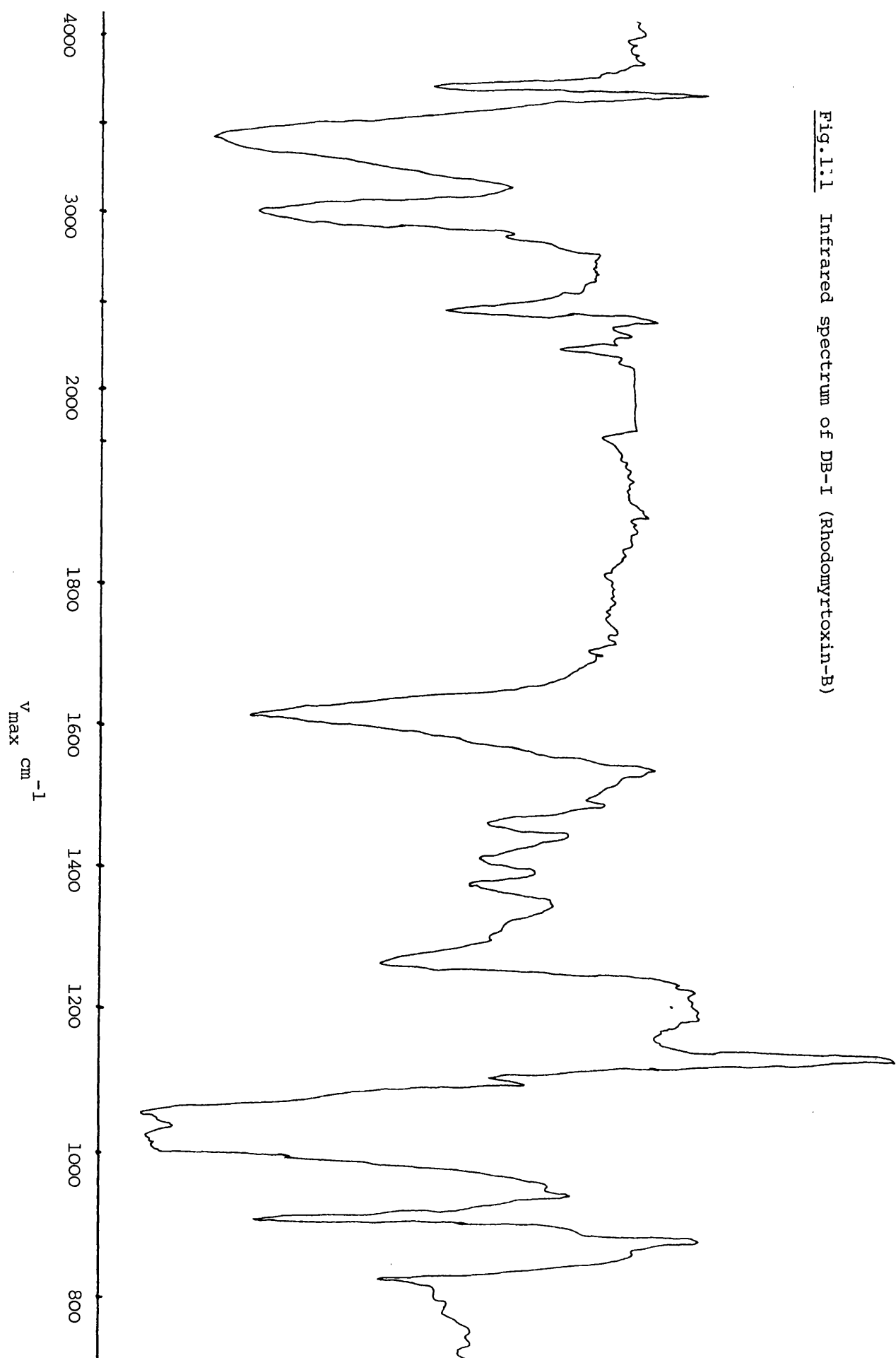
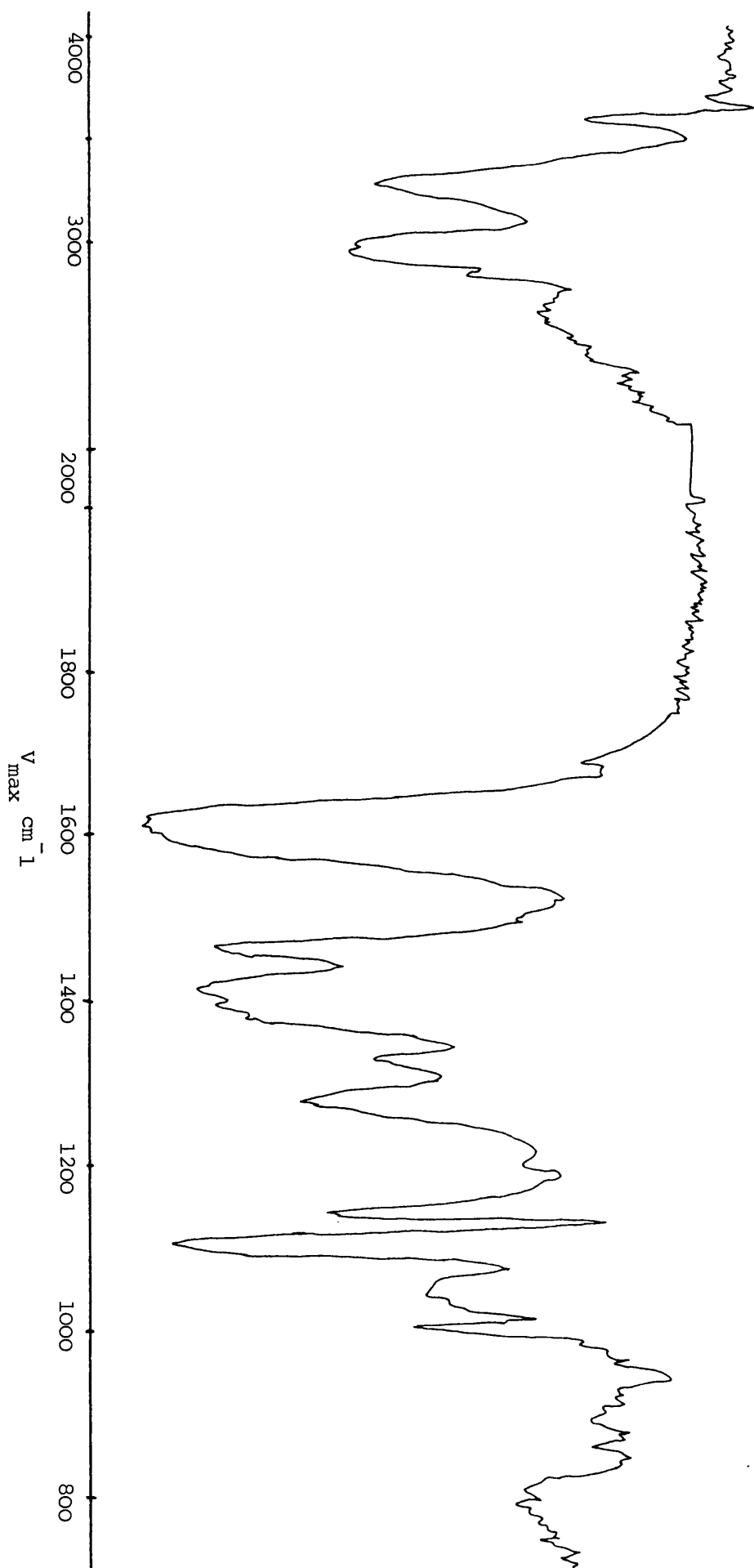


Fig. 1.2. Infrared spectrum of DB-II (Rhodomyltoxoin-C)



3.4.3 RL

RL was isolated as a yellow solid. The infrared spectrum for the solution in chloroform is shown in Fig. 1.3.

Mass spectrum, E.I.M.S. m/z (relative intensity)

428 $[M]^+$ (100.0), 414 (19.2) 371 $[M-C_4H_9]^+$ (99.2), (see Fig. 1.6).

Ultraviolet spectrum, λ_{max}^{EtOH} nm (log ϵ):

277 (4.47), 312 (4.39) (see Fig. 1.8)

3.5 DISCUSSION

The mass spectrum of DB-I furnished a molecular ion at m/z 428 which was also the base peak. This is consistent with the molecular formula $C_{24}H_{28}O_7$. The fragment at m/z 410 corresponds to $[M-H_2O]^+$ and was supported by the presence of a metastable ion at m/z 392.8. The intense peak at m/z 371 $[M-C_4H_9]^+$ indicates the loss of a butyl group from the molecular ion and was supported by the presence of a metastable ion at m/z 321.6. This is probably due to the loss of a side-chain from the structure of the rhodomyrtoxins by cleavage of the bond α to the carbonyl group. The peak at m/z 314 $[M-C_4H_9-C_4H_9]^+$ corresponds to the loss of two butyl groups from the molecular ion, and is consistent with the presence of two $-C(=O)-C_4H_9$ sidechains in the rhodomyrtoxins. The fragment at m/z 353 attributable to $[M-C_4H_9-H_2O]^+$ was also supported by the presence of a metastable ion at m/z 335.9. The mass

Fig. 1.3. Infrared spectrum of RL (ψ -rhodomyrtoxin)

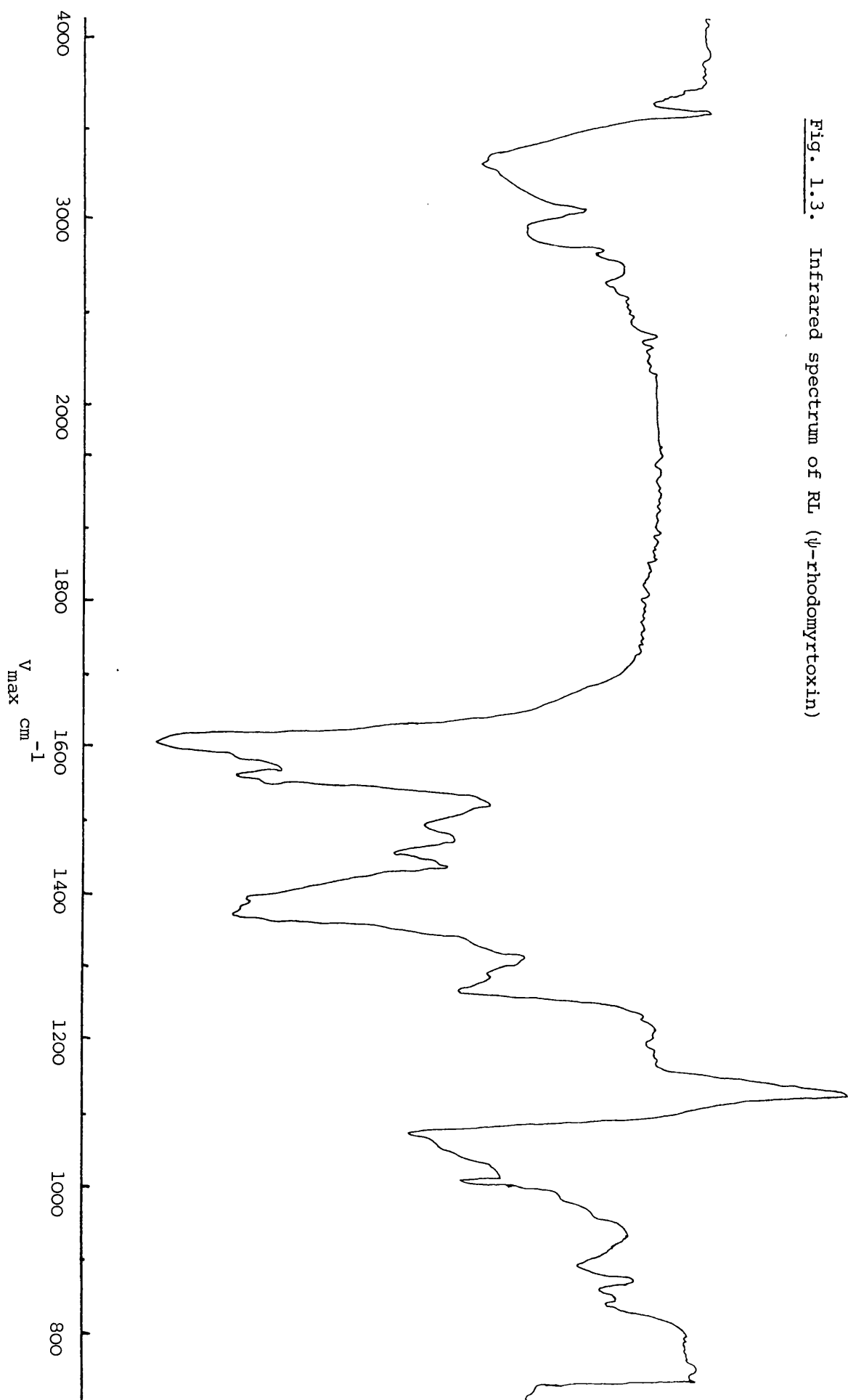


Fig. 1.4. Mass spectrum of DB-I (rhodomyrtxin-B)

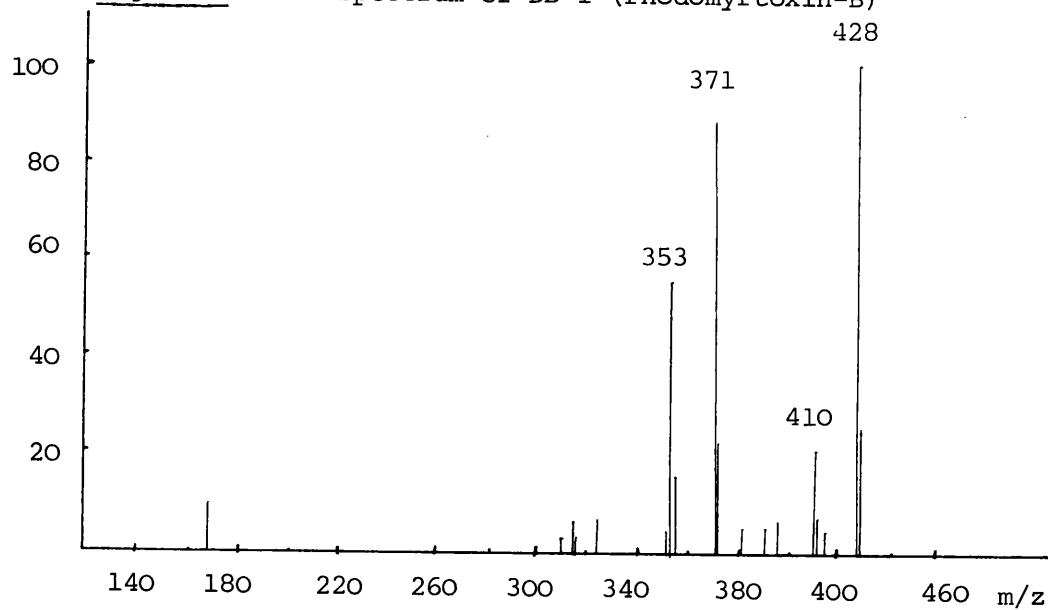


Fig. 1.5. Mass spectrum of DB-II (rhodomyrtxin-C)

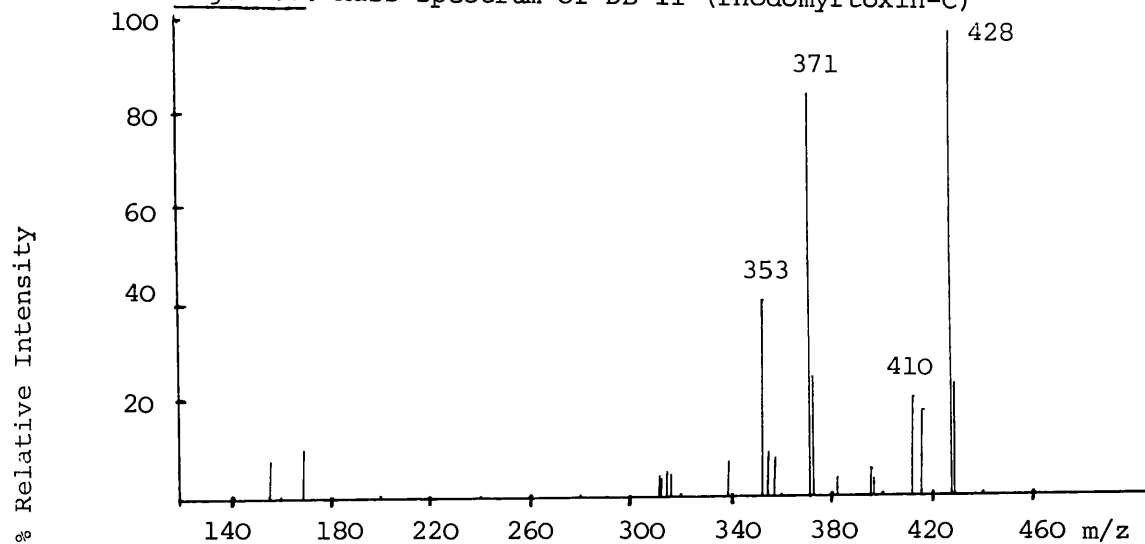
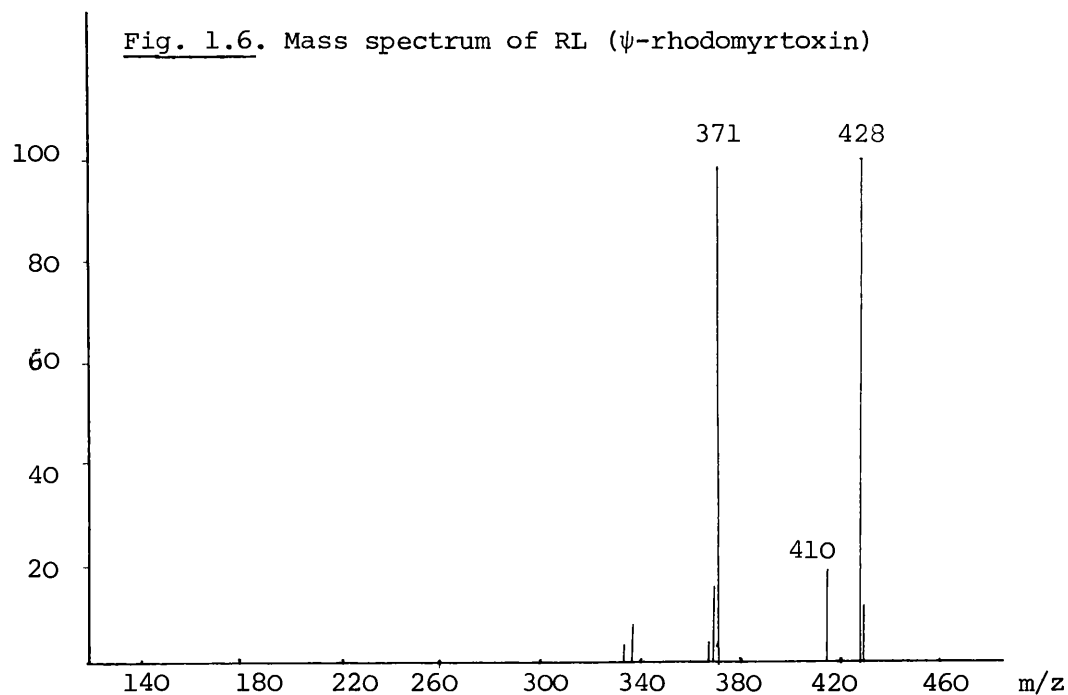


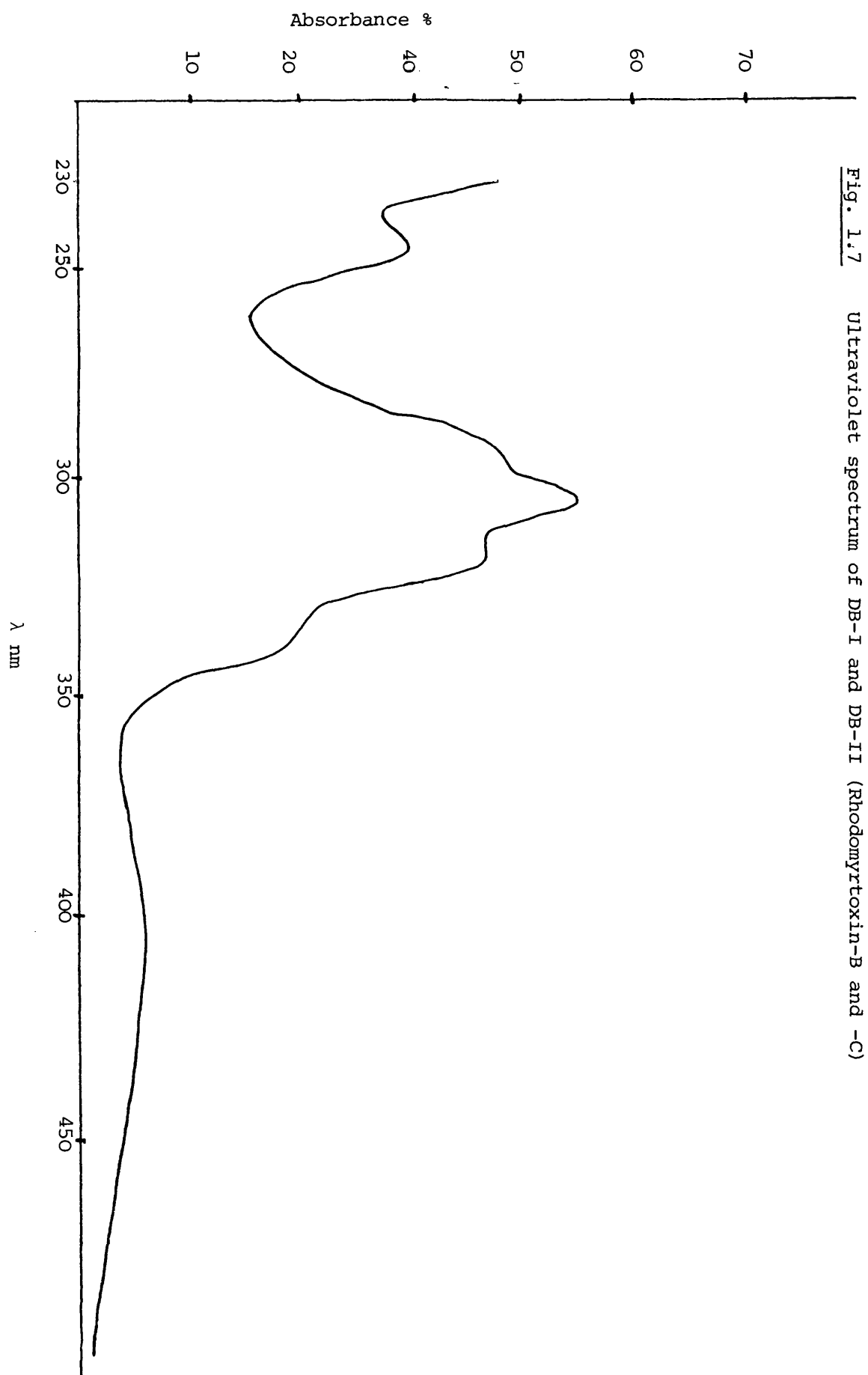
Fig. 1.6. Mass spectrum of RL (ψ -rhodomyrtxin)



spectra of DB-II and RL are identical to that of DB-I except for differences in the relative intensities of the peaks. The three compounds are clearly isomeric.

The ultraviolet spectrum of RL (λ_{max} 277 and 312 nm) was similar to that reported by Anderson *et al.*⁶ for ψ -rhodomyrtoxin whereas the spectra of DB-I and DB-II are identical (λ_{max} 234, 307 and 395 nm) and are similar to that reported by Trippett⁵ for rhodomyrtoxin. This observation is suggestive of the existence of similar chromophoric patterns in RL and ψ -rhodomyrtoxin, and in DB-I, DB-II and rhodomyrtoxin.

The ^1H -NMR spectral data on DB-II (Table 1.IV) is superficially similar to that of ψ -rhodomyrtoxin reported by Anderson *et al.*⁶. A three-proton doublet at δ 1.22 ($J = 6.8$ Hz) and a one-proton multiplet centred near δ 4.0 suggest the presence of the 2-methylbutanoyl moiety whilst doublets at δ 1.00 (6H, $J = 6.5$ Hz) and δ 3.10 (2H, $J = 7.0$ Hz) indicate the presence of a 3-methylbutanoyl moiety as in ψ -rhodomyrtoxin. However, a major difference was the absence of any hydroxyl proton signal near δ 4.0, the only hydroxyl protons being at δ 11.9 (2H, singlet) and δ 12.20-13.50 (2H, broad singlet). Anderson *et al.*⁶ referred peaks in this region to chelated hydroxy-protons, this assignment being supported by the work of Crombie *et al.*⁹ and Finnegan *et al.*¹⁰ on Coumarins from *Mammea americana*. Thus the ^1H -NMR suggests the structure (7) for DB-II in which all four hydroxy-protons may form internal hydrogen bonds with the oxo groups.



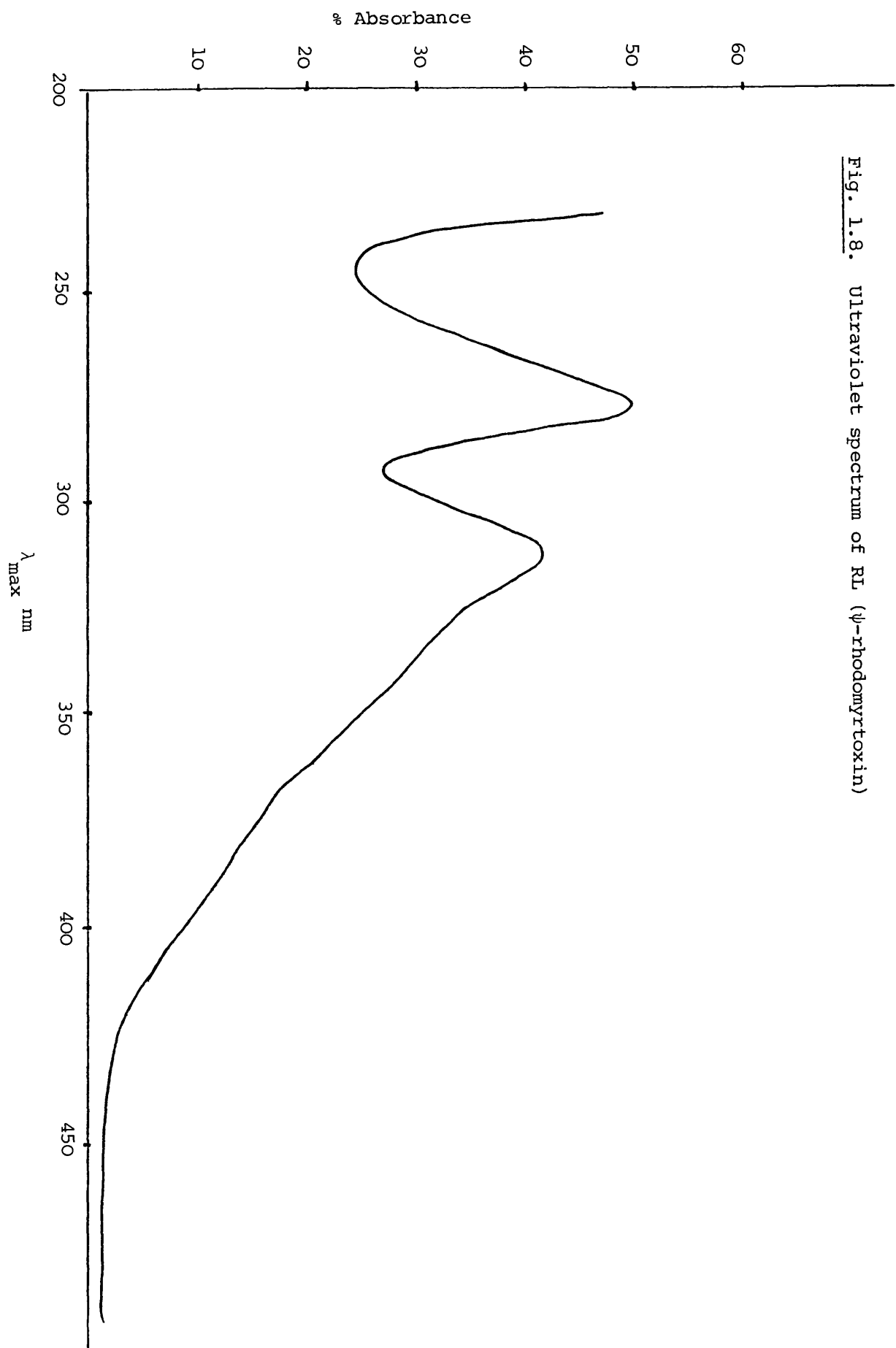


Fig. 1.8. Ultraviolet spectrum of RL (ψ -rhodomyrtxin)

Table 1.IV

footnotes

- a) 100 MHz, reference TMS
- b) Solvent CDCl₃; DMSO-d₆ (10:1)
- c) Solvent DMSO-d₆
- d) Accurate integration of peaks was not obtained with this compound.
- e) Numbering system as in Structure (7)

Table 1.IV $^1\text{H-NMR}^a$ chemical shifts (δ) for dibenzofurans^e isolated from *Rhodomyrtus macrocarpa*

Proton(s)	Rhodomyrtoxin B ^b (DB-I)	Rhodomyrtoxin C ^c (DB-II)	possible ψ -Rhodomyrtoxin ^c (RL) ^d
Ar-CH ₃	2.29 (6H, s)	2.28 (6H, s)	1.98 (s)
2'	3.97 (2H, m)	3.97 (1H, m)	3.46 (m)
3'	1.3-2.1 (4H, br.m)	1.3-2.1 (br.m)	1.36-1.92 (m)
4'	0.95 (6H, t)	0.95 (3H, t)	0.88 (t)
5'	1.22 (6H, d)	1.22 (3H, d)	1.22 (d)
2''	-	3.10 (2H, d)	3.16 (d)
3''	-	1.3-2.1 (br.m.)	1.36-1.92 (m)
4''	-		
5''	-	1.0 (6H, d)	1.0 (d)
-OH (1+9)	11.8 (2H, s)	11.9 (2H, s)	4.0-5.4 (br.s)
-OH (3+7)	12.0-13.0 (2H, br.s)	12.2-13.5 (br.s)	14.10 (s) 14.33 (s)

Fig. 1.9. ^1H -NMR spectrum of DB-I (Rhodomyrtoxin-B)

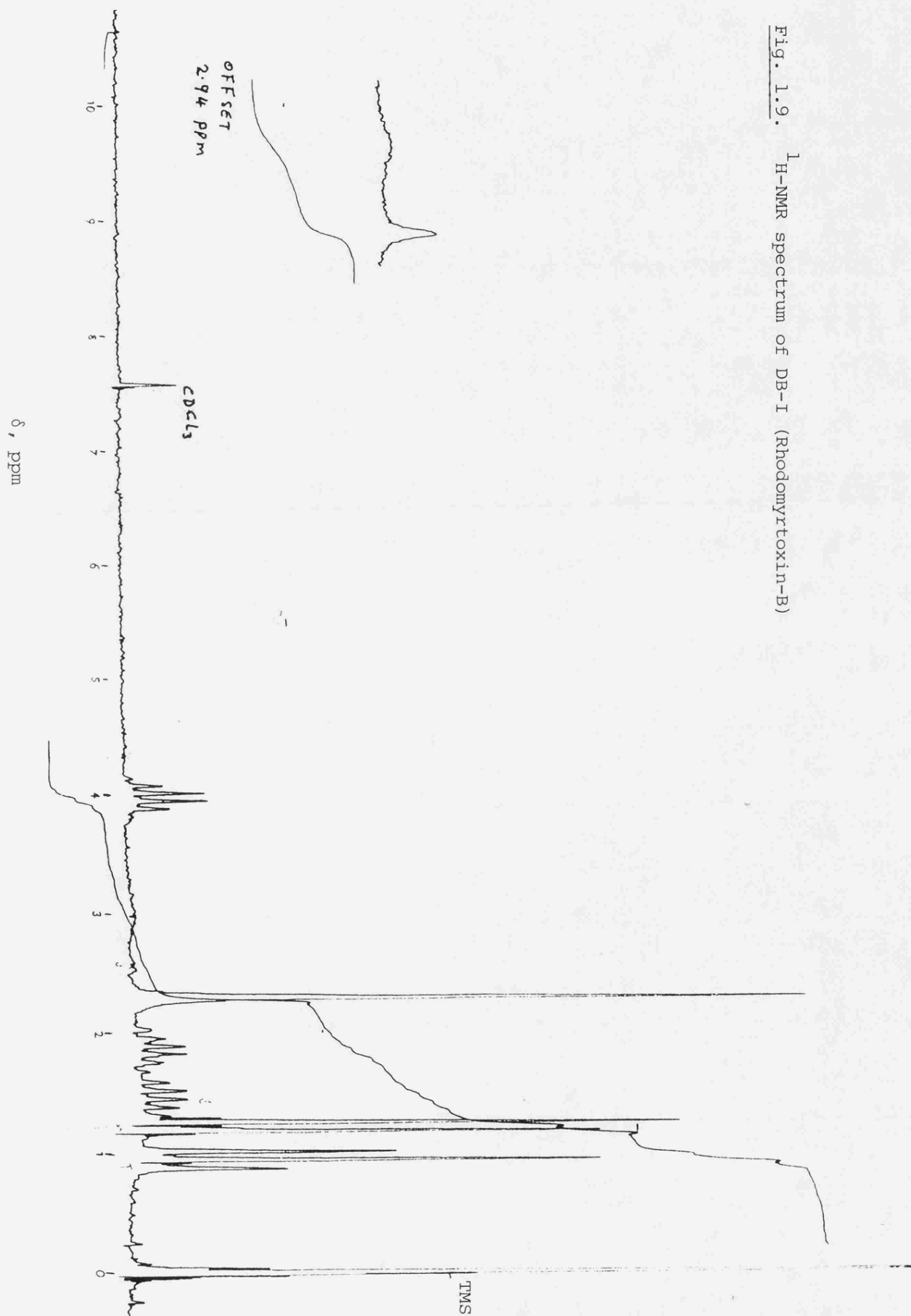
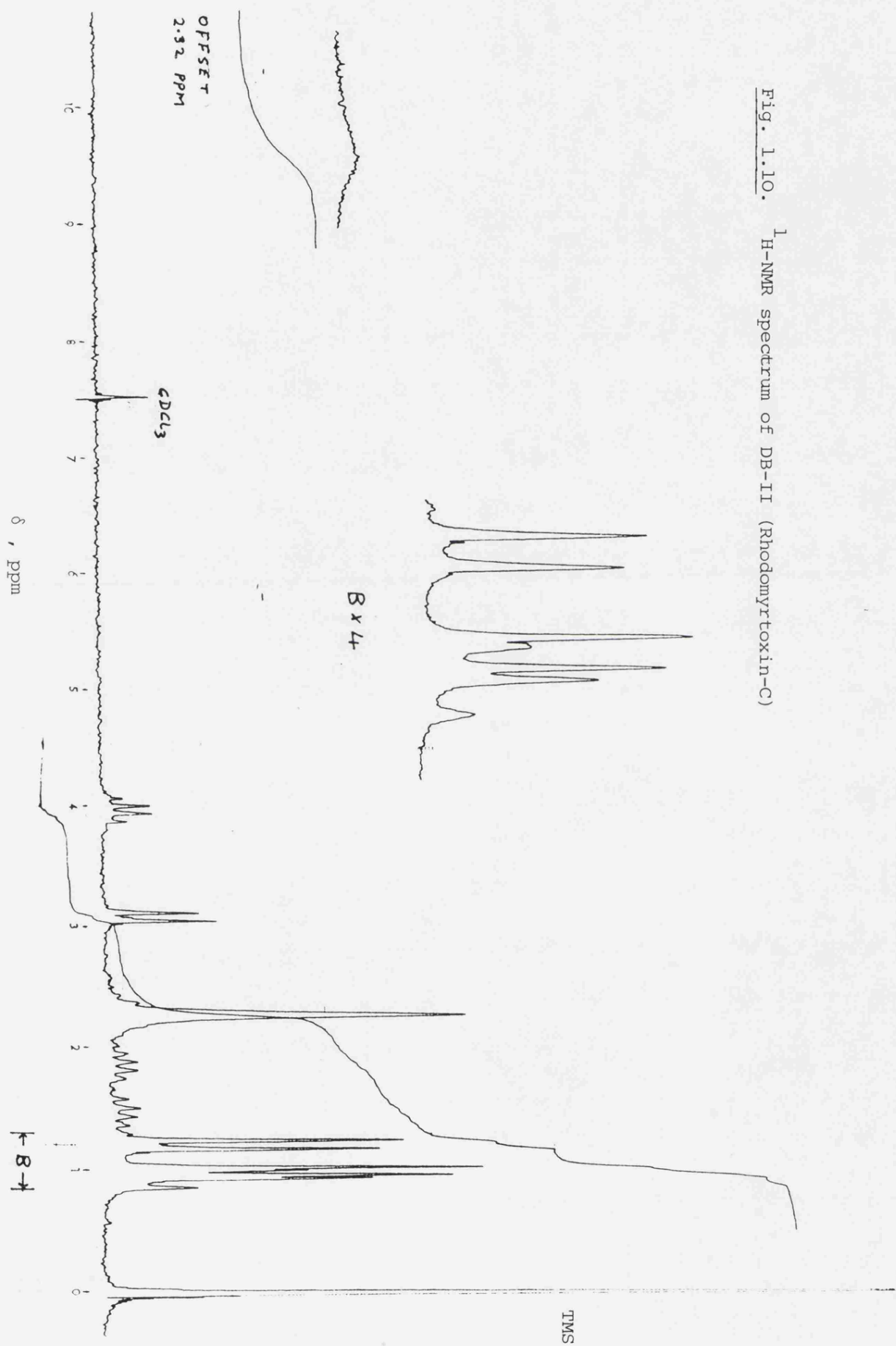


Fig. 1.10. ^1H -NMR spectrum of DB-II (Rhodomyrtoxin-C)



The ^1H -NMR spectral data on DB-I (Table 1.IV) clearly shows the absence of the 3-methylbutanoyl moiety. The two acyl moieties being 2-methylbutanoyl suggesting the symmetrical structure (8). The symmetrical nature of DB-I is supported by the ^{13}C -NMR data (Table 1.V) in which the number of signals seen correspond to exactly half the number of carbon atoms in the structure.

The most polar of the dibenzofurans, RL, was obtained in an insufficiently pure state for unambiguous NMR data to be obtained. However, the ^1H -NMR spectrum showed the presence of both 2-methylbutanoyl and 3-methylbutanoyl side chains, and a broad hydroxy-proton signal at $\delta 4.0-5.3$ integrating to two protons and exchanged on deuteration. In addition, the ultraviolet spectrum of this compound (Fig. 1.8) is similar to that of ψ -rhodomyrtoxin⁶ and unlike that of DB-I and DB-II (Fig 1.7). Thus this component may be identical to the ψ -rhodomyrtoxin (1) of Anderson *et al.*⁶ The TLC behaviour of RL compared with that of DB-I and DB-II (Table 1.III) may be rationalized by consideration of the position of the acyl substituent on the aromatic ring. In non-polar solvents (dichloroethane) DB-I and DB-II have fairly high R_f values whilst RL was hardly moved from the base line. But on addition of methanol to the mobile phase the increase in the R_f values of DB-I and DB-II was 0.05 - 0.11 whilst for RL the R_f value increased by about 0.45. With phenols, hydrogen-bonding of the hydroxyl group is an important sorption mechanism and intramolecular hydrogen-bonding of the hydroxyl group decreases

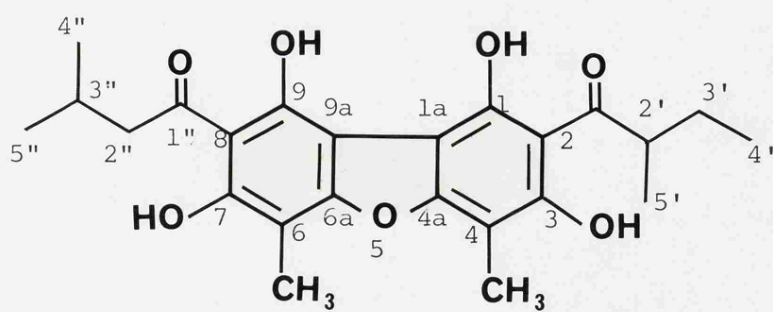
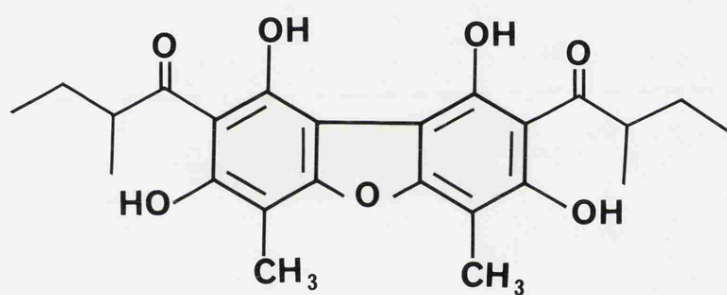
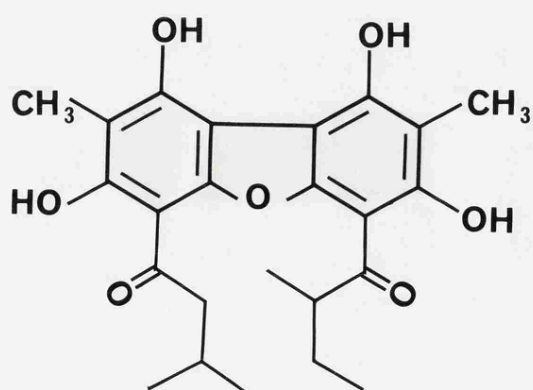
(Rhodomyrtxin-C) DB-II (7)(Rhodomyrtxin-B) DB-I (8)(ψ-Rhodomyrtxin) RL (1)

Table 1.V. footnotes

a. 22.5 MHz

b - e. as in Table 1.IV

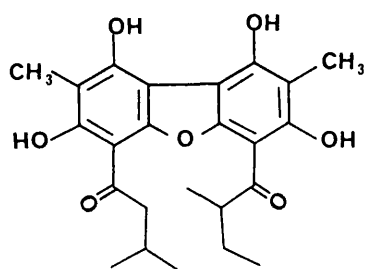
f. Off-resonance decoupled spectrum was not obtained for this compound.

Table 1.V. ^{13}C -NMR^a chemical shifts (δ) for dibenzofurans^e isolated from *Rhodomirtus macrocarpa*

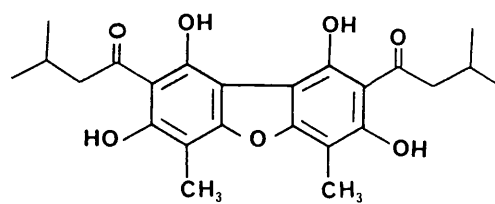
Carbon Atom	Rhodomirtoxin B ^b (DB-I)	Rhodomirtoxin C ^c (DB-II)	possible ψ -Rhodomirtoxin C,f (RL)
Ar-CH ₃	8.1 q	8.1 q	7.8
1			
3	159.6 s	159.6 s	163.4
4a	158.8 s	158.8 s	162.7
6a	152.2 s	152.2 s	152.4
7			
9			
1a			
2		106.7 s	108.1
4	106.4 s	106.4 s	105.2
6	104.0 s	104.0 s	99.3
8	100.7 s	100.7 s	98.5
9a			
1'	211 s	212.1 s	203.8 or 199.1
2'	45.2 d	46.0 d	49.6
3'	26.3 t	26.9 t	26.2 or 25.1
4'	11.7 q	11.9 q	11.5
5'	16.4 q	16.5 q	18.0
1''	-	207.3 s	203.8 or 199.1
2''	-	53.0 t	62.6
3''	-	24.9 d	26.2 or 25.1
4''	-		
5''	-	22.9 q	22.6

the sorption markedly.¹⁸ Thus the low R_f value of RL in dichloroethane is consistent with structure (1) for ψ -rhodomyrtxin in which two of the four hydroxyl groups are chelated and the other two are available for binding to adsorbent. The marked increase in the R_f value of RL in the presence of methanol would reflect competition between the phenolic -OH and that of methanol reducing the binding of ψ -rhodomyrtxin to the silica. Structures (7) and (8) for DB-II and DB-I respectively reflect two O,O-dihydroxy-carbonyl situations in which all the four hydroxy-groups are all able to participate in chelation with carbonyl groups though not both simultaneously. However the hydroxyl group not immediately involved in intramolecular hydrogen-bonding would be sterically hindered by the bulky acyl group. As a result the introduction of a hydroxylic solvent does not bring about a marked increase in their R_f values. It is possible that the difference between the R_f values of DB-I and DB-II is a reflection of the differences in steric hindrance produced by 2-methyl and 3-methyl butanoyl groups.

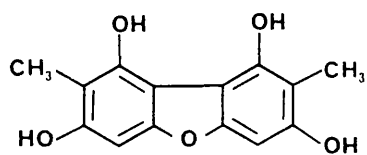
Anderson et al.⁶ reported structure (3) as the thermodynamically most stable degradation product of rhodomyrtxin and ψ -rhodomyrtxin. On this basis, and given that no rearrangement occurred during the degradation of ψ -rhodomyrtxin by base, structure (1) was assigned to ψ -rhodomyrtxin placing the acyl side-chains in the 4 and 6 positions, and structure (4) to isorhodomyrtxin, the product of boron trifluoride-catalyzed reaction between dideisovaleryl rhodomyrtxin and isovaleric acid. Since degradation of rhodomyrtxin was



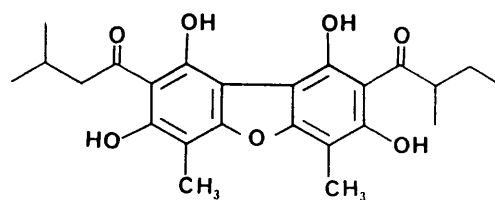
(1)



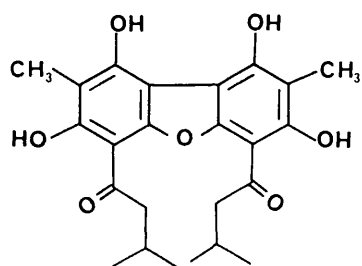
(6)



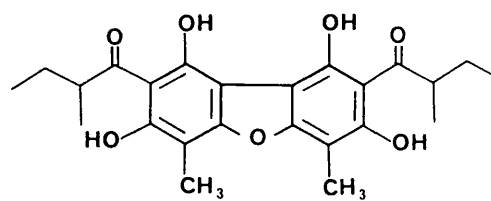
(3)



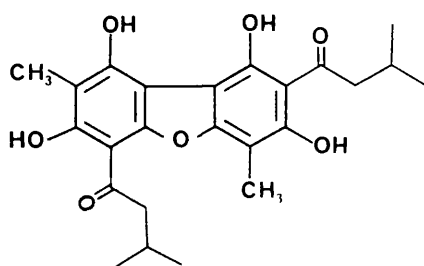
(7)



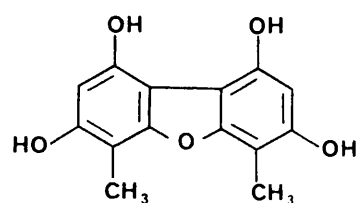
(4)



(8)



(5)



(9)

accompanied by rearrangement⁵, structures (5) or (6) were suggested for rhodomyrtoxin. Sargent *et al.*¹⁸ on the other hand have suggested structure (9), rather than structure (3) as the thermodynamically most stable of the degradation products of rhodomyrtoxin and ψ -rhodomyrtoxin, and cited evidence obtained by synthetic studies and X-ray diffraction in support of their proposal. Consequently they have suggested the revised structures (7) for ψ -rhodomyrtoxin and (6) for isorhodomyrtoxin, and (4) or (5) for rhodomyrtoxin. Following a successful synthesis of structure (5) they found that the physical data of this compound was different from that recorded for rhodomyrtoxin by Trippett⁵. They thus concluded that rhodomyrtoxin must have structure (4) in which the acyl substituents are in the 4 and 6 positions. Sargent *et al.*¹⁸ also synthesized structure (7) which they proposed for ψ -rhodomyrtoxin and discovered that it differed from authentic ψ -rhodomyrtoxin. As a result, they had to accept structure (1) proposed for ψ -rhodomyrtoxin by Anderson *et al.*⁶ as correct. However, according to data reported by Anderson *et al.*⁶ and Trippett⁵ rhodomyrtoxin and ψ -rhodomyrtoxin have different ultraviolet spectra (Sargent *et al.*¹⁸ did not report the ultraviolet spectra of their compounds) whereas compounds (1) and (4) might be expected to possess the same ultraviolet chromophore. In support of this, our compounds DB-I and DB-II (7 and 8) which differ only in the nature of the acyl groups and not in their positions had identical ultraviolet spectra. Thus the different ultraviolet spectra of rhodomyrtoxin and ψ -rhodomyrtoxin suggest that they also differ in the positions of their acyl side chains.

Assuming the correctness of their revised structure, (9) for the stable degradation product of rhodomyrtxin and ψ -rhodomyrtxin, they suggested that a rearrangement must have occurred during the degradation of ψ -rhodomyrtxin under basic conditions. The structure (7) which was wrongly proposed for ψ -rhodomyrtxin by Sargent *et al.*¹⁸ is the same as that assigned to one of the dibenzofurans (DB-II) isolated in this study. The spectral data on the synthesized (7) are in good agreement with the data (¹H-NMR, melting point, mass spectrum) on DB-II, and therefore provide additional evidence in support of structure (7) for DB-II. Since DB-II and DB-I have identical ultraviolet spectra, the o,o-dihydroxy-carbonyl situation in the two acyl substituents is also confirmed for DB-I and as such only structure (8) is tenable for DB-I. Further support for structure (6) for rhodomyrtxin and structure (1) for ψ -rhodomyrtxin was found in the ultraviolet spectral correlations between DB-I, DB-II and rhodomyrtxin, and between RL and ψ -rhodomyrtxin (Table 5). Indeed RL may be identical with ψ -rhodomyrtxin.

The exact constitution of isorhodomyrtxin is still doubtful. The ultraviolet spectral data on isorhodomyrtxin (Table 1.IV) is not consistent with either the solely o-hydroxy-carbonyl situation in structure (4) proposed by Anderson *et al.*⁶, or the solely o,o-dihydroxy-carbonyl situation in structure (6) proposed by Sargent *et al.*¹⁸. Thus the only likely alternative is structure (5) in which the two 3-methylbutanoyl side-chains are in positions 4 and 8. This proposal appears to be supported

Table 1.VI Ultraviolet spectra of dibenzofurans from

Rhodomyrtus macrocarpa

Compound	$\lambda_{\text{max}}^{\text{EtOH}}$	nm (log ϵ)
rhodomyrtoxin ⁵	234 (4.29),	296 (4.55), 307 (4.46), 395 (3.61)
isorhodomyrtoxin ⁵	234 (4.37), 280 (4.60),	293 (4.59), 307 (4.46), 395 (3.60)
ψ -rhodomyrtoxin ⁶	278 (4.45),	312 (4.38)
DB-I	234 (4.38)	295 (4.56), 307 (4.47), 395 (3.62)
DB-II	234 (4.38)	295 (4.56), 307 (4.47), 395 (3.62)
RL	277 (4.47)	312 (4.39)

by the complexity of the ultraviolet spectral data on isorhodomyrtoxin (Table 1.VI). However, structure (5) has been assigned to a compound synthesized by Sargent *et al.* Unfortunately, the ultraviolet spectral data on this compound was not reported but other physical data (melting point 209 - 211°C; the tetraacetate was a thick oil) are not in agreement with the data recorded by Trippett⁵ for isorhodomyrtoxin (melting point 231 - 234°C; tetraacetate 190-191°C). So the riddle about the actual constitution of isorhodomyrtoxin remains unresolved.

DB-I and DB-II are new natural products and we have designated them Rhodomyrtoxin-B and Rhodomyrtoxin-C respectively.

On the basis of melting point, infrared, mass spectral,

ultraviolet and NMR evidence, structure (6) is proposed for rhodomyrtxin, structure (7) for Rhodomyrtxin-C, structure (8) for Rhodomyrtxin-B and structure (1) is confirmed for ψ -rhodomyrtxin.

3.6 FRACTIONATION OF THE RIPE FRUIT EXTRACT

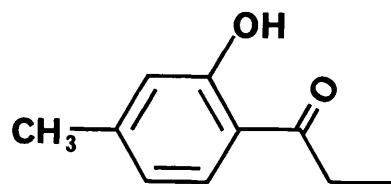
The ripe fruit extract R_B (0.18 g) was fractionated by repeated column chromatography on silica gel eluted with chloroform and chloroform-methanol mixtures. The chloroform fraction yielded trace quantities of a component with similar chromatographic properties to DB (R_f 0.58, Si gel TLC $CHCl_3$ -MeOH, 4:1). Later fractions eluted with chloroform-methanol mixtures gave one prominent yellow spot (R_f 0.29, Si gel TLC $CHCl_3$ -MeOH, 4:1) and traces of more strongly adsorbed components. This could not be purified further because of the small size of the sample (about 4 mg). However, detailed TLC comparison with RL gave a strong indication that the two were identical. The mass spectrum gave a molecular ion at m/z 428 which was also the base peak, as well as other fragments found in the mass spectrum of the dibenzofurans isolated from the unripe fruit extract.

3.7 DEUTERIUM EXCHANGE

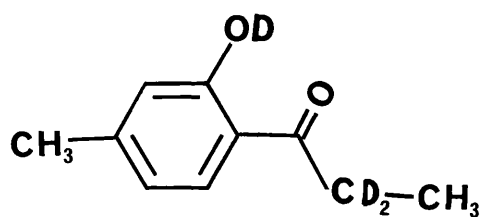
Hydroxy-protons may be exchanged for deuterium atoms merely by shaking with D_2O whilst protons α to carbonyl groups can be deuteriated under basic conditions with comparative ease¹⁶. Thus under basic conditions the structure of Rhodomyrtosin-B (8) would be expected to possess six exchangeable protons, Rhodomyrtosin-C (7), seven, and Trippett's rhodomyrtosin (6), eight. The possible use of mass spectrometry of such deuteriated compounds as a means of determining the different isomers of rhodomyrtosin differing in the nature of their acyl substituents was investigated. It was envisaged that a mixture containing these three isomers will after deuterium exchange give a mass spectrum with molecular ions at m/z 434, 435 and 436 corresponding to deuteriated derivatives of Rhodomyrtosin-B, Rhodomyrtosin-C and rhodomyrtosin respectively.

2-Hydroxy-4-methylpropiophenone (10) possesses one phenolic hydroxyl group and two protons α to a carbonyl group and was therefore chosen as a suitable model compound. In the 1H -NMR spectrum of (10) (Fig. 1.11) the three-proton triplet at $\delta 1.16$ ($J = 8.0$ Hz) was attributed to the side chain methyl group coupled to the methylene group α to a carbonyl group and giving rise to the two-proton quartet ($J = 8.0$ Hz) at $\delta 2.90$. The three-proton singlet at $\delta 2.28$ is attributable to the aromatic methyl signal, and the downfield signals at $\delta 7.56$ (1H, d) and $\delta 6.68$ (2H, m) are due to the aromatic protons. The hydroxy-proton resonated further downfield

at δ 12.36 indicative of a chelated hydroxy-proton as a result of the o-hydroxy-carbonyl situation. The mass spectrum furnished



(10)



(11)

Table 1.VII ^1H NMR chemical shifts (δ) for (10) and (11) in CDCl_3
(internal reference TMS)

Protons	(10)	(11)
Ar-CH ₃	2.28 (3H, s)	2.28 (3H, s)
3	6.68 (2H, m)	6.68 (2H, m)
5		
6	7.56 (1H, d)	7.56 (1H, d)
2'	2.90 (2H, q)	-
3'	1.16 (3H, t)	1.16 (3H, s)
-OH	12.36 (1H, s)	-

a molecular ion at m/z 164. After the exchange the deuteriated derivative (11) showed a molecular ion at m/z 167 which indicated that three protons in the molecule have been exchanged for deuterium atoms. The ^1H -NMR spectrum (Fig. 1.12) did not contain any signal at $\delta 2.90$ due to the methylene protons α to the carbonyl group ($-\overset{\text{O}}{\underset{\text{||}}{\text{C}}}\cdot\text{CH}_2$), and the one-proton singlet at $\delta 12.36$ due to chelated hydroxy-proton in the parent compound was also missing. The three-proton triplet at $\delta 1.16$ due to the aliphatic methyl group coupled to a methylene group in the parent compound was reduced to a sharp three-proton singlet in the deuteriated compound. These data confirmed the successful deuterium exchange of the three exchangeable protons in 2-hydroxy-4-methylpropiophenone. However, an attempt at deuterium exchange under basic conditions with DB proved unsuccessful. The highest peak in the mass spectrum of DB after the attempted deuteration was at m/z 318 corresponding to the molecular weight of dideisovaleryl rhodomyrtxin plus 4 atomic mass units. This could be attributed to the sensitivity of the rhodomyrtxins under alkaline conditions^{5,6}, which must have resulted in degradation of the molecule. Thus it was not possible to employ deuteration under basic conditions as a facile method of detecting the isomers of rhodomyrtxin differing in the nature of their acyl substituents when they occur in a mixture.

Fig. 1.11 ¹H-NMR spectrum of 2-hydroxy-4-methylpropionophenone (10)

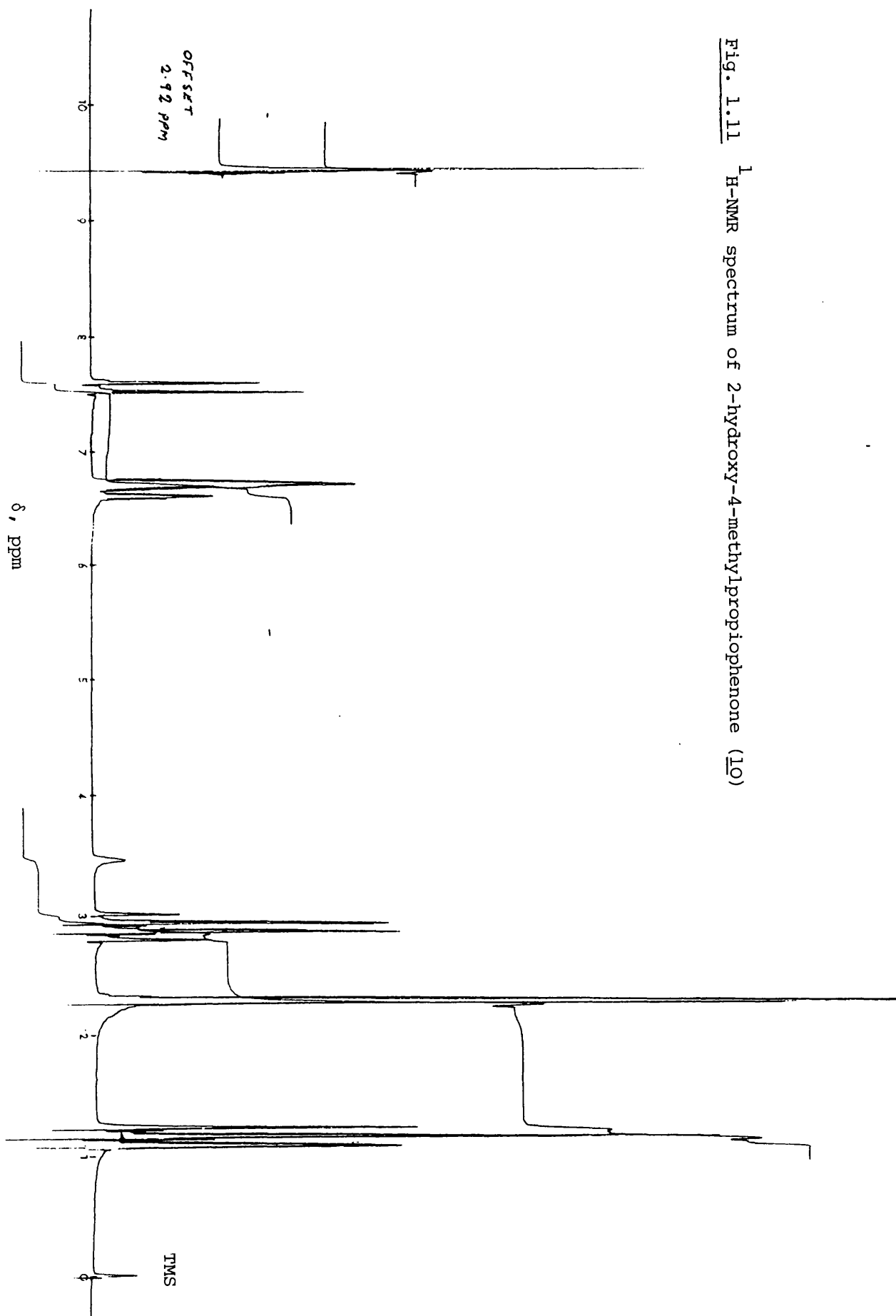
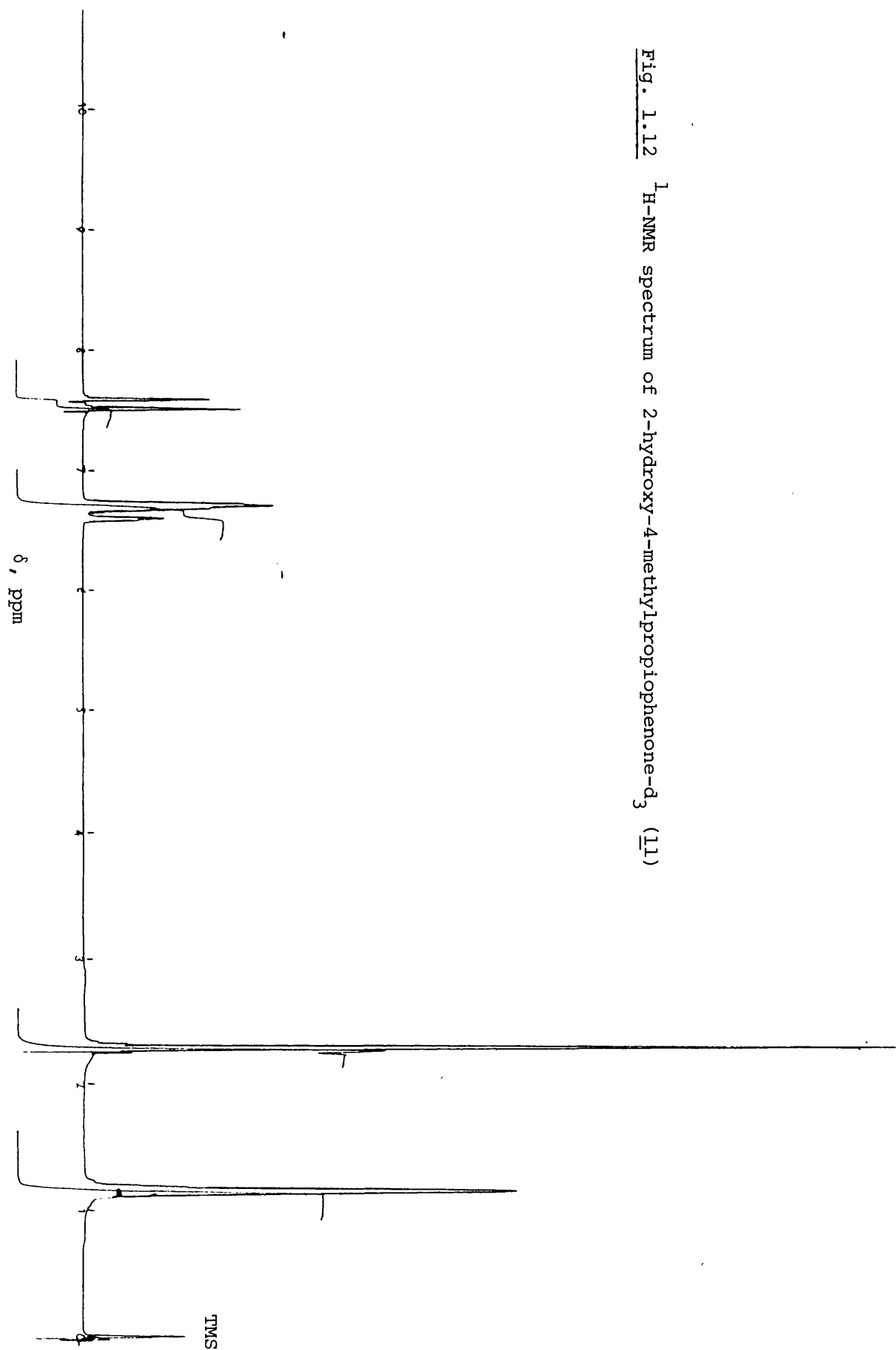


Fig. 1.12 ^1H -NMR spectrum of 2-hydroxy-4-methylpropioophenone- d_3 (11)



3.8 HIGH PERFORMANCE LIQUID CHROMATOGRAPHY (HPLC)

Straight phase HPLC on Lichrosorb Si 60 of the mixed crystalline dibenzofurans (DB) from *Rhodomyrtus macrocarpa* using the different eluents stated in the experimental section did not achieve adequate resolution of the mixture. With eluents containing no methanol the sample was excessively retained in the column. Eluents containing methanol, even as low as 0.5 per cent, eluted the mixture as a single peak with extensive tailing. In reversed phase HPLC on Spherisorb ODS S5 with methanol as the eluent, the mixture was again eluted as a single peak. A lower percentage of methanol in water (65 per cent) gave three poorly resolved peaks, and with less than 65 percent of methanol in water the sample was retained in the injection valve implying that the sample was not sufficiently soluble in the mobile phase. Acetonitrile-water mixtures gave an improved separation. 40 percent acetonitrile in water at a flow rate of 1 ml per min. eluted the mixture as three distinct peaks but these were not well resolved at the baseline. A good resolution was eventually achieved with tetrahydrofuran (THF)-water mixtures. Using a solution of the sample made up in THF-water (35:65) and eluting with the same solvent system at a flow rate of 0.55 - 0.80 ml. per min., the mixture was eluted as three well-resolved peaks with k' values of 2.02, 2.73 and 3.72, and peak area ratios of 2:18:80 respectively (Table 1.VIII). Injection of pure

Table 1.VIII Reversed phase HPLC analysis of DB

Solvent system: THF-water (35:65)

Column: Spherisorb ODS S5 PS 5 μ m 100 mm x 4 mm i.d.

Flow rate (ml/min)	t_R (min)	t_O (min)	κ' $\frac{t_R - t_O}{t_O}$	$W_{1/2}$ (min)	Peak height a (mm)	Peak area (A) $W_{1/2} \times a$ (mm ²)	$\frac{A}{V_A} \times 100$
0.56	42.0	14.0	2.00	5.0	2.5	12.5	1.5
	52.0	14.0	2.71	4.5	32	144.0	17.8
	66.0	14.0	3.71	5.5	119	654.5	80.7
0.61	41.0	13.5	2.02	5.0	3.0	15.0	2.1
	50.5	13.5	2.73	4.0	30.5	122.0	17.5
	63.5	13.5	3.72	5.3	107.0	561.8	80.4

compounds showed that peaks of κ' values of 2.73 and 3.72 were Rhodomyrtoxin-C and Rhodomyrtoxin-B respectively.

Table 1.IX Reversed phase HPLC analysis of Rhodomyrtoxin-B and -C

Chromatographic conditions as in Table 1.VIII.

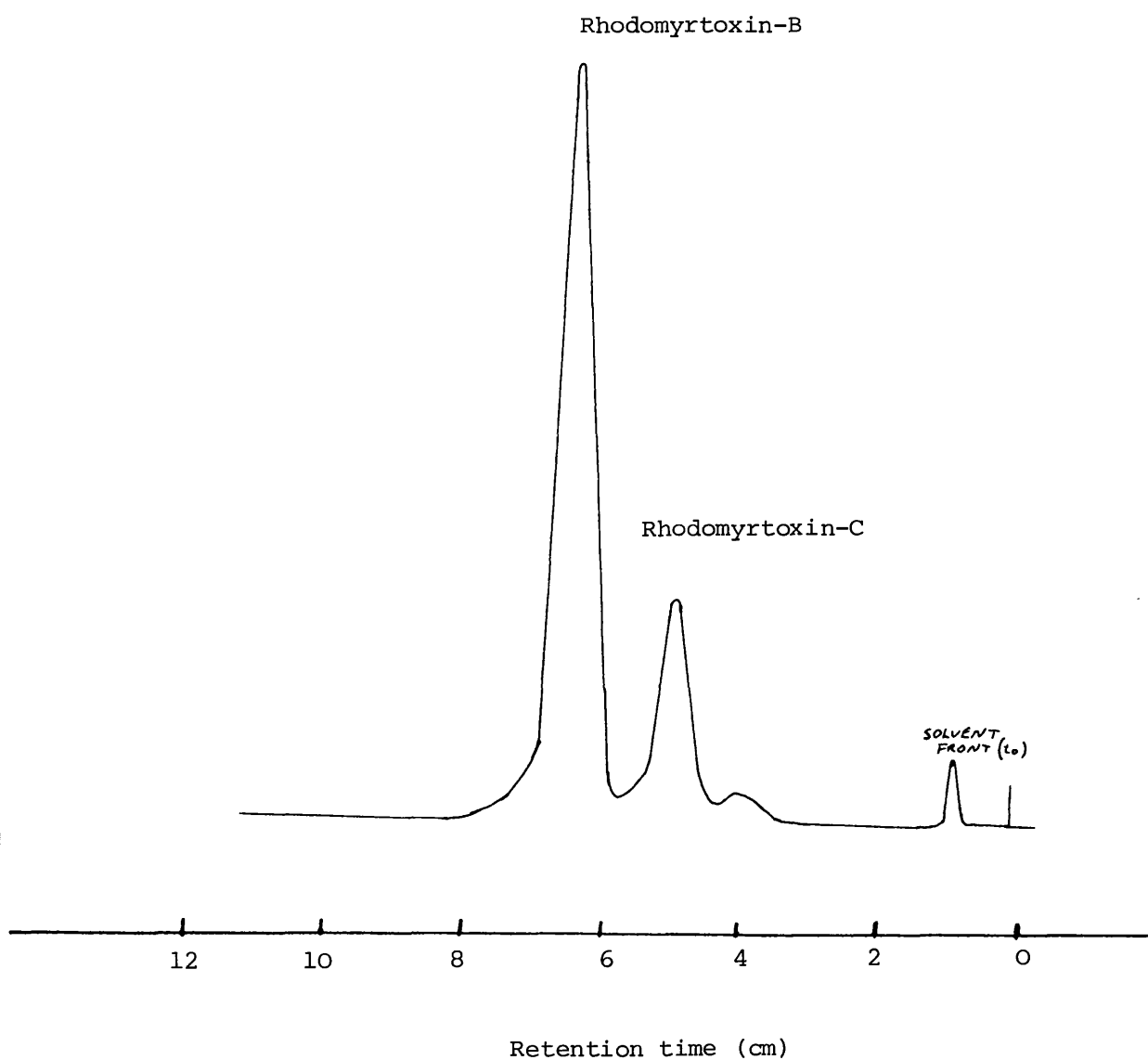
Compound	Flow rate (mls/min)	t_R (mm)	t_o (mm)	κ' $\frac{t_R - t_o}{t_o}$
Rhodomyrtoxin-C	0.62	37.5	10.0	2.74
Rhodomyrtoxin-B	0.60	64.0	13.5	3.72

In reversed phase partition chromatography the more polar compounds exhibit the greater mobility because of their greater affinity for the polar mobile phase. This contrasts with adsorption chromatography in which the more polar substances are more strongly retained by the adsorbent and consequently show the lower R_f values. The compound RL was more strongly retained than Rhodomyrtoxin-B and -C on silica gel TLC as a direct consequence of the unchelated hydroxyl groups which are available for binding to adsorbent. RL being more polar will be expected to exhibit a greater affinity for the polar mobile phase and will thus have a smaller κ' value than Rhodomyrtoxins B and C. The minor peak (2 percent) with a κ' value of 2.02 could possibly be some of RL that co-

Fig. 1.13 Reversed phase HPLC elution chromatogram of DB

Column: Spherisorb S5 ODS

Mobile phase: THF-water (35:65)



crystallized with the mixture in DB or some other isomer of rhodomyrtoxin more polar than Rhodomyrtoxins B and C. The mixture DB is therefore composed of 80 percent Rhodomyrtoxin-B, 18 percent of Rhodomyrtoxin-C and 2 percent of a more polar isomer.

Chemical investigation into the constituents of *Rhodomyrtus macrocarpa* has resulted in the isolation of several different dibenzofurans. Trippett⁵ first examined the fruits and isolated rhodomyrtoxin, whilst a second examination by Anderson et al.⁶ did not yield any rhodomyrtoxin but another isomer, ψ -rhodomyrtoxin. The present study has afforded two dibenzofurans that have not been previously isolated in addition to smaller quantities of a third component which is possibly ψ -rhodomyrtoxin. These differences may be linked with geographical or seasonal variation, level of maturity of the fruit or the existence of different chemical races of *Rhodomyrtus macrocarpa*. These questions could be resolved by an extensive investigation involving fruits collected from different locations at different times of the year and at different stages of maturity. Such a study would require a fast and efficient analytical method. The HPLC system described here offers a direct, rapid and sensitive approach to both qualitative and quantitative analysis of the dibenzofurans from *Rhodomyrtus macrocarpa*. The complete absence of chemical pretreatment significantly reduces possible problems of artifact formation.

3.9 ANALYTICAL DATA ON RH

RH was recrystallized from methanol-chloroform as greyish-white flakes, melting point $279 - 282^{\circ}\text{C}$. The infrared spectrum is shown in Fig. 1.14.

$^1\text{H-NMR}$ (100 MHz) in CDCl_3 (δ , ppm) with TMS as internal standard.

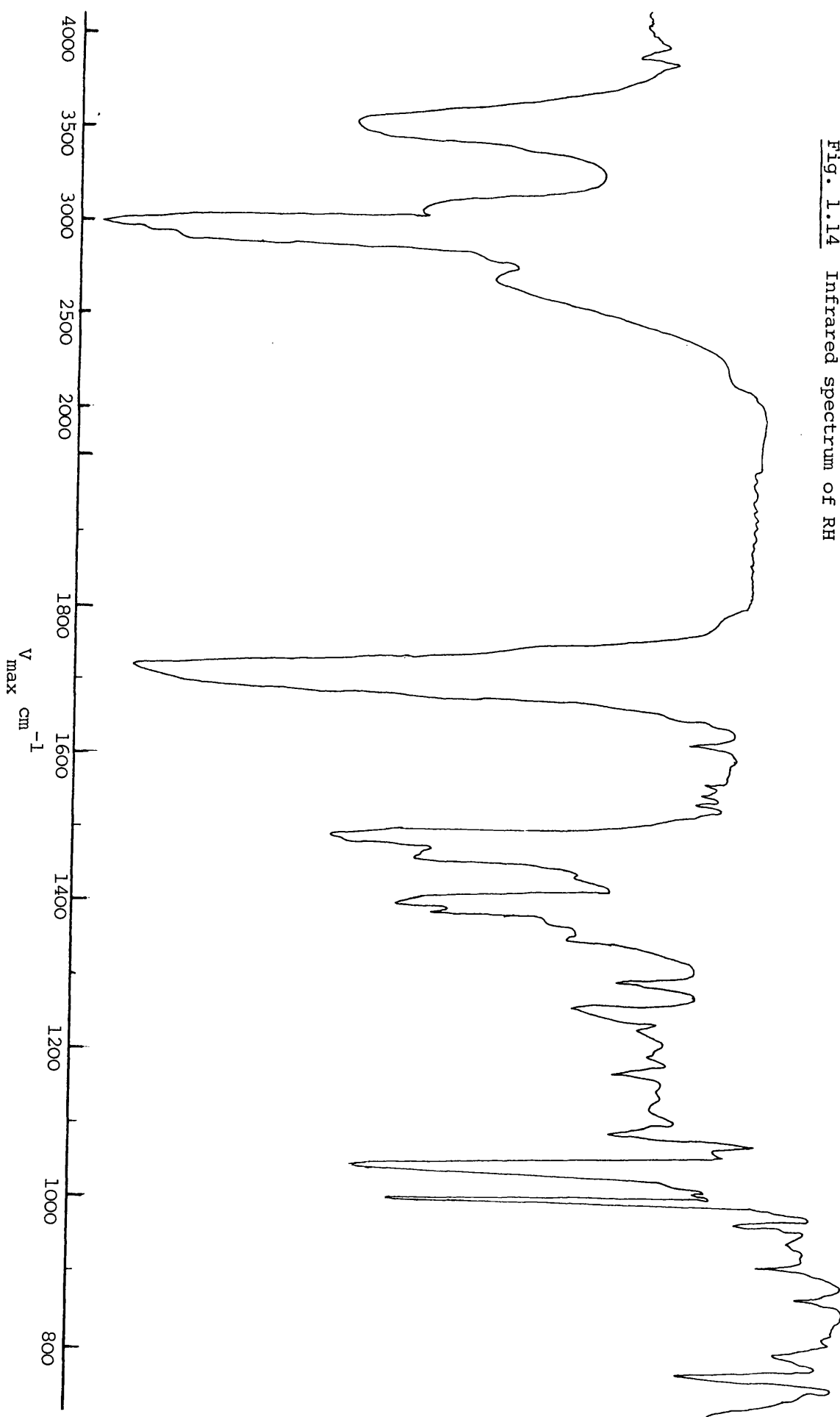
δ 1.24 (3H, s), 1.12 (3H, s), 0.97 (3H, s) 0.87-0.91 (6H), 0.73-0.76 (6H), 3.22 (1H, m), 5.24 (1H, m)

Mass spectrum (E.I.M.S.) in Fig. 1.15.

3.10 CHARACTERISATION OF RH

The compound, RH (R_f 0.82, Si gel TLC, CHCl_3 -MeOH, 4:1) was recrystallized from methanol containing a small amount of chloroform to give greyish-white flakes (8 mg), melting point $279-282^{\circ}\text{C}$. The infrared spectrum exhibited a broad band of moderate intensity at 3480 cm^{-1} indicative of the presence of hydroxyl group. Another broad band at 3080 cm^{-1} is suggestive of a carboxylic hydroxyl group. The presence of a carboxyl group was further indicated by the strong carbonyl absorption at 1715 cm^{-1} . The electron impact mass spectrum at 70 eV furnished a molecular ion at m/z 456. A very characteristic feature of the mass spectrum was provided by the ion at m/z 248 representing the base peak. A molecular weight of 456 is in agreement

Fig. 1.14 Infrared spectrum of RH

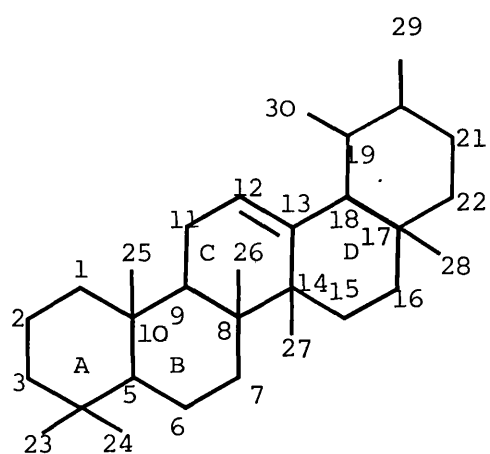


with the molecular formula $C_{30}H_{48}O_3$ which together with the infrared data suggests a monohydroxyl pentacyclic monounsaturated triterpene acid. The presence of a single trisubstituted double bond in the molecule was indicated by the 1H -NMR spectrum which showed resonance for one vinylic proton at $\delta 5.24$.

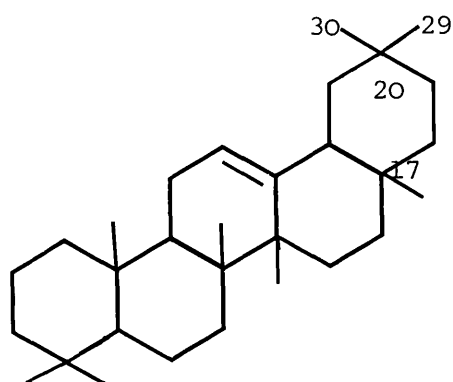
The most common naturally occurring pentacyclic triterpenes are members of the α -amyrin (such as Δ^{12} -ursene,⁽¹²⁾) or β -amyrin (such as Δ^{12} -oleanene, ⁽¹³⁾) series¹¹. These two series are characterised by the presence of a Δ^{12} double bond. This feature has proved recognizable by mass spectrometry since the molecular ion undergoes the equivalent of a retro-Diels-Alder fragmentation to give a very characteristic peak due to ion type 'A',¹¹ (Fig. 1.15). In the absence of substituents which constitute an addition to the basic skeleton, ion 'A' will occur at m/z 218. The mass spectra of a considerable number of triterpenes of the α - and β -amyrin series containing a variety of nuclear substituents have been measured by Budzikiewicz et al.¹², and all exhibit a strong peak corresponding to this process.

Thus, this peak has proved to be of great utility as a mass spectrometric criterion for a Δ^{12} -double bond in the structure elucidation of triterpenoid acids and derivatives¹³.

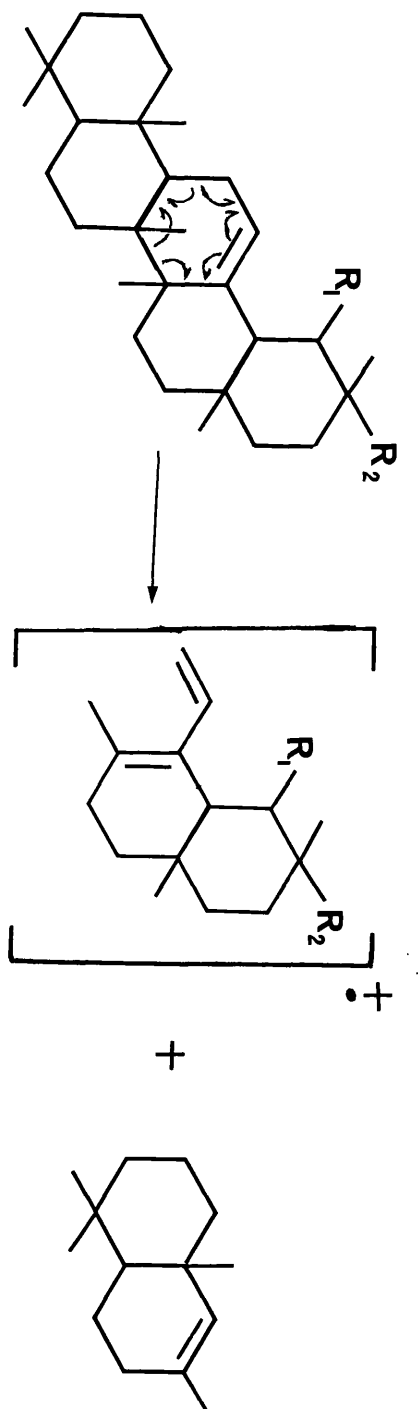
The occurrence of the base peak at m/z 248 in the mass



(12)



(13)

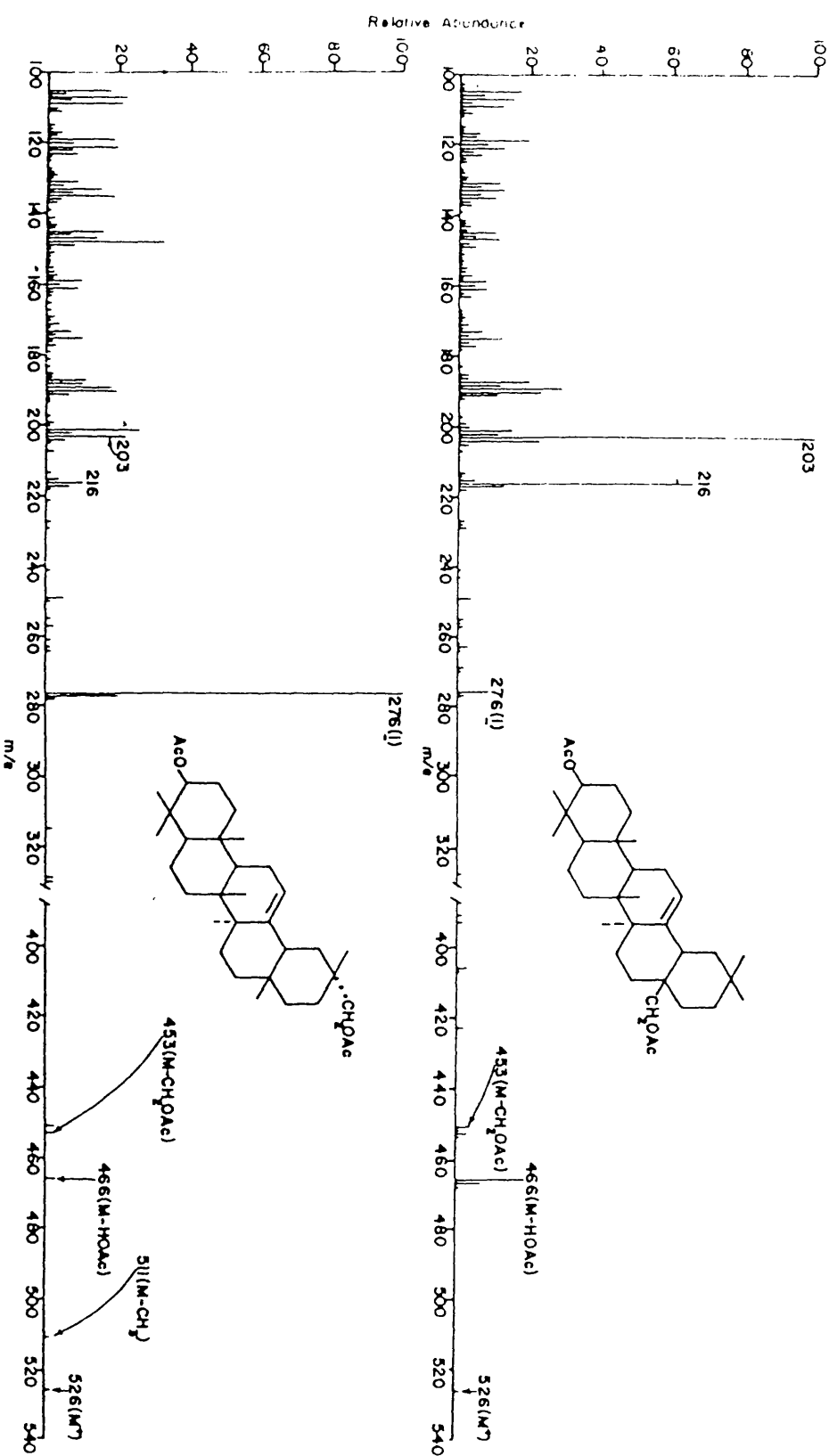


A

Fig. 1.15 R_1 or $R_2 = H$ The other being CH_3

spectrum of RH corresponding to the retro-Diels-Alder fragment of type 'A' is a strong indication that the compound is a pentacyclic triterpenoid acid with a Δ^{12} -double bond and a carboxyl group replacing one of the methyl groups attached to rings D and E (12 and 13). The further fragmentation of the retro-Diels-Alder fragment is also significant. The extent to which this further fragmentation occurs is dependent on the nuclear position of the expelled substituent^{11,12,13}. In general the loss of angular substituents ($-\text{CH}_3$, $-\text{COOH}$, $-\text{CH}_2\text{OAc}$, $-\text{COOCH}_3$) from C-17 is much more pronounced than from C-20. This point is well illustrated by the mass spectra of erythriodiol diacetate and the isomeric diacetate (Fig. 1.16)¹¹. For both compounds the retro-Diels-Alder fragment (ion type 'A') occurs at m/z 276 but in the case of erythriodiol diacetate ($-\text{CH}_2\text{OAc}$ at C-17) further expulsion of acetic acid or a $-\text{CH}_2\text{OAc}$ radical is extremely facile and manifests itself in the abundant ions at m/z 216 and m/z 203 (base peak) respectively. In the isomer with the $-\text{CH}_2\text{OAc}$ group at C-20 the loss of acetic acid or $-\text{CH}_2\text{OAc}$ radical from the retro-Diels-Alder fragment occur to a much smaller degree, and hence m/z 276 (ion type 'A') is much more pronounced and represents the base peak. There is also a peak corresponding to the loss of 15 atomic mass units (loss of C-17 methyl group) from the ion type 'A' while no such peak exists in erythriodiol diacetate. The applicability of this type of argument to carboxyl substituents is supported by the mass spectrum of oleanolic acid¹⁹,

Fig. 1.16.



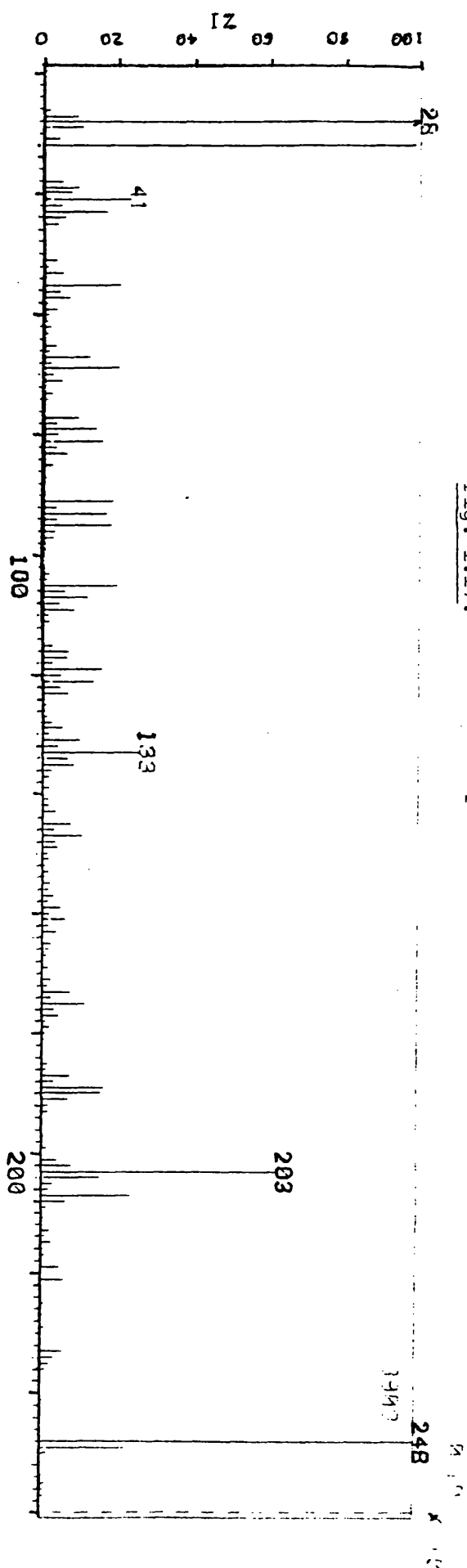
[β -hydroxyolean-12-en-28-oic acid (14)] which furnished a molecular ion at m/z 456 and base peak at m/z 203 (retro-Diels-Alder fragment - COOH). In the light of the above, the fragmentation pattern exhibited in the mass spectrum of RH is very informative. The base peak occurs at m/z 248 corresponding to the retro-Diels-Alder fragmentation of ring C (Fig. 1.18) to give ion type 'A'. This confirmed the presence of the carboxyl group in rings D/E, but suggested that it is unlikely to be at C-17. This was further supported by the presence of peaks at m/z 233 $(248-CH_3)^+$ and m/z 423 $(M-H_2O-CH_3)^+$. Thus the possibility of a carboxyl group at C-17 was ruled out.

The 1H -NMR spectrum of RH indicated the presence of seven tertiary methyl groups. The absence of any secondary methyl group ruled out the possibility of it being an α -amyrin derivative. Hence, RH is most likely to belong to the β -amyrin series (13) with the carboxyl function at C-20 (15).

The 1H -NMR of RH was rather 'noisy' because of the small sample size but the signals for the seven tertiary methyl groups were shown very clearly - δ 1.24 (3H, s), 1.12 (3H, s), 0.97 (3H, s), 0.73-0.76 (6H, two poorly resolved singlets), 0.87-0.91 (6H, two poorly resolved singlets). The one-proton multiplet around δ 3.22 is assignable to $>CHOH$ as expected for the urs-12-ene or olean-12-ene skeleton with

Fig. 1.17.

Mass spectrum (70 eV E.I.) of RH



Relative Abundance

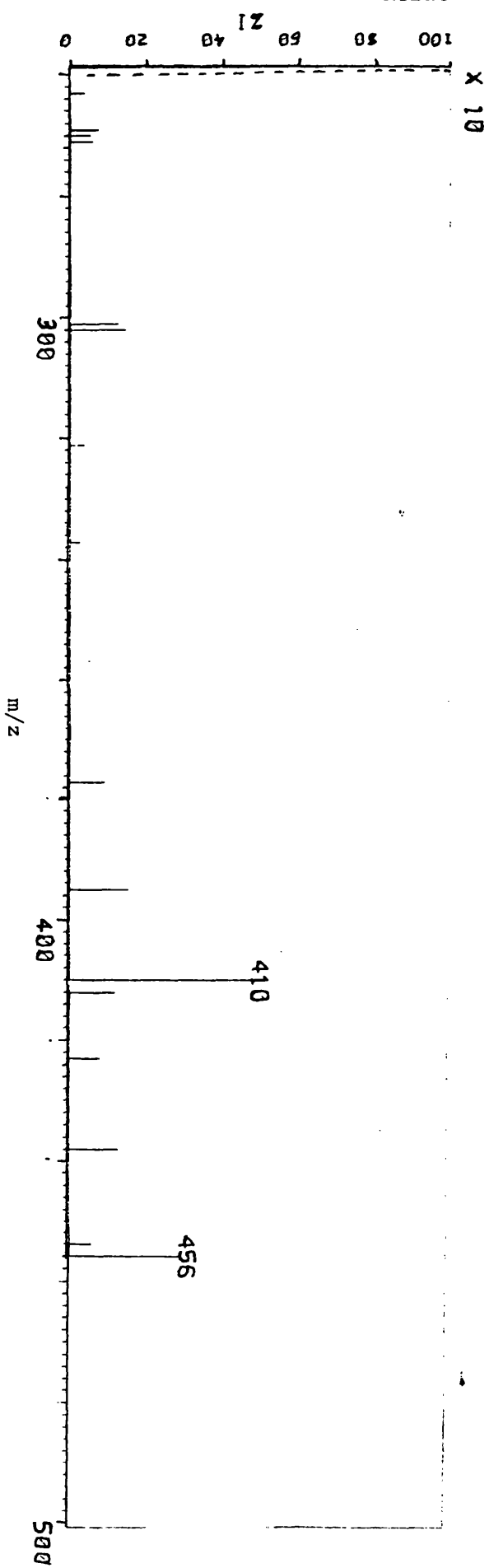
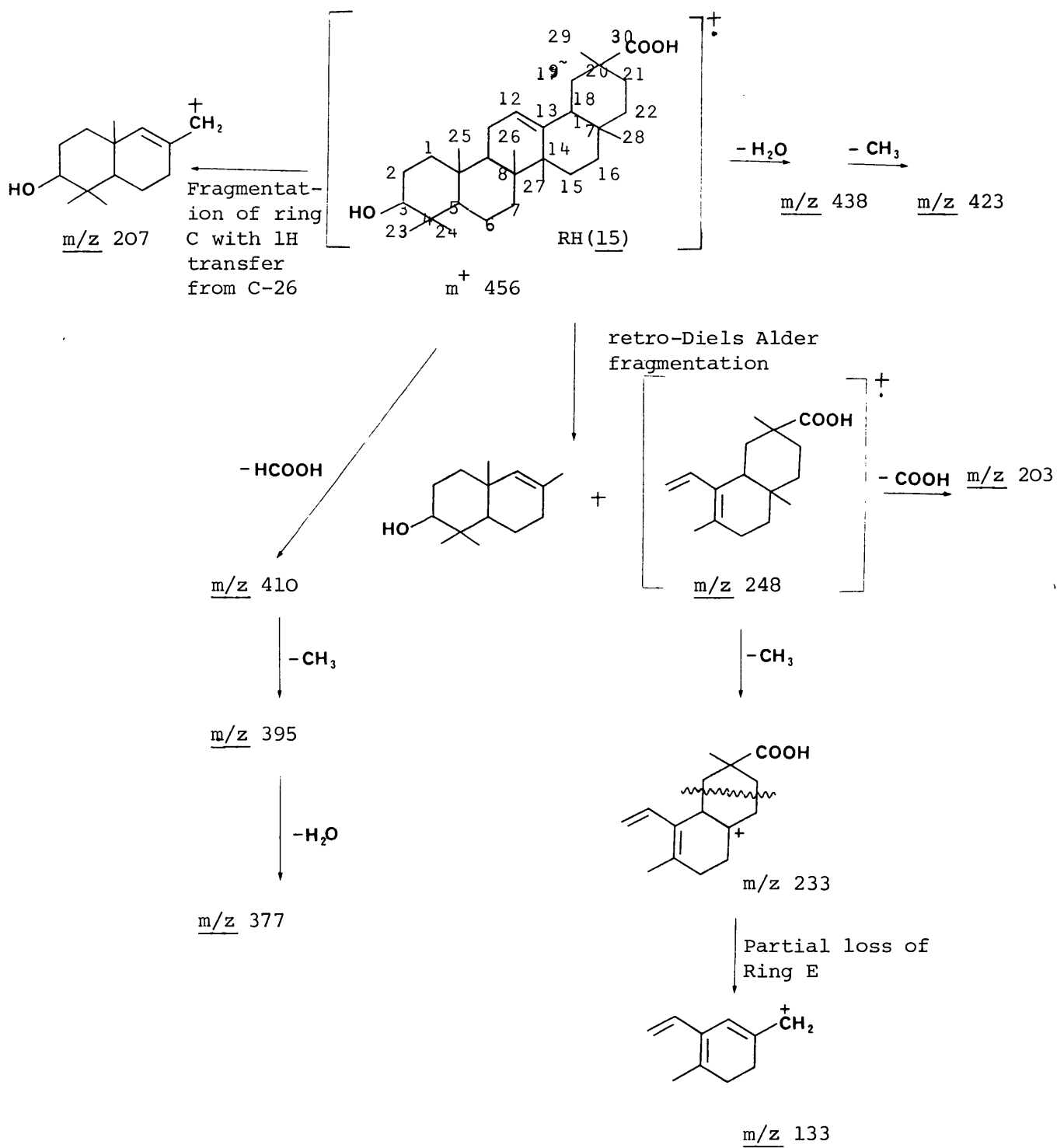


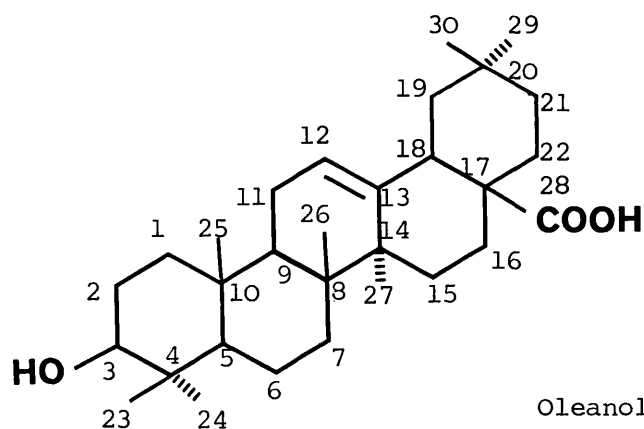
Fig. 1.18. Possible mass spectral fragmentation of RH



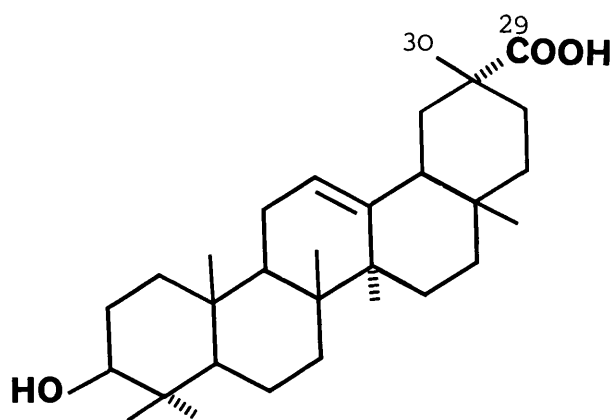
a hydroxyl substituent attached to C-3¹⁵. The C-27 methyl group is homoallylic to the Δ^{12} -double bond and is expected to resonate at lower field than the other methyl groups. Kazuo et al.¹⁵ using lanthanide-induced shifts of the methyl signals of several oleanenes assigned values ranging from δ 1.08 - 1.15 to the C-27 methyl group. Thus the peak at δ 1.12 may be due to the C-27 methyl group. The tertiary methyl signal at δ 1.24 is therefore suggestive of a methyl group strongly deshielded by an electron withdrawing group. This is consistent with a methyl group situated geminal to a carboxyl group and supports the presence of the carboxyl group on C-20. Hence, RH possesses a C-29 or a C-30 carboxyl group. Direct comparison with a gift sample of 3-epikatonic acid (3 β -hydroxyolean-12-ene-29-oic acid) from D. Coxon²⁰ revealed similar mass spectral fragmentation patterns in both compounds (M^+ 456, base peak, 248) which confirmed the gross structure (15) for RH. Additional support was provided by the methyl singlets at δ 1.20 and 1.14 in the ¹H-NMR (100 MHz) of 3-epikatonic acid and attributable to C-27 methyl and C-30 methyl signals (16). But structural identity between RH and 3-epikatonic acid could not be established because of the observed differences in some of the methyl resonances in the two compounds (Table 1.X). RH may differ from 3-epikatonic acid in the orientation of the carboxyl group which could either be α (C-29) or β (C-30), and in the orientation of the proton at C-18. Paucity of sample precluded further investigation.

Table 1.X $^1\text{H-NMR}$ data (δ , ppm) in CDCl_3 C-methyl
resonances in RH and 3-epikatonic acid

3-epikatonic acid	RH
1.20 (3H)	1.24 (3H)
1.14 (3H)	1.12 (3H)
0.99 (3H)	0.97 (3H)
0.96 (3H)	0.88 - 0.91 (6H)
0.93 (3H)	
0.85 (3H)	0.72 - 0.76 (6H)
0.78 (3H)	



Oleanolic acid (14)



3-Epikatonic acid (16)

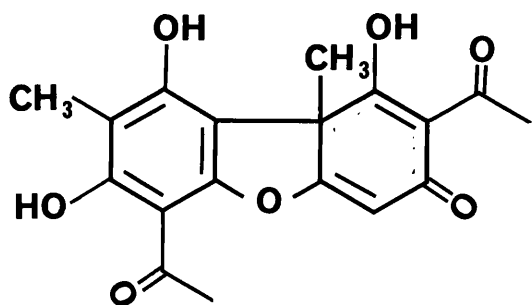
3.11 POSSIBLE RELATIONSHIP BETWEEN BIOLOGICAL ACTIVITY AND CHEMICAL STRUCTURE

Interest in the chemical constituents of the fruits of *Rhodomyrtus macrocarpa* was generated by reports of sporadic toxicity (especially blindness) associated with consumption of the fruits. The nature of the constituents of the fruit appears to vary with the season and the degree of maturity. Different investigations have led to the isolation of different dibenzofurans as the major constituent. Trippett reported that rhodomyrtoxin⁵ has an LD₅₀ of 12 mg per kg in mice and Anderson et al. observed toxic effects in mice at doses of about 30 mg per kg for ψ -rhodomyrtoxin⁶. Administration of ψ -rhodomyrtoxin directly to the eyes of rabbits did not produce any symptoms of temporary or permanent blindness.⁶ On the whole there is no conclusive evidence linking rhodomyrtoxin or ψ -rhodomyrtoxin with the toxicity of the fruits. Given the sporadic nature of the toxicity it is possible that if a link exists between the dibenzofurans and the toxicity that this property will be restricted to only a few of the isomers.

Early reports² on *Rhodomyrtus macrocarpa* have indicated the presence of large amounts of saponin in some of the fruits and no trace of saponin in others (stage of maturity not defined) and the poisonous principle has been described by Tyron and Brunnich²¹ as a saponin. The isolation of a

triterpenoid acid from *Rhodomyrtus macrocarpa* therefore raises the possibility of the presence of pharmacologically active glycosides which might well be responsible for the reported toxicity. The low yield of the triterpenoid acid does not necessarily reflect the extent to which it occurs in the fruit since it is possible that it exists predominantly as a glycoside and was thus largely overlooked by the extraction procedure used in most of the chemical studies reported to date. The presence of phenolic hydroxyl groups in the dibenzofuran derivatives suggests that they also could possibly exist in the fruit as glycosides though significant amounts obviously exist in the free form.

The only other literature reference to *Rhodomyrtus macrocarpa* was an investigation of the antibacterial action of dried Australian plants². Dried powdered mature "finger cherry" was found to be powerfully antibacterial against *Salmonella typhi*, *Staphylococcus aureus* and *Mycobacterium phlei*. The structural relationship between the rhodomyrtoxins and the dibenzofuran antibiotic, usnic acid (17) makes this observation



Usnic acid (17)

particularly interesting. Unfortunately the determination of the bacteriostatic and bactericidal efficacies of the isolated dibenzofurans was not possible.

REFERENCES

1. F.M. Bailey, *The Botany Bulletin*, No. 10, 37 (1895).
2. L.J. Webb, *Guide to the medicinal and poisonous plants of Queensland*, Bull. 232, Council for Scientific and Industrial Research. Melbourne, 1948.
3. H. Flecker, *The Medical Journal of Australia ii*, 183-185 (1944).
4. J.B. Cleland, *The Australian Medical Gazette*, June 1914.
5. S. Trippett, *J. Chem. Soc.* 414 (1957).
6. N.H. Anderson, W.D. Ollis and J.G. Underwood, *J. Chem. Soc.* 2403 (1969).
7. A. Pryde and M.T. Gilbert, *Application of high performance liquid chromatography*. (1979). Published by Chapman and Hall Ltd., London.
8. *High performance liquid chromatography* ed. J. Knox, page 155, Edinburgh University Press (1978).
9. L. Crombie and D.E. Games, *Tetrahedron Letters*, 145 (1966).
- 9b. L. Crombie and D.E. Games, *Tetrahedron Letters*, 151 (1966).
10. R.A. Finnegan and W.H. Mueller, *J. Org. Chem.* 30, 2342 (1965).
11. C. Djerassi, H. Budzikiewicz and J.M. Wilson, *Tetrahedron Letters*, 263 (1962).
12. H. Budzikiewicz, J.M. Wilson and C. Djerassi, *J. Am. Chem. Soc.* 85, 3658 (1963).
13. J.S. Shannon, *Austral. J. Chem.* 16, 683 (1963).

14. T.K. Razdan, S. Harkar, V. Kachroo and G.L. Koul,
Phytochemistry 21, 2339 (1982).
15. T. Kazuo, S. Shyujivo and T. Yutaka, *Chem. and Ind.*, 434
(1975).
16. R.J. Abraham and P. Loftus, Proton and Carbon-13 NMR
Spectroscopy. Heyden and Son Ltd. (1981).
17. L. Olson, *J. Chromatogr.* 106, 139 (1975).
18. M.V. Sargent, P.O. Stransky, V.A. Patrick and
A.H. White, *J. Chem. Soc. Perkin Trans I*, 231
(1983).
19. K.P. Tiwari and M. Masood, *Phytochemistry* 19, 1244 (1980).
20. D.T. Coxon and J.M. Wells, *Phytochemistry* 19, 1247
(1980).
21. H. Tyron and J.C. Brunnich, memoranda to the Under-
Secretary, Dept. of Agriculture and Stock, Brisbane,
December 1 and 2, 1902.

PART II
CHEMICAL INVESTIGATION INTO THE CONSTITUENTS
OF SOME BRITISH MARINE RED ALGAE

CHAPTER ONE

INTRODUCTION

1.1 GENERAL CHARACTERISTICS OF SEaweEDS

Seaweeds belong to the Thallophyta, a group of plants without the differentiation of a shoot into axis and leaf which is characteristic of the higher forms of plant life. They are macroscopic members of the divisions Chlorophyta (green algae), Phaeophyta (brown algae) and Rhodophyta (red algae), living in the sea. They are generally found growing attached to solid substrata between and below the tide marks but may also occur in an unattached state. A typical seaweed is normally composed of a holdfast (attachment organ) and a frond - which are together termed the thallus. Most of the cells are developed in such a way that each can carry out many of the functions of the organism, and any specialized regions that do exist, such as holdfast and reproductive organs are reduced to a minimum. Seaweeds obtain their nourishment by absorption through the thallus. They are primarily photoautotrophic, using sunlight to produce organic matter from mineral ions and water. Many photosynthetic seaweeds are also auxotrophic, that is they require small amounts of organic growth stimulators such as vitamins. The availability of nutrients is one of the key factors regulating the growth, reproduction and biochemistry of seaweeds²⁵.

Epiphytism is widespread and some parasitic species are known. The general distribution of seaweeds is governed by the nature of the substratum, and especially its suitability for attachment, and also by the phenomenon of zoning. At

any one place, the species composition changes on moving down the shore from high to extreme low water mark and beyond into shallow water. On the whole the red seaweeds grow at the greatest depth, the brown occurring in the main in places exposed at every tide or only partially exposed at the lowest tides. The green seaweeds occur high up where they are exposed at every tide or left in shallow rock-pools. The presence of rock-pools upsets the general sequence because it enables plants that would otherwise occur at greater depths to persist nearer high-water mark. Shallow pools near high-water mark become very warm in summer, and the number of species which are able to exist under these conditions is very limited. Nearer low-water the vegetation becomes luxuriant, and below half-tide the plants of the pools are varied and abundant^{23, 24}.

1.2 USES

The abundance and diversity of seaweeds have made them prime material for human use. Use as human food has been recorded as early as 600 - 800 B.C. in China. They are eaten for their food value, flavours, colours, and textures and are typically combined with other types of food. Examples of the major edible seaweeds include *Monostroma* and *Enteromorpha* (green seaweeds), *Laminaria* and *Undaria* (brown seaweeds), *Porphyra*, *Palmaria* and

Gracilaria (red seaweed). Analyses of certain edible seaweeds show that many contain significant amounts of protein, vitamins and minerals essential for human nutrition as well as large amounts of polysaccharides²⁷.

Seaweeds have regularly been fed to livestock in areas where they are conveniently and abundantly available. In most cases they are used as a supplement in the regular diet of livestock rather than as sole diet. Examples of seaweeds used in this way are *Chondrus*, *Palmaria* (red seaweeds), *Ascophyllum* and *Fucus* (brown seaweed)²⁸. Seaweeds are collected from beach drift or harvested especially for agricultural use. The method of application ranges from whole and chopped plants applied wet or dry to composted, liquified, supplemented, and extracted preparations. Ashes or 'kelp' from burnt seaweeds have also been applied to improve the soil. *Fucus* and *Ascophyllum* are very often used in this manner. An advantage of seaweed as fertilizer is that it is free of weed seeds and spores of fungi that are harmful to terrestrial crops²⁹.

Crude preparations and extracts of some seaweeds have been used for their medicinal properties for centuries. Some brown seaweeds were effective for curing goitre because of their iodine content. Other seaweeds have been used as vermifuges and to make cough medicines, soothing lotions and cosmetics³⁰.

Extraction of soda, potash and iodine formed the basis of the seaweed chemical industry. The soda and potash were used in making glass, pottery, soap and leather tanning. Kelp is the source of a fine grade of charcoal used for decolourizing and filtering. A large quantity of seaweeds harvested are used for the extraction of the polysaccharides agar, algin and carrageenan. Agar gels at room temperature and is very often used for microbiological plating media. Because of their excellent gelling properties at moderate temperatures, agar and carrageenan find much use in bakery products and creams. They are also used in the preparation of canned meats and fish and as clarifying agents in wines and beers²⁷. Mixtures of alginic acid and various alginates are often designed for many different gelling and viscosity controlling functions in a wide range of food, biomedical and industrial products such as in bakery and candy products, dyes and paints, and cardboard products²⁸.

One of the major new uses of seaweed presently being considered is as a biomass source for the production of fuel (methane and alcohol), chemicals and large quantities of food. This has stimulated research in growing and harvesting *Macrocystis* in large off-shore farm modules³¹.

1.3 CHEMISTRY OF THE SEaweeds

The most striking feature of the marine natural products

literature is the frequency with which halogenated compounds have been described. The majority of the halogenated marine metabolites contain bromine, with some of these compounds containing both bromine and chlorine, and fewer containing iodine.

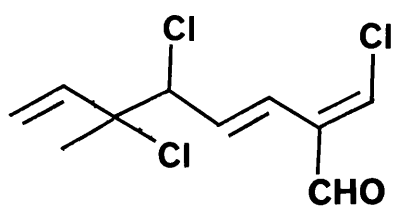
The sea is a dynamic environment, the salinity, oxygen content and nutrient composition varies a great deal from time to time and from one location to another. Many aspects of the chemistry of marine products are also dynamic in a sense. There are strong indications that certain chemical constituents of seaweeds undergo geographical and (or) seasonal variations (quantitative and(or) qualitative). Different populations of the same species of seaweed may accumulate significantly different metabolites in different geographical areas³².

The chemical investigation of the secondary metabolites of seaweeds has yielded a rich variety of novel and interesting compounds including sterols, terpenes, acetylenes, non-terpenoid phenols, amino acids and other low molecular weight nitrogenous compounds and low molecular weight carbohydrates. Some of these compounds are discussed below on a broad structural and biogenetic outline.

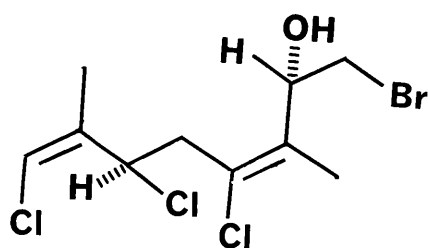
1.3.1 Terpenes

The terpenes are common in certain members of the Rhodophyta and can be grouped according to the number of isoprene units in each molecule. Halogenated monoterpenes have been shown as the major metabolites in *Plocamium* species (Gigartinales) and also in *Desmia hornemanni* (Cryptonemiales). Halogenated sesquiterpenes are perhaps the most commonly reported metabolites in red seaweeds. Most of the brominated sesquiterpenes and diterpenes described occur in various species of *Laurencia*. Species within this genus possess the fascinating ability to synthesize structurally elaborate halogenated natural products.

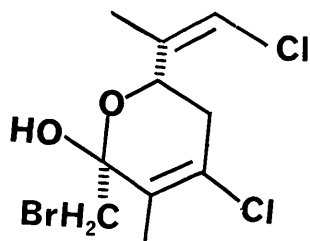
Monoterpenes are C_{10} isoprenoids structurally related to neryl pyrophosphate or its isomers³³. Five structural classes of monoterpenes have been described among seaweeds; four of these occur in red seaweeds of the genera *Chondrococcus*, *Microcladia*, *Ochtodes* and *Plocamium*. The simplest structural class, the acyclic monoterpenes is illustrated by cartilaginal (18), costatol (19) and a host of related di- and trienes from *Plocamium* species and *Chondrococcus hornemanni*^{34,35,36}. Cyclization of an alcoholic intermediate would lead to cyclic dihydropyran monoterpenes such as costatone (20) and the related metabolites of *P. costatum*^{37,38}. Another structural class of monoterpenes, the 1,1,5-trialkylcyclohexanes, may arise from $C_7 \rightarrow C_2$ carbocyclization of acyclic precursors. Examples include



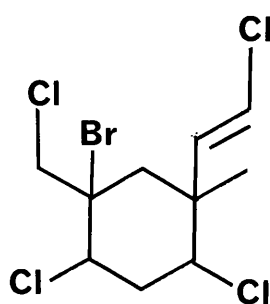
(18)



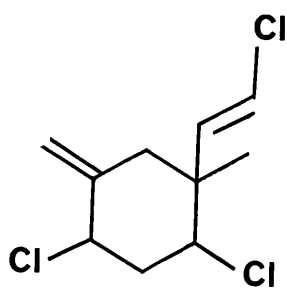
(19)



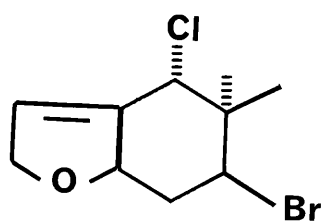
(20)



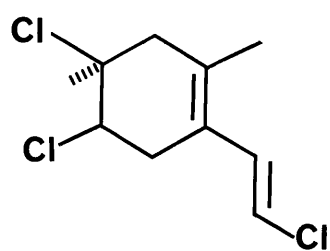
(21)



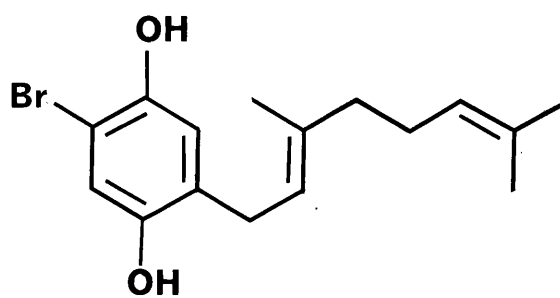
(22)



(23)



(24)



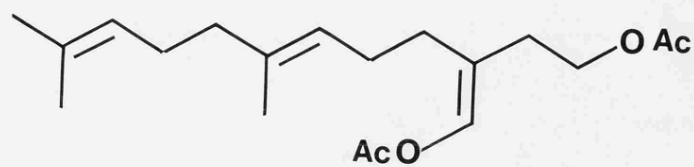
(25)

violacene (21) and the related plocamene D (22), produced by *Plocamium* species and also found in *Microcladia* species^{39,40}, Chondrocole A (23) from *C. hornemanni*⁴¹, and related monoterpenes from *P. cartilagineum*³⁶ and *P. mertense*⁴².

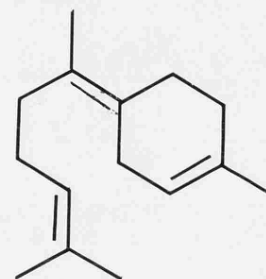
1,2,5-Trialkylcyclohexenes such as plocamene B (24) presumably arise from 1,1,5-trialkylcyclohexanes by trans-vinyl migration⁴³.

A different structural class, monoterpene-substituted hydroquinones, apparently of mixed biosynthetic origin, is known from the calcareous green seaweed *Cymopolia barbata*. This class is exemplified by cymopol (25)⁴⁴. Cymopol and related terpenoid phenols have been shown to possess strong antibiotic activity.

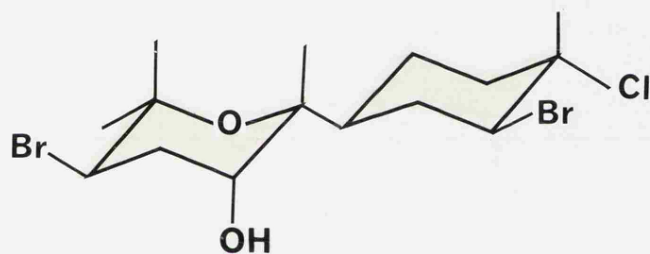
Sesquiterpenes are C₁₅ isoprenoids formally derived from trans, cis-farnesyl pyrophosphate or one of its isomers. Acyclic sesquiterpenes are uncommon in seaweeds. Flexilin (26) isolated from *Caulerpa flexilis* is one of the few examples⁴⁵. Monocyclization of farnesol pyrophosphate could generate the hydrocarbon intermediate, bisabolene (27), leading to the bisabolene based metabolites such as caespitol (28)⁵⁸ and its trans-diaxial isomer isocaespitol (29)⁵⁸. Carbocyclization of a bisabolene intermediate could then yield the Chamigranes such as glanduliferol (30) and spirolaurenone (31) from *Laurencia glandulifera*⁴⁶, and 10-bromo- α -Chamigrene (32) from *L. pacifica*⁴⁷. Rearrangement of trans-diaxial bromochloro bisabolonium intermediates may lead to (+) Chamigranes such as obtusol (33) from *L. obtusa*⁴⁸, or possibly



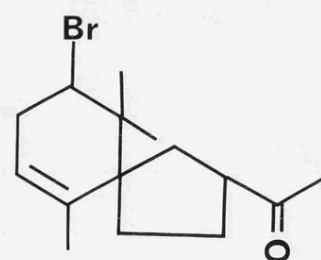
(26)



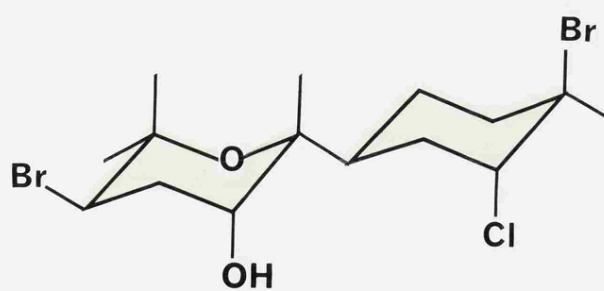
(27)



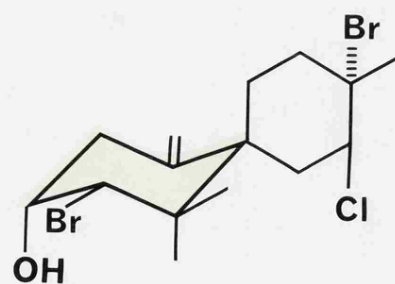
(28)



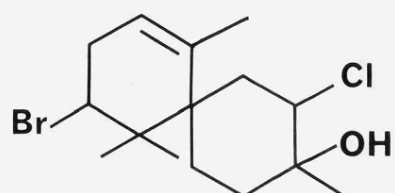
(31)



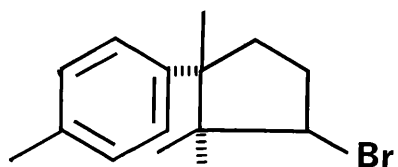
(29)



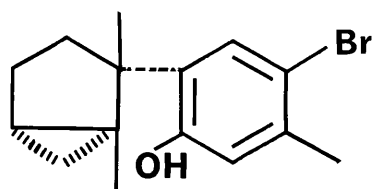
(33)



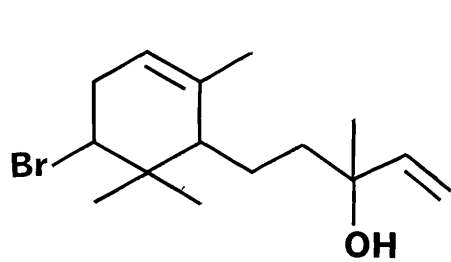
(30)



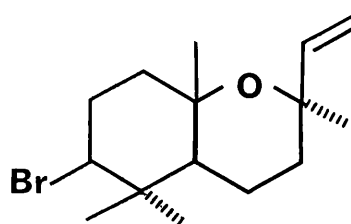
(34)



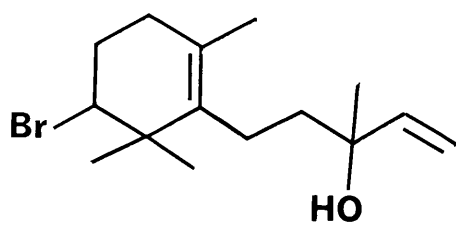
(35)



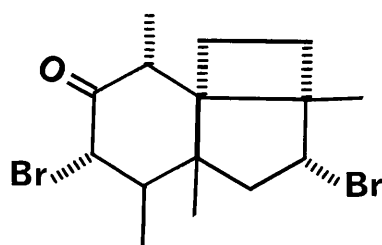
(38)



(39)

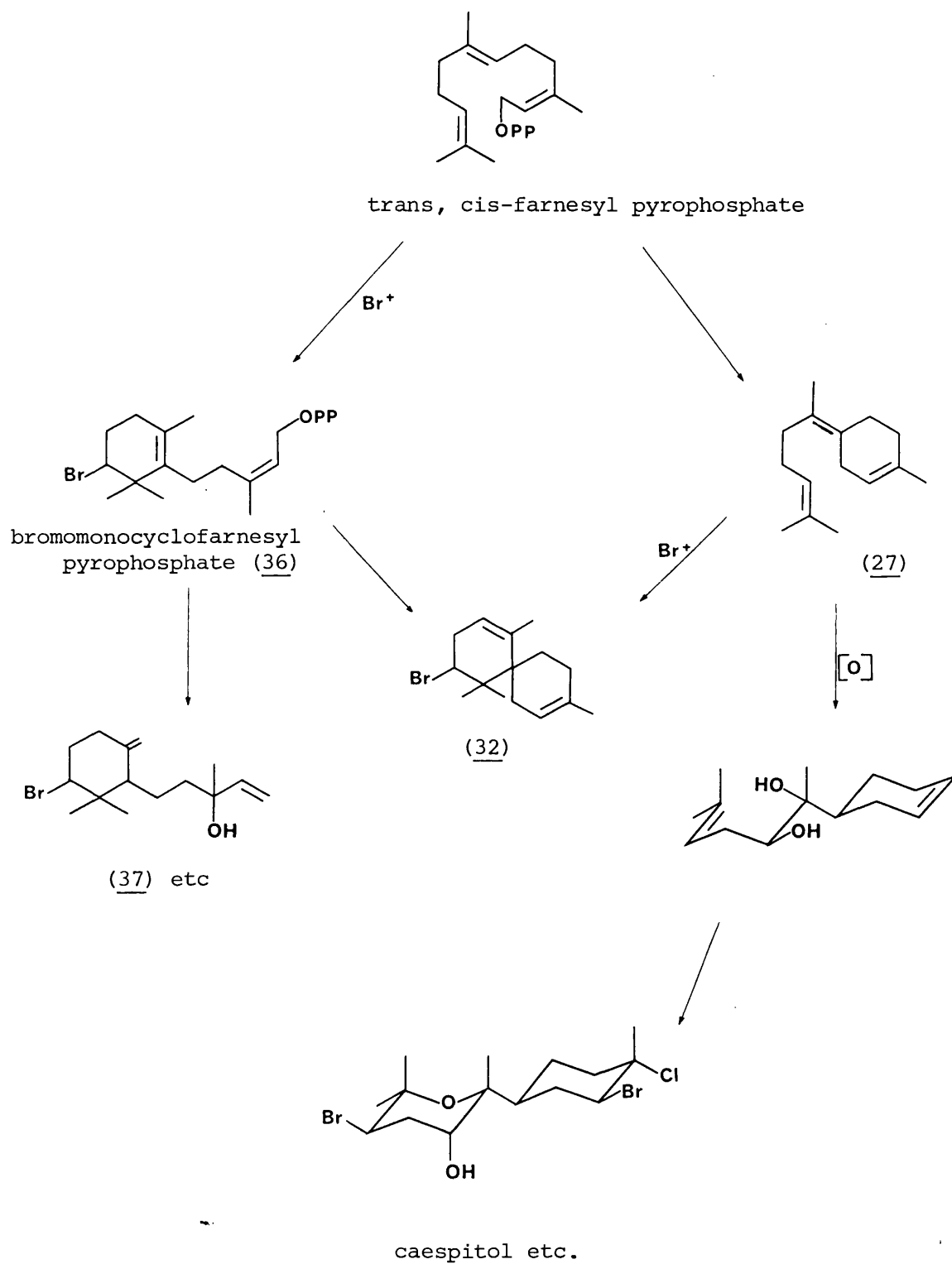


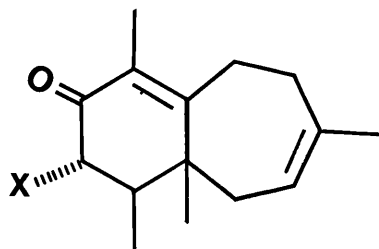
(40)



(41)

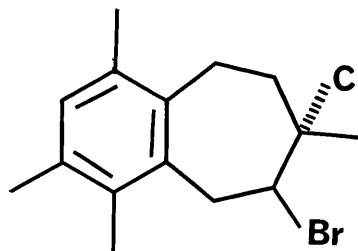
Fig. 2.1 Possible biosynthetic relationship among algal
sesquiterpenes





(42) **X = OH**

(43) **X = Cl**



(44)

certain cuparanes such as α -bromocuparene (34) and laurinterol (35) isolated from *L. okamurai*⁴⁹. Monocyclization of farnesol pyrophosphate to monocyclofarnesol (36), [Figure 2.1], leads to the monocyclofarnesanes exemplified by β -snyderol (37) and α -snyderol (38) from *L. snyderae*⁵⁰ and 3 β -bromo-8-epicaparrapi oxide (39) from *L. obtusa*⁵¹. The isomer of snyderol (40), has been shown to undergo acid catalyzed cyclization to give 10-bromo- α -chamigrene (32) which has been isolated as a minor metabolite of *L. pacifica*⁴⁷.

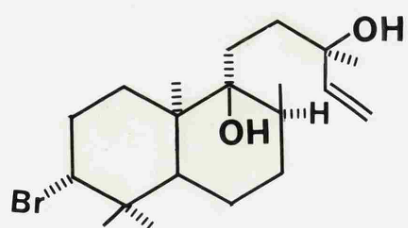
A most unusual series of sesquiterpenes - perforatone (41), perforenone A (42), perforenone B (43) and perforene (44) has been isolated from *L. perforata*⁵². These compounds represent a radical departure from familiar *Laurencia* metabolites and are deemed to be rearranged chamigranes⁵³.

Diterpenes are C₂₀ isoprenoids formally derivable from

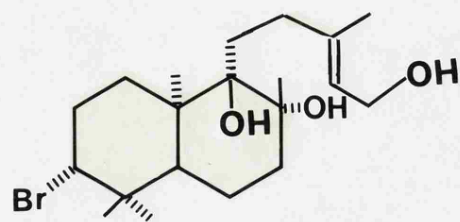
geranylgeranyl pyrophosphate. All the halogenated diterpenes reported so far from algal sources are brominated diterpenes, most of them being *Laurencia* metabolites. Concinndiol (45), isolated from *Laurencia concinna*⁵⁴ belongs to the rather common Labdane ring system which is also present in Aplysin-20 (46) isolated from the herbivorous mollusc *Aplysia kurodae*⁵⁵. The structural similarity between the two compounds has led to the suggestion that Aplysin-20 is also a *Laurencia* metabolite. Irienol (47) and related metabolites from *L. iriei*⁵⁶ are representatives of a different diterpene ring system. Interestingly, part of these diterpene structures are identical to the *Laurencia* sesquiterpene oppositol (48). Sphaerococcenol A (49) and related bromosphaerol (50) obtained from the red alga *Sphaerococcus coronopifolius*⁵⁷ represent a different structural class of diterpenes which have not been found in the *Laurencia* species.

1.3.2 Sterols

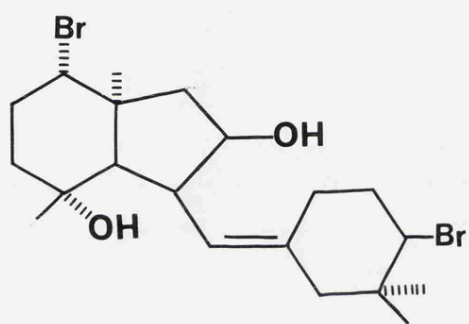
Sterols are terpenoid in nature and are biosynthesised from mevalonic acid via isopentenyl-pyrophosphate and the triterpenoid, squalene. Squalene is oxidized to squalene 2,3-epoxide which can undergo a number of primary cyclizations. In animals, lanosterol (51) is formed, which, after a number of further steps, involving loss of methyl groups at C-4 and C-14, is converted into the 27-carbon compound cholesterol



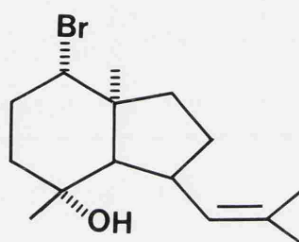
(45)



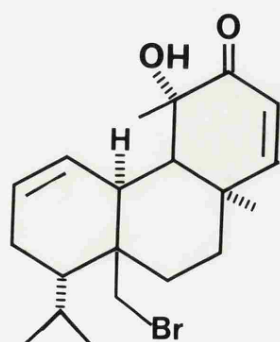
(46)



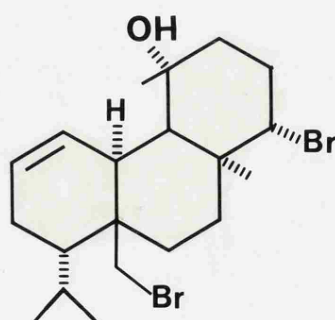
(47)



(48)



(49)



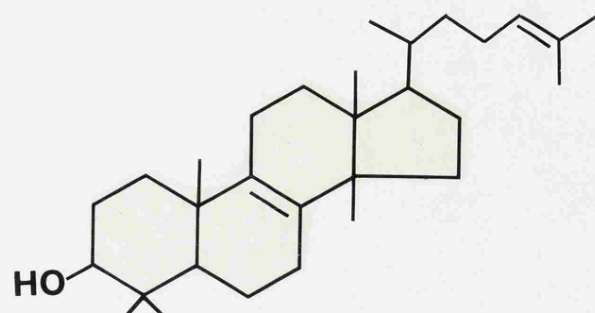
(50)

(52). Lanosterol is also formed in fungi and is the precursor of fungal sterols. However, in higher plants and algae the first product of cyclization in sterol biosynthesis is not lanosterol but cycloartenol (53) thought to be the precursor of all algal sterols⁵⁹.

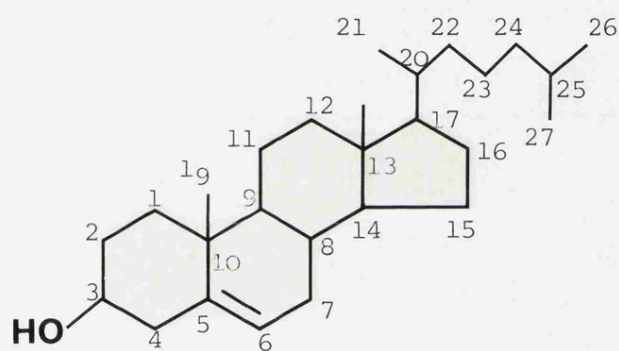
In all the red seaweeds investigated cholesterol, or its biosynthetic precursor desmosterol (54), or 22-dehydrocholesterol (55) is the main sterol component⁶⁰. Other phytosterols which may be present as minor constituents include campesterol (56) and/or its isomer 22-dihydrobrassicasterol; β -sitosterol (57) and/or its 24-S epimer clionasterol; stigmasterol (58) brassicasterol (59), fucosterol (60) and 28-isofucosterol (61); 24-methylenecholesterol (62) and liagosterol (63)⁶¹.

The predominant sterol of all investigated brown seaweeds is fucosterol (60), or in some cases its Δ^{24} [25] isomer⁶². Cholesterol, 24-methylenecholesterol and 22-dehydrocholesterol are also widespread among brown seaweeds. Brassicasterol (59), desmosterol, stigmasterol (58) or its 24-R epimer poriferasterol, a C₂₇ cyclopropanoid cystosterol (64) and the vinyl alcohol saringosterol (65) probably derived by oxidation of fucosterol are less frequently encountered⁶³.

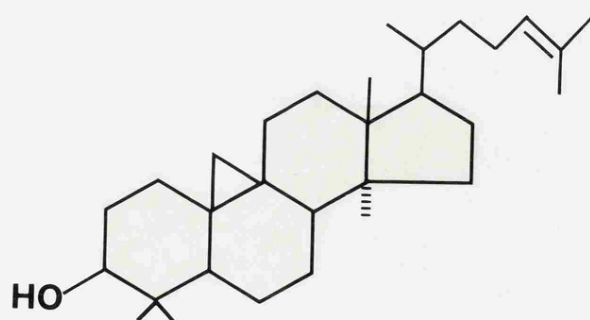
Sterol profiles of green seaweeds are less predictable. β -Sitosterol (57), 24-methylenecholesterol and 28-isofucosterol appear to be present in most, although not all, green seaweeds⁶⁴.



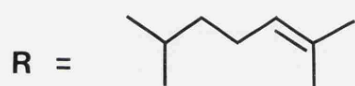
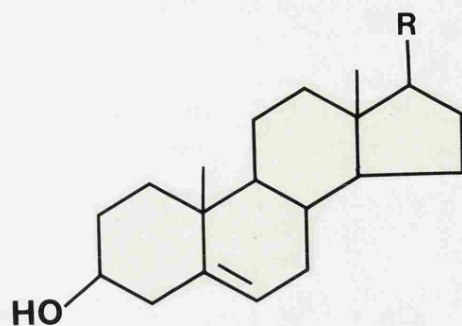
(51)



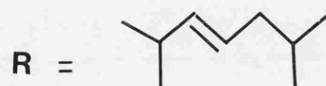
(52)



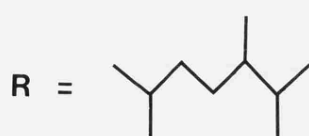
(53)



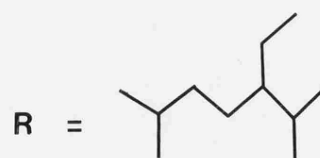
(54)



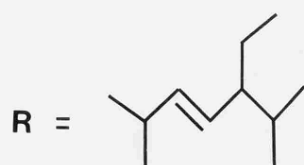
(55)



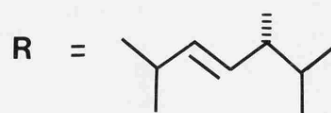
(56)



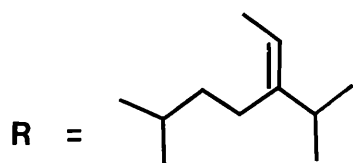
(57)



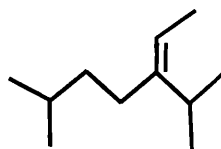
(58)



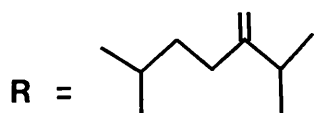
(59)



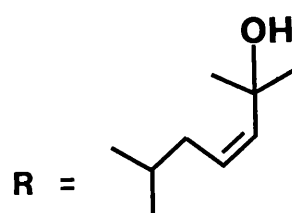
(60)



(61)



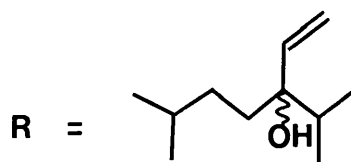
(62)



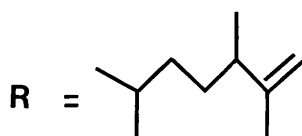
(63)



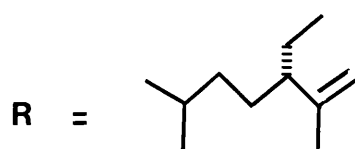
(64)



(65)



(66)



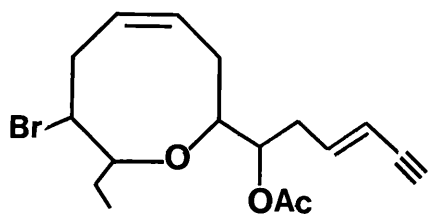
(67)

Campesterol (56), stigmasterol (58) and its 24-R epimer poriferasterol, 22-dehydrocholesterol, desmosterol and fucosterol are reported less frequently. *Codium fragile* and *C. vermilara* differ considerably from other green seaweeds, accumulating only the unusual dienols clerosterol (66) and codisterol (67)⁶⁵. It is notable that no halogenated derivatives of sterols have been reported

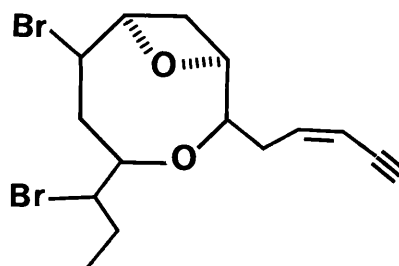
1.3.3 Non-terpenoid acetylenes

Acetylene cyclic ethers are known from several species of *Laurencia* and *Chondria oppositoclada*. The algal acetylenes are all halogenated cyclic ethers based on a linear pentadeca-3-ene-1-yne carbon chain, that is they all contain a conjugated pentenyne group. Examples of the different structural types include laurencin (68) from *L. gladulifera*, which was shown to contain a trans enyne system attached to an 8-membered ether ring⁶⁶; Laureatin (69) and the isomeric isolaureatin (70) isolated from *L. nipponica*⁶⁷. These two isomers elaborated two ether rings - an oxocane ring in which the oxygen linked the C₆ and C₁₂ instead of C₇ and C₁₃ as in laurencin, but laureatin possessed an additional oxetane ring whereas isolaureatin had a tetrahydrofuran ring. They both contain the cis enyne system though the trans isomers have also been described⁶⁸. Laurefucin (71), a bicyclic bromo alcohol and its acetate, acetyllaurefucin (72) were also isolated from *L. nipponica*⁶⁹. Cis- and trans-laurediol (73) isolated in low yield from *L. nipponica* have been suggested as probable biosynthetic precursors of the cyclic ethers⁶⁸.

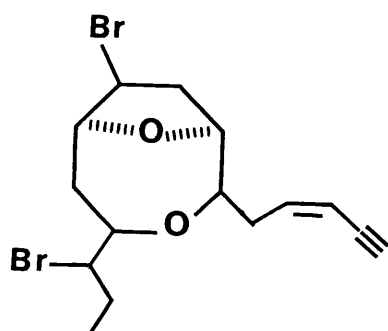
The series of acetylenes containing both bromine and chlorine is illustrated by chondriol (74) isolated from *Chondria oppositoclada*⁷⁰. The structural similarities between chondriol and the *Laurencia* metabolites such as laureatin (69) led to a taxonomic re-examination of the algal source, with the result that *Chondria oppositoclada*



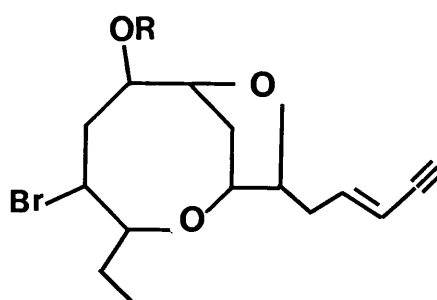
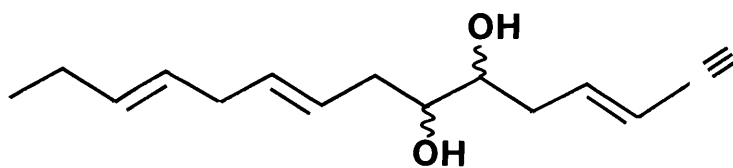
(68)



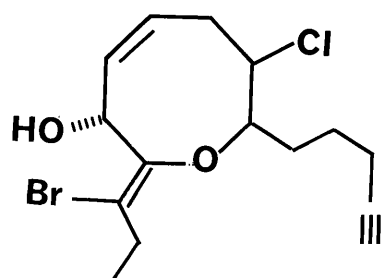
(69)



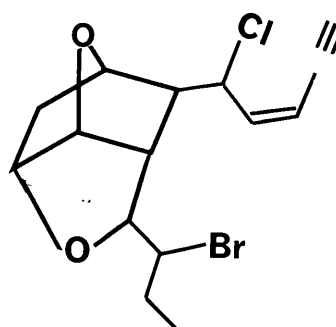
(70)

(71) $R = H$ (72) $R = Ac$ 

(73)



(74)



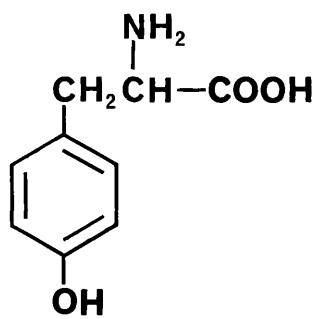
(75)

was reclassified as *Laurencia yamada*⁷¹.

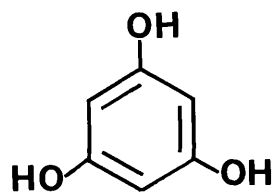
All the acetylenes described so far are cyclic ethers with rings ranging in size from the four-membered oxetane to eight-membered oxocane and containing no carbocyclic rings. A different group of acetylenic compounds, exemplified by cis-maneonene A (75) which contain six-membered (or both five- and six-membered) carbocyclic rings in addition to ether rings was obtained from *L. nidifica*^{72,73}.

1.3.4 Non-terpenoid phenols

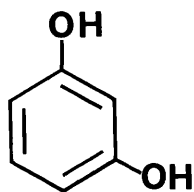
The non-terpenoid phenols from seaweed may be divided into two groups which probably differ in their biosynthetic origins - phenols related to tyrosine (76) and phenols related to phloroglucinol (77) and resorcinol (78). Phenols with an intact C_6-C_3 unit include 3-iodo- and 3,5-diiodotyrosine and triiodothyronine (79) present at low levels in many red and brown seaweeds⁷⁴. In addition, 3,5-dibromo-4-hydroxyphenylacrylic acid (80) has been reported from *Halopytis incurvus* and *H. pinastroides*⁷⁵, and 4-hydroxyphenylpyruvic acid (81) from *Odonthalia floccosa*⁷⁶. Eight-carbon (C_6-C_2) phenols such as 4-hydroxyphenylacetic acid (82) from *H. incurvus*⁷⁵ can arise by decarboxylation of a C_6-C_3 precursor⁷⁷. Related C_6-C_1 phenols include 4-hydroxybenzylalcohol and 4-hydroxybenzaldehyde in *Marginosporum aberrans*⁷⁸. A variety of C_6-C_1 -based brominated phenols, bromochlorophenols and



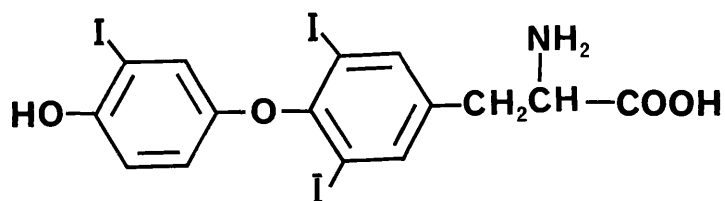
(76)



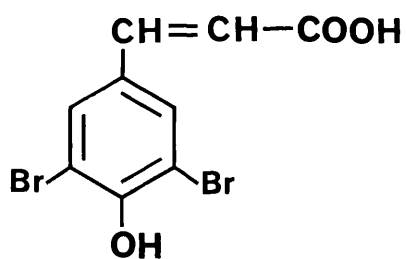
(77)



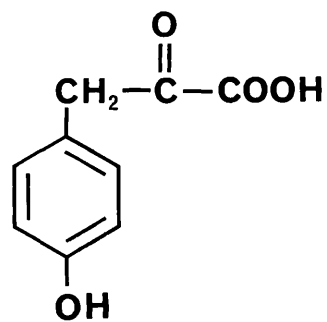
(78)



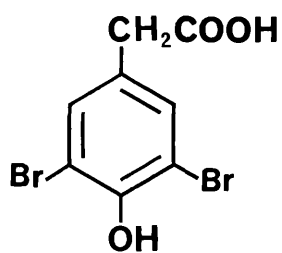
(79)



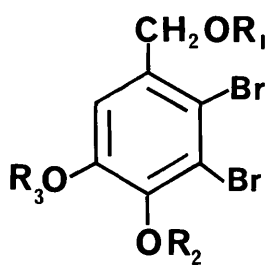
(80)



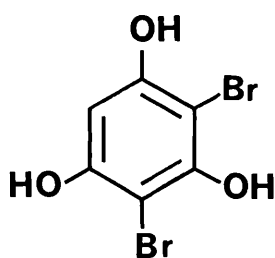
(81)



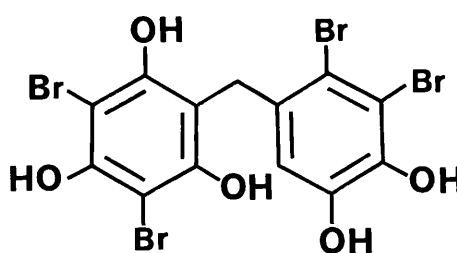
(82)

(83) $R_1 = R_2 = R_3 = H$ (84) $R_3 = H, R_1 = R_2 = SO_3^- K^+$ (85) $R_1 = CH_2CH_3, R_2 = R_3 = H$

bromodiphenylmethanes have been found in certain red seaweeds especially from members of the Rhodomelaceae⁷⁹. The halogenated phenols generally show antibiotic activity. Lanosol (83) is the most abundant and widely distributed of the brominated phenols, being found in more than twelve species of marine algae. Lanosol was first isolated as the dipotassium salt of a disulphate (84)⁸⁰, and many of the simple bromophenols may possibly exist *in vivo* largely as the sulphate esters. Some brominated phenols were also found in *Rytiphlea tinctoria* (Rhodomelaceae). When obtained from



(86)



(87)

the Mediterranean sea, it contained lanosol and its ethyl ether (85), but when collected along the Atlantic coast of France, the same seaweed contained dibromophloroglucinol (86) and the tetrabromo compound (87) which appears to be a condensation product of (83) and (86)⁸¹.

The biological significance of some of these metabolites is still uncertain. Some of them, especially the halogenated phenols and terpene phenols possess strong antimicrobial activity and may be involved in chemical defence against bacteria and parasitic microflora. Lanosol was found to be toxic to microalgae grown in culture⁸². This suggests the involvement of lanosol in deterring epiphytic algal growth. The phenol sulphate ester salts, however, showed no anti-algal activity and, in fact, were found to be mildly growth stimulating. If in fact, the bromophenols occur naturally as their respective sulphates, as is widely speculated, their role in preventing epiphytic growth becomes questionable. On the other hand, these compounds may be stored by seaweeds in the inactive form and rapidly hydrolyzed to the active phenols on the thallus surface by seawater or by an enzymatic process in response to injury.

In most algae, male gametes have been observed to approach and surround the female gametes before fertilization takes place. It was found that the male cells respond to highly volatile compounds secreted by the female gametes⁸³. Some of these compounds have been identified as unsaturated hydrocarbons (examples heneicosahexaene; octatriene). Considering that some of the halogenated metabolites especially the monoterpenes, are volatile in nature it is not unlikely that some of them may function as pheromones especially when their presence is associated with the peak growth periods. A number of the halogenated metabolites, on the other

hand, possess strong odours which are unpleasant and may thus serve to discourage invertebrate predators.

1.3.5 Fatty acids

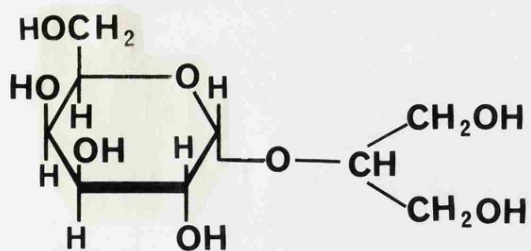
Virtually all the algal fatty acids are straight chain molecules containing an even number of carbon atoms. This is presumably, a direct consequence of their biosynthesis via acetate β -addition. The composition of the fatty acids of red seaweeds (Rhodophyta) is complex, and is remarkable for the relatively high content of C_{20} polyunsaturated fatty acids with 4,5 and even 6 double bonds. The major constituent fatty acids are generally palmitic acid (16:0) and 20:5w3. The only other C_{20} polyunsaturated acid present in significant amounts is 20:4w6. Various C_{18} polyunsaturated acids are present but only in a few cases is the amount of any particular acid greater than 5 percent. A number of C_{16} polyunsaturated acids are present usually in amounts less than 2 percent^{84,85}. Generally, the brown seaweeds (Phaeophyta) have higher proportions of C_{18} polyunsaturated and small proportions of C_{20} polyunsaturated acids than the red seaweeds. Only very small proportions of any C_{16} polyunsaturated fatty acid are present^{85,86}. The green seaweeds (Chlorophyta) tend to accumulate proportionately large quantities of cis-vaccenic (18:1w7), α -linolenic (18:3w3), 18:4w3 and 16:4w3 acids^{84,85,86}. The C_{20} acids are present in smaller amounts than in the Rhodophyta and the Phaeophyta. The three classes of seaweeds contain significantly high amounts of C_{16} saturated

and low percentages of C₁₄ and C₁₈ saturated fatty acids.

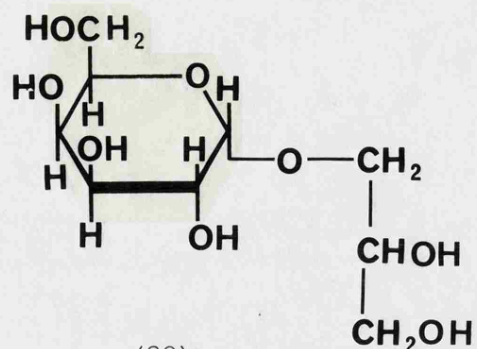
1.3.6 Low molecular weight carbohydrates

The members of the Rhodophyceae differ significantly from most other photoautotrophic plants by the occurrence of certain heterosides. The glycerol glycosides, floridoside (88) and isofloridoside (89) are widely distributed in the Rhodophyceae except in the Rhodomelaceae family where they are largely replaced by sodium mannoglycerate (90) and mannitol⁸⁷. Floridoside is generally present at several times the concentration of isofloridoside (where they occur together)⁸⁸. These galactosides were thought to be peculiar to red algae but isofloridoside has been found in the Chrysophyte, *Ochromonas malhamensis*, and floridoside is rather common in the Cryptophyceae⁸⁹.

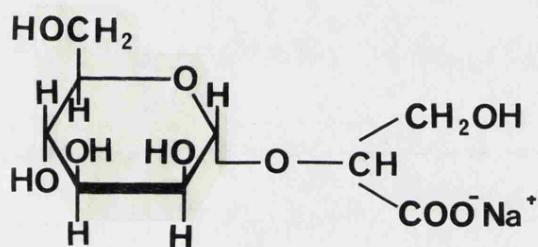
Sugars, polyols and simple glycosides probably contribute significantly to the osmotic balance in algal cells. Direct evidence that the intracellular level of simple carbohydrates could be affected by the salinity of the medium has been provided experimentally by Kaus⁹⁰ who found the cellular concentration of isofloridoside to be directly dependent upon the external osmotic pressure in the medium.



(88)



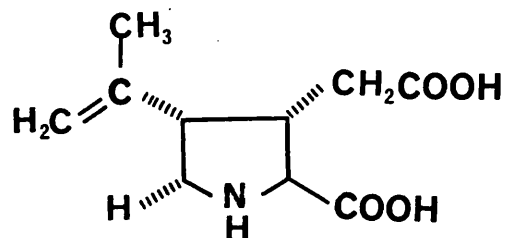
(89)



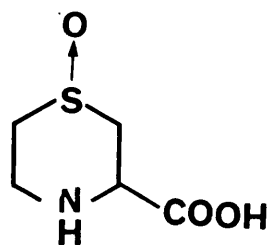
(90)

1.3.7 Amino acids and other low molecular weight nitrogenous compounds

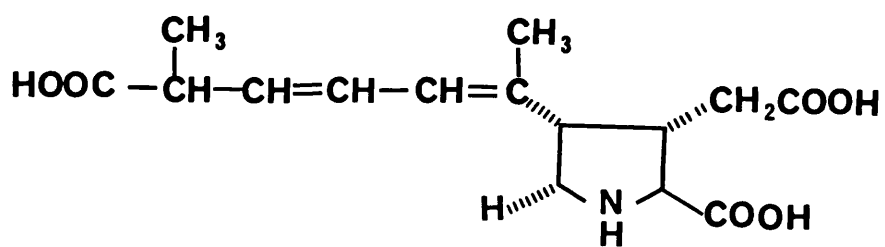
The free amino acid pool in algae is composed of compounds similar to those found in flowering plants⁹¹. Nearly all of the amino acids normally found in proteins are present in the free state in seaweeds. There is a general prevalence of aspartic and glutamic acids, alanine, glycine and serine, and low concentrations of basic amino acids⁹². Other less well-known nitrogenous compounds isolated from seaweeds include the imino acids; L-kainic acid (91) and the isomeric



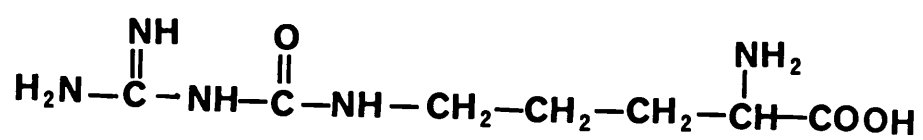
(91)



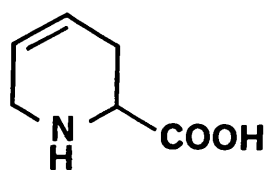
(93)



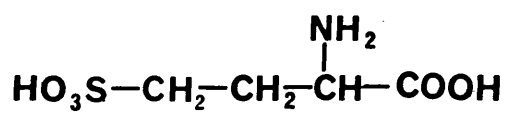
(92)



(94)



(95)



(96)

L-allokalainic acid from *Digenea simplex*⁹³, and domoic acid (92) from *Chondria armata*⁹⁴. The three imino acids are said to possess useful anthelmintic properties. Iodoamino acids are characteristic components of brown and red seaweeds, particularly diiodotyrosine from *Laminaria* species⁹⁵. Other non-protein amino acids from seaweeds include chondrine (93), gigartinine (94), L-baikiaian (95), methylated histidines⁹⁶ and D-homocysteic acid (96)⁹⁷.

The foregoing represents a summary review of the chemical constituents of seaweeds giving a general picture of seaweed-derived natural products and the structural and probable biosynthetic relationship between compounds isolated from different species. Since seawater is a halogen-rich environment, it is not surprising that marine organisms are capable of the synthesis of halogenated metabolites. However, it is remarkable that brominated compounds are more abundant than chlorinated compounds since seawater contains a much higher concentration of chloride ion than bromide ion. This has been attributed to the relative ease of formation of Br^+ as opposed to Cl^+ .

In the present study it is proposed to carry out a chemical examination of some British seaweeds and in particular to extract and characterize low molecular weight constituents. In addition, it is proposed to screen a variety of seaweeds for antimicrobial activity and to consider the possibility of an activity-directed chemical investigation.

CHAPTER TWOGENERAL MATERIALS AND METHODS

•
•
;

SECTION A

2.1 PLANT MATERIAL^{22,23}

2.1.1 *Polysiphonia lanosa* (= *Polysiphonia fastigiata*)

(Rhodomelaceae)

The plants are dark reddish brown, 7 - 8 cm long. They are usually found growing in tufts on *Ascophyllum nodosum* on which they are believed to be parasitic. The main stem bears alternate or dichotomous branches in all planes around the long axis. The branches become shorter from the base from which numerous rhizoids invade the host's tissue.

Habitat: very common wherever *Ascophyllum* is to be found. Samples used in this study were collected at Berwick-on-Tweed (Northumbria) and Kimmeridge Bay (Dorset).

2.1.2 *Corallina officinalis* (Corallinaceae)

The plants are dull purple when growing in deep water, becoming red, yellow and finally white on exposure. They grow in tufts with fronds 5 - 12 cm long. The main stem bears branches arranged exactly opposite; the branches in their turn bear opposite branchlets. The plant consists of numerous calcified segments which are longer than broad, and which are linked by pliable joints to form the frond. The holdfast is chalky and encrusting.

Habitat: The plant is to be found growing on rocks

between tidemarks and in rock pools at all levels of the middle shore. The sample used in this study was collected at Portland (Dorset).

2.1.3 *Palmaria palmata* (= *Rhodymenia palmata*)

(Rhodymeniaceae)

The frond is purplish or reddish brown, leathery or membranaceous, 10 - 30 cm long with no stipe and gradually expands from the wide, disc-like holdfast to form a flattened, dichotomous fan. The younger parts are delicate, and the older parts are tougher and darker and may bear small peripheral 'leaflets'.

Habitat: To be found growing on rocks and on laminarian stipes on lower shore and in shallow water. Samples used in this study were collected at Dawlish, Devon and Kimmeridge Bay, Dorset.

2.1.4 *Laurencia pinnatifida* (Rhodomelaceae)'

The colour of the frond is variable depending on position on the shore, but is often purple-brownish and may be green-yellow in the middle tide range. The frond is flattened, cartilaginous in texture, and 2 - 30 cm long with well-developed main stem alternately branched and the branches subdivided into smaller branchlets. The holdfast is disc-like with rhizoids.

Habitat: To be found growing on rocks and in crevices from the middle shore down to shallow water. The sample used in this study was collected at Portland, Dorset.

2.1.5 Lomentaria articulata (Rhodymeniaceae).

The fronds are dull purple to bright red, shiny and transparent, 5 - 25 cm long. The frond consists of a hollow stem and branches which are repeatedly constricted to give a jointed or beaded effect. The branches only occur at the joint between two beads. The primary branching is dichotomous and the secondary often opposite or somewhat pinnate. The plant has a very small holdfast and attachment runners from the stem.

Habitat: To be found growing attached to rocks and other seaweeds on the upper, middle and lower shores. The sample used in this study was collected at Portland, Dorset.

2.2 PRELIMINARY EXTRACTION

All solvents used in this study were either of spectroscopic grade or redistilled before use.

In all cases, except where indicated, species were separated, transported to the laboratory in plastic bags and

frozen for storage prior to study. For analyses, samples were thawed slowly at room temperature and rinsed briefly in distilled water. All obvious foreign material was removed and the algal material allowed to air-dry overnight at room temperature. The basic extraction technique employed was to extract the half-dried material at room temperature with an appropriate organic solvent usually chloroform-methanol (2:1) and followed by aqueous methanol or ethanol. The combined extract was concentrated *in vacuo* and then partitioned between water and diethyl ether to give polar and non-polar extracts respectively. The non-polar extract was then shaken with three portions of 300 ml 5 percent potassium hydroxide solution to extract acidic components. The organic phases were combined, washed with 1M hydrochloric acid followed by distilled water, dried over anhydrous sodium sulphate and evaporated to leave ether-soluble neutral material. The combined alkaline aqueous solutions were acidified with a calculated volume of 6M hydrochloric acid and extracted with diethyl ether. The ether extract was washed with distilled water, dried over anhydrous sodium sulphate and the solvent removed *in vacuo* to leave an ether-soluble acidic mixture. Subsequent treatment of the polar, ether-soluble acidic and neutral extracts varied to some extent with the different species.

2.3 CHROMATOGRAPHY

2.3.1 Column and thin layer chromatography

Column chromatography of the non-polar extracts was carried out on silica gel slurried with an appropriate solvent and packed into glass chromatographic columns. Thin layer chromatographic analyses were carried out on silica gel G plates 0.25 mm in thickness. For preparative TLC, silica gel H plates, 2.0 mm in thickness, were used. 3% ferric chloride solution and 50% sulphuric acid followed by heating at 110°C for 5 min were used as TLC spray reagents.

2.3.2 Ion-exchange chromatography

The concentrated polar extracts were fractionated by passage through a column of Dowex 50W- x 8 (H^{+} form) packed in 0.1 M hydrochloric acid and washed with deionised water until the eluate was neutral. After the sample was applied onto the column it was eluted with deionised water to give neutral components and then with 2 M ammonia solution. The ammonia eluate was concentrated *in vacuo* and further fractionated by passage through a column of Amberlite IRA 400 (Cl^{-} form) which was converted to OH^{-} form by passing 1 M sodium hydroxide solution through the column until the eluate was basic. The column was then washed with water until the eluate was neutral. The concentrated sample was then applied onto the column. Neutral and basic amino acids

were eluted from the column with deionised water whilst acidic amino acids were eluted with 1 M hydrochloric acid.

2.3.3 Paper Chromatography

Paper chromatographic analyses were carried out by the ascending technique using Whatman 3 mm chromatography paper. The following solvent systems were used:

- a) Butanol-acetic acid-water (4:1:1), for preparative paper chromatography of low molecular weight glycosides and as the second system in two dimensional paper chromatographic analysis of amino acids.
- b) Phenol-water (3:1, w/v) in the presence of strong ammonia vapour. Solution of phenol was effected by warming at 40°C. This was used as the first system in two dimensional paper chromatographic analysis of amino acids.
- c) Isopropanol-pyridine-water-acetic acid (8:8:4:1). This was used for paper chromatographic analysis of sugars and hydrolysis products of low molecular weight glycosides. After development, the chromatograms were usually left to air-dry overnight in the fume cupboard before sparying with an appropriate spray reagent and heating at 105°C for 2 - 3 minutes (where necessary).

The following spray reagents were used:

- i) 3% ferric chloride solution
- ii) 3% *p*-anisidine HCl solution
- iii) 0.01 M potassium permanganate solution prepared

by dissolving 0.48 g of potassium permanganate in water to a volume of 10 ml. 1 ml of this stock solution was then diluted to 30 ml with acetone immediately before use. This solution is stable for about one hour.

- iv). Ninhydrin reagent prepared from ninhydrin (0.2 g), acetic acid (5 ml), water (5 ml) and acetone (90 ml).
- v) 0.1 M sodium molybdate ($\text{Na}_2\text{MoO}_4 \cdot 2\text{H}_2\text{O}$) solution.

2.3.4 Gas-Liquid Chromatography

Gas-liquid chromatographic analyses were carried out on a Perkin-Elmer F33 Gas Chromatograph fitted with flame ionisation detector (F.I.D.) and connected to a Servogor 220 recorder. Sterol analysis was carried out on a 2-metre long glass column containing a non-polar stationary phase which consisted of 100 - 120 mesh Chromosorb W-Hp coated with 3% SE-30. The operating conditions were: oven temperature, 245°C , and injector/detector temperature 270°C , and carrier gas nitrogen at a pressure of 320 kN/m^2 .

Analysis of fatty acid methyl esters was on a 1-metre glass column packed with 3% SE-30 on 100 - 120 mesh Chromosorb W-Hp. The operating conditions were: oven temperature 180°C and injector/detector temperature 200°C and carrier gas nitrogen at a pressure of 280 kN/m^2 .

2.4 SPECTROSCOPIC EXAMINATION

Ultraviolet spectra were measured for solutions in methanol with or without the addition of sulphuric acid using a Perkin-Elmer 550S UV-VIS double beam recording spectrophotometer.

Infrared spectra were recorded for thin oily films and for potassium bromide discs using a Unicam SP 200 G grating Infrared Spectrophotometer.

Electron impact mass spectra were recorded either on an AEI MS12 or a VG7070E mass spectrometer at ionising potentials of 12 and 70 eV.

Field desorption mass spectra were determined by Mr. M. Rossiter at the Department of Chemistry, University College Cardiff, Using a Varian CH-5D Mass Spectrometer on-line to a Varian 621 1 computer.

Chemical ionisation mass spectra were determined on a VG 7070E mass spectrometer using isobutane as the reagent gas.

Fast atom bombardment mass spectra were determined on a VG 7070E mass spectrometer fitted with an FAB source using argon as the reagent gas.

Proton magnetic resonance (^1H -NMR) spectra at 100 MHz were recorded on a JEOL PS 100 NMR spectrometer, and the 220 MHz ^1H -NMR spectra were recorded at the Physico-Chemical Measurements Unit, Harwell. ^{13}C -NMR spectra were recorded on a JEOL FX 90Q Fourier Transform NMR Spectrometer. The ^1H -NMR spectra of polar compounds were determined in D_2O with DSS (sodium 2,2-dimethyl-2-silapentane-5-sulphonate, $\text{Me}_3\text{SiCH}_2\text{CH}_2\text{CH}_2\text{SO}_3\text{Na}$) as internal standard ($\delta_{\text{H}} = 0.00$) whilst the spectra of non-polar compounds were determined in suitable deuteriated organic solvents using TMS (tetramethylsilane, $\text{Si}(\text{CH}_3)_4$) as an internal standard ($\delta_{\text{H}} = 0.00$). ^{13}C -NMR spectra of the non-polar compounds were also recorded in suitable deuteriated organic solvents with TMS ($\delta_{\text{C}} = 0.0$) as internal standard but for the polar compounds, D_2O was used as the solvent with methanol ($\delta_{\text{C}} 49.5$) or dioxan ($\delta_{\text{C}} 67.4$) as internal standard.

2.5 PREPARATION OF FATTY ACID METHYL ESTERS⁹⁸

To an aliquot of fatty acid solution in 1 ml of toluene in a centrifuge tube was added 14% Boron trifluoride-methanol reagent in the proportion 1 ml reagent per 25 mg of lipid, and the tube was tightly stoppered. The tube was then heated in a boiling water bath for 5 - 10 minutes, cooled and opened. Water (10 ml) was added and the esters extracted with n-hexane (2 x 10 ml). The organic extract was dried over anhydrous sodium sulphate and the solvent removed with a stream of

nitrogen. Where necessary, further purification was achieved by preparative TLC on silica gel H with toluene as the mobile phase.

2.6 SYNTHESES OF POTASSIUM SULPHATE ESTERS OF PHENOL AND BENZYL ALCOHOL⁹⁹

Phenol (1.9 g, 0.02 mole) was dissolved in pyridine (20 ml) and pyridine-SO₃ complex (3.2 g, 0.02 mole) was added slowly to the solution with continuous stirring. After addition of the pyridine-SO₃ complex the reaction mixture was stirred continuously overnight at room temperature. Excess solvent was evaporated *in vacuo* at 35°C. The syrupy residue was treated with a solution containing potassium carbonate (3 g) in water (60 ml) until there was no more effervescence, at which point the conversion of -SO₃H to -SO₃K was judged to be complete. After stirring for a further 30 min, the solvent was again removed *in vacuo* at 35°C and the resulting solid residue was extracted three times with boiling ethanol followed by hot filtration. Crystallization from the hot filtrate commenced almost immediately. After an hour in the refrigerator the crystalline solid was collected by filtration and purified further by recrystallization from the same solvent to give colourless flakes (Yield 43.2 percent).

2.6.1 Phenyl Sulphate, potassium salt (97)

Infrared spectrum (KBr) in Fig. 2.2.

$^1\text{H-NMR}$ in D_2O (δ , ppm) with DSS as internal standard:

7.24 - 7.60 (complex asymmetric multiplet unlike that of phenol)

$^{13}\text{C-NMR}$ in D_2O (δ , ppm) with dioxan as internal standard:

151.63 (s), 130.62 (d), 126.94 (d), 122.28 (d).

(Off-resonance multiplicities in parentheses).

2.6.2 Benzyl sulphate, potassium salt (98)

The potassium sulphate ester of benzyl alcohol was prepared by the same method used for phenyl sulphate, potassium salt, and also recrystallized from boiling ethanol to give colourless flakes (Yield 44.6 percent).

Infrared spectrum (KBr) in Fig. 2.3.

$^1\text{H-NMR}$ in D_2O (δ , ppm) with DSS as internal standard:

4.92 (2H, s), 7.40 (5H, m). (Compared with δ 4.55 (2H, s), 7.40 (5H, m) and 5.28 (1H, s, exchanged on D_2O shake) for benzyl alcohol in DMSO)

$^{13}\text{C-NMR}$ in D_2O (δ , ppm) with dioxan as internal standard:

137.45 (s), 128.07 (d), 127.53 (d), 127.42 (d), 67.88 (t).

(Off-resonance multiplicities in parentheses).

Fig. 2.2 Infrared spectrum of phenyl sulphate, potassium salt

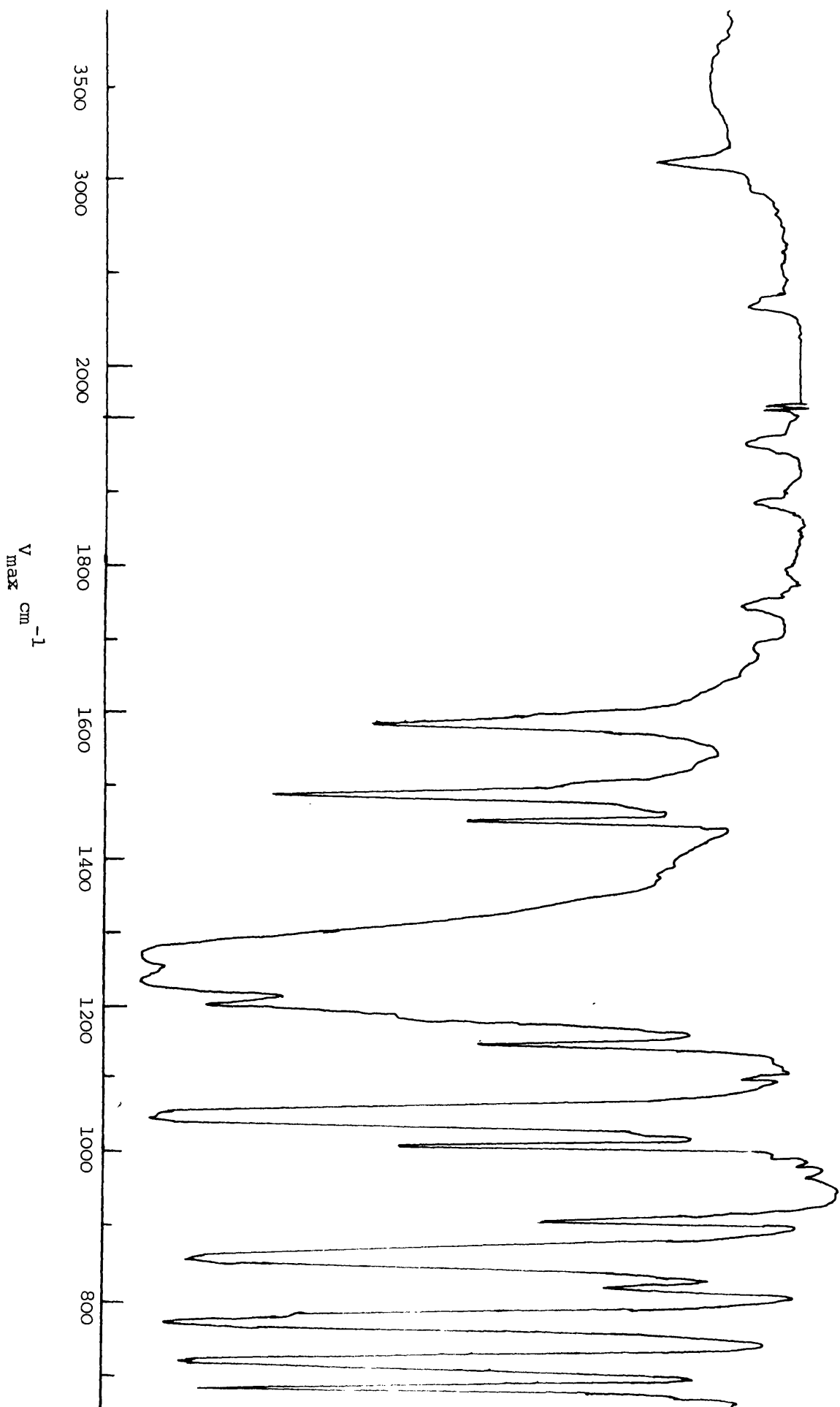
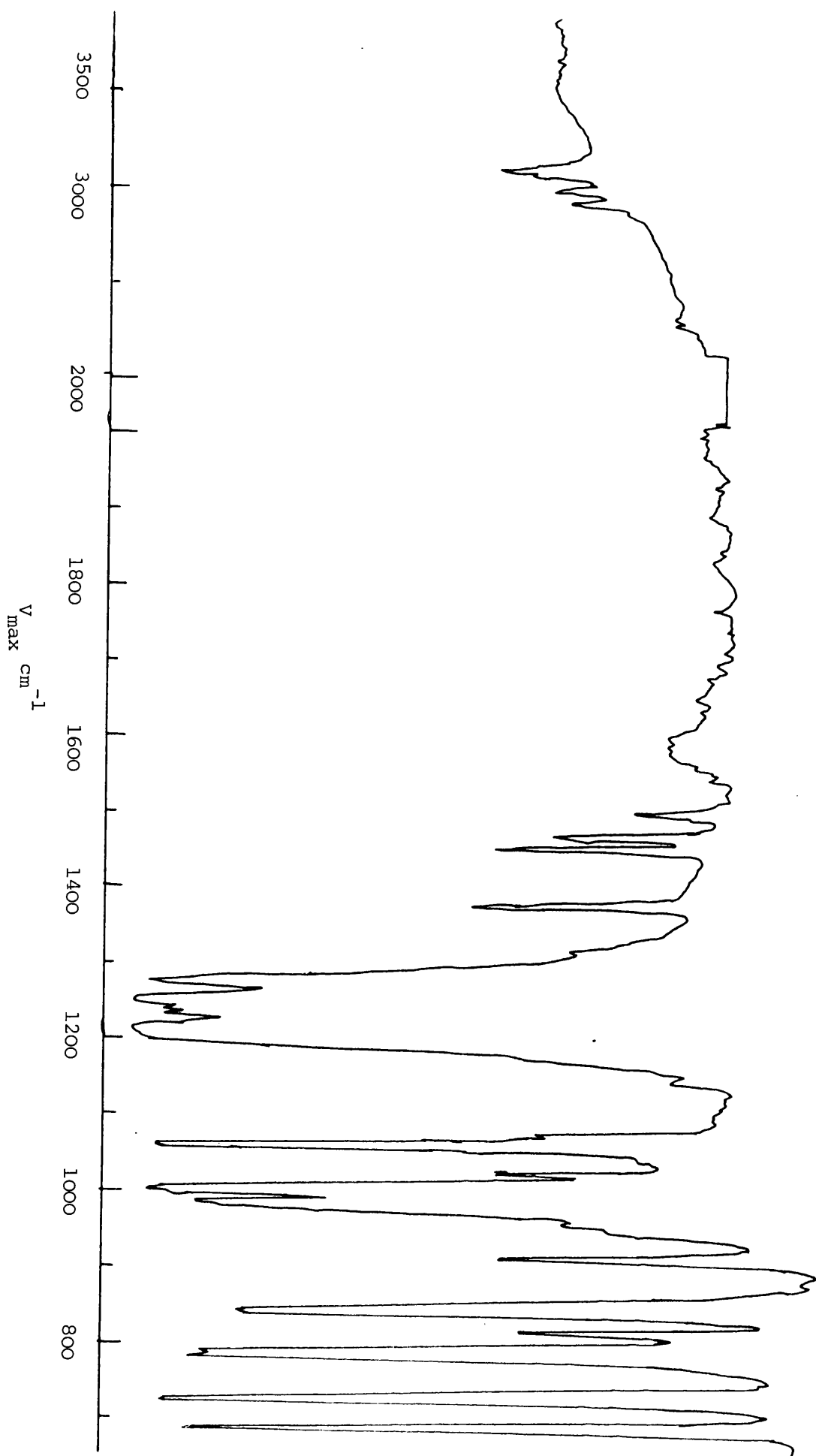


Fig. 2.3 Infrared spectrum of benzyl sulphate, potassium salt



SECTION B

SCREENING FOR ANTIBACTERIAL ACTIVITY

Many marine organisms are known or thought to contain biologically active substances and as such a serious consideration in the chemical investigation of marine natural products is that of screening so that attention can be directed to the likely sources of biologically active substances. Biological assays of extracts permit a rapid check of an array of substances which might be difficult or time-consuming by other methods. In situations where activity is detected, such assays could form the basis for an activity-directed chemical investigation which may be rewarded by the isolation and characterisation of the active substance(s). However, lack of demonstrable activity may not necessarily mean the absence of active substances and may be an indication that the bioassay procedure is inadequate or inappropriate.

Many species of seaweeds are known to display antimicrobial activities and active principles have been isolated and characterised on the basis of microbiological screening results. Using four species of bacteria as test organisms extracts of the seaweeds shown in Table 2.XXI. were screened for antibacterial activity.

2.7 PREPARATION OF TEST SAMPLES

All the seaweed samples were stored at -20°C prior to extraction. The frozen samples were thawed, rinsed briefly

Table 2.XXI. Species of seaweeds tested for antibacterial activity.

Class	Species	Place and time of collection
Rhodophyceae	<i>Laurencia pinnatifida</i>	Portland, May
	<i>Lomentaria articulata</i>	Portland, May
	<i>Corallina officinalis</i>	Kimmeridge, June
	<i>Palmaria palmata</i>	Kimmeridge, June
	<i>Polysiphonia lanosa</i>	Kimmeridge, June
	<i>Ceramium rubrum</i>	Dawlish, August
	<i>Chondrus crispus</i>	Kimmeridge, June
	<i>Halopteris scoparia</i>	Kimmeridge, June
	<i>Cystoclonium purpureum</i>	Dawlish, August
Phaeophyceae	<i>Laminaria saccharina</i>	Kimmeridge, June
	<i>Desmarestia ligulata</i>	Dawlish, August

in distilled water and allowed to air-dry overnight at room temperature. The half-dried samples were extracted three times at room temperature with a mixture of chloroform and methanol, and twice for two hours with boiling 80 percent aqueous methanol. The combined extracts were eventually divided into water-soluble, ether-soluble neutral and ether-soluble acidic extracts using the general procedures described previously. After removal of solvents *in vacuo*, the different extracts were separately made up into solutions containing 50 mg of extract per ml. The test solutions containing the water-soluble extracts were made up in distilled water whilst those containing the non-polar extracts were made up in diethyl ether. Pure samples of the two solvents were used as controls. The actual microbiological tests were carried out as a service by the Department of Pharmaceutical Microbiology.

2.8 RESULTS AND DISCUSSION

The results of the antibacterial assays of the algal extracts are shown in Table 2.XXII. The ether-soluble acidic extracts of all the species of seaweeds examined exhibit considerable activity against *Alcaligenes faecalis*, *Bacillus cereus* and *Staphylococcus aureus* but only the ether-soluble acidic extract of *Palmaria palmata* was equally active against *Pseudomonas aeruginosa*. All the ether-soluble

Table 2.XXII. Antibacterial activity of algal extracts

Extracts		Test organisms			
		<i>Alcaligenes faecalis</i>	<i>Bacillus cereus</i>	<i>Staphylococcus aureus</i>	<i>Pseudomonas aeruginosa</i>
<i>Laurencia pinnatifida</i>	W N A	- - +	- - +	- - +	- - -
<i>Lomentaria articulata</i>	W N A	- - +	- - +	- - +	- - -
<i>Coralina officinalis</i>	W N A	- - +	- - +	- - +	- - -
<i>Palmaria palmata</i>	W N A	- + +	- - +	- - +	- - +
<i>Polysiphonia lanosa</i>	W N A	- - +	- - +	- - +	- - -
<i>Ceramium rubrum</i>	W N A	- - +	- - +	- - +	- - -
<i>Chondrus crispus</i>	W N A	- - +	- - +	- - +	- - -
<i>Halobacteris</i>	W	-	+	-	-

Table 2.XXII. Continued

Extracts	Test organism			
	<i>Alcaligenes faecalis</i>	<i>Bacillus cereus</i>	<i>Staphylococcus aureus</i>	<i>Pseudomonas aeruginosa</i>
<i>Cystoclonium purpureum</i>	W -	-	-	-
	N -	+	-	-
	A +	+	+	-
<i>Laminaria saccharina</i>	W -	-	-	-
	N -	-	-	-
	A +	+	+	-
<i>Desmarestia ligulata</i>	W -	-	-	-
	N -	-	-	-
	A +	+	+	-

W = water soluble extract;

N = ether soluble neutral extract;

A = ether-soluble acidic extract

+ = positive

- = negative

neutral extracts showed no observable activity against the four test organisms except for *Cystoclonium purpureum* which was active against *Bacillus cereus*. Similarly all the water-soluble extracts were inactive except for *Halopteris scoparia* which showed activity against *Bacillus cereus*.

Previous reports on the antimicrobial activity of marine algae were based on test results using ethereal extracts¹⁵³ and samples of thallus¹⁵⁴. On the whole the results presented here are in agreement with previous findings that the production of antibacterial substances is widespread among algae. In many cases the antibacterial effect has been attributed to non-specific inhibition by such substances as organic acids¹⁵⁵. The lower fatty acids fraction has been shown to contain antibacterial components¹⁵⁶. The most active of these is acrylic acid. In addition, other substances such as terpenoid-lactones¹⁵⁷ and phenols¹⁵⁸ have been implicated.

It was envisaged that the screening of a variety of seaweeds for antibacterial activity would give results that could form a basis for an activity-directed chemical investigation. From this point of view, the results obtained were found to be of little help since antibacterial activity was mostly confined to the ether-soluble acidic extracts and probably attributable to acrylic acid and phenols which are known to be of widespread occurrence in algae. Moreover, such an activity-directed chemical investigation

would detect only those compounds with a specific activity, and other compounds with different pharmacological activities or those that may be interesting from structural, physiological or taxonomic viewpoint would probably be overlooked. For these reasons, the idea of an activity-directed chemical investigation was not pursued further. The basic strategy adopted in this study was that of a random chemical investigation which, though time consuming, was directed at detecting any compounds with interesting structural features irrespective of their biological activity.

CHAPTER THREE

POLYSIPHONIA LANOSA

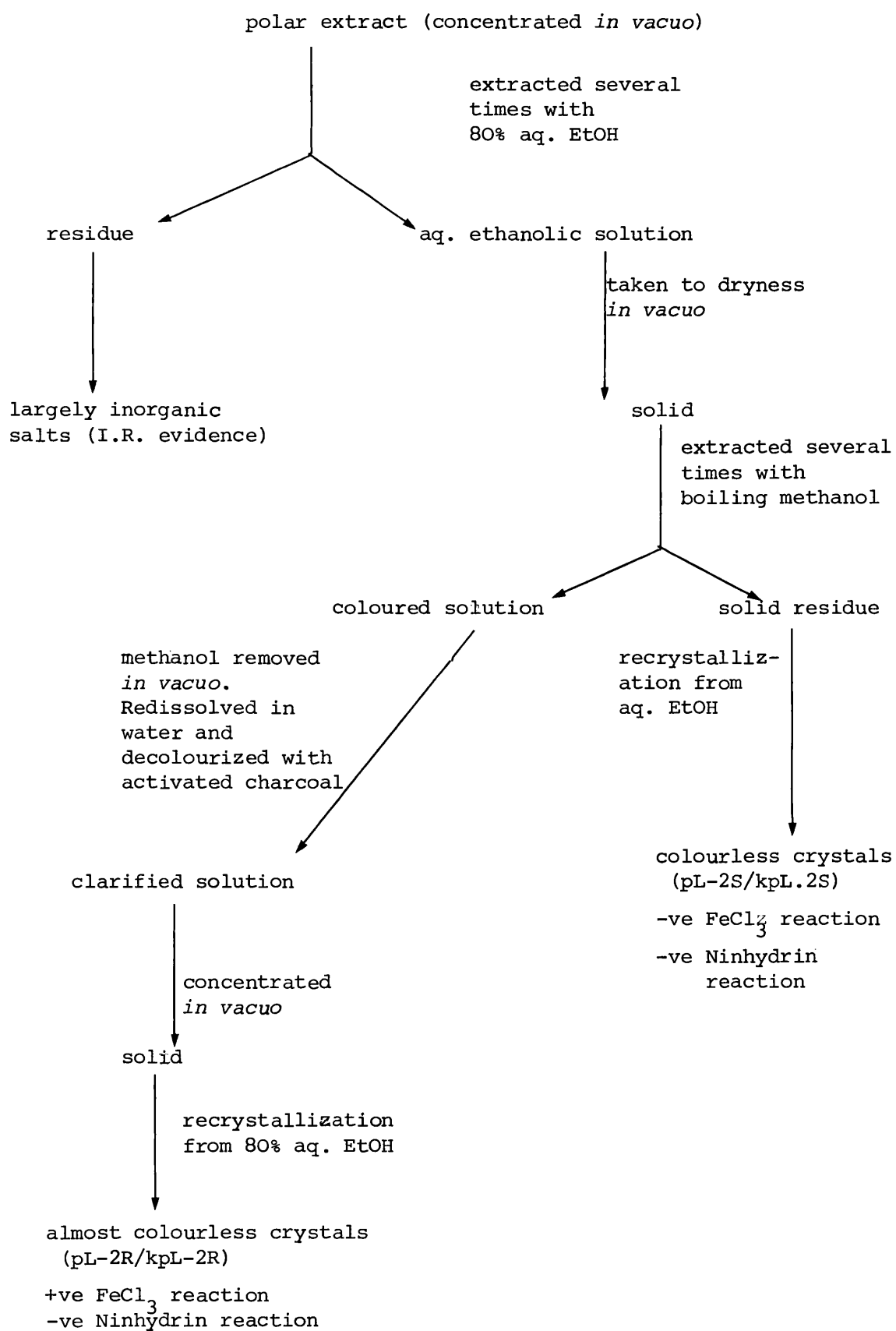
3.1 EXTRACTION AND ISOLATION OF WATER-SOLUBLE COMPOUNDS

The red alga *Polysiphonia lanosa* (Rhodomelaceae) was collected from two different locations:-

- a) Berwick-on-Tweed (North Sea),
September 1979.
- b) Kimmeridge Bay (English Channel),
June 1982.

The sample from Berwick-on-Tweed was stored in ethanol immediately after collection and subsequently extracted several times with more ethanol and with 80 per cent aqueous ethanol at room temperature. After removal of the ethanol *in vacuo* at 45°C, the extract was partitioned between diethyl ether and water to give non-polar and polar extracts respectively.

The Kimmeridge Bay sample was, after collection, transported fresh to the laboratory and stored in a deep freeze at -20°C for about seven months prior to extraction. The sample was thawed, rinsed briefly in distilled water and dried overnight at room temperature. The half-dried alga was then extracted successively at room temperature, twice with chloroform-ethanol (1:2) for 24 hours and three times with 70 percent aqueous ethanol for 24 hours. The combined extract was concentrated under reduced pressure at 45°C. The concentrated extract was partitioned between diethyl ether and water to give non-polar and polar extracts respectively. The polar extract of each batch was subsequently treated as shown in the flow diagram (Fig. 2.4).

Fig. 2.4. Extraction flow-diagram for Polysiphonia lanosa

3.2 CHARACTERISATION OF SODIUM 2'-(1-O- α -D-MANNOPYRANOSYL)

GLYCERATE

3.2.1 Analytical data on KPL-2S

PL-2S and KPL-2S (Fig. 2.4) were isolated from the Berwick-on-Tweed and Kimmeridge Bay samples respectively. The two compounds were found to be identical in all respects.

Melting point, 252-264°C (with decomposition)

Infrared (KBr): Fig. 2.5.

¹H-NMR, 220 MHz and 100 MHz in D₂O (δ , ppm) with DSS as internal standard:

4.86 (1H, d, J = 1.6 Hz),

4.18 (1H, dd, J = 3.5, 6.0 Hz)

4.06 (1H, dd, J = 1.6, 3.0 Hz)

3.60 - 4.00 (7H, complex multiplet) (See Fig. 2.8).

¹³C-NMR in D₂O (δ , ppm from TMS) with methanol as internal standard (δ_c MeOH = 49.5):

177.30 (s), 99.07 (d), 78.43 (d), 73.50 (d), 70.95 (d),

70.68 (d), 67.32 (d), 63.64 (t), 61.47 (t).

(Off-resonance multiplicities in parentheses).

Mass Spectrum: The electron impact mass spectrum of KPL-2S gave a poorly resolved spectrum which suggested that the compound was probably a salt.

[+]⁺ ION FAB: m/z (relative intensity),

313 $[M + Na]^+$ (24), 291 $[M + H]^+$ (21)

207 (85), 115 (100),

(Peak at m/z 207 and 115 are attributable to (2glycerol + Na)

and (glycerol + Na) respectively).

[\leftarrow] ION FAB : $\underline{m/z}$ (relative intensity),
 \vdots
 289 [$M - H$] $^{-}$ (83), 267 [$M - Na$] $^{-}$ (100),
 105 [$M - Na - C_6H_{11}O_5 + H$] $^{-}$ (61), See Fig. 2.6.

3.2.2 Ion-exchange chromatography of KPL-2S

KPL-2S (250 mg) in deionised water (3 ml) was transferred onto a short column of cation exchange resin (Dowex 50W - X8, H^{+} form) and eluted successively with deionised water and 1M ammonia solution. The deionised water eluate was concentrated *in vacuo* at 45°C to give a syrupy residue, KPL-2H (198 mg). The infrared spectrum (thin film) of the syrup was recorded almost immediately (the syrup solidified on cooling) and was found to be comparable with the spectrum of KPL-2S except for a significant shift of the carboxylate absorption band (1615 cm^{-1}) to 1710 cm^{-1} ($-COOH$).

3.2.3 Analytical data on KPL-2H

Infrared spectrum (thin film) $\nu_{\text{max}}^{\text{cm}^{-1}}$:

3350 (O-H stretch); 2930 (C-H stretch), 1710 (C=O stretch)

$^1\text{H-NMR}$, 100 MHz in D_2O (δ , ppm) with DSS as internal standard:

(Fig. 2.9).

4.92 (1H, d, $J = 1.6\text{ Hz}$), 4.45 (1H, t, $J = 3.5\text{ Hz}$),

4.06 (1H, dd, $J = 1.6, 3.0\text{ Hz}$),

3.90 (2H, d, $J = 3.5$ Hz),

3.60 - 3.85 (5H, complex multiplet).

$^{13}\text{C-NMR}$ in D_2O (δ , ppm from TMS) with methanol ($\delta_{\text{C}} 49.5$) as internal standard:

174.37 (s), 99.72 (d), 75.88 (d),

73.99 (d), 70.90 (d), 70.47 (d),

67.32 (d), 62.94 (t), 61.53 (t).

(Off-resonance multiplicities in parentheses).

Mass Spectrum: $[+]$ ION FAB: m/z (relative intensity),

291 $[\text{M} + \text{Na}]^+$ (2), 269 $[\text{M} + \text{H}]^+$ (5), 163 $[\text{C}_6\text{H}_{11}\text{O}_5]^+$ (15)

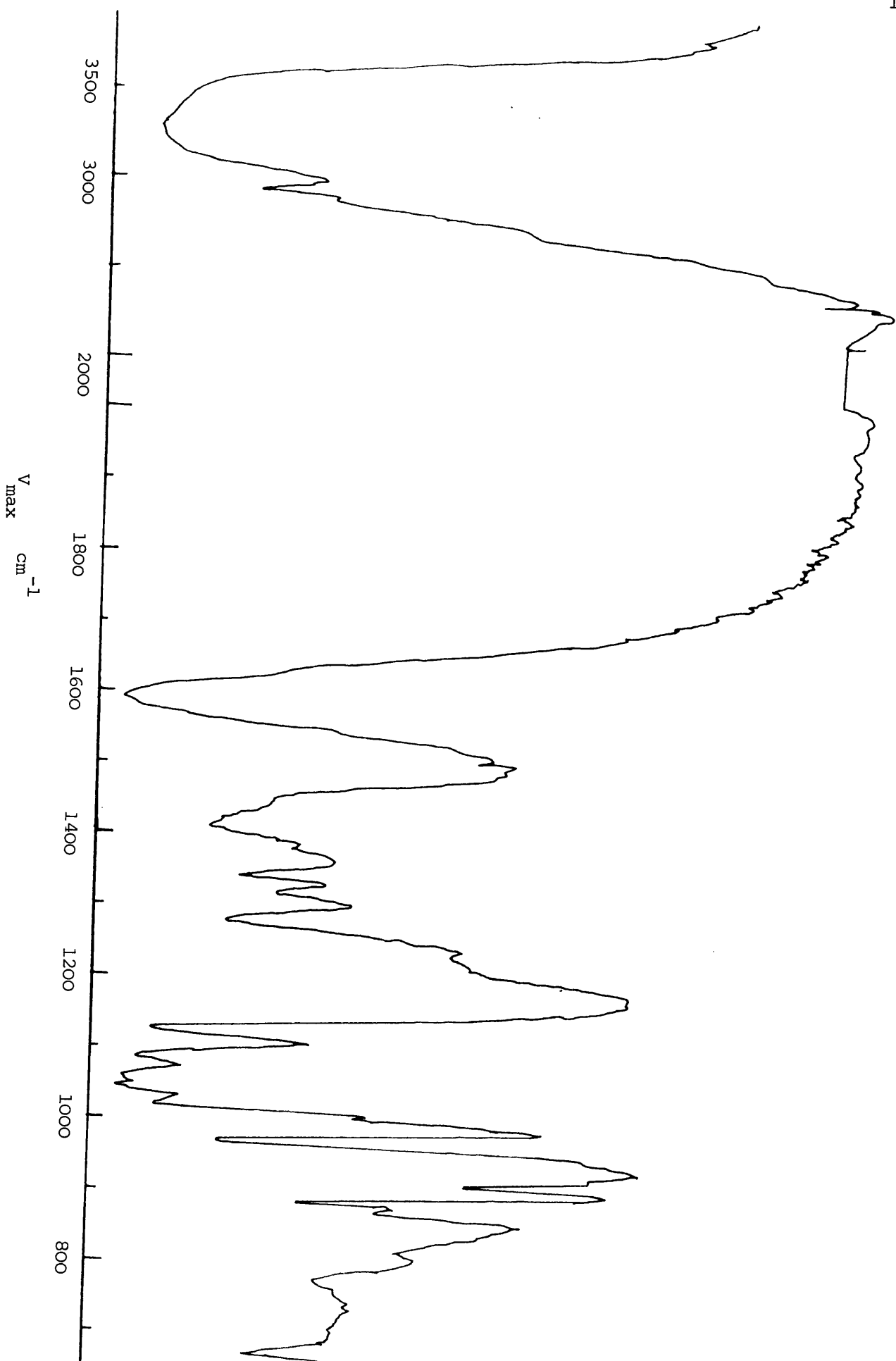
$[-]$ ION FAB: 267 $[\text{M}-\text{H}]^-$ (100), 105 $[\text{M}-\text{C}_6\text{H}_{11}\text{O}_5]^-$ (11) (See Fig. 2.7.)

3.2.4 Acid hydrolysis of KPL-2S

The mass spectral and NMR data of KPL-2S are suggestive of a glycoside structure consisting of one hexose unit and a 3-carbon acid (see discussion). Since the natural product and the corresponding free acid gave no positive ninhydrin reaction, an amino acid glycoside structure was unlikely. The behaviour of the salt on a cation exchange column confirmed that it could not be the salt of an amino acid derivative. A saturated 3-carbon hydroxy-acid immediately brings to mind, glyceric acid.

A small amount of the natural product (45 mg) was hydrolysed with 2M hydrochloric acid (10 ml) under reflux for 10 hours. The hydrolysate was diluted several times with water and

Fig. 2.5. Infrared spectrum of KPL-2S

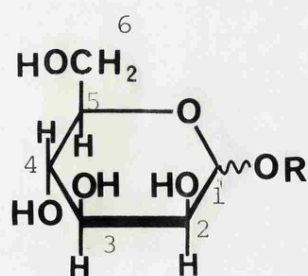


evaporated *in vacuo* over potassium hydroxide pellets. Paper chromatographic analysis of the hydrolysate was carried out using isopropanol-pyridine-water-acetic acid (8:8:4:1) as solvent, and 3% p-anisidine HCl (specific reagent for reducing sugars) and 0.01M potassium permanganate solution (non-specific reagent) as sprays, on two different but concurrently run chromatograms. D-mannose, D-glucose, D-galactose, KPL-2S and glyceric acid were used as reference substances. The hydrolysate gave two spots, identical in R_f values and colour reactions with mannose and glyceric acid. (D-mannose, R_f 0.65; glyceric acid, 0.44; KPL-2S, 0.32; D-galactose, 0.55; D-glucose, 0.58; hydrolysate, 0.65 and 0.45).

3.2.5 Discussion

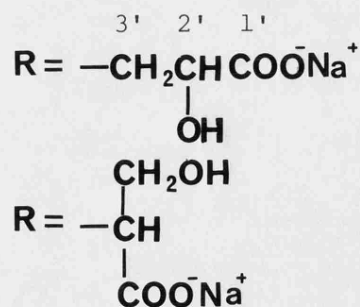
In FAB mass spectrometric measurements, compounds presented to the source in the form of alkali metal salts, for example, carboxylic acid salts of the type R.COONa, gave rise in their positive ion spectra¹⁰⁰ to $[R.COONa_2]^+$. The behaviour of KPL-2S on ion-exchange chromatography is indicative of an alkali metal salt. The pseudomolecular ion at m/z 313 $[M + Na]^+$ in the $[+]$ ion FAB spectrum is therefore of the form $[RCOONa_2]^+$. The peak at m/z 291 corresponds to $[M + H]^+$. This is in accordance with the molecular composition $C_9H_{15}O_9Na$ for KPL-2S. The peak at

m/z 289 in the $[-]$ ion FAB spectrum corresponding to $[M-H]^-$ is also in agreement with this molecular composition. Other fragments in the $[-]$ ion FAB spectrum were seen at m/z 267 and 105 corresponding to $[M-Na]^-$ and $[M-Na-C_6H_{11}O_5 + H]^-$ respectively (Fig. 2.6). The corresponding free acid KPL-2H, obtained after passage through a cation-exchange column gave a $[+]$ ion FAB spectrum with peaks at m/z 269 $[M + H]^+$ and m/z 163 $[C_6H_{11}O_5]^+$. (Here, M refers to the molecular weight of the free acid). The $[-]$ ion FAB spectrum (Fig. 2.7) furnished peaks at m/z 267 and 105 corresponding to $[M-H]^-$ and $[M-C_6H_{11}O_5]^-$ respectively. The mass spectral and infrared data as well as paper chromatographic analysis of the hydrolysis products are therefore consistent with the structure of a glycoside of mannose and sodium glycerate which can, at this stage be represented by the gross structures (99a) or (99b).



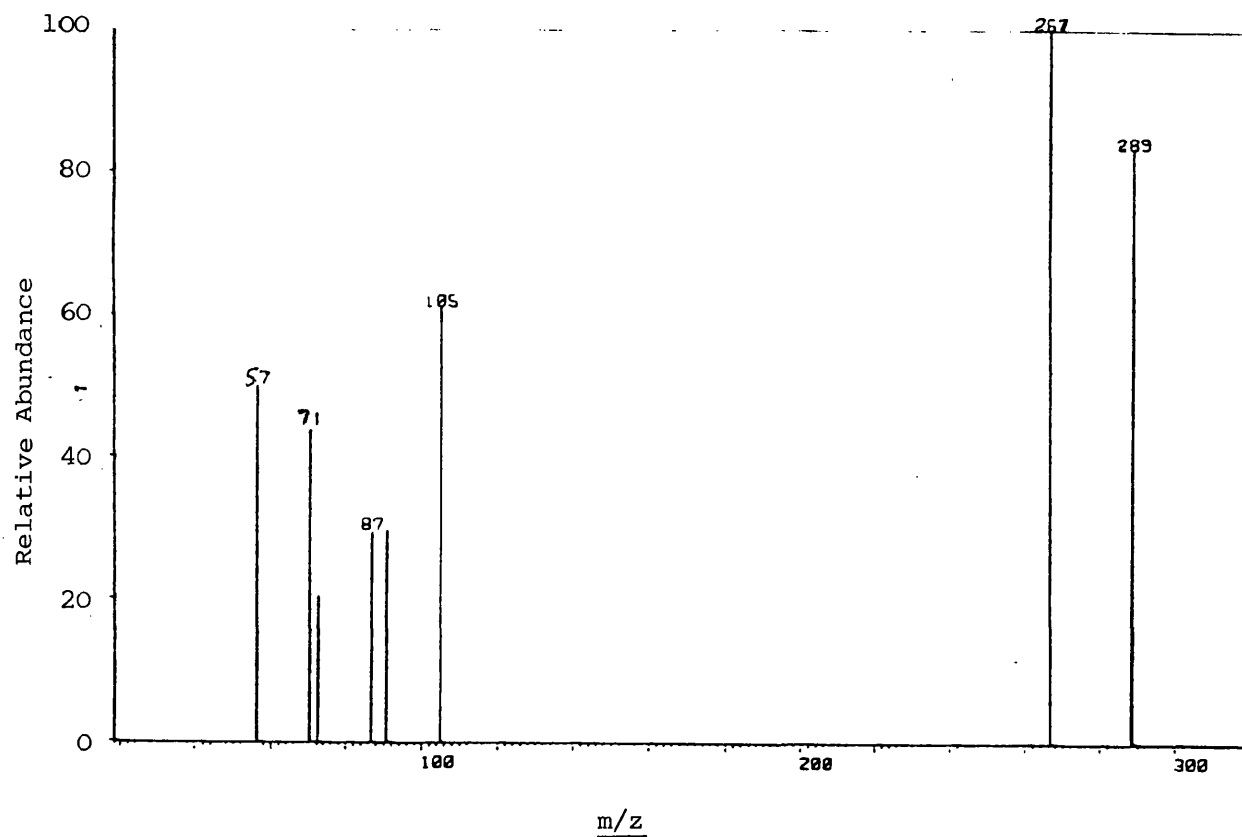
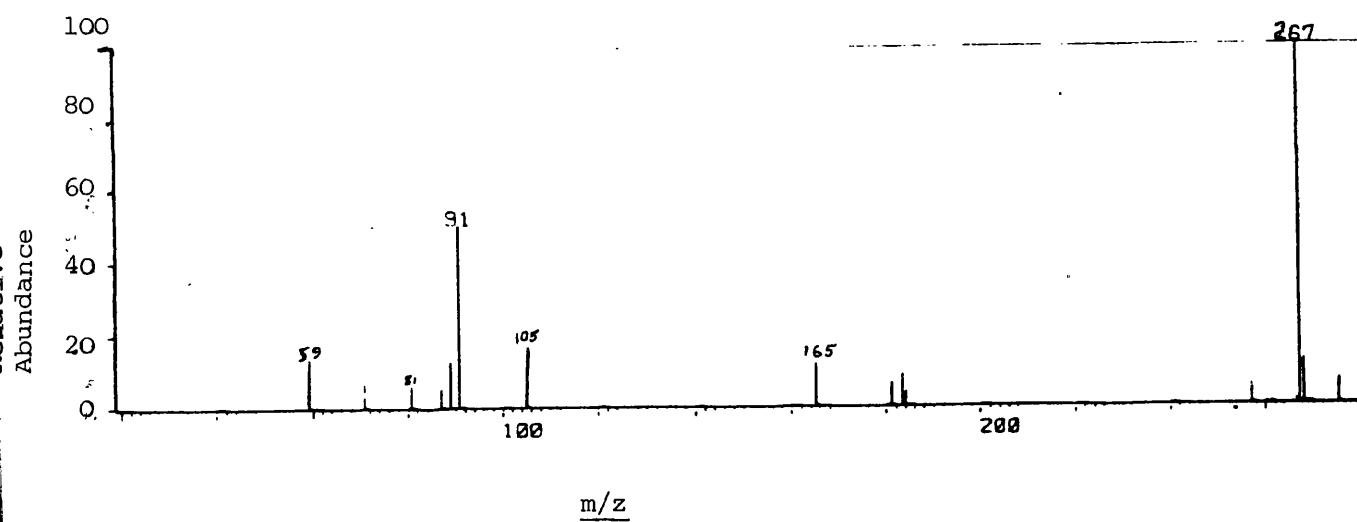
(99a)

(99b)

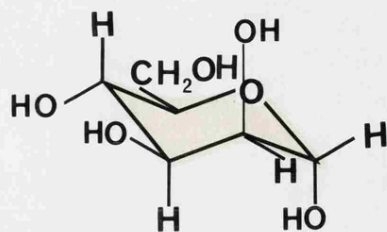


In the 1H NMR (220 MHz, Fig. 2.8) spectrum of the natural product the most downfield doublet (δ 4.86, $J = 1.6$ Hz) is immediately assignable to the anomeric proton¹⁰¹. The doublet

Fig. 2.6. KPL.2S (-)ION FAB

Fig. 2.7. KPL.2H - ION FAB
(-)ION FAB

of doublets at $\delta 4.06$ ($J = 1.6$ Hz, 3.0 Hz) was attributed to H-2 in the mannose ring structure since it has a $^3J_{1,2}$ value of 1.6 Hz and thus is coupled to the anomeric proton. The value of $^3J_{2,3}$ is therefore 3.0 Hz. On the basis of chemical shifts the signal at $\delta 4.18$ (1H, dd, $J = 3.5$, 6.0 Hz) may be due to the methine proton of the glycerate moiety. The doublet of doublet splitting would imply that the methylene protons of the glycerate moiety are chemically inequivalent. It is, however, noteworthy that after conversion of the salt to the free acid by passage through a cation-exchange column, the methine proton of the glyceric acid moiety gave a triplet ($\delta 4.45$, $J = 3.5$ Hz) and the methylene protons, a two-proton doublet ($\delta 3.90$) with $^3J_{2,3}$ value of 3.5 Hz (Fig. 2.9). This implies that both methylene protons now display chemical equivalence. A comparison of the ^1H -NMR data with the ^1H -NMR parameters¹⁰¹ for a number of hexoses in D_2O provide further supportive evidence that the sugar component of the glycoside is mannose especially with regards to the small coupling constant between the anomeric proton (H-1) and H-2. In α -D-mannopyranose (100a) $^3J_{1,2}$ has a value of 1.7 Hz while in β -D-mannopyranose (100b) $^3J_{1,2} = 1.0$ Hz. In the former there is an equatorial-equatorial and in the latter case an axial-equatorial relationship between H-1 and H-2.

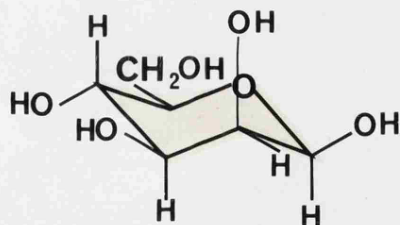


(100a)

 α -D-mannopyranose

$$^3J_{1,2} = 1.7 \text{ Hz}$$

The configuration at C-1 for mannose derivatives can only be assessed by accurate measurement of the spacing of the anomeric proton signal. A 220 MHz ^1H -NMR spectrum of the natural



(100b)

 β -D-mannopyranose $^3J_{1,2} = 1.0 \text{ Hz}$

product provided adequate information in this regard. The observed $^3J_{1,2}$ value was 1.6 Hz and is indicative of the α -anomeric form of the mannose moiety.

Fig. 2.8. 220 MHz ^1H -NMR spectrum of KPL.2S in D_2O

DOH

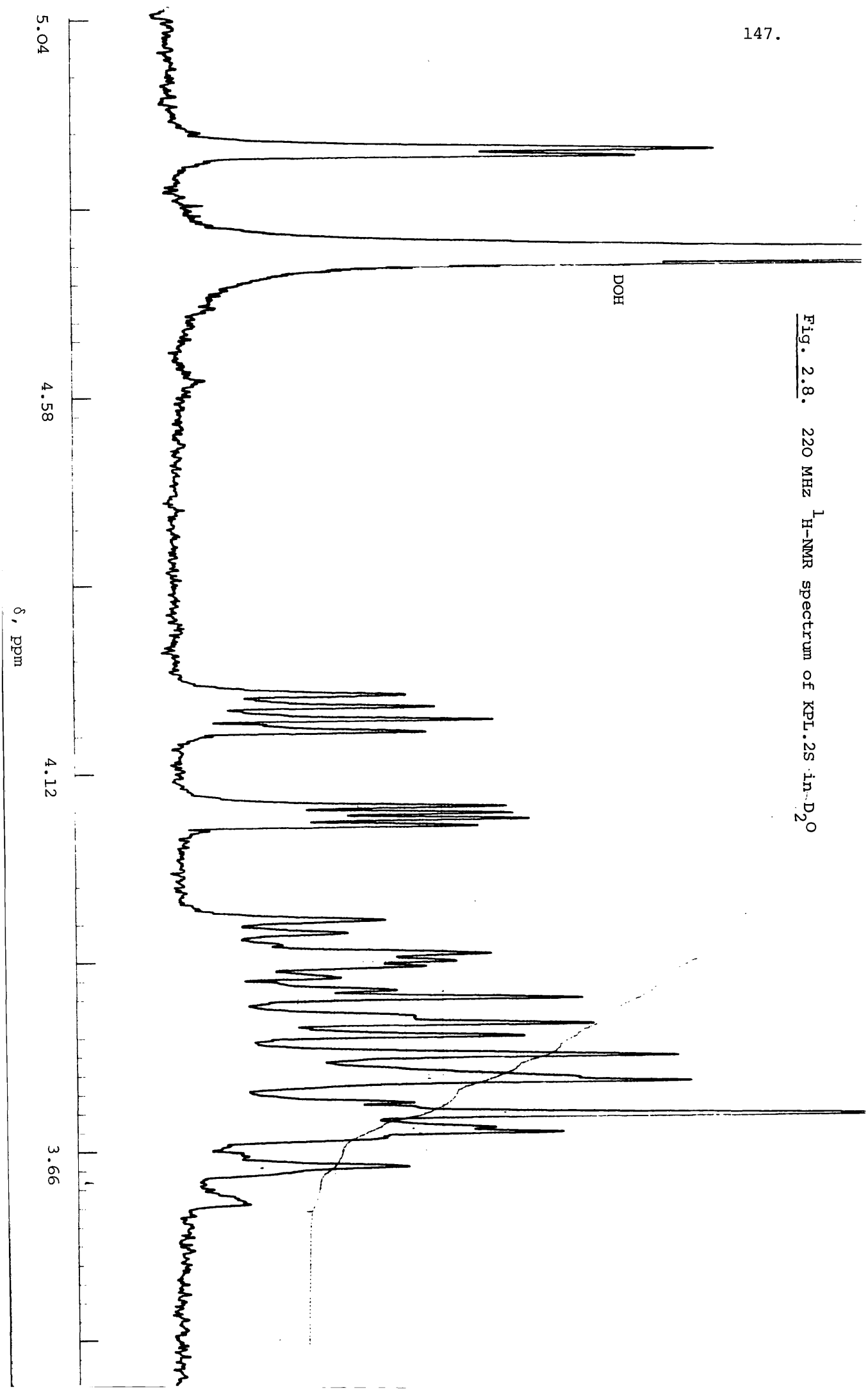
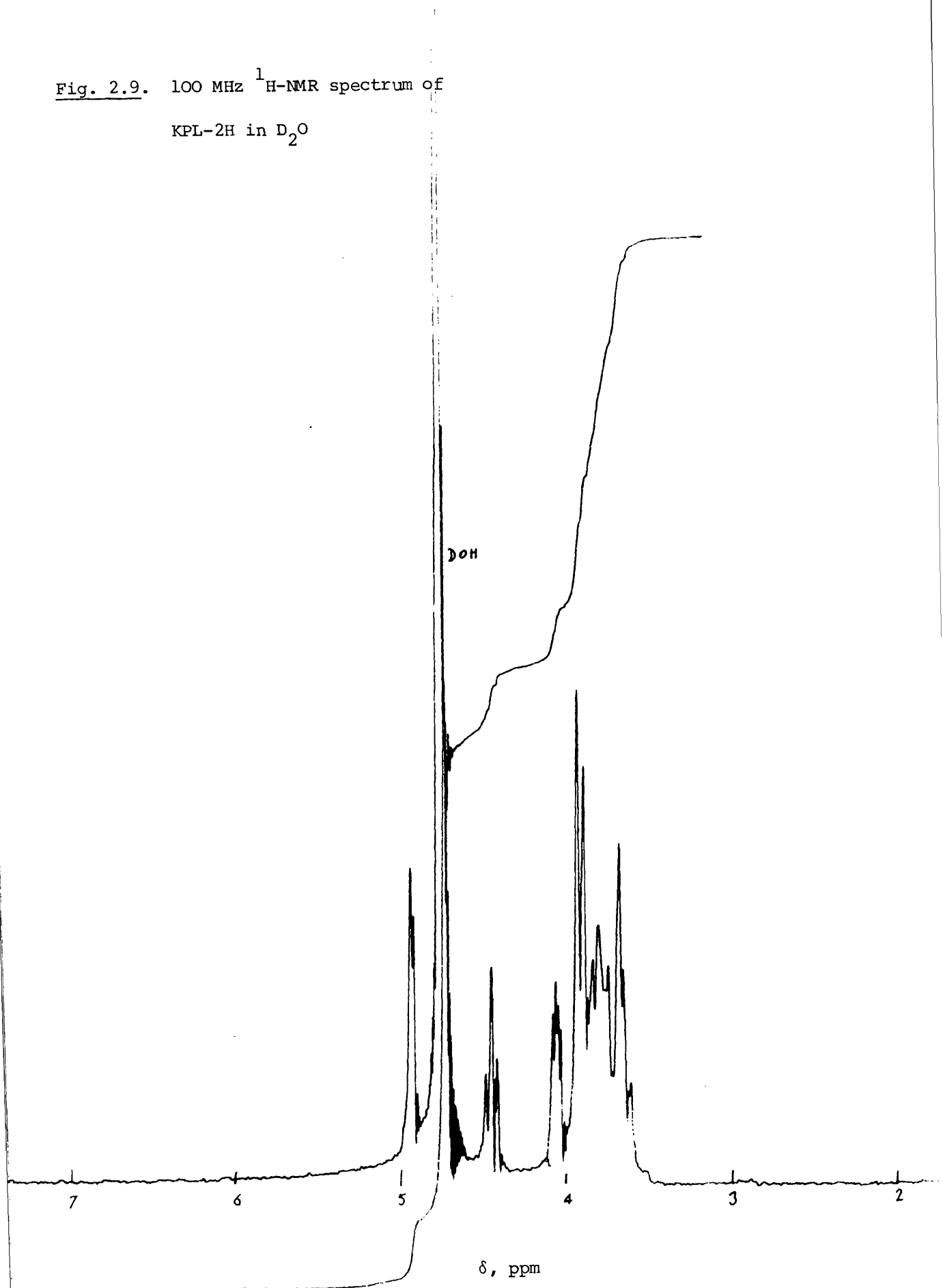


Fig. 2.9. 100 MHz ^1H -NMR spectrum of
KPL-2H in D_2O



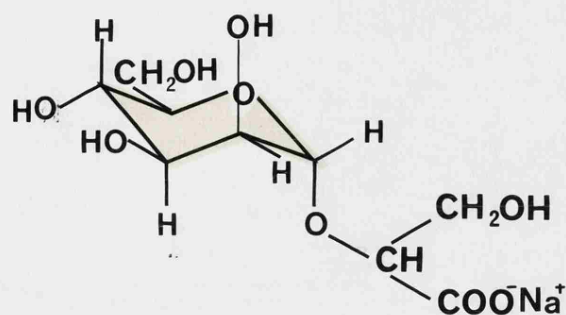
A combination of ^1H - and ^{13}C -NMR techniques have proved to be effective tools for the elucidation of the more subtle features of polysaccharides¹⁰². The ^{13}C -NMR data for the natural product were compared with those of a variety of methyl glycosides¹⁰³. There was very good agreement with α -methylmannoside (Table 2.1) except for the expected differences in the C-1 shifts since the C-1 in mannopyranosyl glycerate will experience additional γ -shielding due to the presence of the glycerate moiety and will thus resonate at higher field than that of methylmannoside.

Having deduced that the natural product is a glycoside of α -D-mannose and sodium glycerate it remains to determine the position of linkage. It was observed that the chemical shift of the C-2' in the natural product was 4.0 ppm (δ 78.4) downfield of the corresponding carbon resonance in glyceric acid hemi-calcium salt (δ 74.4) whereas the C-1' and C-3' resonances were both high field of the corresponding carbon resonances (Table 2.1). Etherification of a hydroxyl group generally causes a downfield shift in the resonance of the carbon atom bearing the etherified hydroxyl groups. The observed differences in the ^{13}C -NMR chemical shifts of the two compounds are therefore consistent with a structure in which the α -D-mannopyranosyl moiety is linked to C-2' rather than to C-3' of the glycerate moiety. It can then be concluded that the structure of the natural product is sodium 2'-(1-O- α -D-mannopyranosyl)-glycerate (101).

Table 2.I. ^{13}C -NMR DATA (δ , ppm from TMS)^a in D_2O

	C-1	C-2	C-3	C-4	C-5	C-6	C-1'	C-2'	C-3'
1-methyl- β -D-mannoside	101.1(d)	70.4(d)	73.1(d)	66.9(d)	76.4(d)	62.1(t)	-	-	-
1-methyl- α -D-mannoside	101.5(d)	71.3(d)	70.6(d)	67.4(d)	73.2(d)	61.6(t)	-	-	-
PL-2H	99.7(d)	70.9(d)	70.5(d)	67.3(d)	74.0(d)	61.5(t)	174.4(s)	75.9(d)	62.9(t)
PL-2S	99.1(d)	71.0(d)	70.7(d)	67.3(d)	73.5(d)	61.5(t)	177.3(s)	78.4(d)	63.6(t)
$ \begin{array}{c} \text{OH} \quad \text{OH} \\ \quad \\ \text{CH}_2 - \text{CH} - \text{COO}^- \\ 2 \quad 1' \end{array} $ (as hemi calcium salt)	-	-	-	-	-	-	179.7(s)	74.4(d)	64.9(t)

a, Internal standard, methanol δ_{C} MeOH=49.5



(101)

The same structure has been assigned to a glycoside isolated from the red alga *Rhodomela larix* by Whyte¹⁰⁴. The structure was derived by interpretation of ¹H-NMR (100 MHz) spectral data of the methyl ester in D₂O and the pentacetate in CDCl₃. However, the ¹H-NMR data presented by Whyte shows appreciable differences from the data obtained in the present study.

It proved impossible to compare the two substances directly but Dr. Whyte kindly provided a copy of his original spectrum. It was notable that the DHO resonance was at δ 5.15 as opposed to δ 4.78 observed throughout the course of this work and thus it is possible that errors in chemical shift measurement were introduced by his use of TMS as an external standard. Alternatively, there is of course the possibility that the two compounds are different, possibly by having opposite configuration at the C-2' atom of the glycerate moiety. A similar situation has been reported in the structural elucidation of isofloridoside (O- α -D-galactopyranosyl-1'-glycerol)¹⁰⁵

Table 2.II $^1\text{H-NMR}$ Data (δ , ppm)

	H_1	H_2	$\text{H}_{2'}$	$\text{H}_{3'}$
PL-2S (sodium salt)	4.86 (1H, d)	4.06 (1H, dd)	4.18 (1H, dd)	*
PL-2H (free acid)	4.92 (1H, d)	4.06 (1H, dd)	4.45 (1H, t)	3.90 (2H, d)
α -D-mannopyranosyl- 2-glyceric acid (J.N.C. Whyte, 1969 ¹⁰⁴)	5.35 (1H, d)	4.49 (1H, m)	4.75 (1H, m)	*
methyl- α -D-manno- pyranosyl-2- glycerate ¹⁰⁴	5.43 (1H, d)	4.55 (1H, dd)	5.00 (1H, t)	4.40 (2H, d)

* Overlapping signals.

which was eventually found to be an isomorphous mixture of the diastereoisomeric D- and L-glycerol derivatives. This conclusion was reached by the successful synthesis of the two diastereoisomers.

The configuration of the glycerate part of sodium-2'-(1-O- α -D-mannopyranosyl)-glycerate has not been investigated. There is thus the possibility that if the two compounds are indeed different they could be the diastereoisomeric D- and L-glycerate forms. On the other hand, one could be a pure isomer of either form and the other an isomorphous mixture of the two forms. The ultimate solution probably lies in the successful synthesis of the two diastereoisomeric forms.

3.3 CHARACTERISATION OF 2,3-DIBROMO-5-HYDROXYBENZYL-1',4-DISULPHATE, DIPOTASSIUM SALT

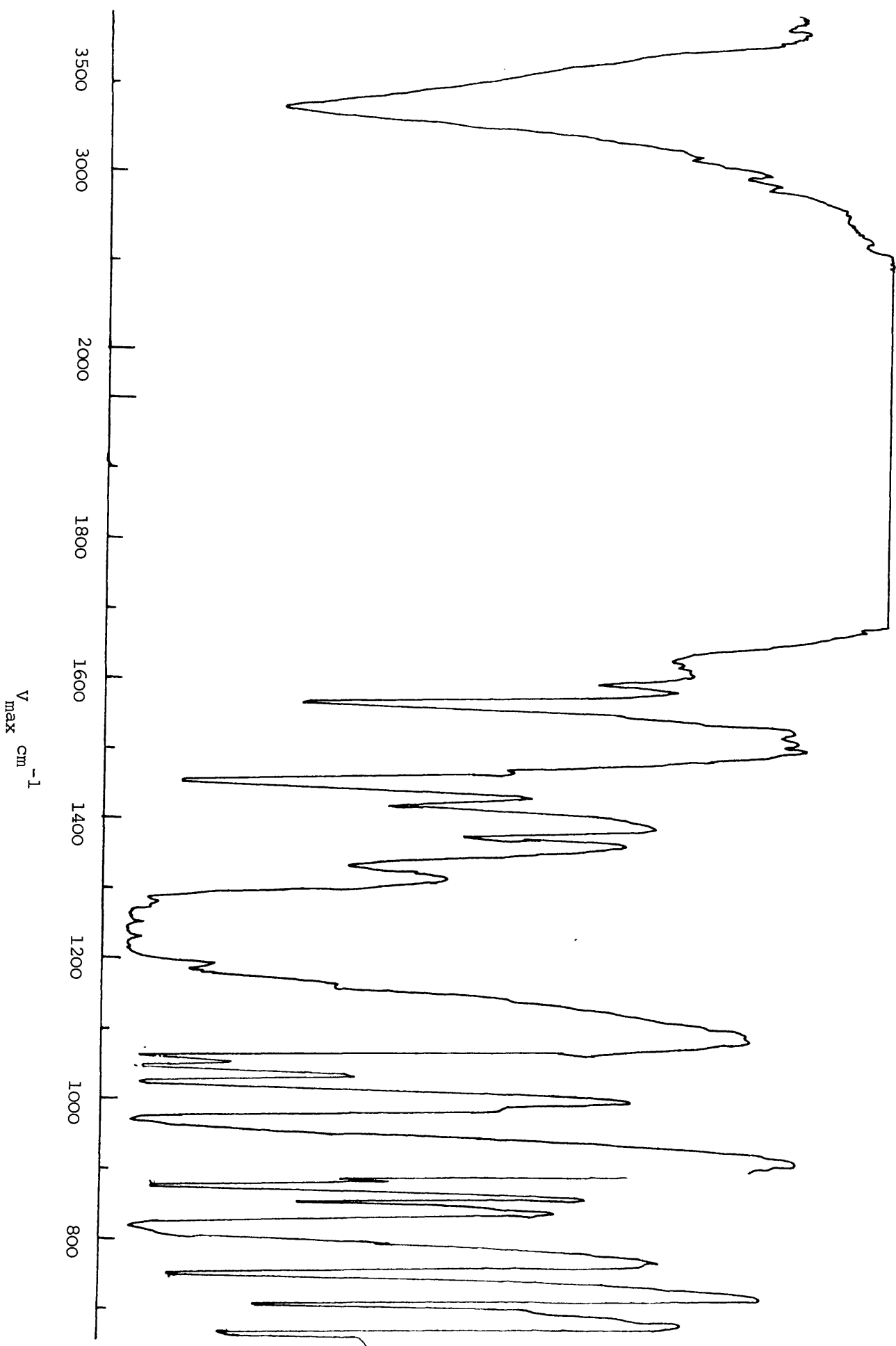
3.3.1 Analytical data on KPL-2R

KPL-2R and PL-2R (Fig. 2.4) were isolated from the Kimmeridge Bay and Berwick-on-Tweed samples respectively. Both compounds were identical in all respects. Infrared spectrum (KBr): Fig. 2.10

$^1\text{H-NMR}$, 100 MHz in D_2O (δ , ppm) with DSS as internal standard:

5.04 (2H, s), 7.16 (1H, s).

Fig. 2.10. Infrared spectrum of KPL-2R



^{13}C -NMR in D_2O (δ , ppm from TMS) with methanol (δ_{C} 49.5) as internal standard:

149.78 (s), 138.62 (s), 135.42 (s), 122.69 (s),
118.25 (d), 116.25 (s), 71.12 (t).

(Off-resonance multiplicities in parentheses)

Mass Spectrum - the E.I.M.S. of the KpL-2R did not give a molecular ion but a 1:2:1 triplet at m/z 282, 280, 278. Other prominent fragment ions were at m/z 254, 252, 250 (1:2:1), 133;131 (1:1); 82, 80 (1:1).

[$-$] ION FAB, m/z (relative intensity):

497 (21), 495 (42), 493 (21), 417 (20), 415 (21),
297 (15), 295 (30), 293 (15), 217 (22), 215 (21),
81 (100), 79 (100).

Ultraviolet spectrum $\lambda_{\text{max}}^{\text{H}_2\text{O}}$ nm (log ϵ): 290 (3.36)

$\lambda_{\text{max}}^{\text{0.1 NaOH}}$ nm (log ϵ): 250 (4.07), 310 (3.58)

3.3.2 Hydrolysis of KPL-2R

KPL-2R (200 mg) was dissolved in water (20 ml) and heated under reflux for one hour. The hydrolysate was extracted with ethylacetate. Evaporation of the organic solvent under reduced pressure left a brownish deposit which was re-crystallized from toluene-ethylacetate to give light-brownish needles, KPL-RH.

3.3.3 Analytical data on KPL-RH

Melting point, 127 - 9°C.

Infrared spectrum (KBr): Fig. 2.11

¹H-NMR, 100 MHz in CD₃COCD₃ (δ, ppm) with TMS as internal standard:

3.20 - 4.20 (3H, broad singlet, exchanged on D₂O shake),

4.60 (2H, s), 7.20 (1H, s).

¹³C-NMR in DMSO (δ, ppm) with TMS as internal standard:

144.86 (s), 142.22 (s), 133.82 (s), 115.65 (d), 114.45 (s),

112.96 (s), 64.99 (t).

(Off-resonance multiplicities in parentheses).

Mass spectrum, (E.I.M.S.): m/z (relative intensity)

300 (25), 298 (49), 296 (24), 282 (14), 280 (27),

278 (13), 254 (6), 252 (11), 250 (6), 219 (27),

217 (27), 190 (22), 188 (22).

3.3.4 Discussion

KPL-2R gave a greenish-blue colour with ferric chloride suggestive of a phenolic compound. The infrared spectrum (KBr disc) showed the presence of OH (3350 cm⁻¹), an aromatic ring (1600, 1580, 880 cm⁻¹), sulphate ester group (1295 - 1200 cm⁻¹) and no carbonyl absorption (Fig. 2.10). Mass spectrometric (FAB) measurements were in good agreement with the formula C₇H₄O₉S₂Br₂K₂. The negative ion FAB mass spectrum (Fig. 2.12) gave a 1:2:1 triplet at m/z 497/495/493 attributable to [M-K]⁻ and

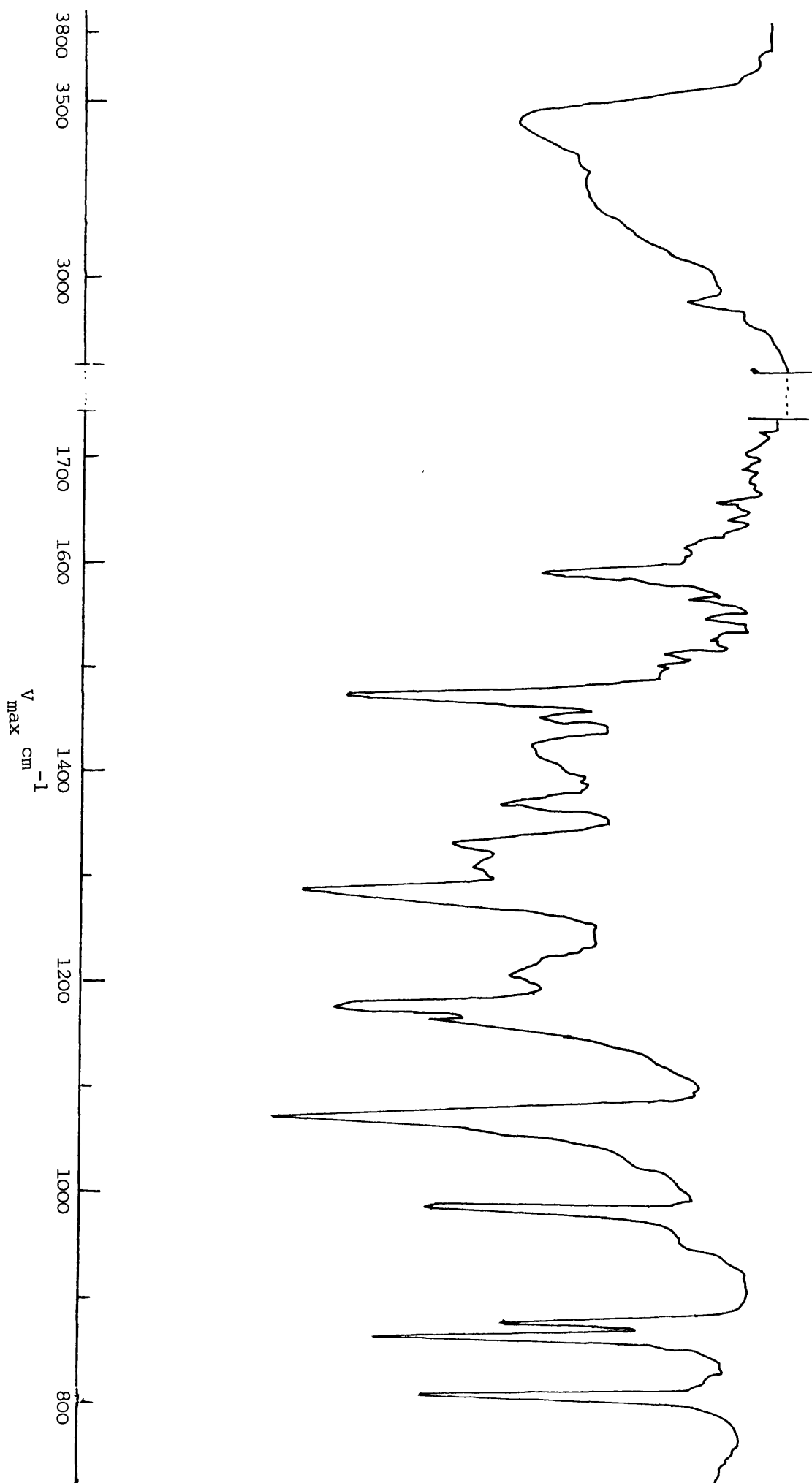


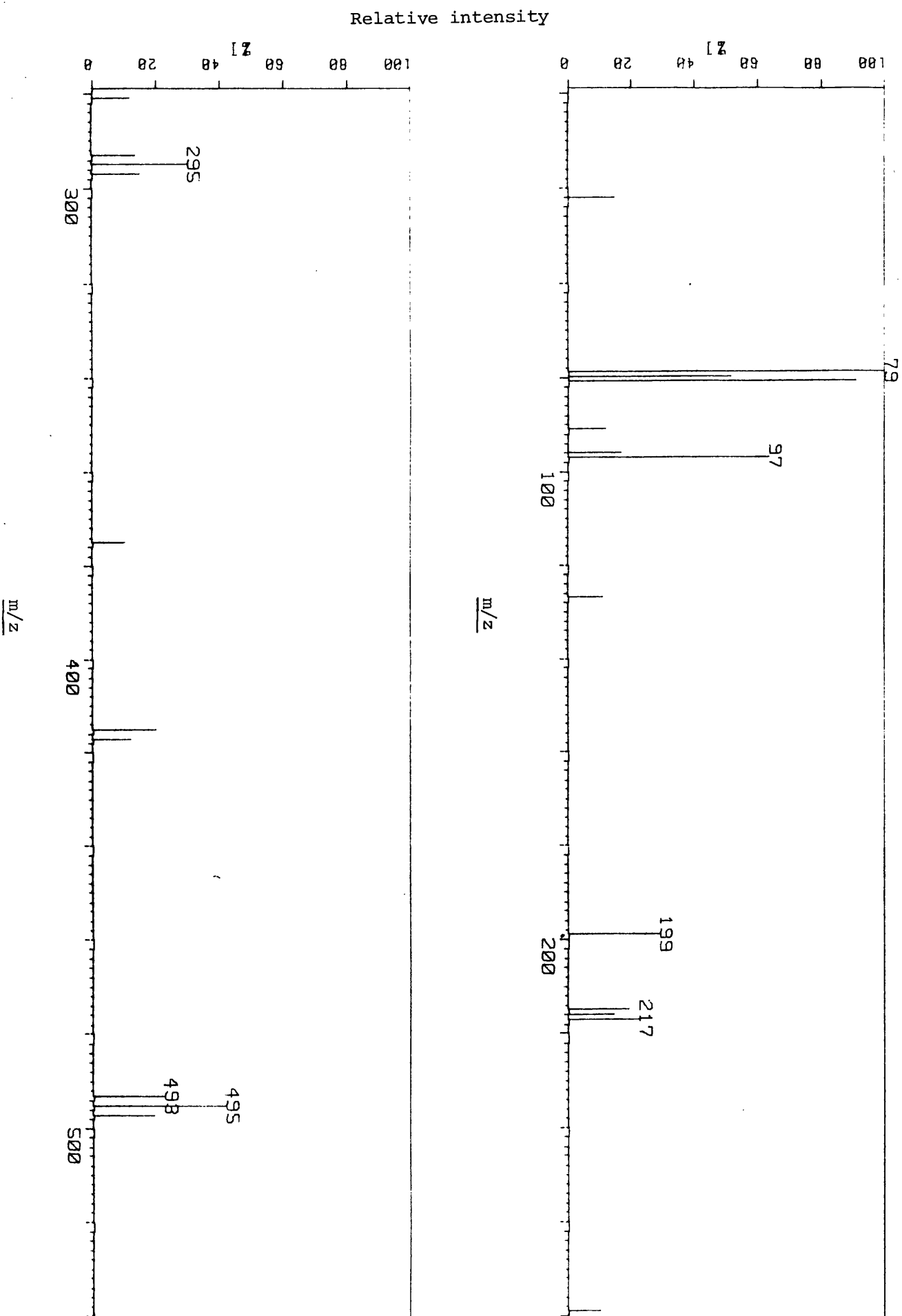
Fig. 2.11. Infrared spectrum of KPL.RH

consistent with a dibrominated compound. The fragment at m/z 471/415 corresponds to $[M-K-Br + H]^-$ and that at m/z 297/295/293 to $[M-H-2SO_3K]^-$. This fragment gives an indication of the presence of two sulphate ester groups per molecule with K^+ as the naturally occurring counter ion. The fragment with the highest m/z value (282/280/278) in the E.I.M.S. corresponds to $[M-K_2S_2O_7]^+$.

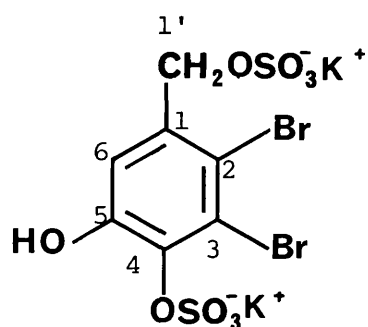
The ultraviolet spectrum was similar to that of phenolic compounds with a broad peak at $\lambda_{\max}^{H_2O}$ 290 nm which shifted to 310 nm in a basic medium. The 1H -NMR in D_2O indicated the presence of a single aromatic proton at $\delta 7.16$ and a benzylmethylene group at $\delta 5.04$ (2H, singlet). This compound was identical (UV, infrared, and 1H -NMR) with 2,3-dibromo-5-hydroxybenzyl-1',4'-disulphate, dipotassium salt (102) previously described by Hodgkin et al.¹⁰⁶ from the same algal source.

The most striking difference in the infrared spectrum of (102) and that of the hydrolysis product, (103), is the absence of the broad (strong) peak at $1295 - 1200\text{ cm}^{-1}$ due to the sulphate ester group (Figs. 2.10 and 2.11). The 1H -NMR spectrum of the hydrolysis product in CD_3COCD_3 indicated a single aromatic proton as a sharp singlet at $\delta 7.20$, a sharp two proton singlet at $\delta 4.60$ attributed to a benzylmethylene group, and three hydroxyl protons (broad singlet at $\delta 3.20 - 4.20$) exchanged on shaking with deuterium oxide. The E.I.M.S. gave a molecular ion cluster

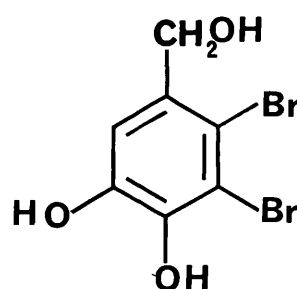
Fig. 2.12. KPL.2R (-)ION FAB



at m/z 300/298/296 as a 1:2:1 triplet, and fragments at m/z 282/280/278 attributable to $[M-H_2O]^+$ and m/z 219/217 corresponding to $[M-Br]^+$. The spectral data are consistent with the assigned structure (103) for the hydrolysis product of (102) and was identical (1H -NMR, UV, IR, M.pt) with 2,3-dibromo-4,5-dihydroxybenzylalcohol (Lanosol)^{106,107}.



(102)

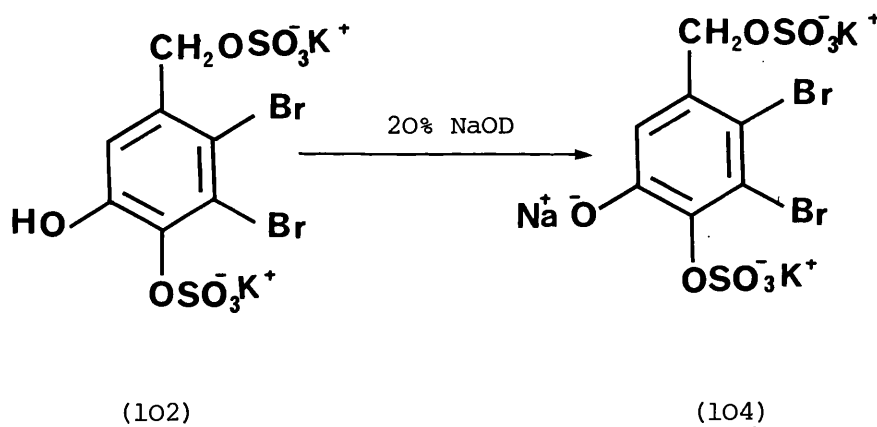


(103)

3.4 ^{13}C -NMR STUDIES ON 2,3-DIBROMO-5-HYDROXYBENZYL-1',4-DISULPHATE, DIPOTASSIUM SALT

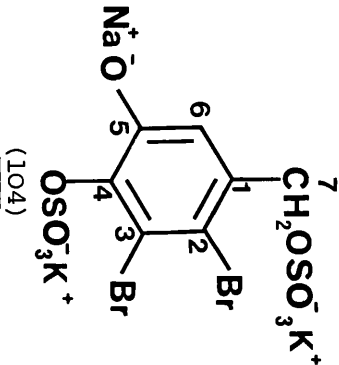
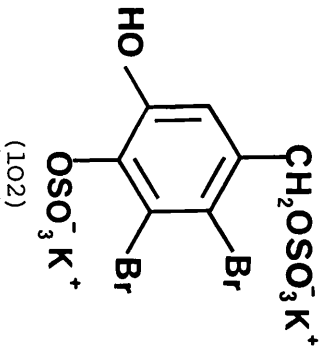
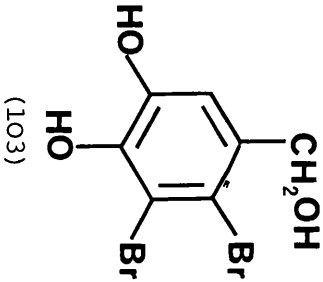
The ^{13}C -NMR spectrum of the naturally occurring phenol sulphate, potassium salt (102) in D_2O (Table 2.III) exhibited seven resonances. The off-resonance spectrum contained one triplet, one doublet and five singlets. The assignment of the high field triplet ($\delta 71.12$) to C-7 is immediately obvious. The doublet at $\delta 118.25$ was unambiguously assigned to C-6 being

the only unsubstituted aromatic carbon atom. Chemical shift assignments of C-4 (the aromatic carbon linked directly to the sulphate ester group) and C-5 (the adjacent carbon atom linked to a hydroxyl group) could not be carried out directly from the spectrum of (102) in D₂O. However, the most downfield signal (δ 149.78) was eventually assigned to C-5 by the pronounced downfield shift (δ 149.78 to δ 161.86) of this signal when the spectrum was recorded in 20 percent NaOD solution (Table 2.III), in consequence of the formation of the corresponding phenolate (104).



The doublet at δ 118.25 already assigned to C-6 experienced a downfield shift (to δ 122.74) of approximately 4.5 ppm in the phenolate. C-4, like C-6, is in *ortho* relationship to C-5 and as such is expected to experience a similar downfield shift. Of the likely chemical shifts, (δ 138.62 or δ 135.42 in (102); δ 142.25 or 134.17 in (104)), the transition δ 138.62 (in (102)) to δ 142.25 (in (104)), representing a downfield shift of approximately 3.7 ppm is in good agreement with the observed downfield shift of the

Table 2.III. ^{13}C -NMR chemical shifts (δC , ppm) for compounds (102), (103), (104).

Carbon			
1	134.17 (s)	135.42 (s)	133.82 (s)
2	106.49 (s)	116.25 (s)	114.45 (s)
3	122.04 (s)	122.69 (s)	112.96 (s)
4	142.25 (s)	138.62 (s)	144.86 (s)
5	161.86 (s)	149.78 (s)	142.22 (s)
6	122.74 (d)	118.25 (d)	115.65 (d)
7	72.31 (t)	71.12 (t)	64.99 (t)

(Off-resonance multiplicities in parentheses)

C-6 resonance. The resonances at $\delta 138.62$ (in (102)) and $\delta 142.25$ (in (104)) were thus attributed to C-4. The signals at $\delta 116.25$ and $\delta 122.69$ in the spectrum of (102) were assigned to the brominated carbon atoms on the basis of chemical shift correlations and the typically low relative intensity of the signals as a result of the relatively long relaxation time values of non-protonated halogen-bearing carbon atoms¹⁰⁸. The signal at $\delta 135.42$ was finally assigned to C-1. In (104), the signals at $\delta 106.49$ and 122.04 were similarly assigned to the brominated carbon atoms, and that at $\delta 134.17$ to C-1. The C-1 resonance can then be seen to have experienced a high field shift of about 1.2 ppm in (104). Again, C-1 is in *meta* relationship to C-5 and it is thus expected that the resonance due to C-3 (also *meta* to C-5) would experience a somewhat similar highfield shift. Of the two pairs of brominated-carbon resonances ($\delta 116.25$ and $\delta 122.69$ in (102); $\delta 106.49$ and 122.04 in (104)), the pair $\delta 122.69$ and 122.04 could then be assigned to C-3 in (102) and (104) respectively indicating a highfield shift of 0.65 ppm. It follows directly that the signals at $\delta 116.25$ and 106.49 belong to C-2 in (102) and (104) respectively (Table 2.III).

A confirmation of these assignments was provided by the substituent chemical shift effect for $-\text{OH} \rightarrow \text{O}^-$ on the benzene ring¹⁰⁹ (Table 2.IV). On the carbon of attachment there was a large downfield shift of +12.7 ppm compared to the observed +12.1 ppm for C-5 in (102) \rightarrow (104). The *ortho*

Table 2.IV. ^{13}C -NMR substituent chemical shift effect ($\Delta\delta_{\text{C}}$, ppm) for $-\text{OH} \rightarrow \text{O}^-$

Carbon relationship to substituent	$\Delta\delta$ (ppm) Phenol \rightarrow Phenolate ¹⁰⁹	$\Delta\delta$ (ppm) (<u>102</u>) \rightarrow (<u>104</u>)
<i>ipso</i>	+12.7	+12.1
<i>ortho</i>	+ 4.4	+3.6 to + 4.5
<i>meta</i>	+ 0.1	-0.6 to -1.2
<i>para</i>	- 5.7	-9.7

carbons experienced a downfield shift of +4.4 ppm. This value compares favourably with the observed values of +3.6 and +4.5 ppm for C-2 and C-4 respectively. The largest upfield shift of -5.7 ppm was reported for the carbon in *para* relationship compared with the largest upfield shift of -9.7 ppm observed for C-2 in (102) \rightarrow (104).

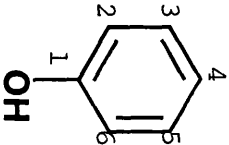
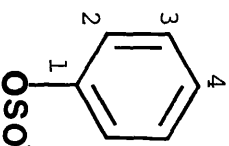
The natural product, (102), was on hydrolysis converted to the corresponding phenol, (103). The ^{13}C -NMR spectrum of (103) in DMSO revealed seven signals appearing as one triplet, one doublet and five singlets in the off-resonance spectrum. On the basis of chemical shift correlations and relative intensity of the signals, the resonances at δ 114.45 and 112.96 were assigned to the brominated-carbon atoms (C-2 and C-3). C-3 has hydroxyl groups in positions *ortho* and *meta* to it while C-2 has hydroxyl groups in positions *para* and *meta* to it. Since the highfield shift due to an *ortho* hydroxyl group is generally greater than that due to a *para* hydroxyl group then the higher field signal (δ 112.96) was assigned to C-3 and the signal at δ 114.45 to C-2. Of the two signals (δ 142.22 and 144.86) assignable to C-4 and C-5 (aromatic carbon atoms directly bonded to hydroxyl groups), the lower field signal was assigned to C-4 on the grounds that it would experience an additional downfield effect due to an *ortho* bromine substituent.

If the chemical shift assignments in (102), (103) and (104) are correct, then a consistent substituent chemical shift effect

due to the sulphate ester groups should be seen. Using (103) as a model the substituent chemical shift changes attributable to the presence of the sulphate ester groups in (102) were determined (Table 2.VII). The carbon (C-1) in *para* relationship to the phenolic sulphate ester group and β to the benzyl sulphate ester group exhibited a downfield shift of +1.6 ppm; C-2 and C-6 (*meta* to C-4), a downfield shift of +1.8 to 2.6 ppm; C-3 and C-5 (*ortho* to C-4), a large downfield shift of +7.6 to 9.7 ppm; C-4, the aromatic carbon directly linked to the sulphate ester group showed an upfield shift of -6.2 ppm whereas C-7, the aliphatic carbon directly bonded to the other sulphate ester group indicated a downfield shift of +6.1 ppm. This implied opposite chemical shift effects on the two types of carbon nuclei.

In order to further investigate this observation, the potassium sulphate esters of phenol and benzyl alcohol were synthesized as previously described (Materials and Methods section). By examination of the ^{13}C -NMR chemical shifts of phenol and benzyl alcohol together with those of the synthetically prepared potassium sulphate esters, chemical shift effects at different carbon atoms for the replacement of -OH by $-\text{OSO}_3\text{K}$ were calculated (Tables 2.V, 2.VI, 2.VII). The good agreement between the replacement effect data obtained from the chemical shift assignments in (102) and (103), and values calculated from these model studies served as additional evidence in support of the chemical shift assignments. It was notable that the ^{13}C -NMR chemical shift

¹³
 Table 2.V. C-NMR data (δ_c in ppm) for phenol to phenyl sulphate

Carbon	<div style="display: flex; justify-content: space-around; align-items: center;">   </div>		Replacement effect for -OH \rightarrow -OSO ₃ K ₃
	$\Delta\delta$ (ppm)	$\Delta\delta$ (ppm)	$\Delta\delta$ (ppm)
1	157.2 (s)	151.6 (s)	-5.6
2,6	115.4 (d)	122.3 (d)	+6.9
3,5	129.1 (d)	130.9 (d)	+1.5
4	118.0 (d)	126.9 (d)	+8.9

Footnotes to Tables 2.V and 2.VI

1. Resonances due to C-2+C-6, C-3+C-5 and C-4 in the sulphate esters were assigned by comparison with the chemical shifts of benzyl alcohol and phenol, and by taking into account the relative intensities of the signals - especially to distinguish between the resonances due to C-2+C-6 and C-4 where the intensity of the signal assigned to C-4 was 56 per cent that of C-2 + C-6.
2. Off-resonance multiplicities in parentheses: s = singlet, d = doublet, t = triplet.

Table 2.VI. ^{13}C -NMR data (δc , ppm) for benzyl alcohol to benzyl sulphate

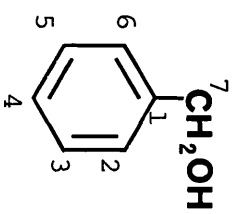
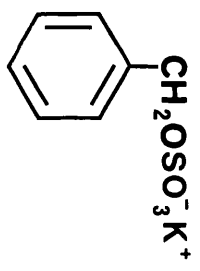
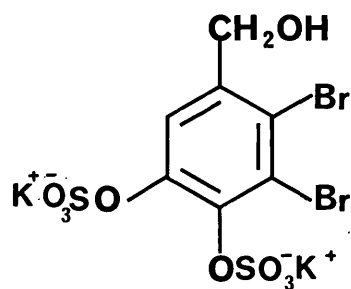
Carbon					Replacement effect $-\text{OH} \longrightarrow -\text{OSO}_3\text{K}$ $\Delta\delta$ (ppm)
	δc (ppm)		δc (ppm)		
1	142.5 (s)		137.5 (s)		-5.0
2,6	126.6 (d)		127.5 (d)		+0.9
3,5	128.1 (d)		128.1 (d)		0
4	126.7 (d)		127.4 (d)		+0.7
7	63.2 (t)		67.9 (t)		+4.7

Table 2.VII ^{13}C -NMR substituent chemical shift effect for
 $-\text{OH} \rightarrow -\text{OSO}_3\text{K}$ ($\Delta\delta$ in ppm)

Carbon	observed $\Delta\delta$ for (<u>103</u>) \rightarrow (<u>102</u>)	calculated values *
1	+1.6	+ 3.9
2	+1.8	+ 2.4
6	+2.6	
3	+9.7	+ 6.9
5	+7.6	
4	-6.2	- 4.9
7	+6.1	+ 4.7

* Calculated from values in Tables 2.V and 2.VI.



(105)

changes due to $\text{-OH} \rightarrow \text{-OSO}_3\text{K}$ indicated a trend similar to the effects of acetylation on phenol and benzyl alcohol.

An alternative structure, (105) was originally assigned to this salt by Hodgkin *et al.*¹⁰⁶ and was later revised to (102) by Glombitza *et al.*¹¹¹ as a result of extensive degradation studies. The present ¹³C-NMR data provides additional evidence in support of the revised structure.

3.5 FRACTIONATION OF THE ETHER-SOLUBLE ACIDIC EXTRACT

The acidic fraction obtained from the ether-soluble extract of the Kimmeridge Bay batch was chromatographed on a column of silica gel and eluted with toluene and toluene-ethylacetate with the proportion of ethylacetate increased gradually. The column fractions were monitored by TLC on silica gel (toluene-methanol, 4:1). The first fraction eluted with toluene was found to contain fatty acids (R_f 0.41) on the basis of infrared evidence, and was preserved for analysis by gas chromatography.

Fractions eluted with toluene-ethylacetate (9:1) afforded a mixture of compounds (R_f 0.38 and 0.34). The fractions were combined and concentrated *in vacuo*. Purification was achieved by recrystallizing from chloroform-methanol to give greyish-white rosettes corresponding

to the compound with R_f 0.34 as the major component (980 mg). This was designated compound A. The mother liquor was concentrated and found to contain mainly the compound with R_f 0.38. This was isolated in a pure form by chromatography on a short column (15 g) of silica gel and eluted with toluene-methanol (98:2). The compound B was recrystallized from chloroform-methanol as colourless prisms (90 mg).

Column chromatography of the ether-soluble acidic extract from the Berwick-on-Tweed batch yielded only fatty acids and no phenolic compounds.

3.6 CHARACTERISATION OF BROMINATED PHENOLIC COMPOUNDS

3.6.1 Analytical data on Compound A

Melting point, 202 - 203°C.

Infrared spectrum (KBr disc): Fig. 2.13

Ultraviolet spectrum, $\lambda_{\max}^{\text{MeOH}}$ nm (log ϵ):

239 (4.08), 292 (3.92), 352 (3.89)

$\lambda_{\max}^{(\text{MeOH}+\text{H}_2\text{SO}_4)}$ nm (log ϵ): 240 (3.85), 296 (3.45)

$^1\text{H-NMR}$ (100 MHz) in CD_3COCD_3 (δ , ppm) with TMS as internal standard:

7.40 (1H, s), 8.40 - 9.60 (2H, broad signal exchanged on deuteration), 10.16 (1H, s).

$^{13}\text{C-NMR}$ in CD_3COCD_3 (δ , ppm) with TMS as internal standard:

191.99 (d), 151.64 (s), 145.95 (s), 128.07 (s),
121.46 (s), 114.74 (d), 114.31 (s)

(Off-resonance multiplicities in parentheses).

Mass Spectrum, EIMS (70 eV) m/z (% relative intensity)

298/296/294 (51.5: 100.0: 50.8) M^+ ;
297/295/293 (48.7: 97.8: 49.0) $[M-H]^+$;
270/268/266 (1.5: 3.1: 1.6) $[M-CO]^+$;
269/267/266 (3.4: 6.8: 3.5) $[M-CHO]^+$;
216/214 (2.6: 2.4) $[M-H-Br]^+$;
188/186 (6.6: 6.5) $[M-H-Br-CO]^+$;
187/185 (3.6: 3.2).

3.6.2 Analytical data on Compound B

Melting point, 128 - 130°C

Infrared spectrum (KBr disc), Fig. 2.14

¹H-NMR, 100 MHz, in CD₃COCD₃ (δ, ppm) with TMS as internal standard:

3.40 (3H, s), 4.40 (2H, s), 7.06 (1H, s)

8.00 - 8.86 (2H, broad signal exchanged on D₂O shake).

¹³C-NMR in CD₃COCD₃ (δ, ppm) with TMS as internal standard:

145.62 (s), 142.70 (s), 130.94 (s), 115.77 (d), 114.69 (s),
113.60 (s), 75.25 (t), 58.24 (q).

(Off-resonance multiplicities in parentheses).

Mass Spectrum, E'I.M.S. (70 eV)

m/z (% relative intensity):

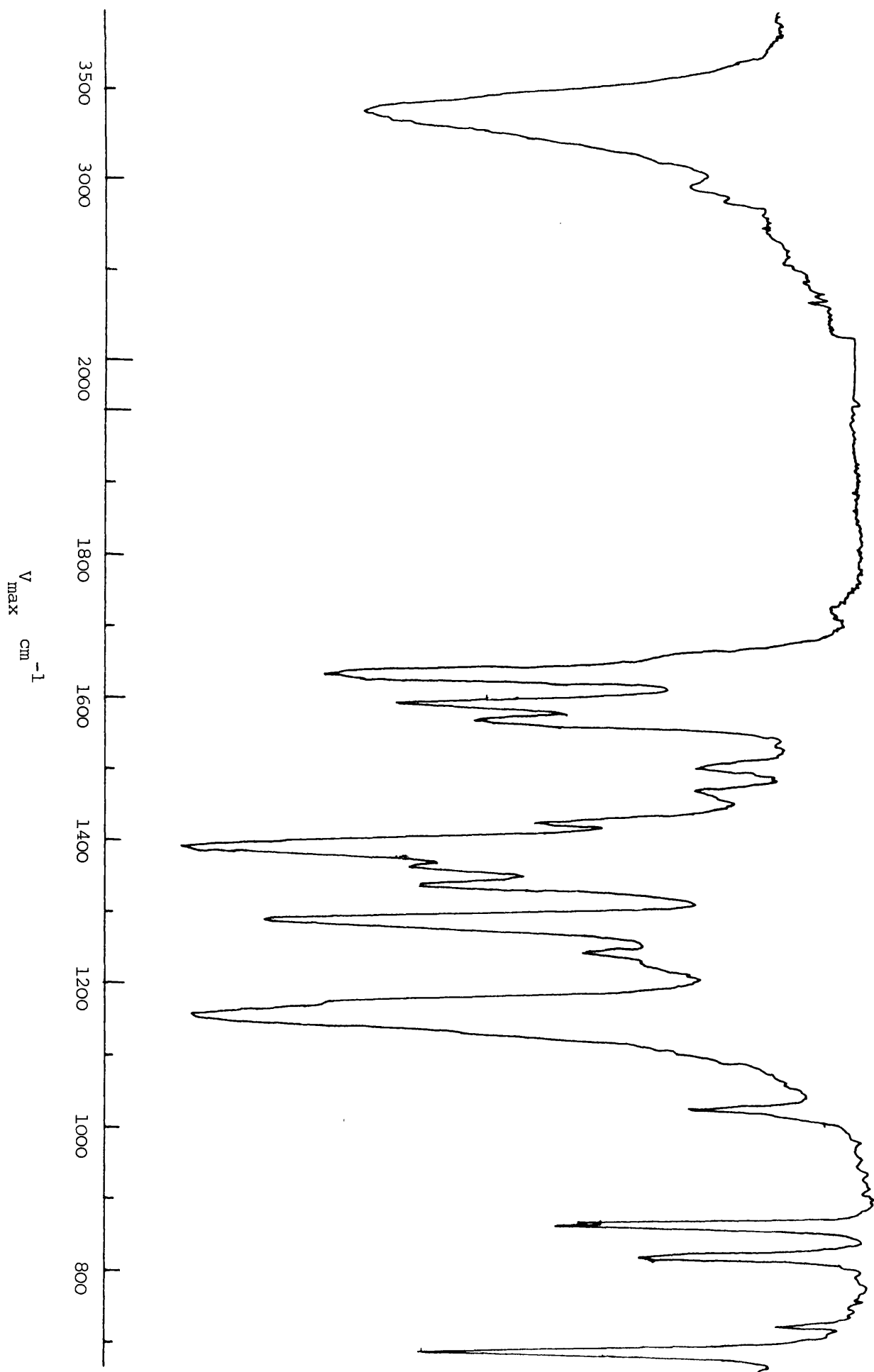
314/312/310 (40:80:41) M^+ ;
283/281/279 (51:100:50) $[M-OCH_3]^+$;

233/231 (69:70) $[\text{M-Br}]^+$.

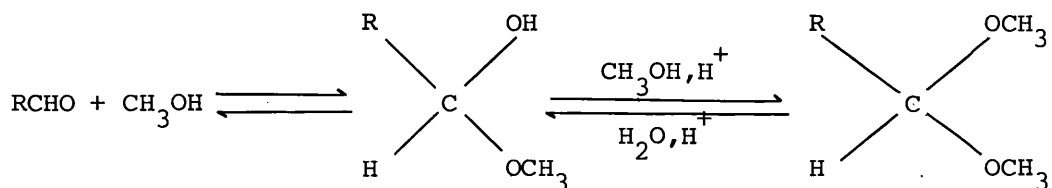
3.6.3 Discussion

Compound A, melting point $202 - 203^\circ\text{C}$, gave an intense green colour with ferric chloride. This indicated that the compound is probably a phenol. It also gave an immediate yellow colour with sodium molybdate suggesting that it is probably a catechol. The infrared spectrum (Fig. 2.13) showed peaks due to the presence of hydroxyl groups at 3300 cm^{-1} (O-H stretch), an aromatic ring at $1595, 1575\text{ cm}^{-1}$ (C=C stretch) and 870 cm^{-1} (C-H deformation), and a carbonyl group at 1645 cm^{-1} (C=O stretch). The $^1\text{H-NMR}$ spectrum in CD_3COCD_3 established the presence of an aldehyde proton at $\delta 10.16$, one aromatic proton at $\delta 7.40$ and two hydroxy-protons at $\delta 8.40-9.60$ (demonstrated by exchange with deuterium oxide). The presence of a formyl group was further supported by the ultraviolet spectra in neutral and acidic media. In methanol, the spectrum exhibited maxima at 239 nm ($\log \epsilon, 4.08$), 292 nm ($\log \epsilon, 3.92$) and 352 nm ($\log \epsilon, 3.89$). But when a drop of concentrated sulphuric acid was added to the methanolic solution in the sample cell and the spectrum redetermined, the absorption at 352 nm disappeared, and those at 239 and 292 nm remained almost at the same wavelengths but with reduced intensities ($\lambda_{\text{max}} 240 (3.85)$ and $296 (3.45)$). This change has been attributed¹¹² to the elimination of the carbonyl chromophore

Fig. 2.13. Infrared spectrum of Compound A.

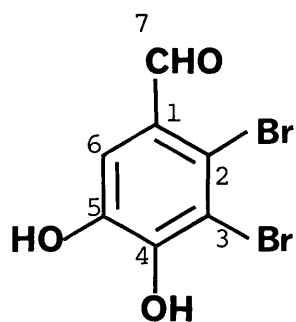


as a result of the acid-catalyzed reaction between the aldehyde and the methanol to form the corresponding acetal according to the following:



Mass spectrometric (E.I.M.S.) measurement established the molecular composition of $\text{C}_7\text{H}_4\text{O}_3\text{Br}_2$, the molecular ion cluster appearing as a 1:2:1 triplet at m/z 298, 296, 294 consistent with a dibrominated compound. Other prominent peaks appeared at m/z 297, 295, 293 $[\text{M}-\text{H}]^+$ cluster (a common aldehyde fragmentation); 270, 268, 266 corresponding to $[\text{M}-\text{CO}]^+$; 216, 214 $[\text{M}-\text{H}-\text{Br}]^+$ appearing as a 1:1 doublet; and at m/z 188, 186 $[\text{M}-\text{H}-\text{Br}-\text{CO}]^+$ also a 1:1 doublet and consistent with a monobrominated species. The infrared, ultraviolet, ^1H -NMR and mass spectral data are therefore consistent with structure (106).

A total of seven peaks observed in the ^{13}C -NMR spectrum of compound A in CD_3COCD_3 was also in agreement with the proposed structure. The signal at $\delta 191.99$ (d) was unambiguously assigned to the carbonyl carbon of the aldehyde group, and the resonance at $\delta 114.74$ (d) was easily attributable to C-6 being the only protonated



(106)

Table 2.VIII. ^{13}C -NMR chemical shifts of (106) in CD_3COCD_3 (δ , ppm)

Carbon	δc in ppm
1	128.07 (s)
2	121.46 (s)
3	114.31 (s)
4	151.64 (s)
5	145.95 (s)
6	114.74 (d)
7	191.99 (d)

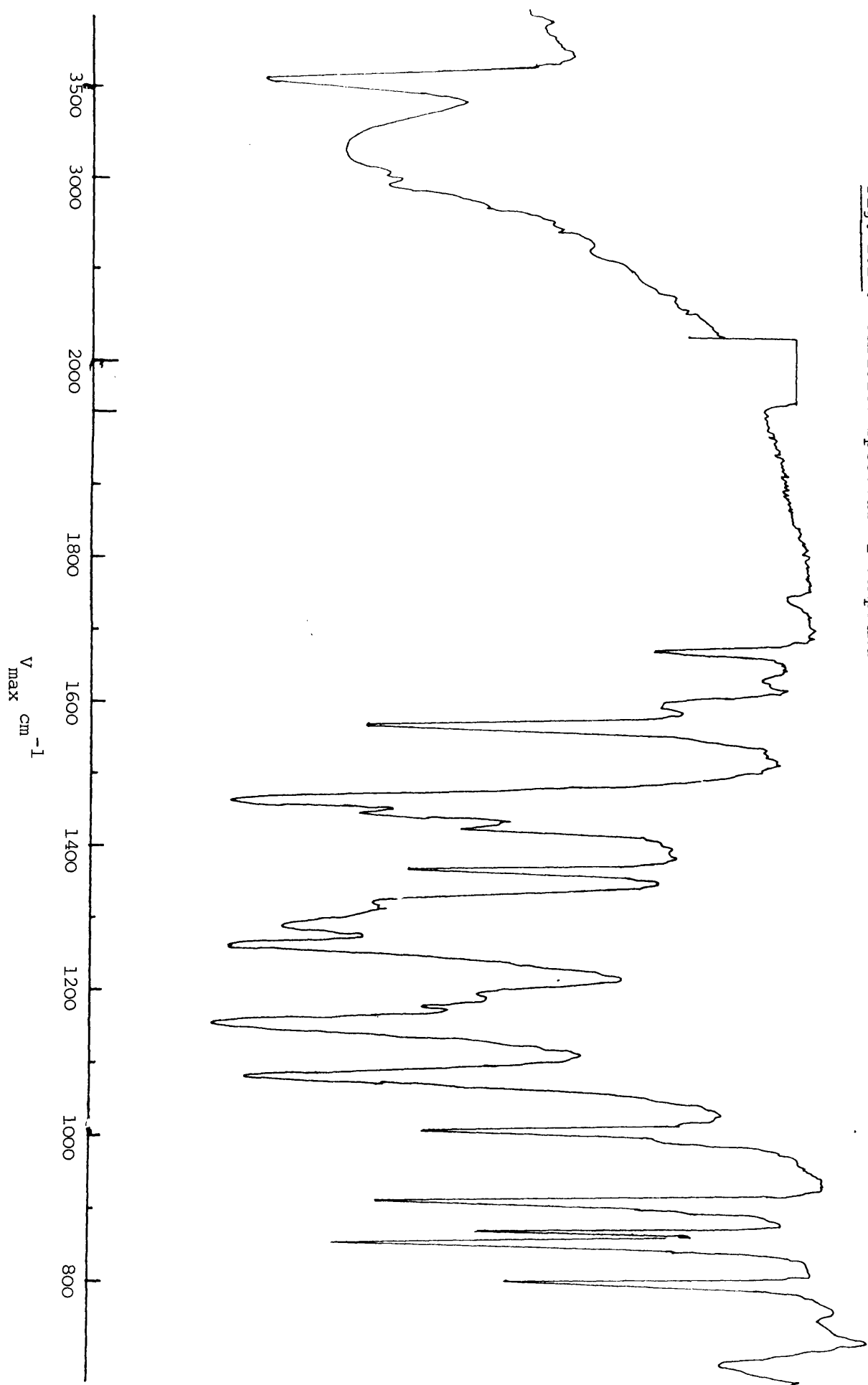
Off-resonance multiplicities in parentheses.

aromatic carbon atom in the molecule. Other assignments (Table 2.VIII) were made by correlation with the carbon resonances in 3,4-dihydroxybenzaldehyde¹¹³. Compound A was found to be identical with 2,3-dibromo-4,5-dihydroxybenzaldehyde (= 5,6-dibromoprotocatechualdehyde) isolated by Katsui *et al.*¹¹⁴ from *Rhodomela larix*, on the basis of melting point, UV, IR and ¹H-NMR data.

Compound B, melting point 128 - 130°C, gave a greenish-blue colour with ferric chloride and a yellow colour with sodium molybdate which again points to compound B being a catechol. The infrared spectrum (Fig. 2.14) revealed the presence of peaks due to hydroxyl at 3480 cm⁻¹ (O-H stretch), aromatic ring at 1600, 1570 (C=C stretch) and 870 cm⁻¹ (C-H deformation) and no carbonyl absorption. The ¹H-NMR spectrum had the following characteristic features: a sharp three-proton singlet at δ3.40 which was assigned to a methoxyl group, a sharp two-proton singlet at δ4.40 attributable to a benzyl methylene group, another sharp one-proton singlet at δ7.06 assignable to an aromatic proton, and finally a broad signal integrating to two protons (δ8.00 - 8.86) which were exchanged on shaking with deuterium oxide and were therefore attributed to two hydroxy-protons.

In the electron impact mass spectrum the molecular ion cluster was clearly visible as a 1:2:1 triplet at

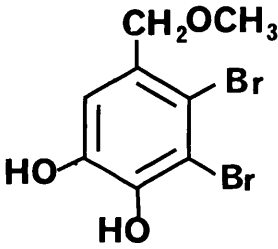
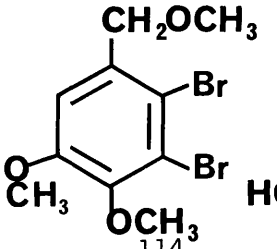
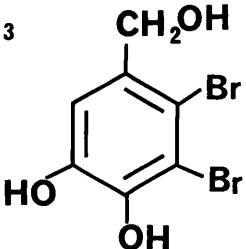
Fig. 2.14. Infrared spectrum of compound B



m/z 310, 312, 314 consistent with a dibrominated compound. The presence of two bromine atoms per molecule was further supported by the loss of 79 a.m.u. to give a daughter ion as a 1:1 doublet at m/z 231, 233, consistent with a monobrominated fragment. The 1:2:1 triplet at m/z 279, 281, 283 suggested the loss of $-OCH_3$ (31 a.m.u) from the molecular ion. The mass spectral analysis is consistent with the molecular formula $C_8H_8O_3Br_2$. The three oxygen atoms were accounted for by the two $-OH$ and one $-OCH_3$ groups in the 1H -NMR spectrum; and the remaining carbon and hydrogen atoms by a pentasubstituted benzene ring and a benzyl methylene group. The mass spectral, infrared and 1H -NMR data are therefore consistent with structure (107).

The relative positions of the methoxy- and hydroxy-groups was resolved by comparing the 1H -NMR data of compound B with those of 2,3-dibromo-4,5-dimethoxybenzyl-methylether (108) and 2,3-dibromo-4,5-dihydroxy-benzyl alcohol (103) (Table 2.IX). From the similarities in the chemical shifts for the benzylmethylene groups in (107) and (108) (δ 4.40 and δ 4.43 respectively) in contrast to δ 4.60 in (103); and the signals at δ 3.40 (107) and δ 3.44 (108) due to aliphatic methoxy-groups in contrast to δ 3.77 and 3.83 for phenolic methoxy-groups in (108), it could be inferred that the methoxy-group in (107) is aliphatic in nature and that the benzylmethylene group is not linked to a hydroxy-group. This constituted good

Table 2.IX. ^1H -NMR data (δ , ppm)

protons	 (107)	 (108) ¹¹⁴	 (103)
$-\text{CH}_2\text{O}-$	4.40	4.43	4.60
$-\text{OCH}_3$ (aliphatic)	3.40	3.44	-
$-\text{OCH}_3$ (aromatic)	-	3.77, 3.83	-

evidence for structure (107). Final proof of the structure was achieved by comparison ($^1\text{H-NMR}$, IR, UV, MS, M.pt) with data obtained for 2,3-dibromo-4,5-dihydroxybenzylmethyl ether isolated from *Rhodomela larix*¹¹⁴.

The $^{13}\text{C-NMR}$ spectrum of compound B displayed eight resonances (Table 2.X). These included resonances attributable to one methoxy-carbon at $\delta 58.43$ (q), one benzylmethylene carbon at $\delta 75.25$ (t) and six aromatic carbon atoms in the form of two brominated quaternary carbons ($\delta 114.69$ and 113.60), two oxygenated quaternary carbons ($\delta 145.62$ and 142.70), one other quaternary carbon and finally one methine carbon at $\delta 115.8$ (d). The different carbon types were distinguished by means of the off-resonance decoupled spectrum (multiplicities in parentheses) and chemical shift correlations with the carbon resonances in 2,3-dibromo-4,5-dihydroxy-benzyl alcohol (103). The carbon resonance due to the hydroxylated benzylmethylene group in (103) was at $\delta 64.99$ (t) (Table 2.III) and the carbon resonance attributed to the benzylmethylene group in (107) was observed at 10.26 ppm lower field ($\delta 75.25$) (Table 2.X). Since etherification of a hydroxyl group generally causes a large downfield shift in the resonance of the carbon bearing the etherified hydroxyl group, this observation thus confirmed that the methoxyl group is on the benzylmethylene group. The $^{13}\text{C-NMR}$ data is therefore consistent with the structure of 2,3-dibromo-4,5-dihydroxybenzyl-methyl ether (107).

Table 2.X. ^{13}C -NMR chemical shifts of (107) (δ , ppm) in CD_3COCD_3

Carbon	δ (ppm)
1	130.94 (s)
2	114.69 (s)
3	113.60 (s)
4	145.62 (s)
5	142.70 (s)
6	115.77 (d)
7	75.25 (t)
8	58.24 (q)

Off-resonance multiplicities in parentheses

It has been suggested by Weinstein *et al.*¹⁰⁷ that reports of (103), (106) and (108) as natural constituents of various red algae are probably incorrect, and that their occurrence is attributable to the various isolation procedures, which employed hot aqueous acid or methanolic-acid extraction; and that the salt (102) and similar sulphate esters are responsible for the wide variety of bromophenol derivatives described in literature.

In the present study, great care was taken to extract the algal material in the mildest possible way to avoid the formation of artifacts due to chemical reaction during the

isolation procedure. Two batches of algal material collected from different geographical locations were investigated. The water-soluble fractions from both batches yielded 2,3-dibromo-5-hydroxybenzyl-1',4-disulphate, dipotassium salt (102). The batch from Kimmeridge Bay (English Channel) also afforded compounds (106) and (107) in the ether soluble acidic fraction which were not detected in the batch from Berwick-on-Tweed (North Sea). Since both batches were extracted under identical conditions it was difficult to attribute the presence of (106) and (107) to the formation of artifacts as a result of the isolation procedure. This view was reinforced by the fact that the most obvious artifact (103) was not observed in our ether-soluble extracts along with (106) and (107). Moreover, ethanol rather than methanol was used during the extraction and this makes it even more unlikely that (106) and especially (107) are extraction artifacts.

To further investigate this view, the salt (102) was subjected to conditions identical to those employed in the isolation procedure. 2,3-dibromo-5-hydroxybenzyl-1',4-disulphate, dipotassium salt (200 mg) was added to a washed and air-dried sample of *Palmaria palmata* (20 g), a species of red seaweed known not to contain phenolic compounds and extracted under conditions identical to those used for *Polysiphonia lanosa*. A control was similarly set up except that the sulphate ester salt was not added. The ether-soluble acidic and neutral fractions in both

cases contained no phenolic components as determined by TLC on silica gel (toluene-methanol, 4:1) and polyamide (methanol-water, 9:1) with (103), (106) and (107) as standards. The water-soluble fraction from the experimental batch gave a positive reaction with ferric chloride whilst that from the control did not. The aqueous extracts from both the experimental and control were heated under reflux for one hour and thereafter extracted with ethyl acetate. The resulting extracts in both cases were concentrated and examined by TLC. Again, phenolic components were detected in the experimental but not in the control. This evidence gives a strong indication that the isolation procedure employed was not drastic enough to convert 2,3-dibromo-5-hydroxybenzyl-1',4-disulphate, dipotassium salt (102) to the related ether-soluble phenolic compounds, and as such the isolated compounds (106) and (107) are not likely to have been derived from (102) by the isolation procedure.

The presence of (106) and (107) in the Kimmeridge Bay sample and their absence in the Berwick-on-Tweed sample may be attributed to geographical or seasonal variation since the sample from Berwick-on-Tweed was collected in September and that from Kimmeridge Bay in June. The two samples of *Polysiphonia lanosa* were subjected to different treatments before extraction. The sample from Berwick-on-Tweed was stored in ethanol immediately after collection while that from Kimmeridge Bay was transported fresh to the laboratory and stored in a deep freeze at -20°C for seven

months prior to extraction. There is thus the possibility that the observed differences in the isolated components of the two algal samples might be related to the different treatments. Storage in ethanol would kill the seaweed and arrest enzymatic activity while at -20°C , certain seaweeds have been shown to survive for weeks and then die rather slowly¹¹⁵. Low temperature treatment thus represents an injury state to the seaweed and could induce an enzymatic response.

Thus it is possible that (106) and (107) may be formed by a natural process in response to injury. There is also the possibility that they may be natural products in their own right. The salt (102) has been shown to be moderately active against certain bacteria while the ether-soluble phenols have strong antibacterial activity⁸². This is an indication that the ether-soluble phenols in seaweeds may be involved in chemical defence and might be formed from the less active sulphate ester salt in response to injury.

3.7 FRACTIONATION OF THE ETHER-SOLUBLE NEUTRAL EXTRACT

The ether-soluble neutral extract from both samples of *Polysiphonia lanosa* was chromatographed in toluene and toluene-methanol mixtures on a column of silica gel.

Only fatty acid esters and sterols were isolated (TLC and infrared evidence). The sterol fraction was further analyzed by gas-liquid chromatography (see Chapter Seven).

CHAPTER FOUR

PALMARIA PALMATA

4.1 EXTRACTION AND ISOLATION

The red alga *Palmaria palmata* was collected from two different locations - Dawlish (in August) and Kimmeridge Bay (in September). Both samples were extracted in exactly the same manner. The frozen seaweed was thawed, rinsed quickly in distilled water and allowed to air-dry overnight at room temperature. The half-dried material was then extracted twice at room temperature with chloroform-methanol (2:1) followed by 70 percent aqueous methanol at 70°C for 2 hours (twice). The combined extract was concentrated *in vacuo* at 40°C and thereafter partitioned between ether and water to give non-polar and polar extracts respectively.

The polar extract was concentrated to about 300 ml under reduced pressure at 40°C and then clarified over activated charcoal. The clear filtrate was concentrated to a small volume and refrigerated overnight. The inorganic salts (infrared evidence) which were deposited were filtered off. The filtrate was passed through a column of Dowex 50W-X8 (H⁺ form) and eluted successively with deionised water and 2M ammonia solution. The ammonia eluate contained amino acids and was preserved for further analysis. The deionised water eluate was further purified by passage through a column of Amberlite IRA-400 (Cl⁻ form) and eluted with deionised water. The neutral effluent gave a negative ninhydrin reaction and was taken to dryness *in vacuo* to give a syrupy residue. This was extracted with hot 80 percent ethanol and filtered. The concentrated filtrate from the Kimmeridge Bay sample gave crystalline deposits after several days at 0 - 5°C.

The crystals were collected and recrystallized twice from boiling methanol to give colourless rosettes coded KPP-A. The concentrated filtrate from the Dawlish sample did not give any crystalline material and was concentrated to give a syrupy residue. The deionised syrup was chromatographed on 3mm filter paper developed with Butanol-Acetic acid-Water (4:1:1). A strip cut out from the chromatogram was visualised by spraying with 0.01 M potassium permanganate solution. The main component was found to have a much lower R_f than KPP-A. Using sprayed strips as markers, the bands were cut out and the components eluted with distilled water. After several unsuccessful attempts at recrystallization, the concentrated syrup (PP-I) was freeze-dried and then submitted to mass spectral analysis.

4.2 FORMATION OF ACETYL DERIVATIVE OF KPP-A

KPP -A (720 mg) was dissolved in pyridine (20 ml), the solution cooled to 4°C, and cold acetic anhydride (8 ml) was added slowly with stirring. The reaction mixture was left at 4°C for 24 hours and then stirred continuously at room temperature for two days. The reaction mixture was then poured into 70 ml of ice-cold distilled water with stirring. The resulting crystals were collected by filtration after one hour in the fridge. The crystals were washed with cold 80 percent ethanol and recrystallized from 95 percent ethanol to give colourless crystals (Yield, 1.38 g).

4.3 ACID HYDROLYSIS OF KPP-A.

45 mg of KPP-A was hydrolysed with 2 N HCl (20 ml) under reflux for 6 hours. The hydrolysate was cooled and neutralised with solid sodium bicarbonate and then taken to dryness *in vacuo* at 40°C. The residue was extracted three times with pyridine and the pyridine extract taken to dryness under reduced pressure at 40°C. The solid residue was redissolved in 10 percent pyridine in water for paper chromatographic analysis. Whatman 3 mm chromatography paper was used and isopropanol-pyridine-water-acetic acid (8:8:4:1) as the solvent system. The spray reagents were 3% p-anisidine hydrochloride and 0.01 M potassium permanganate solution on two different but concurrently run chromatograms. D-mannose, D-glucose, D-galactose and glycerol were used as reference compounds.

4.4 ANALYTICAL DATA ON KPP-A

KPP-A was recrystallized from hot methanol as colourless crystals. Melting point 126 - 128°C.

Specific rotation, $[\alpha]_D$ 166.7 (1.2% solution in water).

Infrared spectrum (KBr disc): Fig. 2.16a.

220 and 100 MHz ^1H -NMR in D_2O (δ , ppm) with DSS as internal standard:

5.23 (1H, d, $J = 3.5$ Hz), 4.16 (1H, t, $J = 6.0$ Hz), 4.07 (1H, d, $J = 3.0$ Hz), 4.01 - 3.72 (9H, complex multiplet).
(see Fig. 2.17b).

^{13}C -NMR in D_2O (δ , ppm from TMS) with methanol as internal standard: (Fig. 2.18b).

98.64 (d), 79.40 (d), 71.55 (d), 69.98 (d), 69.82 (d),
69.06 (d), 61.96 (t), 61.69 (t), 60.98 (t).

(Off-resonance multiplicities in parentheses).

Mass spectrum, (+ve) ion FAB: m/z (relative intensity):

255 $[\text{M}+\text{H}]^+$ (100), 163 $[\text{C}_6\text{H}_{11}\text{O}_5]^+$ (64), (-ve) ion FAB:

253 $[\text{M}-\text{H}]^-$ (100).

Acetyl derivative - Recrystallized from 95% aqueous ethanol as colourless crystals, melting point $102 - 103^\circ\text{C}$.

Specific rotation, $[\alpha]_{\text{D}}$ 113.6 (1.0% solution in acetone).

Infrared spectrum (KBr disc): Fig. 2.16b

100 MHz ^1H -NMR in DMSO (δ , ppm) with TMS as internal standard:

5.40 (1H, multiplet), 5.32 (1H, dd, $J = 10.0, 3.0$ Hz)

5.10 (1H, dd, $J = 10.0, 3.5$ Hz), 4.90 (1H, d, $J = 3.5$ Hz), .

4.28 - 4.48 (1H, m), 3.88 - 4.24 (7H, m),

2.12 (3H, s), 2.08 (3H, s), 2.04 (6H, s), 2.00 (3H, s),

1.96 (3H, s).

^{13}C -NMR in DMSO (δ , ppm from TMS):

170.16 (s), 170.05 (s), 169.89 (s), 169.46 (s),

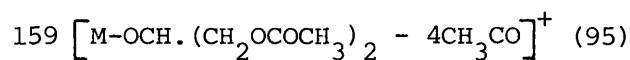
95.02 (d), 73.46 (d), 67.99 (d), 67.45 (d), 66.85 (d),

66.47 (d), 63.33 (t), 62.79 (t), 61.54 (t), 20.32 (q)

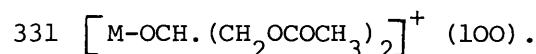
(Fig. 2.18a).

Mass spectrum, (+ve) ion FAB: m/z (relative intensity) -

507 $[\text{M}+\text{H}]^+$ (4), 447 $[\text{M}-\text{CH}_3\text{COO}]^+$ (3), 331 $[\text{M}-\text{OCH}(\text{CH}_2\text{OCOCH}_3)_2]^+$ (100),

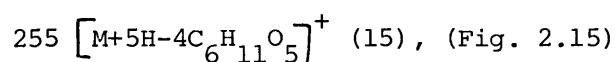
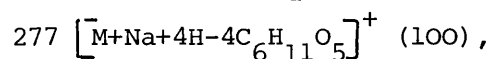
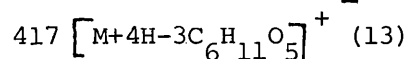
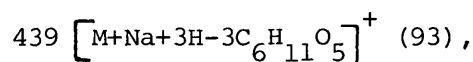
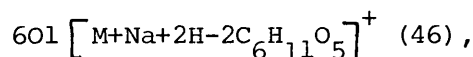
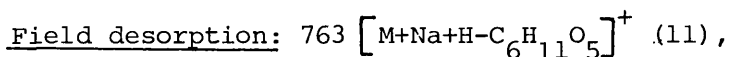
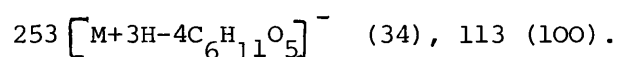
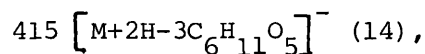
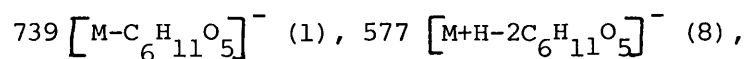
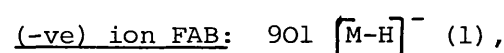
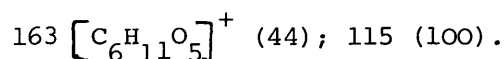
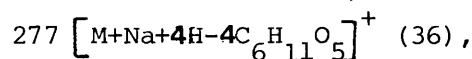
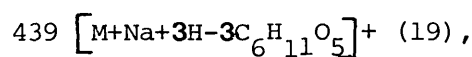
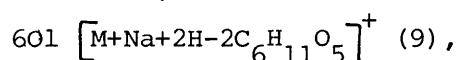
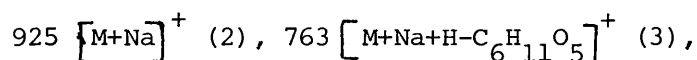


Chemical ionisation (isobutane): $447 \left[\text{M-CH}_3\text{COO} \right]^+ \quad (3),$



4.5 ANALYTICAL DATA ON PP-I

Mass spectrum, (+ve) ion FAB: m/z (relative intensity)



On acid hydrolysis PP-I yielded only glycerol and galactose.

Table 2.XI. Paper chromatographic analysis of the hydrolysate

Solvent system: Isopropanol-pyridine-water-acetic acid (8:8:4:1)

	R_f	Spray Reagents	
		3% Anisidine HCl	0.01 M $KMnO_4$
mannose	0.63	greyish-brown	yellow-white
glucose	0.57	greyish-brown	yellow-white
galactose	0.54	greyish-brown	yellow-white
hydrolysate	0.54	greyish-brown	yellow-white
	0.70	-	yellow-white
glycerol	0,70	-	yellow-white
KPP-A	0.58	-	yellow-white

4.6 DISCUSSION

4.6.1 Characterisation of 1-D-galactopyranosyl-2'-glycerol

KPP-A was isolated as a colourless crystalline solid which on hydrolysis and paper chromatographic analysis afforded two spots identical in R_f values and colour reactions with glycerol and D-galactose. The infrared spectrum (Fig. 2.16a) was superficially similar to that of sodium 2'-(1-O- α -D-mannopyranosyl) glycerate (Fig. 2.5, Chapter 3) except for the absence of the carbonyl absorption.

The positive ion fast atom bombardment (+ve ion FAB) spectrum showed a pseudomolecular ion at m/z 255 $[M+H]^+$ which was also the base peak. This is consistent with the molecular composition $C_9H_{18}O_8$. The intense peak at m/z 163 (63.8 percent) corresponds to a hexose unit and is indicative of a fission of the glycosidic bond. The (-ve) ion FAB mass spectrum gave a pseudomolecular ion at m/z 253 $[M-H]^-$ which was also the base peak and thus provides additional support for the molecular formula. The (+ve) ion FAB mass spectrum of the acetylated derivative gave a pseudomolecular ion at m/z 507 $[M+H]^+$ which corresponds to hexa-O-acetylhexosylglycerol, $C_9H_{12}O_8 (CH_3CO)_6$. The base peak at m/z 331 $[M-OCH_2(CH_2OCOCH_3)_2]^+$ corresponds to the cleavage of the glycosidic bond. The mass spectral data are therefore indicative of a glycoside composed of one hexose unit and glycerol. This is in agreement with the results obtained by acid hydrolysis and paper chromatographic analysis.

Fig. 2.16a. Infrared spectrum of KPP-A

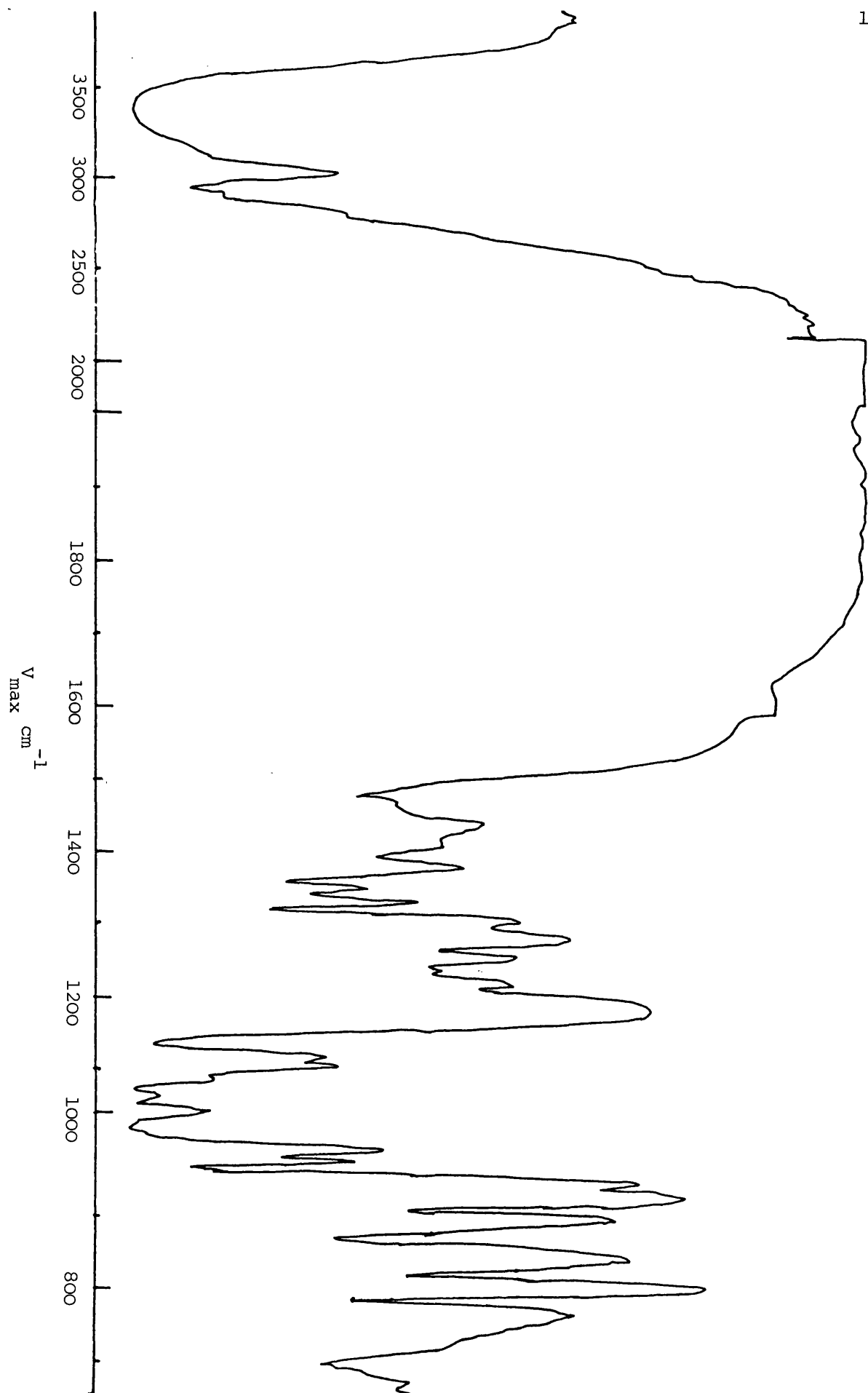
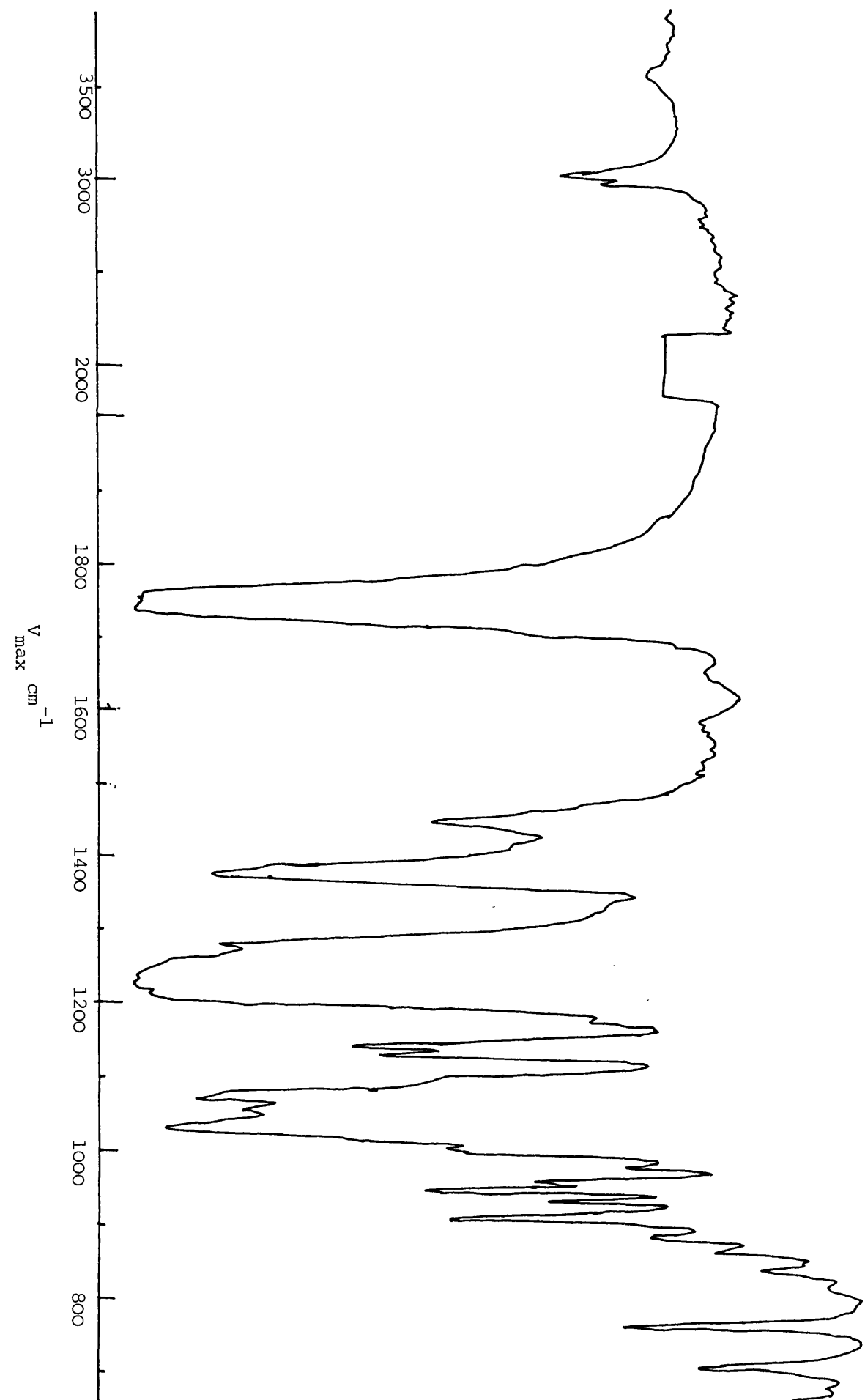


Fig. 2.16b. Infrared spectrum of KPP-A hexaacetate



The ^1H NMR spectrum in D_2O showed a sharp one-proton doublet at $\delta 5.23$ ($J = 3.5$ Hz) easily attributable to the anomeric proton. Spin decoupling at about $\delta 3.82$ (Fig. 2.17a) collapsed the doublet to give a singlet. Therefore, the chemical shift for H-2 is at $\delta 3.82$. The ^1H NMR spectrum in D_2O was determined at 100 MHz and 220 MHz. The spectrum at 100 MHz showed a poorly resolved triplet (1H) overlapping an indistinct doublet (1H) in the region of $\delta 4.0 - 4.2$. A better resolution of these signals was achieved in the 220 MHz spectrum (Fig. 2.17b) which showed the signals as a well-defined triplet ($\delta 4.16$, $J = 6.0$ Hz) fully resolved from a distinct doublet ($\delta 4.07$, $J = 3.0$ Hz). However, the expanded 220 MHz spectrum revealed that both signals have additional small couplings with a J value of about 1 Hz. The nature of this coupling is reminiscent of that observed for $^3J_{\text{H}_4, \text{H}_5}$ in D-galactopyranoses and some of their glycosides in D_2O ¹¹⁶. These signals are readily analyzed due to the presence of an axially oriented hydroxyl group at the 4-position and thus show a large downfield shift of the signal for H-4, and a strong deshielding influence of the axial hydroxyl on the opposing axial H-5. The two methylene protons of the C-6 hydroxymethylene group are frequently chemically equivalent in D-galactopyranose and derivatives unlike those in the sugars of glucopyranose and mannopyranose series^{117,118}. The triplet at $\delta 4.16$ (1H) attributable to H-5 is consistent

Fig. 2.17a. Spin decoupling in 100 MHz

^1H -NMR spectrum of KPP-A

in D_2O

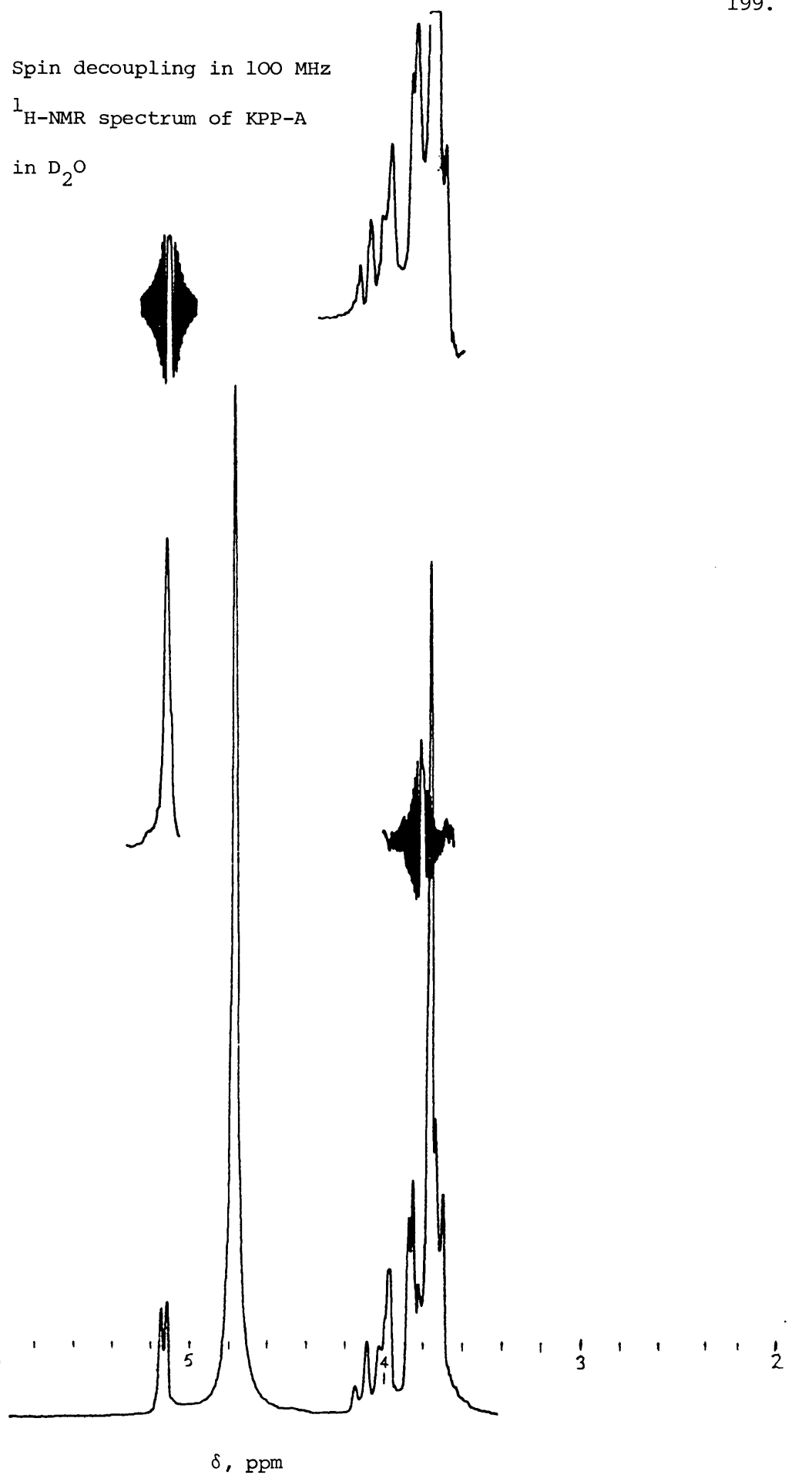


Fig. 2.17b. ^1H -NMR 220 MHz
spectrum of KPP-A
in D_2O

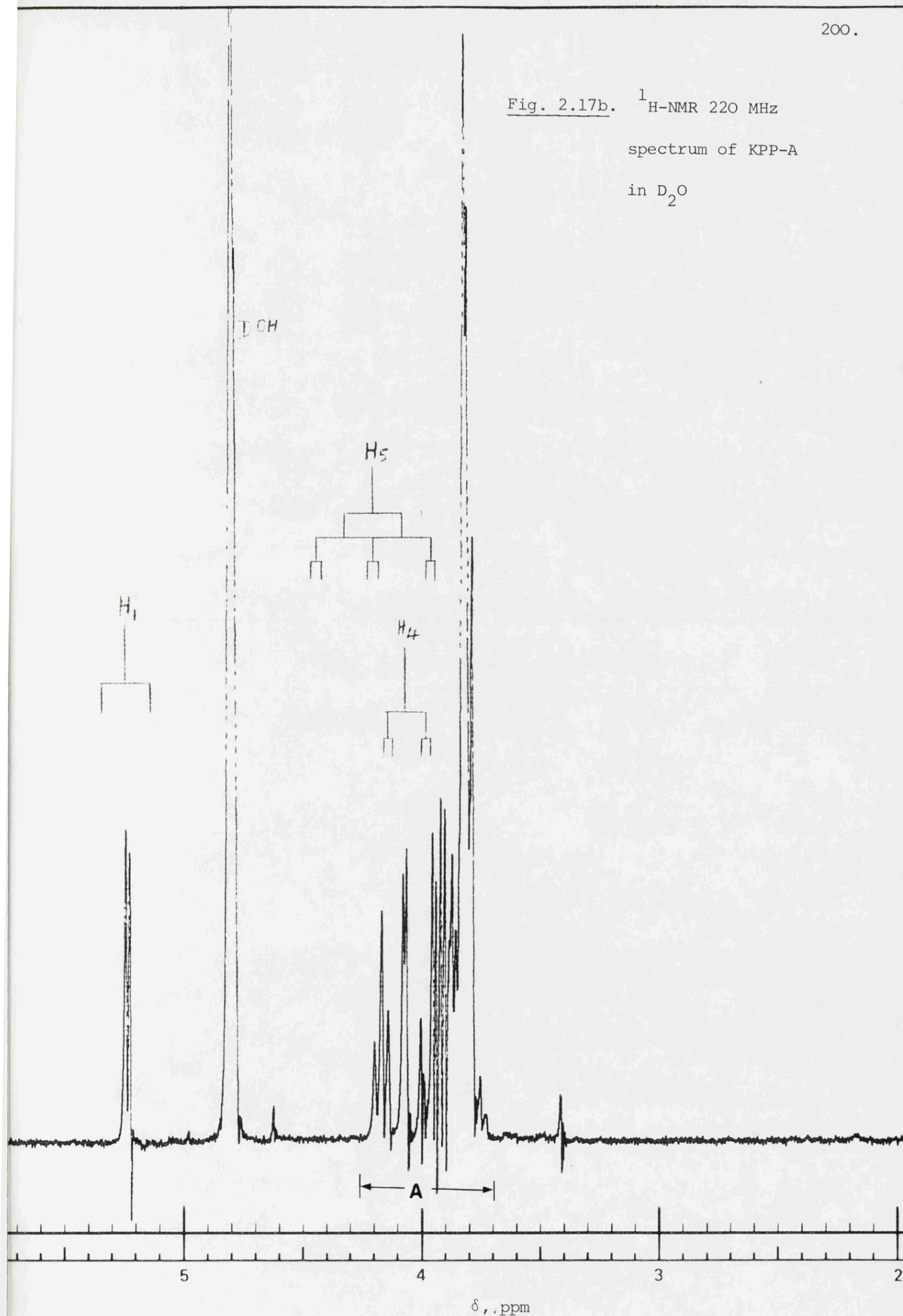
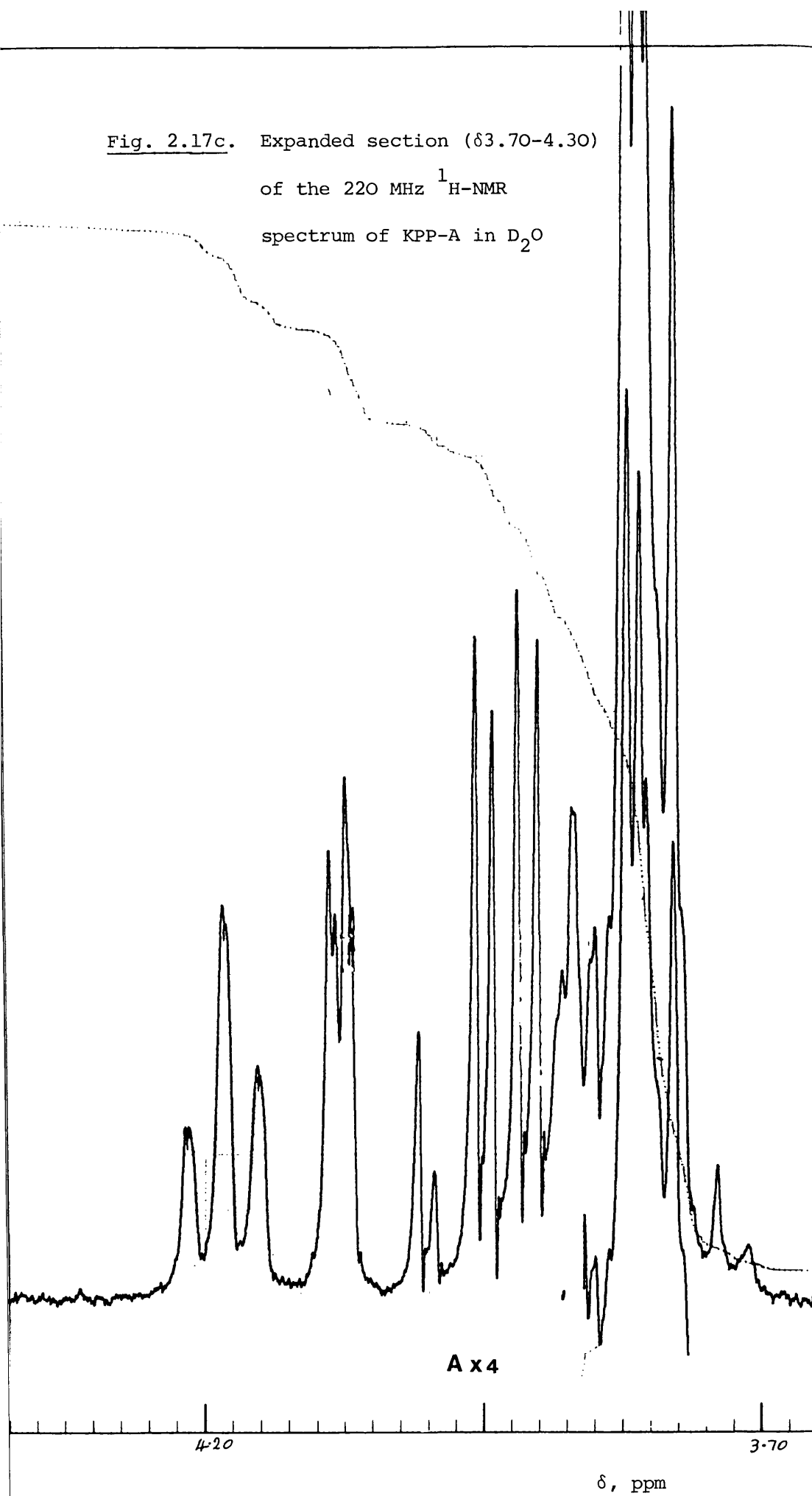


Fig. 2.17c. Expanded section (δ 3.70-4.30)
of the 220 MHz ^1H -NMR
spectrum of KPP-A in D_2O



with these observations in D-galactopyranose. The observed $^3J_{H_3,H_4}$ value of 3.0 Hz and a value of about 1 Hz for the additional coupling attributed to $^3J_{H_4,H_5}$ are in excellent agreement with the structure of D-galactopyranose and derivatives in which the coupling constant between H-4 and H-5 reflecting an axial-equatorial relationship is always markedly lower than that between H-3 and H-4, which reflects another axial-equatorial relationship¹¹⁹. The 1H NMR data thus provides adequate evidence that KPP-A is a D-galactopyranoside. In α -D-galactopyranose and derivatives, H-2 and H-1 are in an axial-equatorial relationship and will thus have a relatively small coupling constant when compared to the β -galactopyranosyl series in which H-2 and H-1 are in axial - axial relationship. The observed splitting of 3.5 Hz (220 MHz 1H -NMR spectrum) in the signal of the anomeric proton is therefore indicative of an α -D-galactopyranoside.

Having deduced that the isolated glycoside is 1-O- α -D-galactopyranosylglycerol, it remains to determine the position of linkage to the glycerol moiety. This could either be at the methine carbon atom or at one of the two methylene carbon atoms of the glyceryl moiety. The correct position can be determined by careful analysis of the 1H - and ^{13}C -NMR spectra of the glycoside and its acetylated derivative.

The 1H -NMR chemical shift assignments of the hexaacetate are given in Table 2.XII. It has been shown¹⁰¹ that an acetoxyl

Table 2.XII. ^1H NMR chemical shift of methine and methylene protons (δ , ppm from TMS).

	1-O-methyl- α -D-galactopyranosyl tetraacetate ¹¹⁷	KPP-A-hexa acetate	KPP-A
Solvent	CDCl_3	DMSO	D_2O
H-1	4.97 (1H)	4.90 (1H)	5.23 (1H)
H-2	5.12 (1H)	5.10 (1H)	(3.82)
H-3	5.32 (1H)	5.32 (1H)	*
H-4	5.43 (1H)	5.40 (1H)	4.07 (1H)
H-5	4.15 (1H)		4.16 (1H)
H-6	4.07 (2H)	4.00 - 4.48 (7H)	
H-1'/H-3'	-		3.72 - 4.01*
H-2'	-	4.28 - 4.48 (1H)	

* Resonances within the complex multiplet.

group in axial orientation not only deshields the geminal proton but also tends to shield the protons in β and γ relationship to it. In structure (110), H-5 does not have an acetoxyl group geminal to it and as such will not experience any deshielding effect. However, the presence of an axially oriented acetoxyl group on C-4 which is in a position β to it will cause a shielding effect, as will the primary acetoxyl group on C-6. H-5 will therefore resonate higher field relative to the H-5 resonance in the non-derivatised glycoside. Considering the magnitude of the shielding effect on H-5, the methine proton signal in the same region as the signal for the six acetoxymethylene protons (δ 4.00 - 4.24, 7H, m) is thus attributable to H-5. H-4 is geminal to an axially oriented acetoxyl group and will be strongly deshielded - the deshielding effect of an axial acetoxyl group on the geminal proton being greater than that of an equatorially oriented acetoxyl group¹⁰¹. As a result, the most downfield signal (δ 5.40), a poorly resolved one-proton doublet of doublets can be assigned to H-4. These assignments are in good agreement with similar assignments in 1-O-methyl- α -D-galactopyranoside tetraacetate¹¹⁷. The signals at δ 5.32 (1H, dd, $J = 10.0, 3.0$ Hz), δ 5.10 (1H, dd, $J = 10.0, 3.5$ Hz), δ 4.90 (1H, d, $J = 3.5$ Hz) were assigned to H-3, H-2 and H-1 respectively by comparison with the ^1H -NMR chemical shifts of 1-O-methyl- α -D-galactopyranoside tetraacetate¹¹⁷. The large value of the $^3J_{\text{H}_2, \text{H}_3}$ coupling constant (10.0 Hz) indicates the trans-diaxial arrangement of H-2 and H-3. The

one-proton multiplet at $\delta 4.28 - 4.48$ is therefore due to the methine proton of the glyceryl moiety. This signal is high field of the corresponding methine proton signal in the triacetyl derivative of glycerol ($\delta 5.04 - 5.28$, 1H, multiplet) where it is geminal to a deshielding acetoxyl group. On the other hand, the acetoxymethylene protons in both derivatives have comparable chemical shifts ($\delta 4.10 - 4.24$ and $\delta 4.00 - 4.36$). This is indicative of the structure having the glycosidic linkage at the methine carbon (C-2') of the glyceryl moiety.

Etherification of a hydroxyl group is known to cause a large downfield shift in the resonance of the carbon bearing the etherified hydroxyl group¹²⁰. Hence in the glycoside the glyceryl carbon atom at the point of linkage will be strongly deshielded being α to the hexose unit and will thus resonate at much lower field than the corresponding hydroxylated carbon atom in glycerol. The ¹³C-NMR chemical shifts for KPP-A, glycerol, and 1-methyl- α -D-galactopyranoside in D₂O are shown in Table 2.XIII. The chemical shifts of KPP-A were assigned by direct comparison with the chemical shifts of 1-methyl- α -D-galactopyranoside¹²¹. The chemical shift of the methine carbon ($\delta 79.40$) in the glyceryl moiety of the isolated galactopyranosylglycerol was observed to be 6.82 ppm lower field than the corresponding carbon resonance ($\delta 72.58$) in glycerol whereas the carbon resonances of the methylene groups in both compounds have comparable chemical shifts. This is clearly indicative of glycosylation at

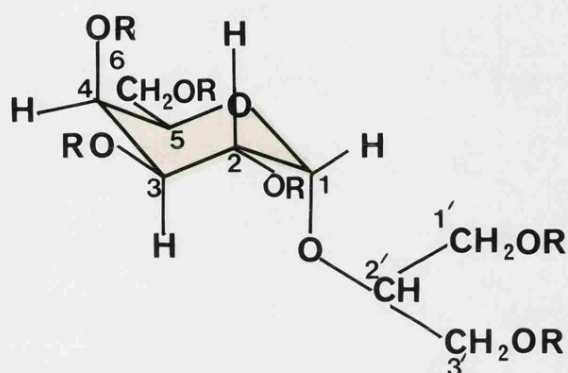
Table 2.XIII. ^{13}C -NMR chemical shifts in D_2O (δ , ppm from TMS)

Internal standard methanol, δ_{C} 49.5.

Carbon	1-O-methyl- α -D-galactopyranoside ¹²¹	KPP-A	glycerol
C-1	99.80 (d)	98.64 (d)	-
C-2	69.90 (d)	69.82 (d)	-
C-3	70.20 (d)	69.98 (d)	-
C-4	68.90 (d)	69.06 (d)	-
C-5	71.20 (d)	71.55 (d)	-
C-6	61.80 (t)	61.96 (t)	-
C-7	55.6 (q)	-	-
C-1'/C-3'	-	60.98/61.69 (t)	63.10 (t)
C-2'	-	79.40 (d)	72.58 (d)

Off-resonance multiplicities in parentheses.

the methine carbon (C-2') of the glycerol moiety and consistent with structure (109) for KPP-A.



(109) $R = H$

(110) $R = OAc$

The ^{13}C -NMR chemical shifts in DMSO of KPP-A and the hexaacetate are given in Table 2.XIV. The assignments are based on those for 1-O-methyl- α -D-galactopyranoside tetraacetate¹²². In the study of pyranoses,¹²¹ acetylation is noted to produce a general shift towards higher field. This has been rationalized on the grounds that the steric effects outweigh the smaller deshielding contribution, to give a net upfield shift. The C-6 resonances unlike all

Table 2.XIV. ^{13}C -NMR acetylation shifts in DMSO

Carbon	Chemical Shifts (δ , ppm)		
	KPP-A	KPP-A-hexaacetate	$\Delta\delta$ (ppm)
C-1	99.14 (d)	95.02 (d)	-4.12
C-2	68.91 (d)	67.99 (d)	-0.92
C-3	69.72 (d)	67.45 (d)	-2.27
C-4	68.75 (d)	66.85 (d)	-1.90
C-5	71.19 (d)	66.47 (d)	-4.72
C-6	61.11 (t)	61.54 (t)	0.43
*C-1'	60.78 (t)	63.3 (t)	2.55
C-2'	80.45 (d)	73.46 (d)	-6.99
*C-3'	60.62 (d)	62.79 (t)	2.17

* Interchangeable

Off-resonance multiplicities in parentheses

others in the spectra are deshielded with respect to their positions in the free pyranoses. This behaviour is apparently related to the primary nature of the C-6 hydroxyl group¹²⁰, and the fact that there is no acetoxyl group at the adjacent carbon. The resonances of the anomeric carbon atoms in the peracetylated pyranoses are noted to undergo large upfield shifts with respect to the free sugars.

On comparing the ¹³C-NMR spectra of KPP-A and the hexacetate (Table 2.XIV), it is noted that resonances due to the three methylene carbons (-CH₂OAc, triplets in the off-resonance decoupled spectrum) are deshielded with respect to their positions in the free glycoside. This observation is indicative of the presence of α-acetoxyl groups on these carbons and none at the adjacent carbon atoms. As expected, the resonances of the anomeric carbon and C-5 underwent large upfield shifts (-4.12 and -4.72 ppm respectively). Both carbons lack α-acetoxyl groups, and are shielded by the acetoxyl group on the adjacent carbons (Structure 110). The largest upfield shift (-7.0 ppm) was observed for the methine carbon (C-2') of the glyceryl moiety. This is suggestive of the shielding effect of two β-acetoxyl groups. The obvious conclusion therefore, is that the glycosidic linkage is at the methine carbon of the glyceryl moiety. This conclusion is in agreement with those reached by the other NMR spectral analyses. The structure of KPP-A is therefore established as 1-O-α-D-galactopyranosyl-2'-glycerol (Structure 109) which has been called floridoside¹²³.

^{13}C -NMR spectra of KPP-A-hexaacetate (Fig. 2.18a) and KPP-A
(Fig. 2.18b) in DMSO
Fig. 2.18a.

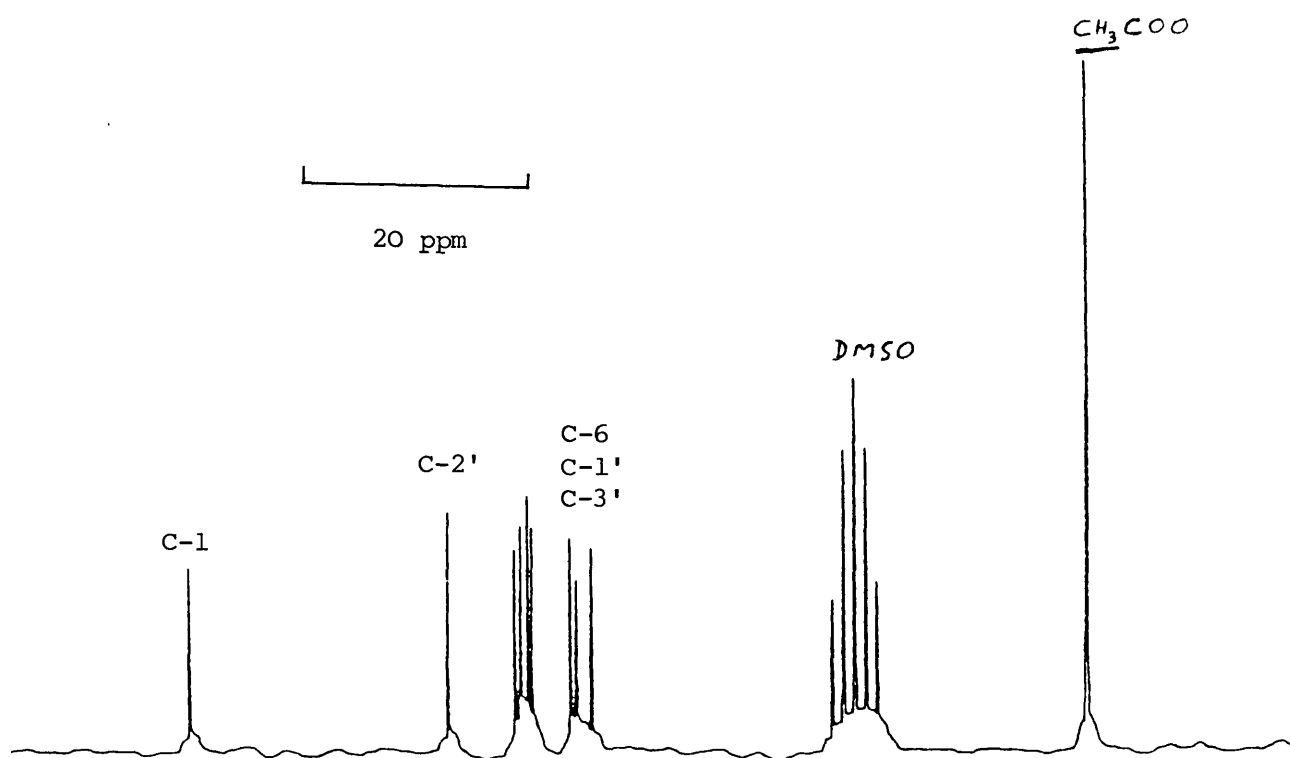
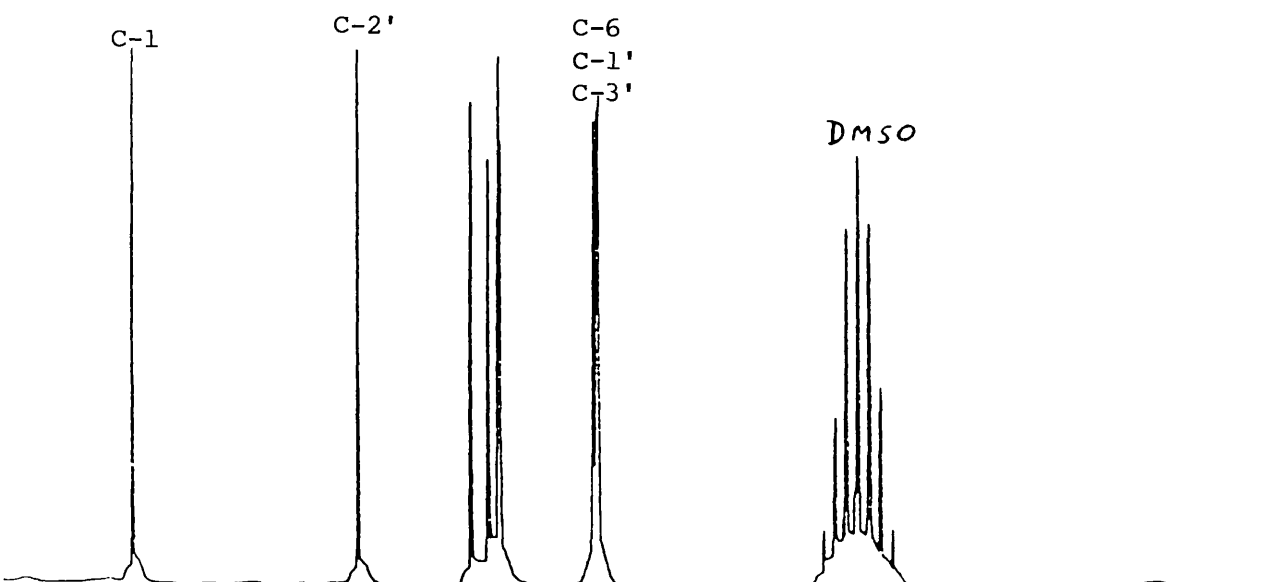


Fig. 2.18b



The melting point of the isolated glycoside, 126 - 128°C and the specific rotation in water, $[\alpha]_D + 166.7^\circ$ (C, 1.2) as well as the melting point of the hexaacetate, 102 - 103°C and the specific rotation in acetone, $[\alpha]_D + 113.6^\circ$ (C, 1.0) are in good agreement with literature values [floridoside, melting point 128.5°C, $[\alpha]_D + 165^\circ$ (C, 3.35); hexaacetate, melting point 101°C, $[\alpha]_D + 114^\circ$ (C, 3)]¹²³.

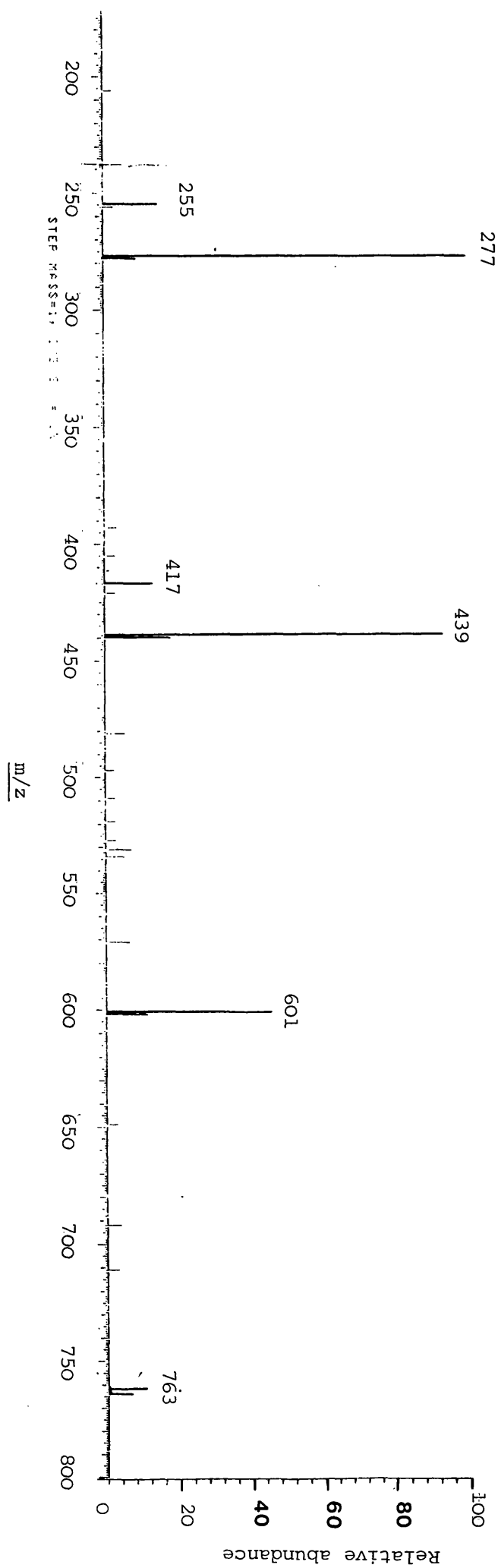
Floridoside is recognized as a common reserve product of the Rhodophyceae^{123,124,125}. In all previous reports, the type and position of the glycosidic linkage were determined by enzymatic hydrolysis and by the use of various chemical methods, chiefly periodate oxidation. The present study furnishes comprehensive spectroscopic data on floridoside, and highlights the usefulness of spectroscopic techniques in determining the configuration at the anomeric carbon atom, and the position of glycosidic linkage. The fact that not more than 200 mg of the compound was actually needed for the entire spectroscopic analysis makes the method very attractive.

4.6.2 Characterisation of Pentagalactosyl Glycerol

The freeze-dried solid PP-I, isolated from the Dawlish sample of *Palmaria palmata* was submitted to different forms of mass spectral examination. In many cases of fast atom bombardment (FAB) and field desorption (FD) mass

spectrometric measurements, especially for carbohydrates, the molecular species is stabilized to give an even-electron species¹⁰⁰ such as $[M+Na]^+$. The (+ve) ion FAB spectrum of PP-I furnished a pseudomolecular ion at m/z 925 $[M+Na]^+$, corresponding to a molecular formula $C_{33}H_{58}O_{28}$. Other fragments were seen at m/z 763 $[M+Na+H-C_6H_{11}O_5]^+$, 601 $[M+Na+2H-2C_6H_{11}O_5]^+$, 439 $[M+Na+3H-3C_6H_{11}O_5]^+$, 277 $[M+Na+4H-4C_6H_{11}O_5]^+$, and the peak at m/z 115 is probably due to $[glycerol + Na]^+$ because of the use of glycerol in the FAB technique though the compound itself could also contribute to this peak. These fragments are indicative of successive losses of four hexose units from the pseudomolecular ion. The molecular weight and the fragmentation pattern are consistent with a structure comprising of five hexose units linked to one molecule of glycerol. The (-ve) ion FAB mass spectrum shows a pseudomolecular ion at m/z 901 $[M-H]^-$. Other key fragments were seen at m/z 577 $[M-2C_6H_{11}O_5+H]^-$, 415 $[M-3C_6H_{11}O_5+2H]^-$ and 253 $[M-4C_6H_{11}O_5+3H]^-$. The pseudomolecular ion and the fragments serve as corroborative evidence for a pentasaccharide structure in glycosidic linkage with a molecule of glycerol. A similar result was also obtained with the field desorption mass spectrum (Fig. 2.15) except that the largest fragment seen was at m/z 763 corresponding to the loss of one hexose unit from the pseudomolecular ion. The spectrum also contained evidence of successive loss of hexose units with the base

Fig. 2.15. Field desorption mass spectrum of PP-1



peak at m/z 277 corresponding to the molecular weight of floridoside plus 23 atomic mass units. Since PP-I on hydrolysis yielded only galactose and glycerol, the gross structure can be represented as (III) but this is by no means the only possible arrangement for a pentagalactosyl glycerol structure.

Gal-Gal-Gal-Gal-Gal-Glycerol

(III)

The ^{13}C - and ^1H -NMR spectra in D_2O were characteristic of a glycoside and superficially similar to those of KPP-A (floridoside) but with complex overlapping of signals. The entire ^1H -NMR spectrum was a fairly narrow band in the region $\delta 3.40 - 5.30$. The ^{13}C -NMR spectrum indicated the presence of at least three anomeric carbon signals ($\delta 103.86, 98.93, 97.42$). These observations are consistent with a pentagalactosylglycerol structure.

In *Ochromonas malhamensis*, it has been shown⁹⁰ that the mechanism for regulating turgor is connected with the formation and degradation of the carbohydrate isofloridoside (1-O- α -D-galactopyranosyl-1'-glycerol). The formation of isofloridoside was found to rapidly increase as the concentrations of osmotically active substances in the nutrient solution was increased. The level of isofloridoside was found to decrease when the suspension of algae was diluted

with water to decrease the osmotic pressure. However, the exact mode of formation and degradation of isofloridoside is not known. In this connection it is noteworthy that a fresh water stream exists in the proximity of the collection site at Dawlish which might lead to local dilution of the seawater. The isolation of pentagalactosylglycerol rather than floridoside from a sample of *Palmaria palmata* growing in an area of apparently low salt concentration, and floridoside from a sample growing in undiluted seawater seems to suggest that floridoside might play a similar role in regulating osmotic balance. And thus it seems possible that the effective concentration of floridoside in the cells may be reduced by polymerisation to form oligosaccharides in glycosidic linkage with one unit of glycerol. When needed, high levels of floridoside could then be easily regenerated by cleavage of the galactose units and subsequent glycosylation with glycerol.

CHAPTER FIVE

CORALLINA OFFICINALIS

5.1 EXTRACTION AND ISOLATION

The red alga *Corallina officinalis* was collected intertidally from Kimmeridge Bay in May and stored at -20°C for four days prior to extraction. The alga was defrosted, rinsed quickly in distilled water and left to air-dry overnight at room temperature. The half-dried alga (1.8 kg) was extracted three times with chloroform-ethanol (2:1) at room temperature followed by 70% aqueous ethanol for one hour at 80°C . The extracts were combined, concentrated *in vacuo* and partitioned between diethylether and water to give non-polar and polar extracts respectively. The non-polar fraction was further divided into ether-soluble neutral and acidic extracts using the method previously described.

The ether-soluble neutral extract (dark-green oil, 2.2 g) was chromatographed on an open neutral alumina column (80 g) and eluted with hexane, hexane-ether mixtures with increasing proportions of ether, and finally with ether. The column fractions were monitored by TLC (silica gel, chloroform). Several fractions eluted with hexane-ether (20:80) contained an oily product. The crude oil was further purified by preparative TLC on silica gel plates developed in chloroform. The pure product was obtained as a colourless oil (42 mg) with R_f 0.38 (silica gel, chloroform) and was coded CN-A.

The later fractions eluted with hexane-ether (20:80) contained a major component with R_f 0.24. This was further purified by preparative TLC using chloroform-methanol (9:1) as the solvent system. The final product was obtained as a light-coloured solid which on recrystallization from chloroform-methanol gave colourless crystals. This was found by infrared, NMR and mass spectral analysis to be a sterol mixture and was further analyzed by gas chromatography (Chapter Seven).

The ether-soluble acidic extract gave 7.2 g of dark oil. This was fractionated by repeated column chromatography on silica gel eluting with chloroform and chloroform-methanol mixtures. The chloroform-methanol (95:5) eluate gave a light brown oil when the solvent was removed under reduced pressure. The oil was found by TLC, infrared and ^1H -NMR spectroscopy to contain a mixture of fatty acids. The ^1H -NMR spectrum revealed the presence of a high proportion of polyunsaturated fatty acid but the ratio of the proton integral $-\text{CH}=\text{CH}-$ (δ 5.40) to $-\overset{|}{\underset{|}{\text{C}}}=\overset{|}{\underset{|}{\text{C}}}-\text{CH}_2-\overset{|}{\underset{|}{\text{C}}}=\overset{|}{\underset{|}{\text{C}}}-$ (δ 2.84) suggested that these were not all of the usual type with an entirely methylene interrupted double bond arrangement ¹²⁵. A sample of the oil was methylated and analyzed by gas-liquid chromatography carried out on a non-polar 3% SE-30 column. The percentages of individual acids were determined by the ratio of peak areas on the chromatogram. The oil was found to contain about 70 percent of C_{20} polyunsaturated fatty acid.

5.2 ISOLATION OF C₂₀ POLYUNSATURATED FATTY ACID AS THE METHYL ESTER

A sample of the oil (1 g) was subjected to a sequence of low temperature crystallizations¹²⁷. The oil was dissolved in acetone (20 ml) and the solution kept at -20°C for two weeks. The resulting crystals were filtered off and the filtrate was again maintained at -20°C for another week. The acidic fraction recovered from the final filtrate was converted into methyl ester by esterification with 14% BF₃-methanol⁹⁸. The resulting fatty acid ester was purified by preparative TLC on silica gel PF₂₅₄ plates developed in toluene and visualised in ultraviolet light. The band corresponding to the fatty acid methyl ester was scraped off the plate and was recovered by eluting with diethyl ether. The ether was removed under nitrogen to give an almost colourless oil. This was found by gas-liquid chromatography to contain about 80 percent of the C₂₀ polyunsaturated fatty acid methyl ester with methyl palmitate as the main contaminant. Further purification was achieved by the urea adduct method¹²⁸. The fatty acid methyl ester (420 mg) was dissolved in ethanol (10 ml) containing urea (500 mg). The solution was kept at -20°C for 4 hours. At low temperatures the urea-adduct of saturated and the less unsaturated fatty acid esters crystallize out of solution whilst the more unsaturated fatty acid ester-urea complex remains in solution. Crystals of fatty acid ester-urea

complex were filtered off and the filtrate containing the polyunsaturated fatty acid ester-urea complex was then treated with 1N HCl (10 ml) to liberate the methyl ester. The liberated methyl ester was extracted with diethyl ether and dried over anhydrous sodium sulphate. The ether was removed under nitrogen to leave an almost colourless oil coded CA-A.

5.3 FORMATION OF PYRROLIDIDE¹²⁹ OF CA-A

Fatty acid esters react quantitatively with pyrrolidine in the presence of acid to form pyrrolidides according to the following equation:



CA-A (0.1 ml) as the methyl ester was dissolved in freshly distilled pyrrolidine (5 ml) and acetic acid (0.5 ml) was added. The mixture was heated to 100°C in a tightly stoppered tube for half an hour and thereafter cooled to room temperature. The cooled reaction mixture was partitioned between dichloromethane and 1N hydrochloric acid. The organic layer was then washed with water and dried over

magnesium sulphate. The dichloromethane was removed with a stream of nitrogen and the product was then submitted to electron impact mass spectrometry.

5.4 ANALYTICAL DATA ON CN-A

CN-A was obtained pure as a clear colourless oil.

Infrared spectrum (neat): Fig. 2.19

^1H -NMR (100 MHz) in CDCl_3 with TMS as internal standard

(δ , ppm):

0.84 (6H, d, $J=6.0$ Hz), 0.86 (6H, d), 1.08 - 1.36 (19H, m),
1.66 (3H, s), 1.98 (2H, t, $J=7.0$ Hz), 4.12 (2H, d, $J=6.5$ Hz),
5.38 (1H, t, $J=6.5$ Hz)

^{13}C -NMR in CDCl_3 with TMS as internal standard (δ , ppm):

140.20 (singlet), 123.36 (doublet), 59.48 (triplet),
39.98 (triplet), 39.49 (triplet), 37.49 (triplet),
36.78 (triplet), 32.88 (doublet), 29.74 (quartet),
28.06 (doublet), 25.25 (triplet), 24.87 (triplet),
24.60 (triplet), 22.75 (quartet), 19.83 (quartet),
16.20 (quartet).

(Off-resonance multiplicities in parentheses).

Mass spectrum (E.I.M.S., 70 eV), m/z (% intensity):

296 (1.0) M^+ , 278 (2.5) $[\text{M}-\text{H}_2\text{O}]^+$, 263 (0.5) $[\text{M}-\text{H}_2\text{O}-\text{CH}_3]^+$,
71 (100) $\left[\begin{array}{c} \text{CH}_3 \\ | \\ +\text{C} \end{array} = \text{CH}-\text{CH}_2\text{OH} \right]$ (Fig. 2.20)

Chemical ionisation: 297 $[\text{M}+1]^+$ (18)

5.5 ANALYTICAL DATA ON CA-A

CA-A was obtained pure in the form of the methyl ester as an almost colourless oil.

Infrared spectrum (neat): Fig. 2.21

^1H -NMR (100 MHz) in CDCl_3 with TMS as internal standard

(δ , ppm):

0.96 (3H, t, $J=8.0$ Hz), 1.92 - 2.46 (10H, m), 2.84 (6H, m), 3.68 (3H, s), 5.39 (10H, m).

^{13}C -NMR in CDCl_3 with TMS as internal standard (δ , ppm):

173.85 (s), 132.02 (d), 128.88 (d), 128.61 (d), 128.23 (d), 128.12 (d), 127.91 (d), 127.09 (d), 51.41 (q), 33.64 (t), 27.30 (t), 26.60 (t), 25.69 (t), 20.97 (t), 20.64 (t), 14.30 (q).

Mass spectrum (chemical ionisation), m/z (relative intensity)

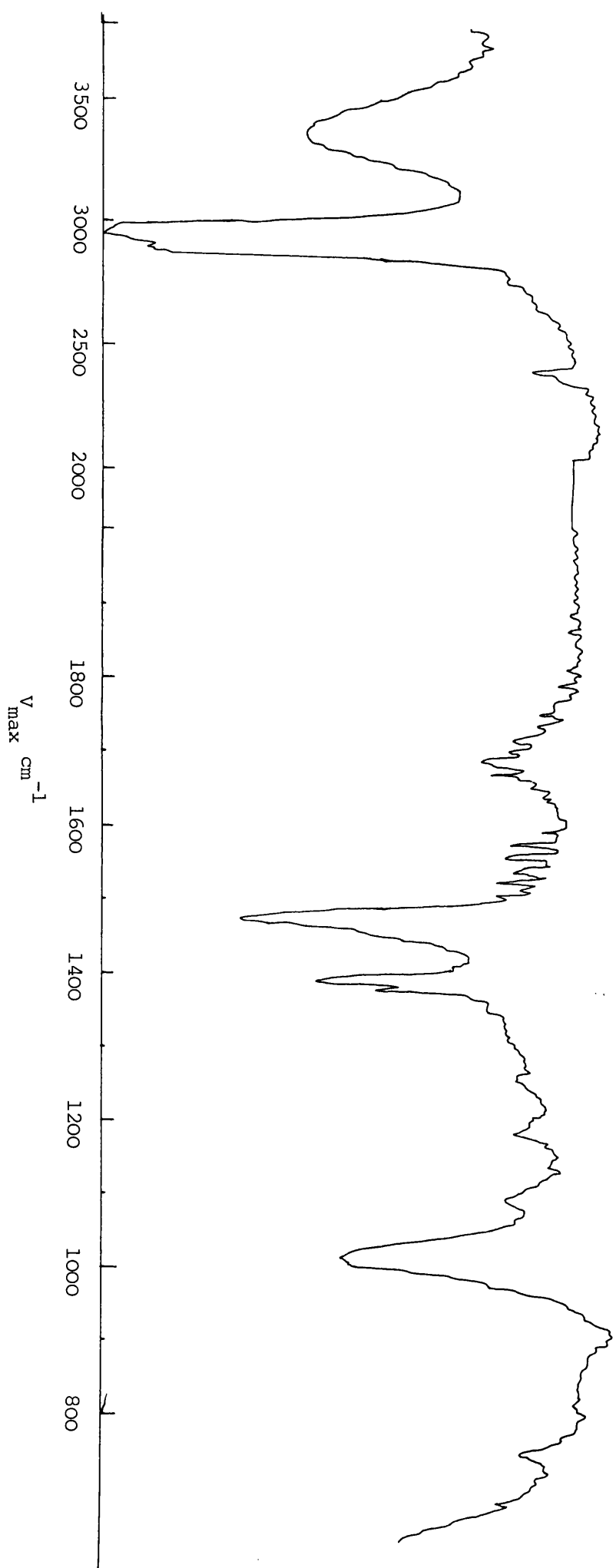
317 $[\text{M} + \text{i}]^+$ (82), 271 (100), 131 (71), 74 $[\text{CH}_2=\underset{\text{OH}}{\text{C}}-\text{OMe}]^+$ (24)

5.6 DISCUSSION

5.6.1 CN-A

The colourless oil from the neutral fraction CN-A, gave only one peak on gas-liquid chromatography (OV-17, 1 metre column at 170°C with nitrogen as carrier gas at a pressure of 140 kN/m^2). The infrared spectrum (Fig. 2.19) showed the presence of hydroxyl group (3380 cm^{-1} , O-H stretch) and double bond (3020 , C-H stretch and 1670 cm^{-1} C=C stretch). The mass spectral

Fig. 2.19. Infrared spectrum of CN-A



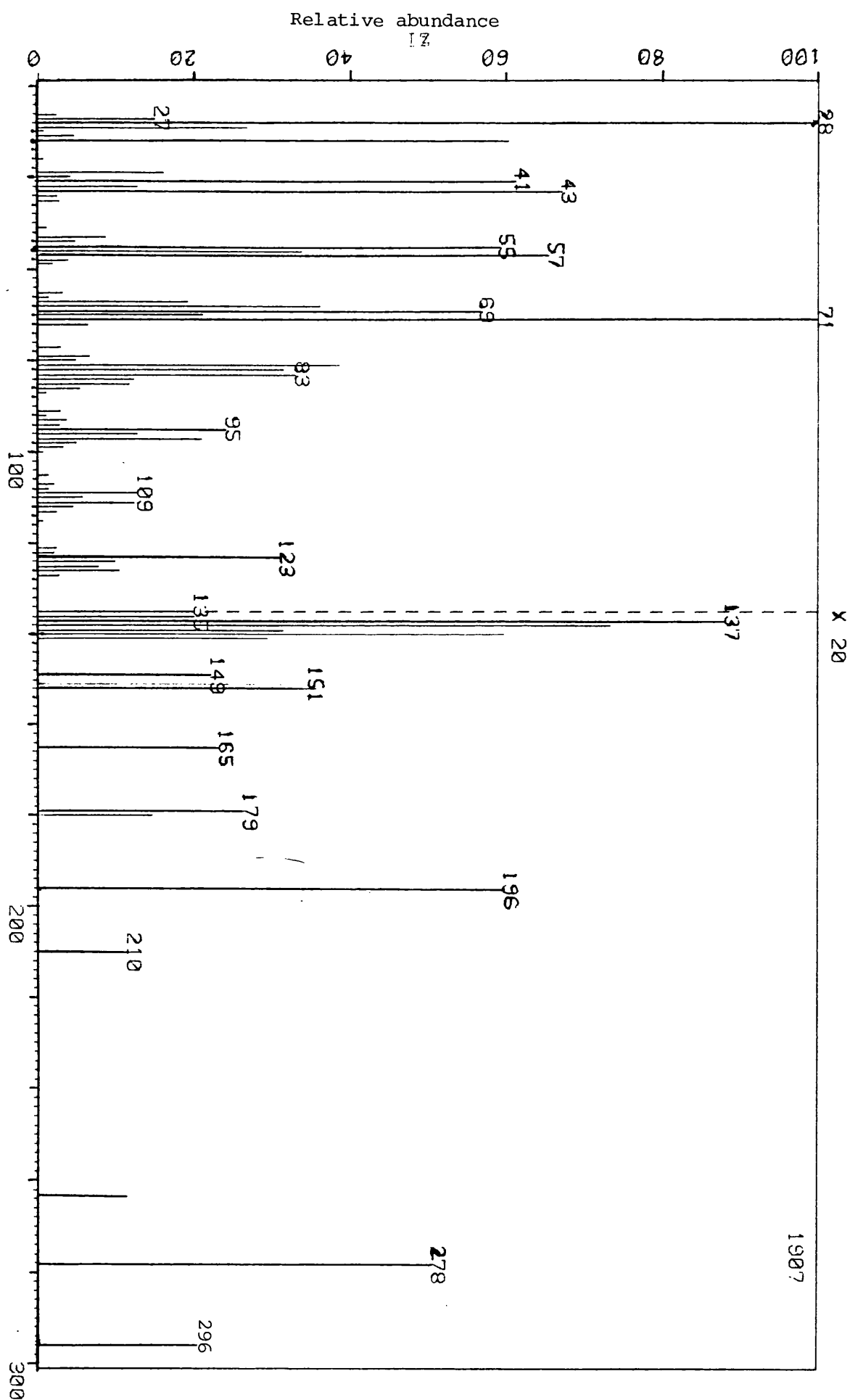
(E.I.M.S.) data (Fig. 2.20) showed a molecular ion peak at m/z 296 (further supported by a peak at m/z 297 $[M+1]^+$ in the chemical ionisation mass spectrum). Other fragments were observed at m/z 278 $[M-H_2O]^+$, 263 $[M-H_2O-CH_3]^+$ and the base peak at m/z 71 $[C(CH_3)=CH-CH_2OH]^+$. A molecular weight of 296 corresponds to the molecular formula $C_{20}H_{40}O$. This formula is suggestive of a diterpene alcohol possessing only one double bond.

The 100 MHz 1H -NMR spectrum in $CDCl_3$ exhibited signals at δ 0.80 - 0.90 which are two superimposed six-proton doublets centred at δ 0.84 and 0.86 and are assignable to two terminal methyl groups and two side-chain methyl groups. The three-proton singlet at δ 1.66 is due to a vinyl-methyl group, and the two-proton doublet ($J = 6.5$ Hz) at δ 4.12 can be attributed to a primary alcohol methylene group adjacent to a trisubstituted carbon atom. The downfield resonance at δ 5.38 (1H, triplet, $J = 6.5$ Hz) can be assigned to a vinyl proton. The 1H -NMR and mass spectral data are consistent with the structure of the diterpene alcohol, phytol. The infrared spectrum is also identical with that published by De Souza and Nes¹³⁰ for phytol.

The ^{13}C -NMR spectrum in $CDCl_3$ exhibited signals at δ 140.20 (s) and 123.36 (d) (off-resonance multiplicities in parentheses) which confirm the presence of $-C=C-$ group (a trisubstituted double bond) in the molecule.

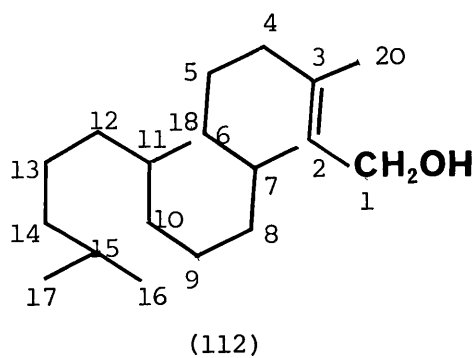
Fig. 2.20. CN-A

70 eV E.I.



The resonance at 59.48 (t) attributable to a primary alcohol-methylene group, the signals at δ 29.74 (q) vinyl-CH₃, 22.75 (q) and 19.83 (q) side chain methyl groups, and 16.20 (q) terminal methyl groups provide additional evidence in support of the isolated diterpene alcohol being phytol.

The published ¹H-NMR data ¹³¹ (determined in CCl₄) on *trans* and *cis*-phytol ((E)- and (Z)-3,7,11,15-tetramethyl-2-hexadecen-1-ol respectively) show the vinyl-methyl signals at δ 1.64 for the former and δ 1.71 for the latter, and the primary alcohol-methylene groups as doublets at δ 4.05 for *trans*-phytol and δ 4.48 for the *cis*-isomer. The signal for the vinyl proton in both isomers was recorded as a triplet at δ 5.33. The three-proton singlet at δ 1.66, the two-proton doublet at δ 4.12 and the one-proton triplet at δ 5.38 in the ¹H-NMR spectrum of CN-A in CDCl₃ point conclusively to the structure (112) of *trans* - phytol ((E)-3,7,11,15-tetramethyl-2-hexadecen-1-ol)



Trans-phytol occurs naturally as a component of chlorophyll from which it is obtained by hydrolysis¹³² while *cis*-phytol occurs naturally only in the free form¹³¹. In this present study members of the red seaweed (Rhodophyta) were investigated for low molecular weight constituents. The diterpene alcohol, phytol, was found in *Corallina officinalis* without a deliberate attempt to hydrolyze the extract but not in any other red seaweed investigated. Since the phytol isolated was unequivocally shown to be the *trans*-isomer it was possibly derived by hydrolysis of chlorophyll. This finding may reflect the calcareous nature of *Corallina officinalis*. The presence of significant quantities of calcium carbonate might render the extraction medium sufficiently alkaline to induce the hydrolysis of chlorophyll.

The presence of *trans*-phytol has been demonstrated in hydrolysed extracts in representatives of brown (Phaeophyta)¹³⁰ blue-green (Cyanophyta)¹³⁰ and green (Chlorophyta)¹³³ algae. Both *cis*- and *trans*-phytol were reported from the red alga *Gracilaria andersoniana*¹³¹. The *trans*-phytol isolated from *Corallina officinalis* in this present investigation showed no evidence of the presence of *cis*-phytol. This finding is in agreement with the presence of only *trans*-phytol in green, blue-green and brown algae. The isolation of both *cis*- and *trans*-phytol from *Gracilaria andersoniana* is therefore not necessarily a general feature of the red algae.

5.6.2 CA-A

CA-A was isolated from the fatty acid fraction by a sequence of low temperature crystallizations¹²⁹. After conversion into the methyl ester and subsequent purification, it was found by gas-liquid chromatography to contain mainly C₂₀ polyunsaturated fatty acid methyl ester. The infrared spectrum of the methyl ester Fig. 2.2.1 was characteristic of that of an unsaturated fatty acid methyl ester and indicated the presence of non-conjugated double bonds absorptions (3020, C-H stretch, and a weak band at 1650 cm⁻¹, C=C stretch). The absence of any significant absorption at 965 cm⁻¹ indicated the absence of *trans*-olefinic unsaturation implying that all the double bonds have the *cis*- configuration.

The chemical ionisation (isobutane) mass spectrum exhibited a molecular ion at m/z 317 $[M + 1]^+$ indicating a C₂₀ polyunsaturated fatty acid methyl ester with five double bonds or equivalent unsaturation, and an empirical formula, C₂₁H₃₂O₂. However, as is the case with electron impact mass spectra of unsaturated esters, no information concerning the double bond positions could be gained from the spectrum.

¹H-NMR spectroscopy has been shown to be of immense value in the structural elucidation of fatty acids^{126,134,135}. The ¹H-NMR spectrum of the methyl ester of CA-A was structurally very informative (Table 2.XV). The pattern

Fig. 2.21. Infrared spectrum of CA-A

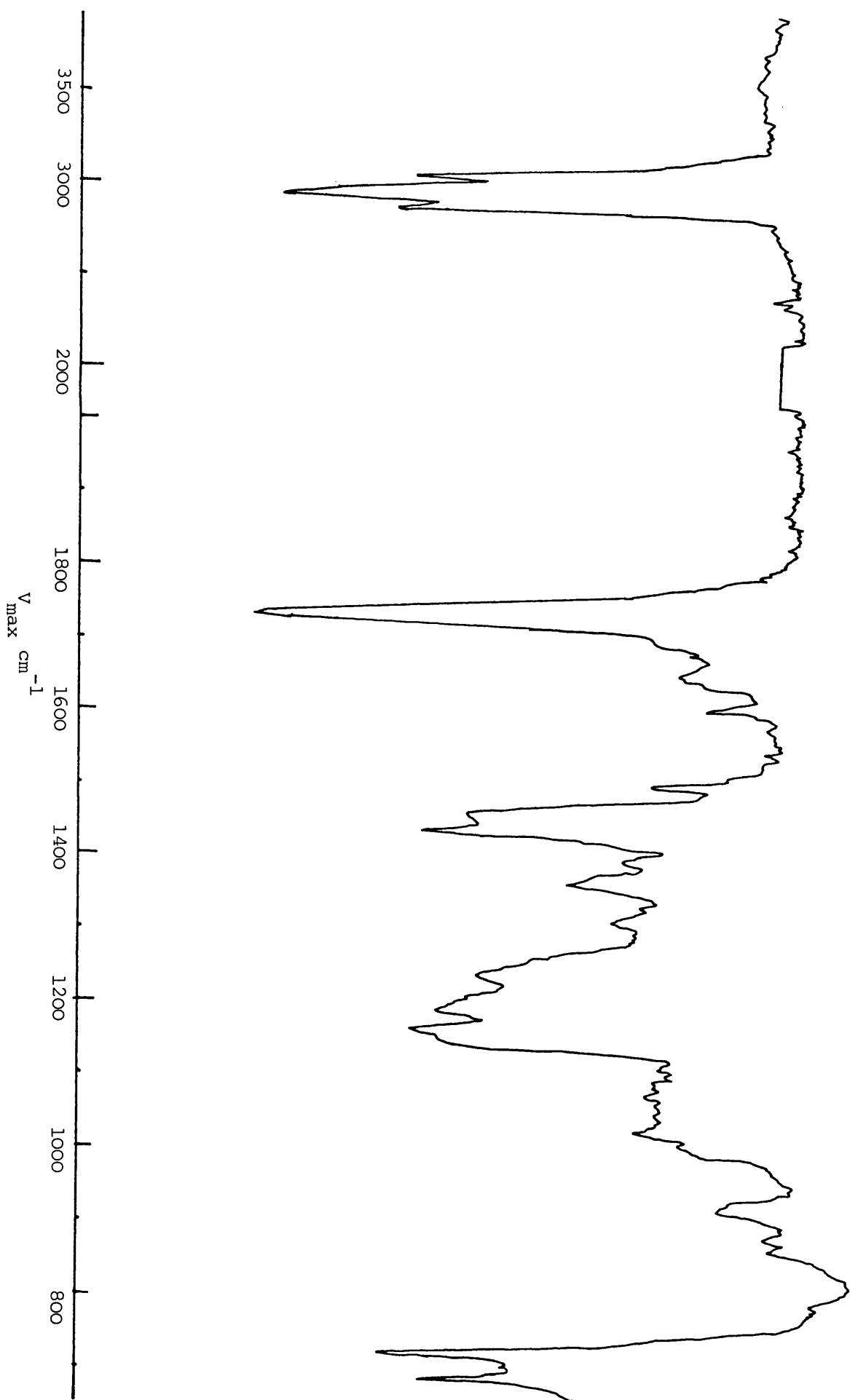


(Fig. 2.22) of the signal (well-defined triplet, $J = 8.0$ Hz) centred at $\delta 0.96$ (3H) is that of the terminal methyl group characteristic of fatty acids with ω_3 unsaturation¹³⁰ indicating the presence of double bond β - to the terminal methyl group (The notation ω , indicates the position of the double bond counted from the terminal methyl group while Δ denotes the double bond position counted from the carboxylic group). This signal is superimposable on the corresponding signal (Fig. 2.23) for methyl linolenate (18:3 ω_3). Hence the C_{20} pentaene acid is considered to have an ω_3 double bond. There was no signal at $\delta 3.05$ due to methylene protons α - to both an olefinic group and a carboxylic group. This, coupled with the absence of any signal at $\delta 5.55$ due to olefinic protons situated β - to the carboxylic group¹²⁸ ruled out the presence of a Δ_3 double bond ($-\text{CH}=\text{CH}.\text{CH}_2\text{CO.O-}$). The absence of a Δ_2 unsaturation in which the double bond is in conjugation with the carboxylic group ($-\text{CH}=\text{CH}.\text{CO.O-}$) was established by the absence of any signal downfield of that due to the isolated olefinic protons, and was confirmed by the absence of strong infrared absorption bands at 1650 and 1715 cm^{-1} , characteristic of $\alpha\beta$ -unsaturated esters¹²⁸. The signal at $\delta 2.84$ (6H, multiplet) is in the usual position for allylic methylene groups ($=\text{CH}.\text{CH}_2.\text{CH}=\text{}$). The occurrence of six protons in the allylic position requires at least four of the double bonds to be in the familiar 1,4 relationship (methylene-interrupted or divinylmethane arrangement), as in linolenic acid. The multiplet centred at $\delta 5.39$ (10H)

Fig. 2.22 ^1H -NMR spectrum of CA-A

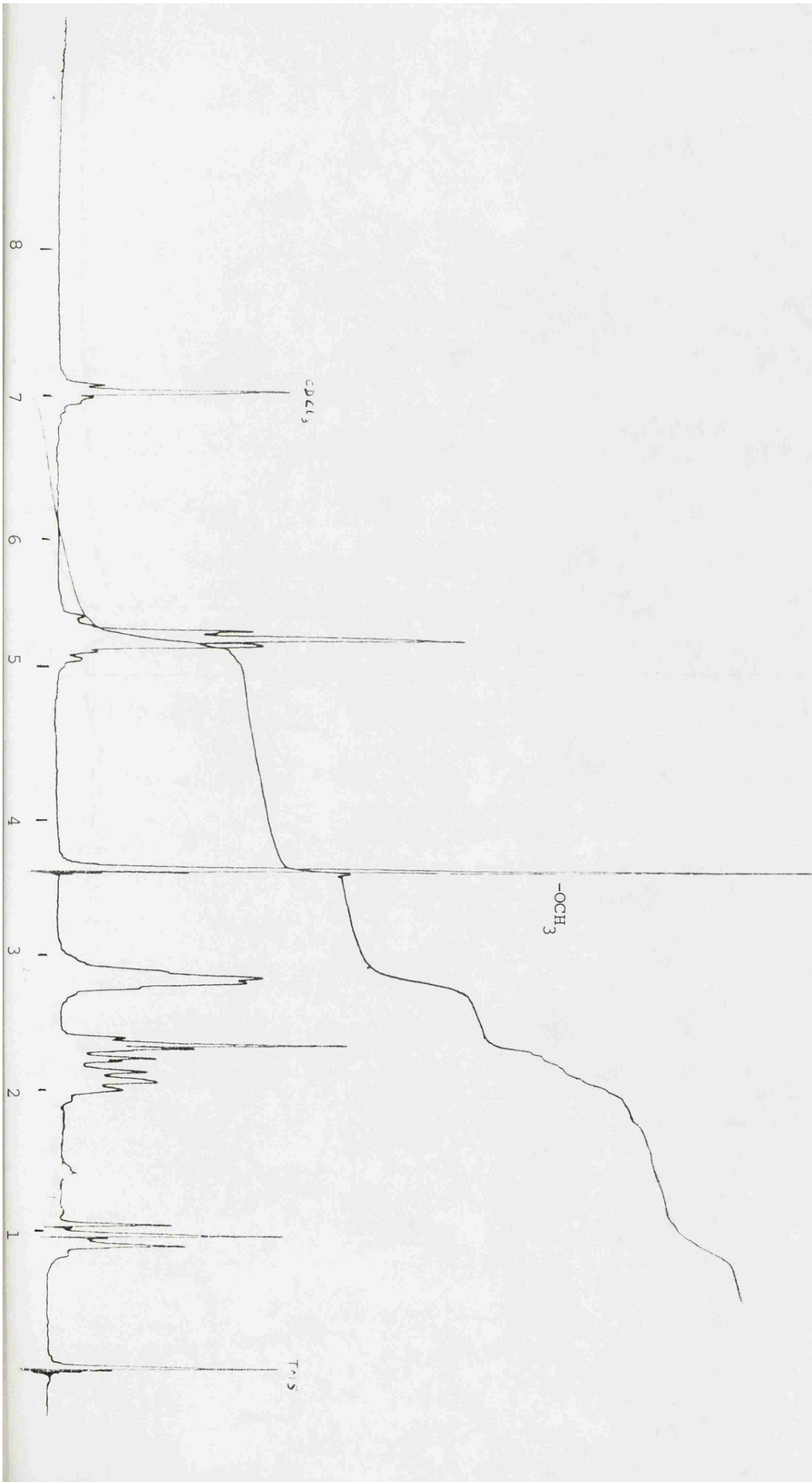


Fig. 2.23 ^1H -NMR spectrum of methyl linolenate (18:3 δ 3)

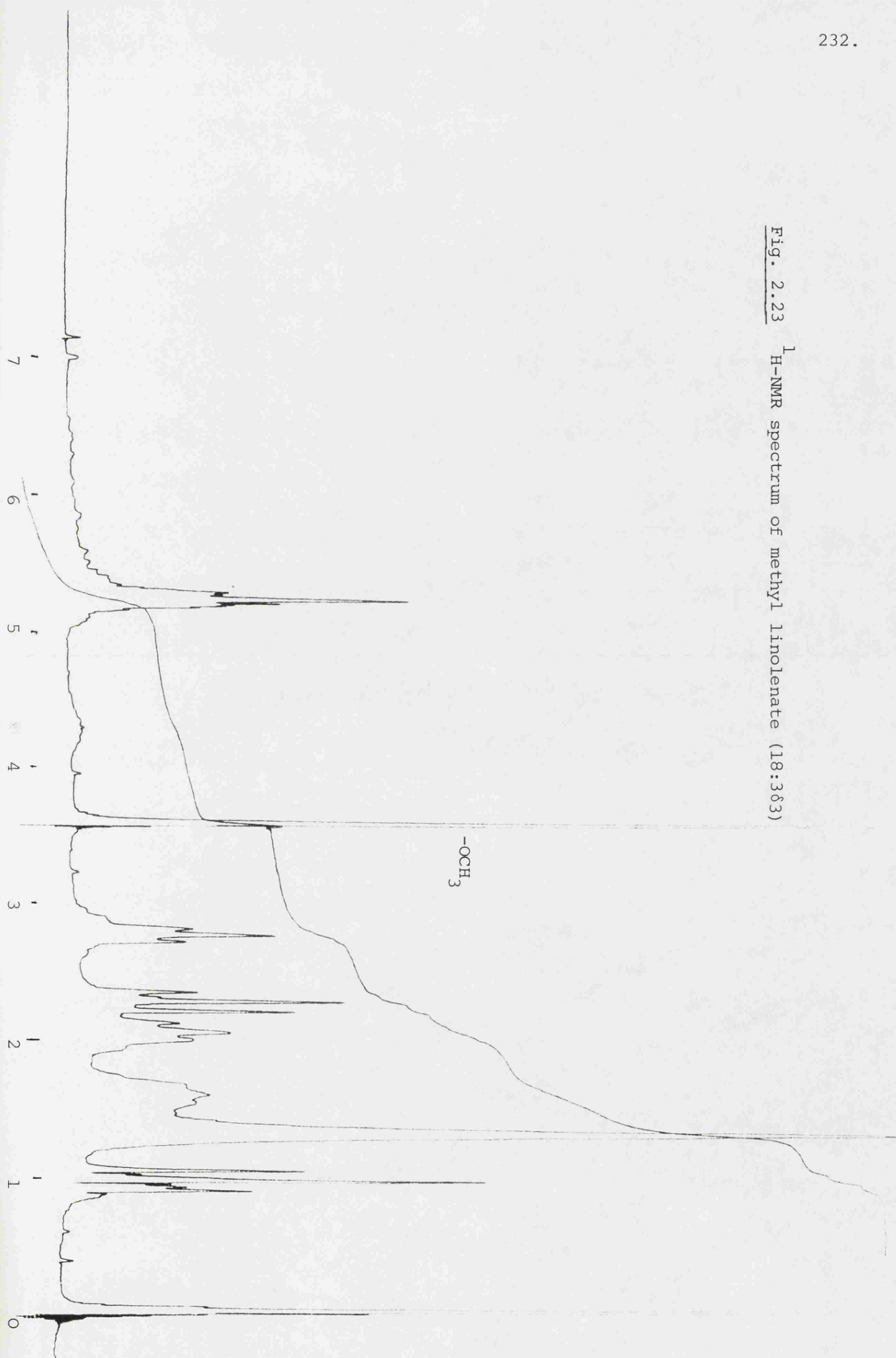


Table 2.XV. ^1H -NMR data on CA-A (methyl ester) in CDCl_3 (δ , ppm). Internal reference, TMS = 0

Chemical Shift (δ , ppm)	Multiplicity of signal	No. of protons	Assignment
0.96	triplet	3	$\overset{*}{\text{CH}}_3 \cdot \text{CH}_2 \cdot \text{CH} =$
1.92 - 2.46	multiplet	10	$=\text{CH} \cdot \overset{*}{\text{CH}}_2 \cdot \overset{*}{\text{CH}}_2 \cdot \text{CH} =$ and $-\overset{*}{\text{CH}}_2 \cdot \text{CO} \cdot \text{O}-$
2.84	multiplet	6	$=\text{CH} \cdot \overset{*}{\text{CH}}_2 \cdot \text{CH} =$
3.68	singlet	3	$-\text{CO} \cdot \text{OCH}_3$
5.39	multiplet	10	$-\text{CH}_2 \cdot \overset{*}{\text{CH}} = \overset{*}{\text{CH}} \cdot \text{CH}_2 -$

* relevant protons

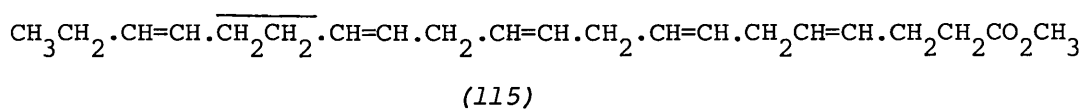
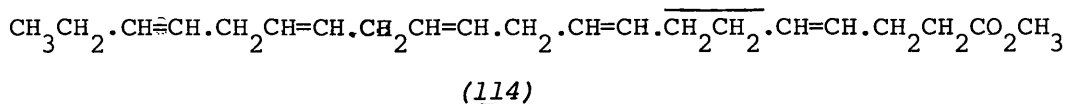
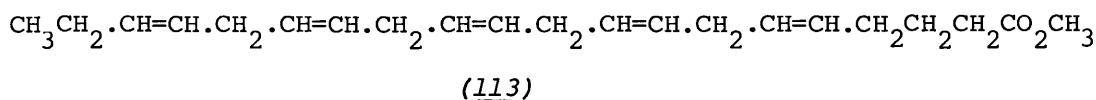
is assignable to the olefinic protons, and confirms the presence of five disubstituted double bonds. The three-proton singlet at $\delta 3.68$ is due to the methyl ester group ($-\text{COO} \cdot \text{CH}_3$). The ^1H -NMR spectrum has so far indicated the presence of the following partial structures:

$\text{R}' \cdot \text{CH} = \text{CH} \cdot \text{CH}_2 \cdot \text{CH} = \text{CH} \cdot \text{CH}_2 \cdot \text{CH} = \text{CH} \cdot \text{CH}_2 \cdot \text{CH} = \text{CH} \cdot \text{R}^2$ (three divinyl methane ($=\text{CH} \cdot \text{CH}_2 \cdot \text{CH} =$) groups), $\text{CH}_3 \cdot \text{CH}_2 \cdot \text{CH} = \text{CH} -$ (ω3 double bond), $-\text{CH}_2 \text{CH}_2 \text{CO}_2 \cdot \text{CH}_3$ (absence of Δ^3 and Δ^2 double bonds).

The complex multiplet at $\delta 1.92 - 2.46$ integrating to about ten protons is attributable to the methylene group α to the carboxylic group, and to methylene groups α to single double-bonded carbons. It has been shown¹²⁶ that the divinylethane arrangement of double bonds, if present

in highly unsaturated fatty acids, would have the signal of the dimethylene groups ($=\text{CH}.\text{CH}_2.\text{CH}_2.\text{CH}=\text{}$) overlapping with that of the α -methylene groups.

Hashimoto *et al.*¹²⁶ have established that the ratio of the area intensity of signals of $=\overset{|}{\text{C}}.\text{CH}_2.\overset{|}{\text{C}}=$ to $-\text{CH}=\text{CH}-$ (ratio A), and the ratio of the area intensity of signals of α -methylene groups to $-\text{CH}=\text{CH}-$ (ratio B) are of diagnostic value in distinguishing between polyunsaturated fatty acid esters with solely a divinylmethane arrangement of the double bonds and those with one divinylethane in addition to divinylmethane groups. In structure (113) where the C-20 pentaenoic fatty acid methyl ester has solely divinylmethane (methylene interrupted) arrangement of double bonds there are ten olefinic protons ($-\text{CH}=\text{CH}-$), four divinylmethane groups ($=\overset{|}{\text{C}}-\text{CH}_2-\overset{|}{\text{C}}=$, eight protons), and six α -methylene ($-\overset{|}{\text{C}}=\overset{|}{\text{C}}.\text{CH}_2.\overset{|}{\text{C}}-$ and $-\text{CH}_2.\text{COO}-$) protons. Thus theoretically, for structure (113), ratio A = 0.80, and ratio B = 0.60. (114) is a possible structure for a C-20 pentaenoic fatty acid methyl ester with one divinylethane and three divinylmethane groups in the double bond arrangement. It contains ten olefinic protons, three divinylmethane groups (six protons) and ten α -methylene protons. The theoretical values of ratios A and B for structure (114) are thus 0.60 and 1.00 respectively. In the ^1H -NMR spectrum of CA-A, the ratio of the proton integrals for the signals at $\delta 2.84$ ($=\text{C}.\text{CH}_2.\text{C}=\text{}$) to the signals at $\delta 5.39$ ($-\text{CH}=\text{CH}-$), ratio A was found to be 0.63, and for the signals at



($\overline{\quad}$ = divinylethane group)

δ 1.92 - 2.46 (α -methylene and divinylethane protons) to the signals at δ 5.39, the proton integral ratio (ratio B) was found to be 0.94. These values are, within the limit of experimental error,¹²⁶ in good agreement with the theoretical values (0.60 and 1.00 respectively) for a C-20 pentaenoic acid with one divinylethane and three divinylmethane groups in the double bond arrangement. Given that the presence of ω 3 unsaturation, three divinylmethane groups and the absence of Δ 3 and Δ 2 double bonds have been established by chemical shift parameters, it is not possible to devise a structure for CA-A with more than one divinylethane group. The correct structure for CA-A is therefore limited to two possibilities - (114) and (115) - in which both have theoretical values of 0.60 and 1.00 for ratios A and B respectively.

Anderson and Holman¹²⁹ reported that mass spectra of pyrrolidides of monounsaturated, straight chain fatty acids contain principally ions from the polar end of the molecule. Their interpretative rule for such spectra

states that:

"If an interval of 12 atomic mass units, instead of the regular 14, is observed between the most intense peaks of clusters of fragments containing n and $n-1$ carbon atoms of the acid moiety, the double bond occurs between carbons n and $n+1$ in the molecule".

This rule was shown to be valid for 18:1 isomers, and was used successfully to characterize 18-carbon monoenes with unsaturation in the 4, 16 and 17 positions. The rule was used with limited success by Joseph¹³⁵ to locate the positions of ethylenic bonds in 18:5 ω 3. The spectrum of the pyrrolidide derivative was found to contain numerous fragments of odd m/z which were particularly troublesome. The E.I.M.S at 70 eV of the pyrrolidide derivative of CA-A has the base peak at m/z 113 formed by a McLafferty rearrangement¹³⁶ (Fig. 2.24), and the molecular ion at m/z 355. These peaks confirm the successful preparation of the pyrrolidide derivative. The molecular ion of the pyrrolidide also constitutes additional evidence in support of the molecular weight, 302, of the free acid corresponding to a 20:5 acid. However, the rest of the spectrum contained cleavage patterns in the high mass region with peaks 14 atomic mass units apart, and only one pair of peaks at m/z 126 - 138 corresponding to C_3-C_4 are 12 atomic mass units apart. According to the interpretative rule, this locates a double bond in the $\Delta 4$ position. Numerous fragments of odd m/z were also seen in the mass spectrum and it was not possible to locate the positions of any

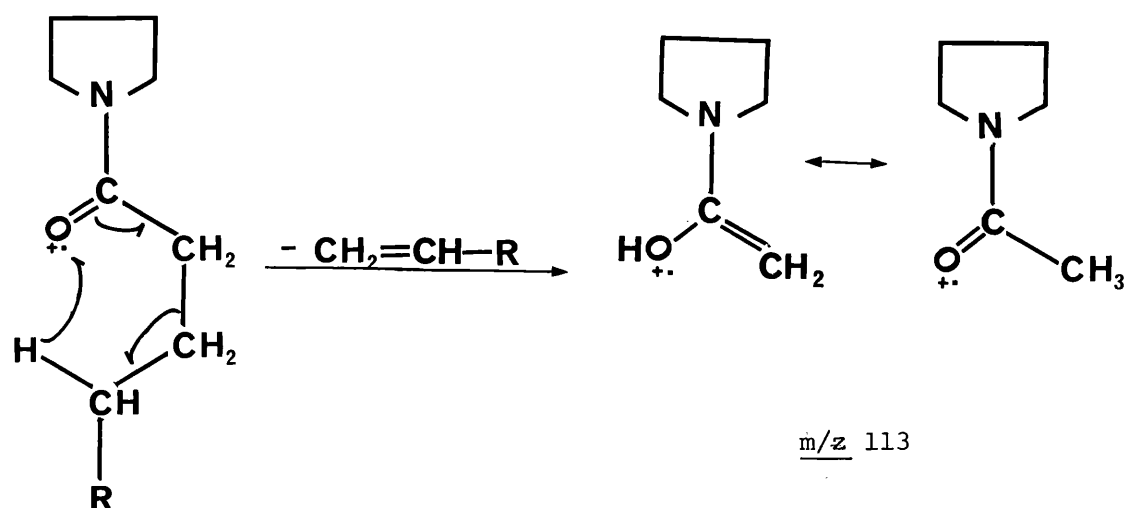


Fig. 2.24. McLafferty rearrangement in a fatty acid pyrrolidide.

other double bond with certainty. The pyrrolidide derivative of methyl linolenate (18:3 ω 3) was prepared and the mass spectrum determined under similar conditions. Apart from the molecular ion at m/z 331 and the base peak at m/z 113, the mass spectrum contained peaks that are 14 atomic mass units apart. Again, only one pair of peaks at m/z 196 - 208 ($\text{C}_8 - \text{C}_9$) are 12 atomic mass units apart thus locating a double bond in the Δ^9 position.

Again, it was not possible to locate the position of the other double bonds with certainty. It is however notable that in the mass spectrum of both pyrrolidide derivatives, the double bonds located are those closest to the carboxyl end of the molecules. It thus seems that the method has limited application with polyunsaturated fatty acids. It also seems probable that the position of the double bond closest to the carboxyl end in polyunsaturated fatty acids can be located with relative ease using this method.

The two structures, 20:5 ω 3,6,9,12,16 and 20:5 ω 3,7,10,13,16 (shorthand notation for chain length: number of double bonds, and positions counted from the terminal methyl group) [4, 8, 11, 14, 17 - and 4, 7, 10, 13, 17- eicosapentaenoic acid respectively] cannot be distinguished by simple oxidative splitting since both would give the same products. Both structures would also be expected to have the same equivalent chain length and gas chromatographic retention times. The electron impact mass spectrum of the pyrrolidide derivative served to confirm the presence of Δ 4 double bonds in the molecule but could not distinguish between the two probable structures. The ^{13}C -NMR spectrum was characteristic of that of a highly unsaturated fatty acid but did not offer any clue that could help to draw a distinction between the two structures.

Non-methylene interrupted fatty acids are rarely reported in algae although non-methylene interrupted fatty acids 20:2

and 22:2 have been reported in *Corallina officinalis*⁸⁵. Unfortunately, the actual double bond positions in these fatty acids were not stated but it is possible that they may be ethylene-interrupted and may share a common origin with the isolated eicosapentaenoic acid. Non-methylene interrupted fatty acids do occur frequently in marine molluscs¹³⁷ and there has been a strong suggestion that they originate in algae and consequently may pass through the marine food chains into higher trophic levels¹³⁷.

CHAPTER SIX

LAURENCIA PINNATIFIDA

6.1 EXTRACTION AND ISOLATION

The red alga *Laurencia pinnatifida* was collected from Portland in March and stored at -20°C for two weeks prior to extraction. The seaweed was thawed, rinsed briefly in distilled water and dried overnight at room temperature. The half-dried alga (660 g) was extracted three times at room temperature with chloroform-methanol (1:1) and twice at 70°C for two hours with 70 percent aqueous methanol. The extracts were combined and concentrated *in vacuo*. The concentrated extract was partitioned between diethyl ether and water to give non-polar and polar extracts respectively. The non-polar extract was further divided into ether-soluble acidic and neutral extracts by the method described previously.

Column chromatography of the ether-soluble acidic fraction on silica gel eluted with n-hexane and n-hexane-diethyl ether mixtures resulted in the isolation of a mixture of fatty acids which was further analyzed by gas-liquid chromatography (see Chapter 7).

The ether-soluble neutral extract was chromatographed on a column of silica gel eluted with n-hexane, n-hexane-toluene and toluene-methanol mixtures. Fractions from the column were monitored by TLC on silica gel plates and visualised by spraying with 50% sulphuric acid followed by heating at 110°C for 5 min. The initial fractions eluted

with hexane-toluene (20;80) contained a major component, R_f 0.58 (TLC silica gel, toluene), with a purple fluorescence under ultraviolet light λ_{254} , and a minor component with R_f 0.35 which was found to be a mixture of fatty acid glycerides (infrared and ^1H -NMR evidence). The toluene-methanol eluents yielded a sterol mixture which was further analyzed by gas-liquid chromatography (Chapter 7).

The component with R_f 0.58 from the hexane-toluene (20:80) fraction was further purified by preparative TLC on silica gel with toluene as the mobile phase and visualised under ultraviolet light (λ_{254}). The component was scraped off the plate and eluted from the adsorbent with diethyl ether. The ether was removed *in vacuo* to leave a light yellow oil which solidified on refrigeration. The oil was coded PLP-NB.

6.2 PERMANGANATE-PERIODATE OXIDATION¹²⁷ OF PLP-NB

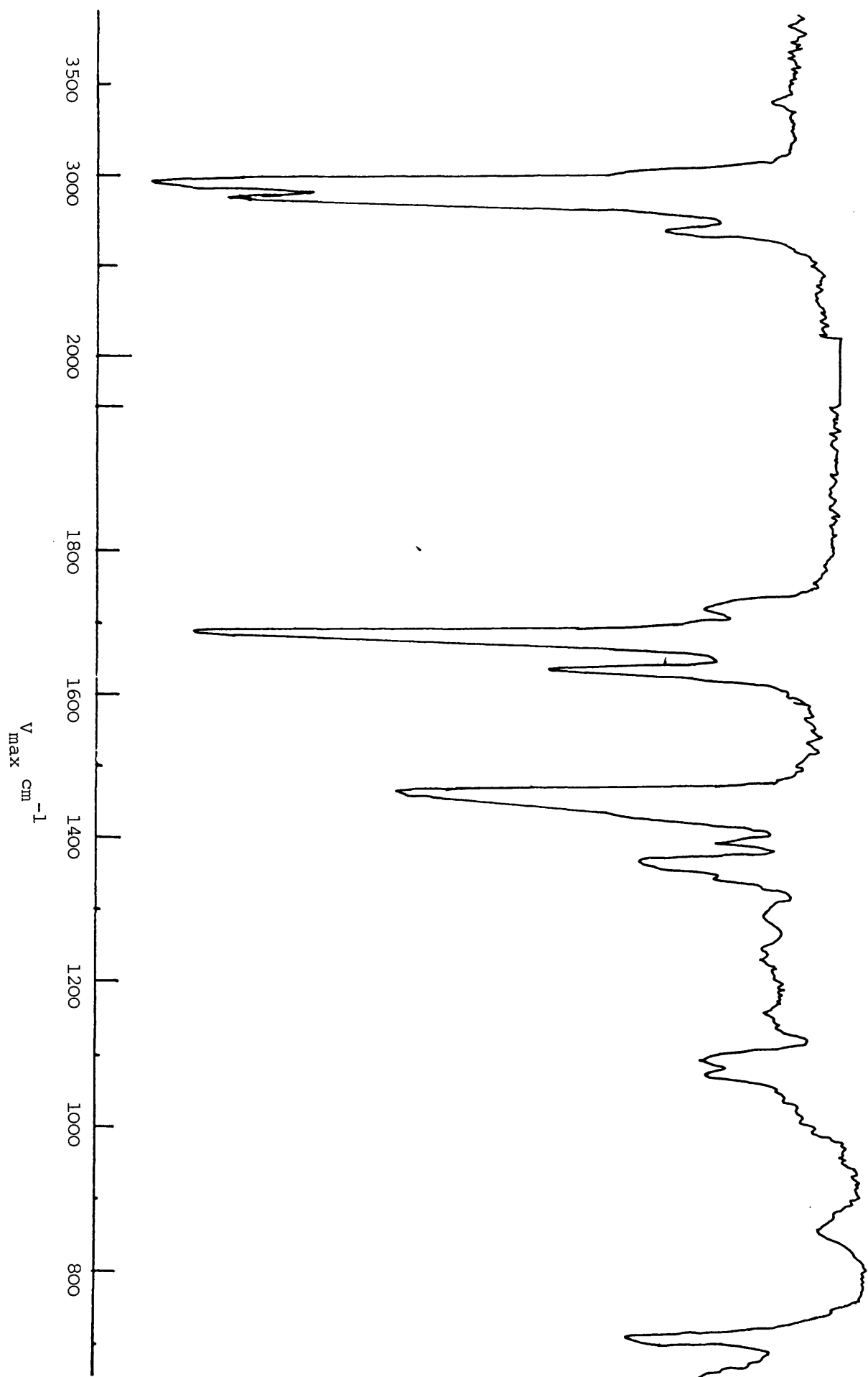
PLP-NB (15 mg) was stirred at room temperature for 3 days with potassium carbonate (25 mg), sodium periodate (100 mg), potassium permanganate (1.5 mg) and water (25 ml). The reaction mixture was thereafter chilled and acidified with 6N hydrochloric acid. Excess reagents were reduced by adding sodium bisulphite until the reaction mixture became colourless. It was then extracted with diethyl ether, the organic layer washed with

water, dried over magnesium sulphate and filtered. The filtrate was concentrated with a stream of nitrogen and then methylated with BF_3 -methanol complex. The methylated product was analyzed by gas-liquid chromatography on a 3% SE-30 column.

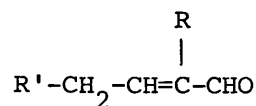
6.3 RESULTS AND DISCUSSION

PLP-NB was obtained as a light-yellowish oil which solidified on refrigeration. The infrared spectrum (neat) Fig. 2.25 exhibited C-H stretching at 2960, 2880 and 2700 cm^{-1} . The weak absorption band at 2700 cm^{-1} is suggestive of an aldehyde C-H stretching vibration. The absorption bands at 1690 (conjugated C=O stretch) and 1640 cm^{-1} (C=C stretch) are suggestive of a conjugated carbonyl system. The ^1H -NMR spectrum (ppm, in CDCl_3) showed a sharp one-proton singlet $\delta 9.34$ attributable to an aldehyde proton, and a one-proton triplet at $\delta 6.42$ attributable to a vinyl proton and indicative of the presence of a trisubstituted double bond ($-\text{CH}_2\text{CH}=\overset{\text{I}}{\text{C}}-$). The absence of secondary and tertiary methyl signals suggests that it is not a terpenoid. The ^{13}C -NMR spectrum (ppm, in CDCl_3) furnished a signal at $\delta 194.97$ (d) and thus confirmed the presence of an aldehyde carbonyl group (off-resonance multiplicities in parentheses). The signals at $\delta 154.78$ (d) and 144.05 (s) confirmed the presence of a trisubstituted double bond. The infrared, ^1H - and ^{13}C -NMR spectra are consistent with the partial structure

Fig. 2.25. Infrared spectrum of PLP-NB



(116) for PLP-NB:



(116)

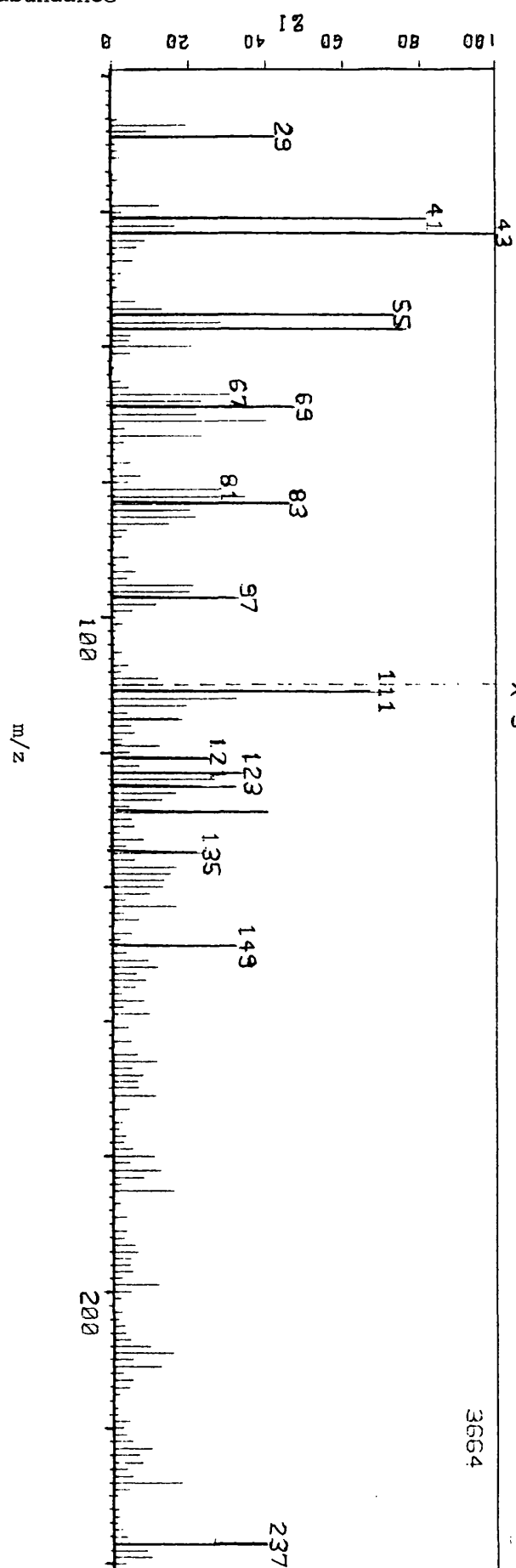
Mass spectral (70 eV E.I.) analysis (Fig. 2.26) revealed a molecular ion at m/z 434 and an $[M-28]^+$ (presumably $[M-\text{CO}]^+$) fragment at m/z 406. The low eV (E.I.) mass spectrum (Fig. 2.27) served to confirm the peak at m/z 434 as the molecular ion and the peak at m/z 406 as a fragment from the molecular ion and not due to a contaminant. However, the mass spectrum did not show any sign of bromination or chlorination. Though the presence of monoisotopic halogens (fluorine and iodine) could not be ruled out from the nature of the molecular ion cluster, the absence of peaks corresponding to HI, HF, $[M-\text{F}]^+$, $[M-\text{HF}]^+$, $[M-\text{I}]^+$, or $[M-\text{HI}]^+$ seems to suggest that PLP-NB is not halogenated. The ^1H - and ^{13}C -NMR spectra equally did not show any indication of halogenation.

In order to determine the nature of R and R' in (116), PLP-NB was subjected to oxidative cleavage by permanganate-periodate. The product was esterified using BF_3 -methanol and was shown by gas-liquid chromatography to contain two fatty acid esters tentatively identified as C_{14} and C_{15} fatty acid esters. The structure of PLP-NB may thus be

Fig. 2.26.

PLP-NB 70eV E.I.

X 5



Relative abundance

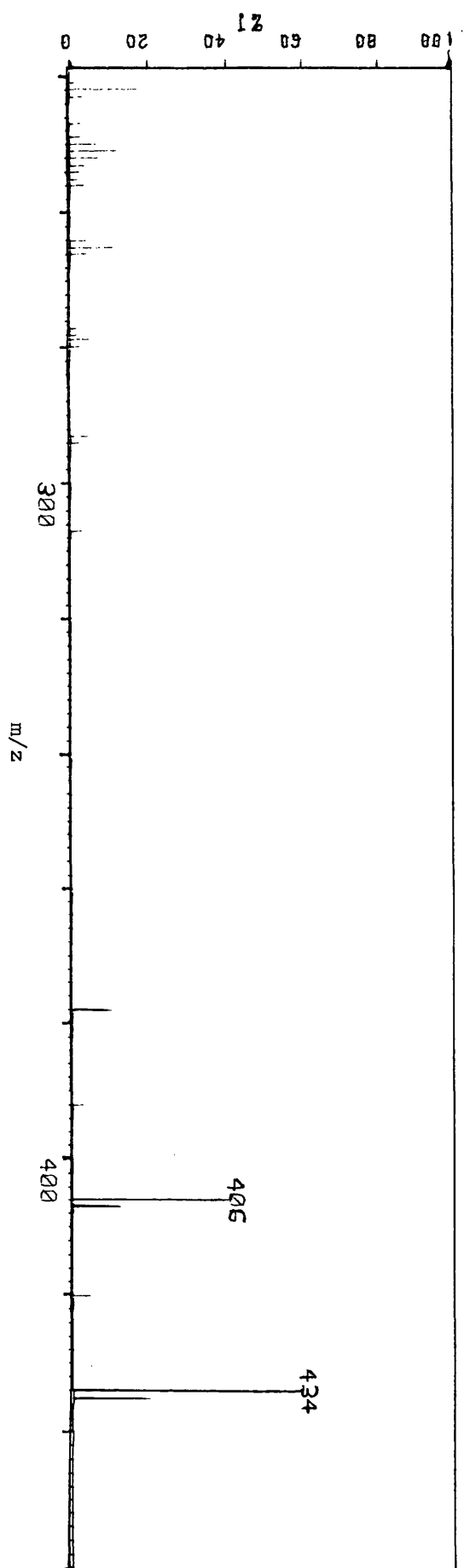
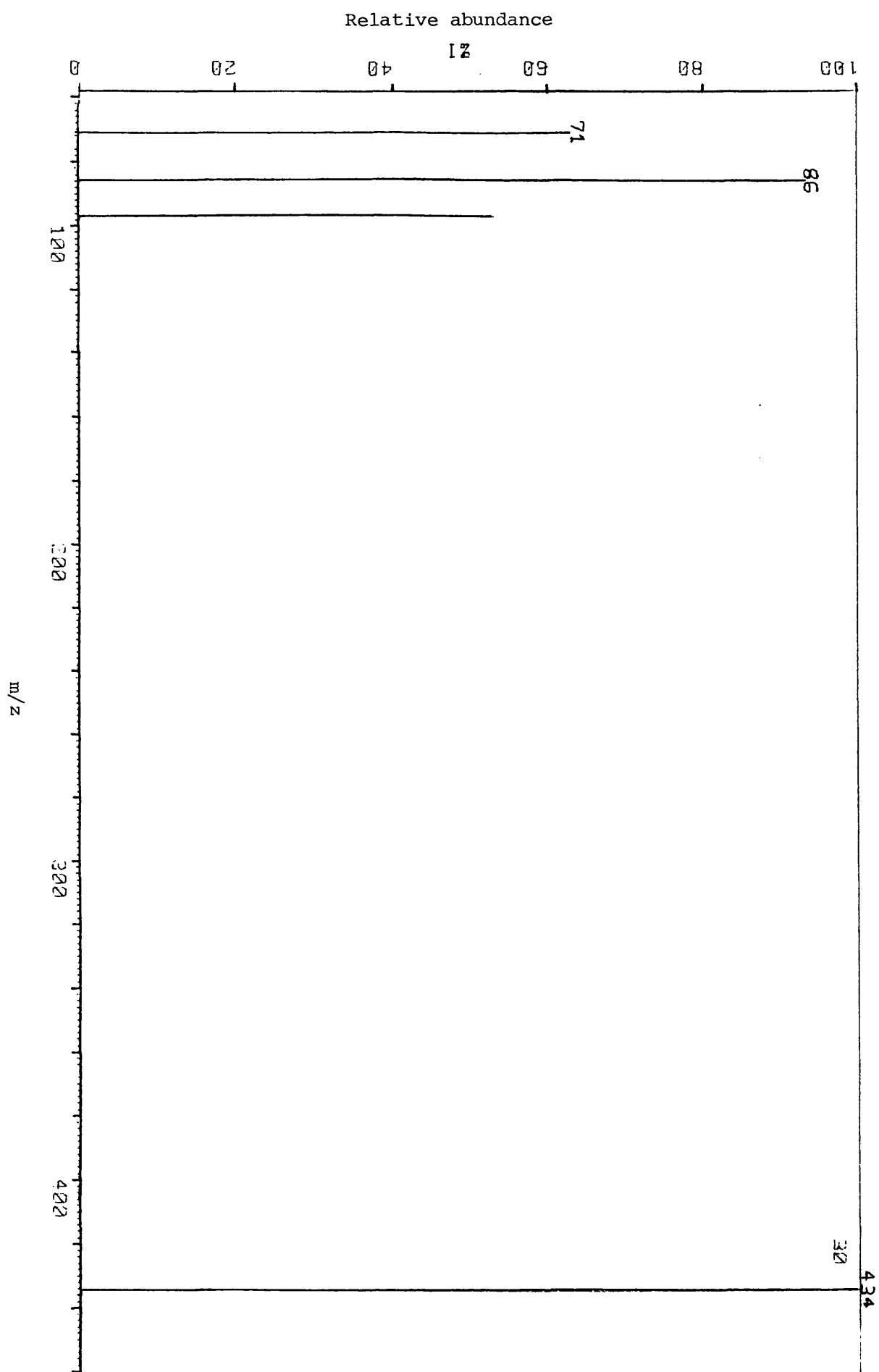
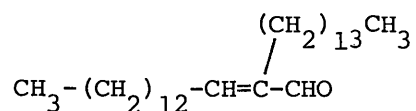


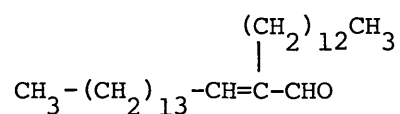
Fig. 2.27 PLP-NB LDM EV E. I.



tentatively represented as (117) or (118)



(117)



(118)

Both structures have a molecular weight of 434 and possess all the characteristic features indicated by the infrared, ^1H - and ^{13}C -NMR spectra. The small amount of sample obtained (28 mg) was not in a sufficiently pure state to allow unequivocal determination of its structure.

Marine red algae of the genus *Laurencia* have yielded such a variety of halogenated metabolites - sesquiterpenes, diterpenes, acetylenes etc. - that it is frequently assumed that an investigation of a *Laurencia* species would result in the isolation of halogenated metabolites. In this present study, the extracts of *Laurencia pinnatifida* did not yield any halogenated metabolite but an aliphatic aldehyde tentatively identified as (117) or (118) which is presumably a fatty acid derived natural product. This result may be interesting for two reasons -

i. this species of *Laurencia*, contrary to expectation, yielded no halogenated metabolites

ii. Few aldehydes have been isolated from algal sources.

It is noteworthy that the plant material was collected at the peak growth period. In the light of this, and considering that long chain unsaturated hydrocarbons serve as attractants for spermatozoa during the reproductive stages in brown algae, it is possible that the isolated aliphatic aldehyde may function as a pheromone.

CHAPTER SEVEN

ANALYSES OF STEROL, FREE FATTY ACID AND FREE AMINO
ACID COMPOSITION OF SOME RHODOPHYTA SPECIES

In addition to the compounds considered in the previous chapters, sterols, free fatty acids and free amino acids were routinely isolated from the species examined. The five species concerned are listed in Table 2.XVI.

Table 2.XVI. Species of Rhodophyta examined for sterols, free fatty acids and free amino acids

Order	Family	Genus and species	Place and time of collection
Ceramiales	Rhodomelaceae	<i>Laurencia pinnatifida</i>	Portland, April
Ceramiales	Rhodomelaceae	<i>Polysiphonia lanosa</i>	Kimmeridge Bay, June
Ceramiales	Rhodomelaceae	<i>Lomentaria articulata</i>	Portland, May
Rhodymeniales	Rhodymeniaceae	<i>Palmaria palmata</i>	Kimmeridge Bay, September
Cryptonemiales	Corallinaceae	<i>Corallina officinalis</i>	Kimmeridge Bay, June

7.1 STEROL ANALYSES BY GAS-LIQUID CHROMATOGRAPHY

7.1.1 Sample preparation and operating conditions

The sterol fractions obtained by column chromatography of the ether-soluble neutral extracts were further purified by preparative TLC on silica gel P₂₅₄ developed in toluene-methanol (9:1). Cholesterol was chromatographed as a marker, and the sterol bands detected under ultraviolet light. The sterol zones were then scraped off and eluted with diethyl ether.

Using available standards, the optimum gas-liquid chromatographic conditions were determined on a 2 metre column of 3% SE 30 on Chromosorb W-Hp. The operating conditions were: oven temperature 245°C, injector/detector 270°C, carrier gas nitrogen at a pressure of 320 kN/m² and flame ionisation detection. Sterol samples were injected as solutions in chloroform.

7.1.2. Results and discussion

A number of different gas chromatographic methods for the identification of sterols have been published involving a variety of different sterol derivatives such as acetates¹³⁸, methyl ethers¹³⁹, and trimethylsilyl ethers¹⁴⁰ in addition to free sterols¹⁴¹. Many of these systems have been compared in the comprehensive work of Patterson¹⁴² in which the gas chromatographic characteristics of ninety-two sterols were

determined on several liquid phases. With few exceptions (involving especially the C-4 methyl and C-4 dimethyl sterols), the relative retention time of a sterol relative to cholesterol was found to be identical to that of sterol acetate relative to cholesterol acetate. More importantly, the separation factors between compounds differing by a single double bond, and the effects of *cis* and *trans* Δ^{22} double bonds were determined on four different liquid phases including 3% SE-30. For instance, the relative retention time on 3% SE-30 of a sterol with *trans* Δ^{22} double bond was found to be 0.91 that of the corresponding sterol with a saturated side chain while that of the *cis* Δ^{22} isomer was 0.87. All the sterols examined were found to behave in a predictable manner in gas chromatography enabling the relative retention times of most sterols to be calculated from their structures and the data on separation factors. As a result it is possible to deduce the identity of unknown sterols from experimentally determined or calculated relative retention time data without necessarily having to obtain a large number of known sterols for comparison.

The relative retention times obtained for the available sterol standards on 3% SE-30 were in good agreement with the data of Patterson¹⁴². The relative retention time (relative to cholesterol) for brassicasterol (59) and chalinasterol (119) were calculated using the *trans* and *cis* Δ^{22} double bond separation factors relative to campesterol (56). This gave the relative retention time for brassicasterol as (0.87 x 1.29) 1.12, and that for chalinasterol as (0.91 x 1.29) 1.17. The

Table 2.XVII. Relative retention data^a of sterol standards

Sterol	Relative retention times ^b
Cholesterol	1.00
Cholestanol	1.03
Desmosterol (<u>54</u>)	1.09 ^c
Brassicasterol (<u>59</u>)	1.12
Chalinasterol (<u>119</u>)	1.17 ^d
24-Methylene cholesterol (<u>62</u>)	1.26 ^c
Campesterol (<u>56</u>)	1.29
Stigmasterol (<u>58</u>)	1.41
Lanosterol	1.55
β -Sitosterol (<u>57</u>)	1.63

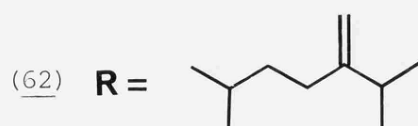
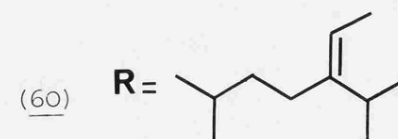
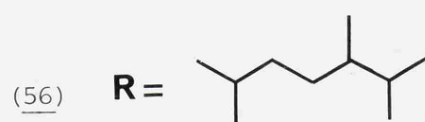
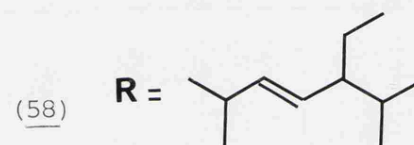
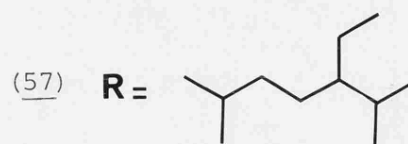
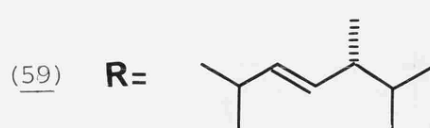
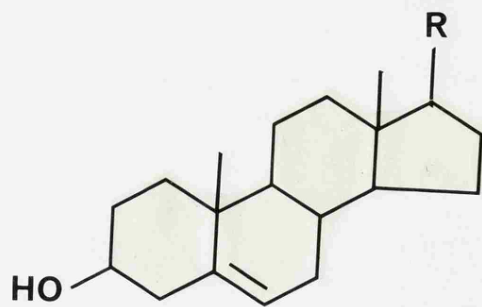
a, Column 2 metre, 3% SE-30 on 100-120 mesh Chromosorb W.Hp.

Column temperature 245°C, injector/detector 270°C, carrier
gas nitrogen at a pressure of 320 kN/m²

b, relative to cholesterol

c, values from G.W. Patterson¹⁴⁵

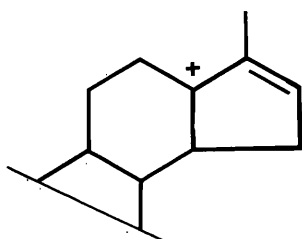
d, calculated



calculated value of 1.12 for brassicasterol is the same as the experimentally determined figure.

The various sterols detected and their relative percentage composition are shown in Table 2.VIII. *Corallina officinalis* was found to contain primarily cholesterol in agreement with the results of Doyle et al.¹⁴³. Additional evidence for the identity of cholesterol was provided by the mass spectrum of the isolated sterol which showed a molecular ion at m/z 386 which was also the base peak. Other peaks were observed at m/z 371 $[M-CH_3]^+$, 368 $[M-H_2O]^+$, 353 $[M-CH_3-H_2O]^+$, 301, 275, 273 $[M\text{-side chain}]^+$, 255 $[M\text{-side chain}-H_2O]^+$, 247, 231 $[M\text{-side chain-part of ring D-H}]^+$ ¹⁴⁴ and 213.

Laurencia pinnatifida was shown by gas-liquid chromatography to contain two sterols, the major sterol being cholesterol (78.4 percent) whilst the minor sterol was identified as desmosterol (21.6 percent) on the basis of retention data. The presence of desmosterol was further supported by a peak at m/z 384 equivalent to its molecular ion and an intense peak at m/z 271 in the mass spectrum corresponding to the loss of the side chain together with two hydrogen atoms from the steroid nucleus - a rearrangement process favoured by the formation of the allylically stabilized ion 'Z'¹⁴⁴



'Z' (m/z 271)

Table 2.XVIII. Sterol composition of Rhodophyta species

Red algae	Relative ^(a) retention times	Identity of sterols and relative percentage composition ^(b)
<i>Corallina officinalis</i>	1.00	cholesterol, 100
<i>Laurencia pinnatifida</i>	1.00 1.09	cholesterol, 78.4 desmosterol, 21.6
<i>Lomentaria articulata</i>	1.00 1.09 1.63	cholesterol, 30.4 desmosterol, 66.4 β -sitosterol, 3.2
<i>Polysiphonia lanosa</i>	1.00 1.17 1.26 1.63	cholesterol, 61.2 chalinasterol, 25.7 24-methylene cholesterol, 6.7 fucosterol, 6.4
<i>Palmaria palmata</i>	1.00 1.09	cholesterol, 3.0 desmosterol, 97.0

a, relative to cholesterol

b, mean of three determinations.

Area of peak = $W^{\frac{1}{2}}h$, where $W^{\frac{1}{2}}$ = width at half height, and

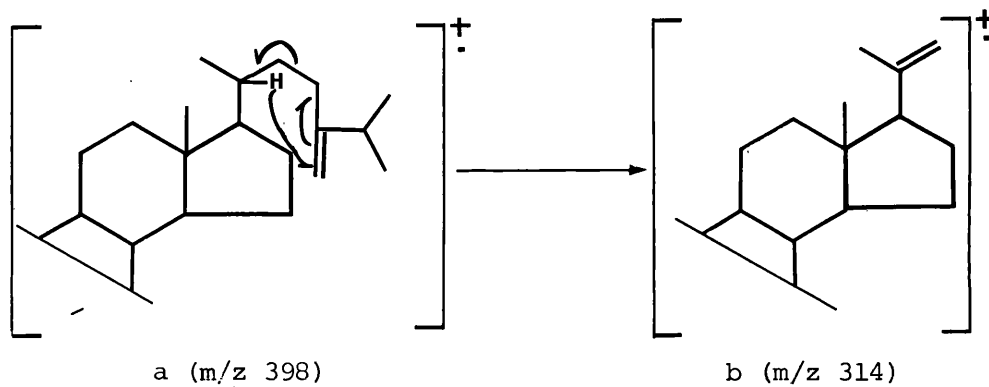
h = height of peak.

Palmaria palmata was found to contain two sterols. The major sterol in this case was desmosterol (97 percent) with cholesterol as the minor sterol. The identifications of the two sterols were again supported by diagnostic peaks in the mass spectrum of the sterol mixture.

Lomentaria articulata was shown to contain three sterols which were identified as desmosterol, cholesterol and β -sitosterol on the basis of retention time data. β -sitosterol cannot be distinguished from fucosterol (60) on 3% SE-30 but the distinction was based on the presence of a peak at m/z 414 in the mass spectrum corresponding to the molecular weight of β -sitosterol (57). The identification of the major sterol as desmosterol was confirmed by peaks at m/z 384 and 271 (base peak) in the mass spectrum.

The red alga *Polysiphonia lanosa* was shown by gas-liquid chromatography to contain at least four sterols in significant amounts. The major sterol was cholesterol (61.2 percent) whilst the minor sterols were tentatively identified as chalinasterol (25.7 percent), 24-methylene cholesterol (6.7 percent) and fucosterol (6.4 percent) on the basis of retention times. The presence of cholesterol as the principal sterol was confirmed by the mass spectrum. The presence of 24-methylene cholesterol (62) was also supported by the presence of a significant peak at m/z 398 equivalent to the molecular ion and a dominant peak at m/z 314 corresponding to the cleavage of the 22-23 bond together with one hydrogen

transfer from the charge retaining moiety and rationalized by a McLafferty type rearrangement ($a \rightarrow b$).



Chalinasterol (119) also has a molecular weight of 398 but support for its presence was provided by the peak at m/z 300 characteristic of sterols with Δ^{22} double bond, and presumed to arise by the vinylic cleavage of the side chain with one hydrogen transfer¹⁴⁴. The presence of fucosterol (60) was supported by a peak at m/z 412 corresponding to the molecular weight. However, the barely discernible peak at m/z 414 may indicate the presence of β -sitosterol in trace quantities.

Previous reports^{143, 145} have indicated that cholesterol, a characteristic animal sterol, or the closely related sterol, desmosterol, was found to occur without exception in the red algae. Results from the present work are in agreement with these reports. The occurrence of desmosterol as the predominant sterol (97 percent) and cholesterol as the minor sterol in *Palmaria palmata* is also in agreement with the findings of Gibbons et al.¹⁴⁵. Desmosterol was also found in considerable

proportions in *Laurencia pinnatifida* (21.6 percent) and *Lomentaria articulata* (66 percent). This result for *Laurencia pinnatifida* is at variance with the findings of Gibbons *et al.*¹⁴⁵ in which cholesterol accounted for 98 percent and desmosterol only 2 percent, of the sterol content. The sterol fraction from *Polysiphonia lanosa* presented a picture that is very different from the earlier report by Gibbons *et al.*¹⁴⁵ Their report indicated only the presence of cholesterol whereas at least four sterols were detected in significant proportions in the present study (Table 2.XVIII). Traces of unidentified sterols were also present in all the investigated red alga. Overall, this is in agreement with the observation made by Wyllie and Djerassi¹⁴⁴ that most of the naturally occurring sterols of marine origin - reported as pure compounds in the literature - were in fact mixtures of two to ten components. The detection of β -sitosterol, fucosterol, chalinasterol and 24-methylene cholesterol in some of the red algae negates the report¹⁴⁵ that cholesterol or closely related C-27 sterols occur in the Rhodophyta unaccompanied by any sterols containing a C-24 alkyl group.

Cholesterol has been reported in small amounts in various higher plants^{146, 147, 148} where it accompanies sterols containing an extra alkyl group at C-24. It seems that the situation is reversed in the Rhodophyta where the principal sterol is cholesterol or the related C-27 sterol, desmosterol, accompanied by smaller amounts of sterols alkylated at C-24.

7.2 ANALYSES OF FREE FATTY ACIDS BY GAS-LIQUID CHROMATOGRAPHY

7.2.1 Sample preparation and analytical conditions

The free fatty acid fractions isolated from the ether-soluble acidic extracts by column chromatography were esterified with 14% BF_3 -methanol complex⁹⁸. The esterified product was purified by preparative TLC on silica gel PF_{254} with toluene as the developing solvent and visualised in ultraviolet light. The fatty acid ester zones were scraped off and eluted with diethyl ether. The recovered fatty acid esters were analyzed as solutions in n-hexane by gas-liquid chromatography using a one metre long glass column packed with 3% SE-30 on Chromosorb W-Hp, 100 - 120 mesh. The analysis was carried out isothermally at an oven temperature of 180°C and injector/detector temperature of 200°C using purified nitrogen as the carrier gas at a pressure of 280 kN/m^2 . The components of the fatty acid ester mixtures were identified provisionally by comparison of the relative retention times (relative to stearic acid) of the peaks with those of standard esters analyzed under the same chromatographic conditions (Table 2.XIXa). Purification of the fatty acid methyl esters by preparative thin layer chromatography prior to gas-liquid chromatographic analysis did not introduce any obvious qualitative or quantitative difference in the composition of the fatty acid methyl esters as indicated by the chromatograms. This procedure was thus subsequently omitted.

Table 2.XIXa. Relative retention time data of fatty acid
methyl ester standards

Fatty acid methyl esters	Relative retention times *
12:0	0.10
14:0	0.21
16:0	0.43
16:1w9	0.37
18:0	1.00
18:1w9	0.86
18:2w6	0.84
18:3w3	0.83
20:0	1.76
20:2w3	1.52
20:5w3	1.46

* Relative to methyl stearate (18:0)

7.2.2 Results and discussion

The result of the analyses carried out on the free fatty acid methyl esters of the five Rhodophycean seaweeds are shown in Table 2.XIXb. The fatty acid distribution is broadly characteristic of the Class Rhodophyta, with C_{16} saturated fatty acid as the predominant saturated fatty acid, and high relative levels of C_{18} and C_{20} unsaturated fatty acids. C_{16} Unsaturated fatty acids were detected in low levels, usually less than 2 percent except in the case of *Polysiphonia lanosa* where up to 8 percent was detected. This result is in agreement with the observations of Jameison and Reid⁸⁶ who found C_{16} unsaturated fatty acids in amounts less than 2 percent of the total fatty acids in twelve Rhodophycean algae. This may suggest that these acids are not significantly involved in glyceride formation. The absence of C_{20} unsaturated fatty acids in *Palmaria palmata* is rather odd and is at variance with earlier reports^{149,150}. Since these earlier reports were based on the total fatty acids the present finding may imply that the C_{20} unsaturated fatty acids in *Palmaria palmata* exist only as glyceride esters. The absence of free C_{20} unsaturated fatty acids in *Palmaria palmata* may have taxonomic usefulness although more species would have to be examined and more data acquired on the seasonal variations of the free fatty acid distributions.

The very high level of C_{20} unsaturated fatty acids in *Corallina officinalis* (67.5 percent) compared to the levels observed in the other species (less than 40 percent) is again

Table 2.XIXb. Free fatty acid composition of Rhodophyta species

Acid	Percentage ^a of free fatty acids				
	<i>Laurencia pinnatifida</i>	<i>Polysiphonia lanosa</i>	<i>Lomentaria articulata</i>	<i>Palmaria palmata</i>	<i>Corallina officinalis</i>
<u>Saturated</u>					
C ₁₄	2.6	4.5	2.6	12.6	trace
C ₁₆	41.6	33.8	36.2	62.2	20.4
C ₁₈	trace	trace	trace	4.2	1.0
<u>Unsaturated</u>					
C ₁₆	1.6	8.1	1.2	1.1	1.9
C ₁₈	22.7	30.2	21.4	20.0	9.1
C ₂₀	31.5	23.4	38.5	-	67.5

trace = less than 1%

a, mean of three determinations based on peak areas, A. $A = W^{\frac{1}{2}}h$ were $W^{\frac{1}{2}}$ = width at half height, and h = height of peak.

striking and has led to the isolation of an eicosapentaenoic acid with an unusual arrangement of double bonds (see Chapter 5). There have been previous indications of the presence of 20:2 and 22:2 non-methylene interrupted fatty acids in *Corallina officinalis*⁸⁵, though fatty acids of this type are rare in other algae.

Usually fatty acids are bound to alcohols, notably glycerol in the living cells, in the form of glyceride esters. They are mostly in the form of triglycerides which are usually regarded as storage materials, and to a lesser extent as mono- and di-glycerides. Another class of fatty acid glyceride esters have the central hydroxyl and one terminal hydroxyl of the glycerol esterified to fatty acids, and the remaining hydroxyl attached to a more polar group. These are referred to as polar lipids. The free fatty acids are readily separated from the glyceride esters and are contained in the non-polar acidic extracts (soluble in alkaline aqueous solutions) while the glyceride esters remain in the non-polar neutral extracts. The fatty acids involved in glyceride formation can only be liberated after saponification. The major importance of algal lipids probably lies in their participation in biological membranes. It is possible that the occurrence of free fatty acids reflects the activities of lipases during extraction of lipids from the cells.

7.3 ANALYSES OF FREE AMINO ACIDS BY TWO DIMENSIONAL PAPER CHROMATOGRAPHY

7.3.1 Sample preparation and chromatographic conditions

The water-soluble fraction of each algal extract was concentrated *in vacuo* and passed through a column of Dowex 50W-X8 (H^+ form). After washing the column with deionised water, amino acids were eluted from the resin with 2M ammonia solution and the alkaline effluent was evaporated to dryness *in vacuo*. The residue was then dissolved in water and passed through a column of Amberlite IRA 400 (OH^- form). Neutral and basic amino acids were eluted from the column with deionised water and elution with 1N hydrochloric acid allowed the recovery of acidic amino acids. The eluates were taken to dryness *in vacuo* (the acidic solution over sodium hydroxide pellets). The amino acids present in the residues were investigated qualitatively using ascending two-dimensional paper chromatography on Whatman 3 mm chromatography papers. Phenol-water (3:1, w/v) in the presence of concentrated ammonia vapour was used as the first developing solvent, and n-butanol-acetic acid-water (4:1:1) was the second solvent. The amino acid spots obtained after spraying the developed chromatograms with ninhydrin reagent and heating at $110^{\circ}C$ for 5 min were tentatively identified by comparisons with the chromatograms of standard amino acids.

Table 2.XX. Free amino acid profiles in some species of red seaweeds

Amino acids	<i>Lomentaria articulata</i>	<i>Palmaria palmata</i>	<i>Laurencia pinnatifida</i>	<i>Polysiphonia lanosa</i>	<i>Coralina officinalis</i>
Aspartic acid	+++	++	+++	++	+
Asparagine	+	+	+	+	+
Glutamic acid	++	+++	++	+++	++
Glutamine	+	+	+	+	+
Alanine	+++	+++	++	++	++
Glycine	+++	++	+++	+++	+++
Serine	++	++	++	++	++
Proline	++	++	+++	+++	++
Threonine	++	+	+	+	+
Valine	+	+	+	+	+
Phenylalanine	+	++	+	+	+
Isoleucine/leucine	+	+	+	+	++
Lysine	-	++	-	+	++
Arginine	-	-	-	-	-
Histidine	-	+	-	-	+
Homocysteic acid	-	++	-	-	-

+++ = strong ninhydrin-reaction colour
 ++ = moderate ninhydrin-reaction colour
 + = weak ninhydrin-reaction colour

7.3.2 Results and Discussion

Table 2.XX shows the relative intensities of the amino acid spots after ninhydrin treatment of the chromatograms. The amino acids appeared as purplish spots except for proline, hydroxyproline and histidine which appeared as yellowish spots. Leucine and isoleucine could not be easily separated by the two systems, and formed a composite spot. The amino acid distribution in all the species examined show a general prevalence of acidic amino acids - aspartic and glutamic acids - as well as alanine, glycine, proline and serine. The levels of basic amino acids were generally low. A fairly high level of homocysteic acid was indicated only in *Palmaria palmata*. This is in agreement with the work of Laycock et al.⁹⁷. It was however not possible to comment on the quantitative aspects of the amino acid composition. Moreover, quantitative variations in algal amino acids are influenced to a large extent not only by genetically controlled factors but also by differences in physiological and environmental conditions^{151, 152}. The amino acid fraction of *Laurencia pinnatifida* contained an unidentified sky-blue ninhydrin-reacting spot appearing just above serine on the chromatogram.

REFERENCES TO PART II

22. L. Newton, A handbook of British Seaweeds. A. Wheaton and Co. Ltd. Exeter (1962).
23. A.C. Campbell, The Hamlyn Guide to the Seashore and Shallow seas of Britain and Europe. Hamlyn, London, (1982).
24. J.R. Lewis, The Ecology of Rocky Shores. English Universities Press, London (1964).
25. J.A. De Boer, in The Biology of Seaweeds, ed. C.S. Lobban and M.J. Wynne, Blackwell Scientific Publications, London (1981).
26. J.E. Bardach, J.H. Ryther and W.O. McLarney, Aquaculture, The Farming and Husbandry of Freshwater and Marine Organisms; Wiley - Interscience, New York (1972).
27. T. Levring, H.A. Hoppe and O.J. Schmid, Marine Algae: A Survey of Research and Utilization. Cram, De Gruyter and Co. Hamburg (1969).
28. J.R. Waaland, in Biology of Seaweeds, ed. C.S. Lobban and M.J. Wynne. Blackwell Scientific Publications. London (1972).
29. G. Blunden, *Proc. Int. Seaweed Symp.*, 7, 584 (1972).
30. L. Newton, Seaweed Utilization, Sampson Low, London, (1951).
31. A. Flowers and A.J. Bryce, Energy from Marine Biomass. *Sea Technology* (Oct. 1977).

32. J.S. Mynderse and D.J. Faulkner, *Phytochemistry* 17, 237 (1978).
33. B.V. Charlwood and D.V. Banthorps, *Progr. Phytochem.* 5, 65 (1978).
34. D.J. Faulkner and M.O. Stallard, *Tetrahedron Lett.* 1171, (1973).
35. J.S. Mynderse and D.J. Faulkner, *Tetrahedron*, 1963 (1975).
36. D.B. Stierle and J.J. Sims, *Tetrahedron* 35, 1261 (1979).
37. R. Kazlauskas, P.T. Murphy, R.J. Wells and J.F. Blount, *Tetrahedron Lett.* 4451 (1976).
38. D.B. Stierle, R.M. Wing and J.J. Sims, *Tetrahedron Lett.* 4455 (1976).
39. J.S. Mynderse and D.J. Faulkner, *J. Am. Chem. Soc.* 96, 6771 (1974).
40. P. Crews, P.Ng, E. Kho-Wiseman and C. Pace, *Phytochemistry* 15, 1707 (1976).
41. D. Van-Engen, J. Clardy, E. Kho-Wiseman, P. Crews, M.D. Higgs and D.J. Faulkner, *Tetrahedron Lett.*, 1401 (1978).
42. R.S. Norton, R.G. Warren and R.J. Wells, *Tetrahedron Lett.*, 3905 (1977).
43. P. Crews, in *Marine Natural Products Chemistry*. eds. D.J. Faulkner and W. Fenical, 211-223. Plenum Press, New York and London (1973).
44. H.E. Hogberg, R.H. Thomson and T.J. King, *J. Chem. Soc., Perkin Trans 1*, 1696 (1976).

45. A.J. Blackman and R.J. Wells, *Tetrahedron Lett.*, 3053 (1978).
46. M. Suzuki, E. Kurosawa and T. Irie, *Tetrahedron Lett.*, 4995 (1970).
47. D. J. Faulkner and L.E. Wolinsky, *J. Org. Chem.* 41, 597 (1976).
48. A.G. Gonzalez, J.M. Aguilar, J.D. Martin and M.L. Rodriguez, *Tetrahedron Lett.*, 137 (1976).
49. T. Irie, M. Suzuki and Y. Hayakawa, *Bull. Chem. Soc. Jpn.*, 42 , 843 (1969).
50. B.M. Howard and W. Fenical, *Tetrahedron Lett.*, 41 (1976).
51. D.J. Faulkner, *Phytochemistry* 15, 1992 (1976).
52. A.G. Gonzalez, J.M. Aguilar, J.D. Martin and M. Norte, *Tetrahedron Lett.*, 2499 (1975).
53. J.D. Martin and J. Darias, in *Marine Natural Products, Chemical and Biological Perspectives*, Vol. 1, ed. P.J. Scheuer, 161-3, Academic Press, London and New York (1978).
54. J.J. Sims, G.H.Y. Lin, R.M. Wing and W. Fenical, *J. Chem. Soc. B., Chem. Comm.* 470 (1973).
55. H. Matsuda, Y. Tomie, S. Yamamura and Y. Hirata, *Chem. Commun.* 898 (1967).
56. W. Fenical, B.M. Howard, K.B. Gifkins and J. Clardy, *Tetrahedron Lett.*, 2983 (1975).
57. W. Fenical and J. Clardy, *Tetrahedron Lett.*, 731 (1970).
58. A.G. Gonzalez, J.Darias, J.D. Martin and C. Perez, *Tetrahedron Lett.*, 1249 (1974).
59. M.A. Ragan and D.J. Chapman, *A Biochemical Phylogeny of the Protists*. Academic Press, London and New York (1978).

60. E. Fattorusso, S. Magno, C. Santacroce, D. Sica, G. Impellizzeri, S. Mangiafico, M. Piattelli and S. Sciuto, *Biochem. Syst. Ecol.*, 4, 135 (1976).
61. E. Fattorusso, S. Magno, C. Santacroce, D. Sica, G. Impellizzeri, S. Mangiafico, G. Oriente, M. Piattelli and S. Sciuto, *Phytochemistry* 14, 1579 (1975).
62. T. Komura, S. Wada and H. Nagayama, *Agr. Biol. Chem.* 38, 2275 (1974).
63. T.W. Goodwin, Sterols. In *Algal Physiology and Biochemistry*, ed. W.D.P. Stewart, 266. Blackwell Scientific Publications, Oxford (1974).
64. G.F. Gibbons, L.J. Goad and T.W. Goodwin, *Phytochemistry* 7, 983 (1968).
65. L.G. Dickson, G.W. Patterson and B.A. Knights, *Proc. Int. Seaweed Symp.* 9, 413 (1979).
66. T. Irie, M. Suzuki and T. Masamune, *Tetrahedron Lett.* 1091 (1965).
67. T. Irie, M. Izawa and E. Kurosawa, *Tetrahedron* 26, 851 (1970).
68. E. Kurosawa, A. Fukuzawa and T. Irie, *Tetrahedron Lett.*, 2121 (1972).
69. A. Furusaki, E. Kurosawa, A. Fukuzawa and T. Irie, *Tetrahedron Lett.*, 4579 (1973).
70. W. Fenical, K.B. Gifkins and J. Clardy, *Tetrahedron Lett.*, 313 (1973).
71. W. Fenical and J.N. Norris, *J. phycol.* 11, 104 (1975).
72. S.M. Waraszkiewicz, H.H. Sim and K.L. Erickson, *Tetrahedron Lett.*, 3021 (1976).

73. H.H.Sun, S.M. Waraszkiewicz and K.L. Erickson, *Tetrahedron Lett.*, 4227 (1976).
74. R. Scott, *Nature (Lond)* 173, 1098 (1954).
75. J.M. Chantraine, G. Combaut and J. Teste, *Phytochemistry* 12, 1793 (1973).
76. S.L. Manley and D.J. Chapman, *Phytochemistry* 19, 1453 (1980).
77. S.L. Manley and D.J. Chapman, *F.E.B.S. Lett.* 93, 97 (1978).
78. K. Ohta and M. Takagi, *Phytochemistry* 16, 1085 (1977).
79. M. Pedersén, *Phytochemistry* 17, 291 (1978).
80. K.W. Glombitza and H. Stofflen, *Planta med.* 22, 391 (1972).
81. A.M. Chevolol-Magneur, A. Cave, P. Potier, J. Teste, A. Chiaroni and C. Riche, *Phytochemistry* 15, 767 (1976).
82. J. McLachlan and J.S. Craigie, *J. Phycol.* 2, 133 (1966).
83. D.G. Müeller, G. Gassmann and K. Lüning, *Nature (Lond)* 279, 430 (1979).
84. R.G. Ackman and J. McLachlan, *Proc. Nova Scotian Inst. Sci.* 28, 47 (1977).
85. R.B. Johns, P.D. Nichols and G.J. Perry, *Phytochemistry* 18, 799 (1979).
86. G.R. Jameison and E.H. Reid, *Phytochemistry* 11, 1423 (1972).
87. J.S. Craigie, In *Algal Physiology and Biochemistry*, ed. W.D.P. Stewart, 206. Blackwell Scientific Publications, Oxford (1974).
88. J.S. Craigie, J. McLachlan and R.D. Tocher, *Can. J. Bot.* 46, 605 (1968).

89. J.S. Craigie and J. McLachlan, *Can. J. Bot.* 42, 777 (1964).
90. H. Kaus, *Nature (Lond.)* 214, 1129 (1967).
91. L. Fowden, *Nature (Lond.)* 167, 1030 (1951).
92. G. Impellizzerri, S. Mangiafico, G. Oriente, M. Piattelli, S. Sciuto, E. Fattorusso, S. Magno, C. Santacroce and D. Sica, *Phytochemistry* 14, 1549 (1975).
93. S. Murakami, T. Takemoto and Z. Shimuzu, *J. Pharm. Soc. Japan* 73, 1026 (1953).
94. K. Daigo, *J. Pharm. Soc. Japan* 79, 356 (1959).
95. R. Scott, *Nature (Lond.)* 173, 1098 (1954).
96. K. Miyazawa, *Bull. Jpn. Soc. Sci. Fish.* 37, 788 (1971).
97. M.V. Laycock, A.G. McInnes and K.C. Morgan, *Phytochemistry* 18, 1220 (1979).
98. W.R. Morrison, and L.M. Smith, *J. Lipid Res.* 5, 600 (1964).
99. M.A. Ragan, *Can. J. Chem.* 56, 2681 (1978).
100. M. Barber, R.S. Bordoli, R.D. Sedgwick and A.N. Tyler, *Nature* 293, 270 (1981).
101. R.U. Lemieux and J.D. Stevens, *Can. J. Chem.* 44, 249 (1966).
102. A.S. Perlin, B. Casu and H.J. Koch, *Can. J. Chem.* 48, 2596 (1970).
103. J.B. Stothers, *Carbon-13 NMR Spectroscopy*, 461. Academic Press, New York and London (1972).
104. J.N.C. Whyte, *Can. J. Chem.* 47, 4083 (1969).
105. Borje Wickberg, *Acta Chem. Scand.* 12, 1187 (1958).
106. J.H. Hodgkin, J.S. Craigie and A.G. McInness, *Can. J. Chem.* 44, 74 (1966).
107. B. Weinstein, T.L. Rold, C.E. Harrel, Jr, M.W. Burns III,

- and J.R. Waaland, *Phytochemistry* 14, 2667 (1975).
108. R.J. Abraham and P. Loftus, Proton and Carbon-13 NMR Spectroscopy, 117. Heyden, London (1981).
109. D.F. Ewing, *Org. Magn. Resonance* 12, 499 (1979).
110. J.B. Stothers, Carbon-13 NMR Spectroscopy, 197. Academic Press, New York and London (1972).
112. E.P. Crowell, W.A. Powell and C.J. Varsel, *Analyt. Chem.* 35, 184 (1963).
113. Bunker, 13-C Data Bank, Vol. 1.
114. N. Katsui, Y. Suzuki, S. Kitamura and T. Irie, *Tetrahedron* 23, 1185 (1967).
115. R. Bieble, In Physiology and Biochemistry of algae, ed. R.A. Lewin, 805. Academic Press, New York and London (1962).
116. A. De Bruyn, M. Anteunis and G. Verhegge, *Acta Cienc. Indica* 1, 83 (1975).
117. K. Izumi, *J. Biochem.* 76, 535 (1974).
118. J. Haverkamp, M.J.A. de Bie and J.F.G. Vliegthart, *Carbohydr. Res.* 39, 201 (1975).
119. K. Izumi, *J. Biochem.* 81, 1605 (1977).
120. D.E. Dorman and J.D. Roberts, *J. Am. Chem. Soc.* 93:18 4463 (1971).
121. K. Bock and C. Pedersen, *J. Chem. Soc. Perkin II* 293 (1974).
122. K. Bock and C. Pedersen, *Acta chem. Scand. B.* 29, 258 (1975).
123. E.W. Putman and W.Z. Hassid, *J. Am. Chem. Soc.* 76, 2221 (1954).

124. H. Colin and G. Guéguen, *Compt. Rend. Acad. Sci.* 191, 163 (1930).
125. J.S. Craigie, J. McLachlan and R.D. Tocher, *Can. J. Bot.* 46, 605 (1968).
126. T. Hashimoto, K. Nukada, H. Shima and T. Tsuchiya, *J. Amer. Oil Chemists' Soc.* 40, 124 (1963).
127. M.P. Bagby, C.R. Smith, Jr., K.L. MikoLajczak and I.A. Wolff, *Biochemistry* 1:4, 632 (1962).
128. C.Y. Hopkins and M.J. Chisolm, *J. Chem. Soc.* 907 (1965).
129. B.A. Anderson and R.T. Holman, *Lipids* 9:3, 185 (1974).
130. N.J. De Souza and W.R. Nes, *Phytochemistry* 8, 819 (1969).
131. J.J. Sims and J.A. Pettus, Jr., *Phytochemistry* 15, 1076 (1976).
132. J.W.K. Burrell, R.F. Garwood, L.M. Jackman, E. Oskay and B.C.L. Weedon, *J. Chem. Soc. (C)*, 2144 (1966).
133. I. Iwata and Y. Sakura, *Agr. Biol. Chem. (Tokyo)* 27, 253 (1963).
134. C.Y. Hopkins, *J. Amer. Oil Chemists' Soc.* 38, 664 (1961).
135. J.D. Joseph, *Lipids* 10:7, 395 (1975).
136. A.M. Duffield and C. Djerassi, *J. Am. Chem. Soc.* 87, 4554 (1965).
137. R.G. Ackman and S.N. Hooper, *Comp. Biochem. Physiol.* 46B, 153 (1973).
138. J.W. Copius-Peereboom, *J. Gas Chromatogr.* 3, 325 (1965).
139. B.B. Clayton, *Biochemistry* 1, 357 (1962).
140. P. Eneroth, K. Hellström and R. Rhyhage, *Steroids* 6, 707 (1965).
141. K. Tsuda, K. Sakai and N. Ikekawa, *Chem. Pharm. Bull.* 9, 835 (1961).

142. G.W. Patterson, *Analytical Chemistry* 43:10, 1165 (1971).
143. P.J. Doyle and G.W. Patterson, *Comp. Biochem. Physiol.* 41B, 355 (1972).
144. S.G. Wyllie and C. Djerassi, *J. Org. Chem.* 33, 305 (1968).
145. G.F. Gibbons, L.J. Goad and T.W. Goodwin, *Phytochemistry* 6, 677 (1967).
146. D.F. Johnson, R.D. Bennett and E. Heftmann, *Science* 140, 198 (1963).
147. C. Djerassi, J.C. Knight and H. Brockmann, *Chem. Ber.* 97, 3118 (1964).
148. R.D. Bennett, S.T. Ko and E. Heftmann, *Phytochemistry* 5, 231 (1966).
149. J.A. Lovern, *Biochem. J.* 30, 387 (1936).
150. L. Chuecas and J. P. Riley, *J. Mar. biol. Ass. UK* 46, 153 (1966).
151. G. Impellizzeri, S. Mangiafico, M. Piattelli, S. Sciuto, E. Fattorusso, C. Santacroce and D. Sica, *Biochem. Syst. Ecol.* 5, 77 (1977).
152. L. Fowden, In *Physiology and Biochemistry of Algae*, ed. R.H. Lewin, 189. Academic Press, London (1962).
153. C.G.C. Chesters and J.A. Stott, *Proc. 2nd Int. Seaweed Symp.*, 49 (1956).
154. I.S. Hornsey and D. Hide, *Br. Phycol. J.* 9, 353 (1974).
155. J. McN Sieburth, *Science* 132, 676 (1960).
156. T. Katayama, In *Physiology and Biochemistry of Algae*, ed. R.A. Lewin, 467-473. Academic Press, New York (1962).
157. L.S. Ciereszko, *Trans. N.Y. Acad. Sci. Ser. II*, 24, 502 (1962).

158. K. Saito and Y. Nakamura, *J. Chem. Soc. Japan, Pure Chem. Sect.*, 72, 992 (1951).